Immune Regulation by Human Colonic Bacteria and Short-chain Fatty Acids

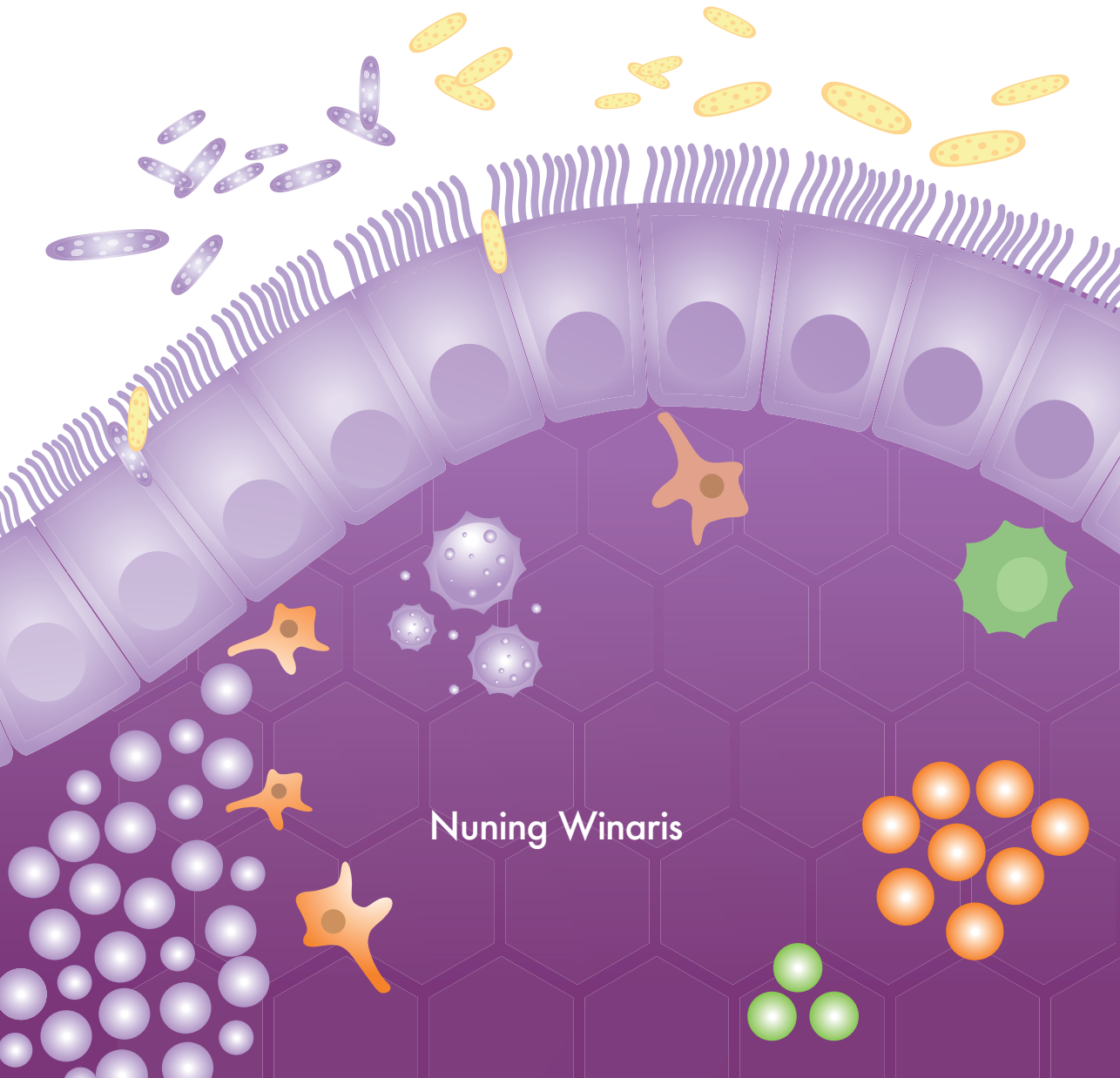

Nuning Winaris

PROPOSITIONS

1 *Faecalibacterium prausnitzii* strains with a 'silent' immune profile give best protective effect against DSS-induced colitis.
(this thesis)

2 Acetate elicits anti-inflammatory effects on immune cells and alters gene expression in epithelial cells through a different mechanism to butyrate.
(this thesis)

3 Staying in space for a year makes you different compared to your identical twin sibling (Garrett-Bakelman *et al*., 2019, Science 364, 144).

4 Research on people who encounter extreme dietary or physiological conditions can further our understanding of human genetics and biology (Ilardo *et al*., 2018, Cell 173, 569–580).

5 Korean wave (*hallyu*) is an influential global phenomenon in the 21st century.

6 At the end, finishing a PhD is all about persistency and endurance.

Propositions belonging to the thesis entitled

"Immune Regulation by Human Colonic Bacteria and Short-chain Fatty Acids"

Nuning Winaris
Wageningen, 14 February 2020

Immune Regulation by Human Colonic Bacteria and Short-chain Fatty Acids

Nuning Winaris

Thesis committee

Promotor

Prof. Dr Jerry M. Wells
Professor of Host-Microbe Interactions
Wageningen University & Research

Co-promotor

Dr Ellen Kranenbarg-Stolte
Researcher at the Host-Microbe Interactomics Group
Wageningen University & Research

Other members

Prof. Dr Hauke Smidt, Wageningen University & Research
Dr Wilma T. Steegenga, Wageningen University & Research
Dr Kenneth Nally, University College Cork, Ireland
Dr Anita Wichmann Hørsholm, Denmark

This research was conducted under the auspices of the Graduate School VLAG
(Advanced studies in Food Technology, Agrobiotechnology, Nutrition and Health Sciences)

Immune Regulation by Human Colonic Bacteria and Short-chain Fatty Acids

Nuning Winaris

Thesis

submitted in fulfilment of the requirements for the degree of doctor
at Wageningen University
by the authority of the Rector Magnificus,
Prof. Dr A.P.J. Mol,
in the presence of the
Thesis Committee appointed by the Academic Board
to be defended in public
on Friday 14 February 2020
at 4 p.m. in the Aula

Nuning Winaris
Immune Regulation by Human Colonic Bacteria and Short-chain Fatty Acids,
212 pages.

PhD thesis, Wageningen University, Wageningen, The Netherlands (2020)
With references, with summaries in English and Dutch

ISBN: 978-94-6395-244-6

DOI: https://doi.org/10.18174/509135

This thesis is dedicated to my family

Table of contents

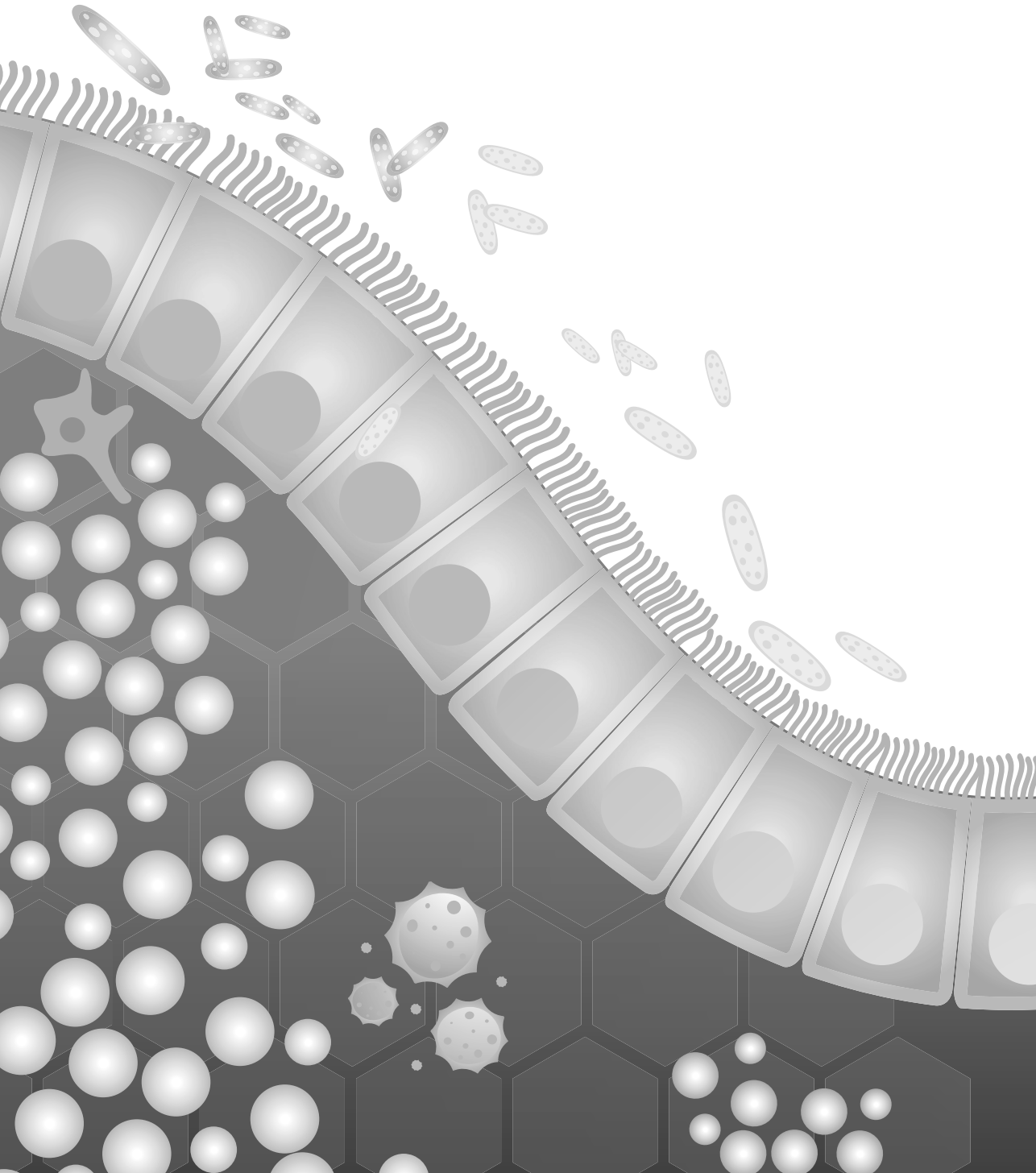

Chapter 1

General Introduction

Nuning Winaris

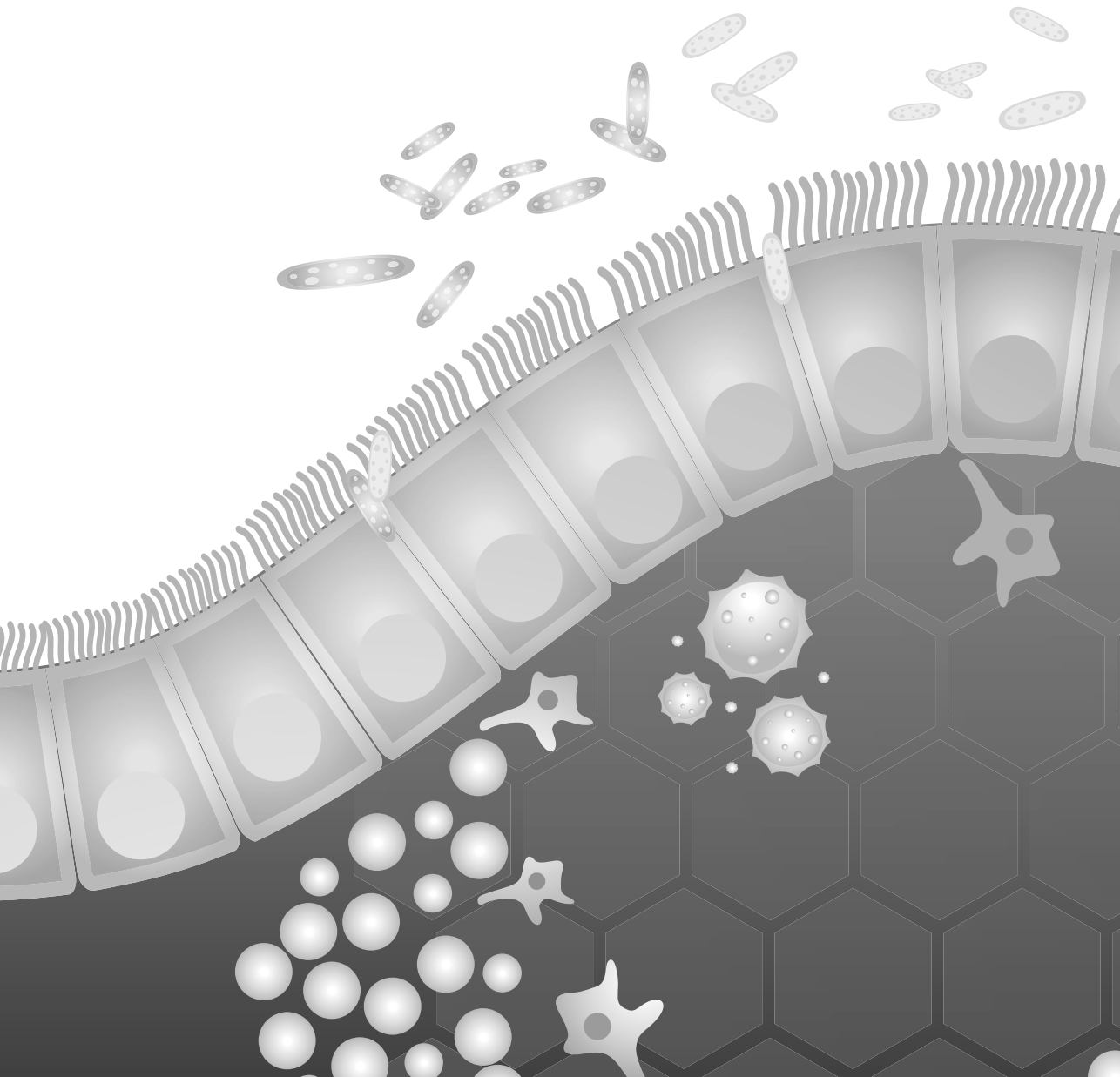

The impact of the gut microbiota on host physiology

More than a decade of research on the interactions between the host and its intestinal microbiota has moved the field into the mainstream scientific arena. A stream of high impact publications has described how the microbiota can modulate the host's immune system, metabolism, and influence host development and physiology. Considerable progress has been made in identifying, isolating and culturing members of the gut microbiota, but we are only beginning to understand the complex interplay between the microbiome, host genetics and host physiology. It is now clear that the microbial community has a beneficial role during normal homeostasis and that the beneficial relationship with the host microbiota is lost under inflammatory conditions leading to the emergence of opportunist pathobionts that can contribute to the pathophysiology of different diseases.
A disrupted microbial balance in the faecal microbiota often referred to as 'dysbiosis' is known to contribute to the pathophysiology of many human diseases, including inflammatory bowel disease (IBD)[1]. IBD is a chronic inflammation of the gut consisting of two readily distinguishable disease types; ulcerative colitis (UC) and Crohn's disease (CD)[2-4]. In CD the inflammation can affect different parts of gastrointestinal tract, whereas in UC the inflammation occurs predominantly in the large intestine or colon[4]. Additionally UC only affects the inner most lining of the colon while Crohn's disease can occur in all anatomical layers of the gut.

The number of IBD cases has steadily increased over the years, with more than 2.5 million people in Europe and 1 million people in the USA (up to 0.5% population) reported to suffer from IBD in 2015[2]. In the USA alone the IBD prevalence is estimated to increase by more than 0.6% over the next decade, which would result in around 2.2 million people suffering from IBD in 2025[5]. Additionally, the incidence of IBD in newly industrialized countries in Asia, the Middle East and South America has also increased notably over the last two centuries[2, 3].

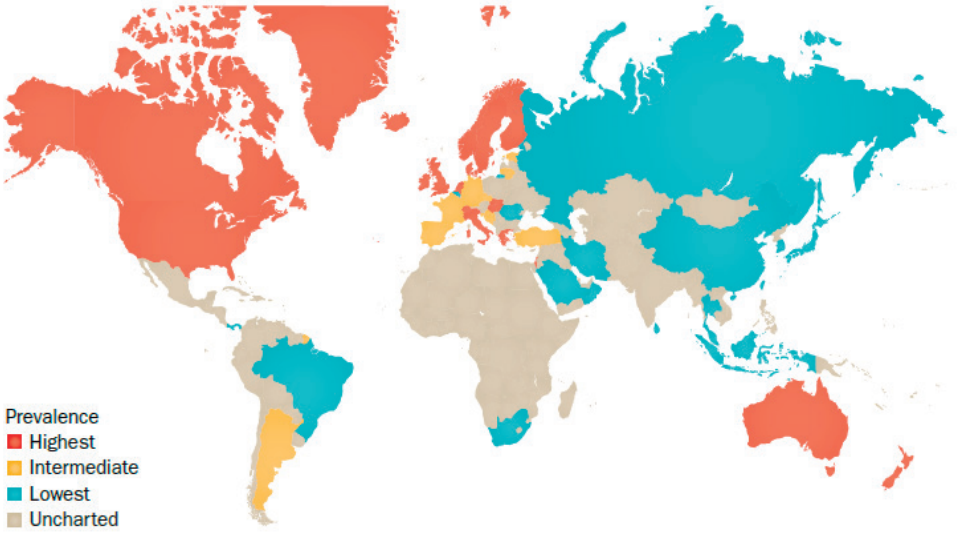

Figure 1.1. The global prevalence of IBD in 2015. Data from Molodecky et al. (2012)[6]. Adapted from an image provided by PresenterMedia. Adapted from Kaplan (2015)[2].

Several factors are known to contribute to IBD, such as the environment (including diet), microbiota composition, genetic predisposition and the host immune response[7]. Studies in monozygotic twins showed that the concordance of IBD in both individuals is between 20 to 50% indicating that the environment plays a crucial role in triggering the disease in genetically susceptible individuals[8-11].

Sartor and Mazmanian (2012) reported that IBD patients have a distinctive gut microbiota composition compared to healthy people. Patients with IBD are characterized by depleted numbers of *Firmicutes* and *Bacteroidetes,* phyla which are associated with a healthy gut condition, as well as with increased numbers of the pathobiont *Proteobacteria*[12]. As this disrupted microbial balance (dysbiosis) is strongly linked to cause the majority of IBD cases, restoring this microbial balance could be the key to IBD treatment.

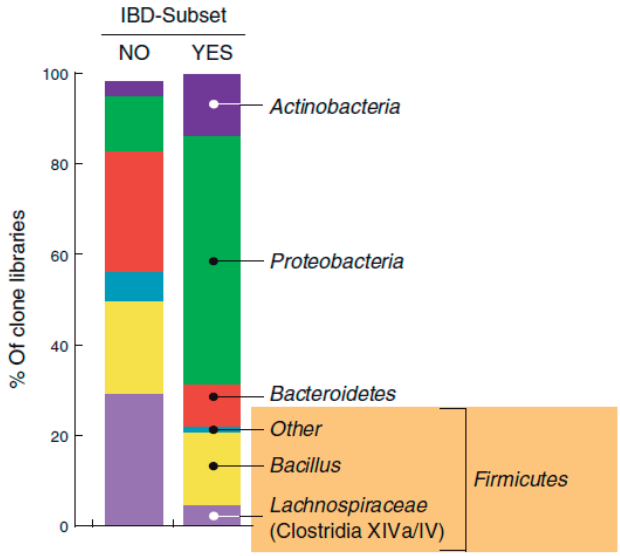

Figure 1.2. The intestinal microbiota in patients with inflammatory bowel disease (IBD) is characterized by a reduction of Firmicutes and Bacteroidetes and an expansion of Proteobacteria. Reproduced with permission from Frank et al. (2007)[13]. Adapted From Sartor and Mazmanian (2012)[12].

Several previous studies have investigated the use of traditional probiotics[14-19] or colonic anaerobes such as *Faecalibacterium prausnitzii* as a prevention or treatment for IBD[20-23]. Indeed, a protective effect of specific commensal bacteria or their components against colitis has been shown in different rodent models. For example, the human commensal *Faecalibacterium prausnitzii* (*F. prausnitzii*), which is reduced in CD patients, protects mice from 2,4,6-trinitrobenzene sulfonic acid (TNBS)-induced colitis (a Th1-driven model for human (IBD)[21, 22]. Another example is *Bacteroides fragilis* that protects mice from *Helicobacter hepaticus*-induced colitis[24]. *B. fragilis* also induces Il-10 secretion in $CD4^+$ T cells and prevents the expansion of inflammatory Th17 cells in mono-associated mice; these effects were reported to be mediated by bacterial polysaccharide A (PSA)[25]. Furthermore, colonization of young conventionally reared mice with a cocktail of 46 strains of commensal Clostridium spp. induced an accumulation of colonic regulatory T cells (cTregs) and reduced sensitivity to inflammatory disease in adult mice[26]. Taken together these findings suggest that not only the bacteria themselves but also specific factors (e.g. metabolites, molecules), play a role in the maintenance of homeostasis and can have beneficial effects. These studies support the concept of using microbial symbionts or their products for novel prophylactic or therapeutic applications in humans.

Next generation therapeutics based on microbial consortia

Previously available treatments for IBD consist of anti-inflammatory medication, such as anti-TNF-α [27] and anti-IL-17 (Ixekizumab)[28], however many IBD patients do not respond, or lose responsiveness to such anti-inflammatory medication[29]. Another known alternative for IBD treatment, which focusses on restoring the microbial balance in the gut, is faecal microbiota transplantation (FMT). FMT is the process of transplantation of faecal bacteria from a healthy individual into a diseased recipient. It has been proven to be a highly effective treatment for patients suffering from *Clostridium difficile* infection, even for the most desperate cases, after failure of multiple courses of antibiotics. The approach addresses the imbalance in the composition and altered activity of the microbiota and represents a new class of therapeutics. For example, Khoruts et al. showed how transplanting the microbial community from a healthy donor to a patient suffering from *Clostridium difficile*-associated disease (CDAD) significantly modified the bacterial composition in the patient [30]. After 2 weeks, the microbiota of the recipient had dramatically changed from a *Firmicutes*- and *Bacteroidetes*-deficient configuration to a community highly similar to that of the donor, dominated by *Bacteroides spp*. This radical shift in the composition of the microbiota was also accompanied by the disappearance of the symptoms associated with CDAD[30].

Several disease phenotypes induced by changes in host genetics cause dysbiosis of the intestinal microbiota, including IBD. Remarkably, these phenotypes can be transferred to germ-free wild-type hosts simply by inoculating them with the microbiota from the diseased donors[31-33]. These findings are raising interest in applying microbial consortia to treat non-*C. difficile* indications. For the past few years, some studies reported the efficacy of FMT treatment in various clinical trials focused on UC patients[34-37]. However, there are concerns about possible transfer of pathobionts and pathogens including viruses by use of faecal donors. Additionally, there are concerns involving the use of undefined faecal material and high donor variability related to the use of FMT in IBD treatment. A safer and more effective option than FMT might be the administration of specific bacteria, a well-defined microbial consortia and/or bacterial metabolites that have a beneficial effect in modulating the host immune response.

Modulation of the immune system by probiotic bacteria

There are numerous studies on immune modulation by traditional probiotics based on lactic acid bacteria and *Bifidobacteria*, which are too numerous to detail in this chapter but have been discussed in several reviews[14-19]. Much of this work has focused on cytokine profiling of PBMC and/or dendritic cells (DCs) stimulated with bacterial strains *in vitro* as well as *in vivo* testing of strains in mouse disease models[14-19]. Dendritic cells have been

of particular interest because they are antigen presenting cells and play a crucial role in maintaining tolerance at mucosal surfaces[38]. For example Foligne et al. (2007) suggested that the IL-10 to IL-12 cytokine ratio measured in human peripheral blood mononuclear cells (PBMCs) as a result of stimulation with lactic acid bacteria could be used to predict their protective capacity in mice colitis models[39].

Another mechanism by which *lactobacillus* probiotics can modulate the immune system is via the induction of regulatory T cells (Tregs). Currently the exploration of gut commensal bacteria in search of novel probiotic candidates, known as next-generation of probiotics, is increasing due to their potential beneficial effects in modulating the intestinal immune response of the host[40-42]. Colonic bacteria that can directly attenuate inflammatory responses in immune cells or enhance host mechanisms to regulate inflammation are of considerable interest as new treatments for the management of IBD[43]. Atarashi et al. (2013) reported that oral inoculation of 17 selected spore-forming *Clostridia* strains in germ-free mice lead to $CD4^+$ $FOXP3^+$ regulatory T (Treg) cell induction which plays an important role in maintaining both mucosal as well as systemic homeostasis. Oral administration of this strain mixture was shown to attenuate clinical symptoms of TNBS-induced colitis[44]. The Firmicutes phylum, includes species of butyrate-producing bacteria such as *Faecalibacterium prausnitzii*, which has shown potential as a novel treatment for IBD[21-23, 45]. In summary, probiotic bacteria have been reported to modulate the immune system by stimulating secretion of anti-inflammatory cytokines, and/or suppressing secretion of inflammatory cytokines or chemokines and inducing Tregs through DC and DC-independent mechanisms.

Innate immune activation by bacteria

Toll-like receptors (TLRs) and other pattern recognition receptors recognise different microbial components which not only leads to activation of the innate immune response, but also triggers the development of the antigen-specific response which is part of the adaptive immune system. Until now, 11 members of the TLR family have been identified in mammals, and each TLR can bind specific microbe-associated molecular patterns (MAMP). Activation of any of these TLRs induces an intracellular cascade resulting in NF-kB activation[46].

In our study we focussed on TLR2, since the majority of gut bacterial strains tested were known to be Gram-positive bacteria. TLR2 is a TLR family member which is able to recognize quite a wide range of molecular patterns including peptidoglycan and lipoteichoic acid, which make up the cell wall of Gram-positive bacteria[47, 48]. It has been suggested that TLR2 is the most 'promiscuous' among the TLR family members, referring to its peculiar capacity to form a heterodimer with TLRs 1 and 6 (forming TLR1/2 and TLR2/6), as well as its association with CD36 in response to diacylated lipoproteins. This enables TLR2 to recognize a wide range of

microbial-associated patterns[49]. When the TLR2 forms the TLR1/2 heterodimer, this TLR is able to recognize triacylated lipopeptides of mycoplasma or Gram-negative bacteria, whereas in the form of TLR2/6, it is able to recognize diacylated lipopeptides of mycoplasma and Gram-positive bacteria[50]. Stimulation of TLRs by their specific ligands leads to activation of NF-κB through the myeloid differentiation primary-response protein 88(MyD88)-and/or TIR-domain-containing adapter-inducing interferon-β (TRIF)-dependent pathway. The activation of NF-kB signalling pathway itself will lead to inflammatory cytokine production, one of the most important mechanisms in the innate immune response, which can subsequently trigger activation of the adaptive immune response[46, 51].

Cytokines and chemokines in IBD

Cytokines are known as the key regulators of inflammation and are therefore of paramount importance in IBD management[43]. Previous studies showed that oral administration of *Lactobacillus* and *Bifidobacterium* strains was able to positively affect both the mucosal and systemic immune response through immunomodulation of cytokine secretion[14, 16, 17]. Previous study by Foligne et al. (2007) proposed to measure the IL-10 to IL-12 cytokine ratio in human PBMC, which could be used to predict protective capacity of lactic acid bacteria in mice colitis models[39]. Other cytokines, such as Tumour Necrosis Factor alpha (TNF-α), which is known as an inflammation mediator is of key importance to balance the regulation of cytokine secretion in IBD. Indeed, anti-TNF has been commonly used as a therapeutic agent for IBD treatment[52]. Other than TNF-α, Singh et al (2016) reported an increased concentration of inflammatory cytokines IL-16, IFN-γ and IL-1β in the blood serum of IBD patients when compared to healthy donors[53]. IL-8 chemokine also known to play important role in modulating the inflammation in IBD. IL-8 is responsible to attract and activate neutrophils. IL-8 concentration is correlated with MPO concentration in colon and is also responsible for an increased CD11b expression and ROS production by neutrophils[54]. Additionally, oxidative stress is also considered to be an important criterium for the assessment of therapeutic candidates for IBD. Oxidative stress itself has been proposed as a mechanism underlying the pathophysiology of IBD[55-57]. Therefore, bacteria that cause excessive production of either nitric oxide (NO) or reactive oxygen species (ROS), might be excluded as potential anti-inflammatory candidates.

Short-chain fatty acids: a candidate microbiome-based metabolite treatment

The anaerobic fermentation of non-digestible dietary fibre by colonic microbiota produces short-chain fatty acids, the most abundant being acetate, butyrate and propionate. Depending

on the nature of fibres consumed, the concentration of SCFAs in the proximal colon ranges from 70 – 140 mM, and from 20 - 70 mM in the distal colon[58, 59]. Butyrate is mainly used by colonocytes as an energy source and scarce amounts are found in the portal vein[60]. Acetate and propionate are transported across the basolateral membrane of the colonocytes mediated by an unknown HCO_3^- exchanger, most likely monocarboxylate transporter (MCT) 4 or 5[61]. Transported SCFAs then reach the liver and blood circulation through the portal vein. Acetate concentrations in the plasma and serum are up to 250 µmol/L, whereas these are only 0.5 - 10 µmol/L for butyrate and propionate[59, 60]. The concentrations of acetate and propionate are anticipated to be much higher in the lamina propria, and the blood vessels leading up to the portal vein[62].

SCFAs are well-known to play an important role in maintaining barrier protection and regulating the inflammatory status in the gut[63]. In addition to local effects on the gastrointestinal mucosal immune function, SCFAs may reach remote organs and modulate immune responses. SCFAs are known to modulate several cellular process including gene expression, chemotaxis, differentiation and apoptosis. SCFAs may activate signalling pathways through activation of G protein-coupled receptors (GPCRs) for SCFAs. Additionally, butyrate and propionate can alter chromatin structure and gene expression through inhibition of histone deacetylases (HDACs), as well as affecting and stabilizing hypoxia-inducible factor (HIF)[64-67].

Several studies report anti-inflammatory activities of butyrate and studies in mice showed its crucial role in the induction of inducible regulatory T cells (Treg) in the colon[26, 68]. The SCFA receptor GPCR43, also known as free fatty acid receptor 2 (FFAR2), plays an important role in regulation of inflammation[69] and mice lacking this receptor exhibit more severe inflammatory responses in disease models[70]. Other SCFA receptors such as GPCR41 (FFAR3), GPCR109a (HCA2) and olfactory receptor-78 (Olfr-78) are known to mediate the effect of SCFAs on leukocyte and epithelial cells (IECs)[71, 72]. These findings support the concept of utilizing viable butyrate-producing bacteria like *F. prausnitzii* to maintain homeostasis and promote anti-inflammatory mechanisms in the host[22].

Besides the anti-inflammatory mechanisms of butyrate in the gut, it can also suppress proliferation of stem/progenitor cells by inhibiting HDAC and increase promotor activity for the negative cell-cycle regulator Foxo3[73]. Additionally, butyrate has been shown to induce apoptosis in colonic tumour cell lines[74]. Acetate, might be a better candidate as an anti-inflammatory compound because it is present in higher concentrations in the large intestine and blood compared to butyrate or propionate. Besides, acetate is reported to suppress pro-inflammatory interleukin (IL-8) production in intra-epithelial cells (IECs) of colonic mucosa[75]. Furthermore, administration of acetate effectively attenuated inflammation in mouse models of trinitrobenzenesulfonic acid (TNBS)-induced colitis and dinitrofluorobenzene-induced

dermatitis[76]. In another mouse model, Thornburn et al. (2015) showed that maternal acetate intake leads to protection against allergic airways disease (AAD) in the offspring[59].

Aim and outline of thesis

As IBD is characterized by a chronic inflammation in the gut, the overarching aim of this thesis was to try to find a novel colonic bacterial strains or bacterial metabolites that have an immunomodulatory (i.e. an anti-inflammatory) function and may therefore be used as a preventive therapy or treatment. To this end we tested 100 colonic anaerobic bacteria obtained from healthy subjects and investigated their immunomodulatory properties in various assays.

In **Chapter 2** we summarize the results of 68 different colonic anaerobic bacteria tested. Most importantly, we found that there is a large variation among the tested strains in their immunomodulatory properties. However, we could identify three different immune profiles, resulting from bacterial stimulation. The first 'immunostimulatory' profile was characterized by secretion of high levels of cytokines and NO and strong NF-κB signalling after TLR activation. The second 'immunomodulatory' profile was characterized by induction of only moderate amounts of cytokines and NO. The final 'immuno suppressive' or 'silent' profile was characterized by a low capacity to induce cytokine or NO secretion.

As several studies showed the importance of relative abundance of *F. prausnitzii* for a healthy gut we examined the immunomodulatory activity of 28 *F. prausnitzii* strains in more detail in **Chapter 3.** After thorough *in vitro* investigation we have to conclude that the immunomodulatory properties are really strain specific, as the properties of the strains tested (cytokine and NO secretion and NF-κB signaling via TLR activation) do not correlate with phylogenetic clustering. We again could distinguish the three different immune profiles as described in Chapter 2. Moreover, the general assumption that all *F. prausnitzii* strains induce strong IL-10 secretion was disproven, as there were some 'silent' strains that hardly induced any IL-10 secretion.

During the *in vitro* screening procedures, we observed that the culture supernatant of all strains tested had anti-inflammatory properties. Further investigations showed that the SCFAs in the bacterial growth medium elicited the same attenuation effect. We investigated this in more detail in **Chapter 4** where we compared the effects of acetate and butyrate on the function of immune cells. We found that butyrate, but not acetate, decreased cell viability when administered at higher concentrations. Interestingly, although both acetate and butyrate were able to attenuate heat inactivated bacteria (HIB) induced secretion of pro-inflammatory cytokines, only acetate was able to increase the anti-inflammatory cytokine

IL-10. To investigate how butyrate and acetate elicited their effects, we tried to determine the molecular mechanisms by examining G protein-coupled receptors (GPCR) and histone acetylation.

As we found clear effects of both acetate and butyrate on cytokine secretion by PBMC and monocyte derived dendritic cells we investigated whether other biological pathways would be affected. We therefore investigated the effect of SCFA on the transcription profile of stimulated $CD14^+$ monocytes in **Chapter 5**. SCFA also attenuated pro-inflammatory cytokine secretion in monocytes. Acetate did not cause major effects in the number of regulated genes, but butyrate significantly affected the regulation of many different (immune) pathways and genes. In **Chapter 6** where we investigated the effect of SCFA on modulation of the epithelial gut function. A transcriptomic analysis was performed on an *ex vivo* 3D ileum porcine organoid model exposed to acetate and butyrate. Butyrate proved to elicited greater changes in gene expression compared to acetate.

To conclude our studies, we tested examples of each of the three 'immune profiles' in an *in vivo* mouse DSS-induced colitis model in **Chapter 7**. Confirming our hypothesis that the bacterial strains which induced an 'silent' profile would be able to reduce the colonic inflammation, we indeed observed attenuation of the clinical symptoms after addition of these 'silent' strains.

In the last chapter, **Chapter 8**, we summarize the combined results from this thesis. We discuss the findings of this thesis with respect to other studies and how these findings could contribute to a better understanding of the immunomodulatory properties of colonic anaerobic bacterial strains and their metabolites, acetate and butyrate. Furthermore we provide suggestions on future studies which could shed more light on the mechanisms by which the immune modulation could be effectuated.

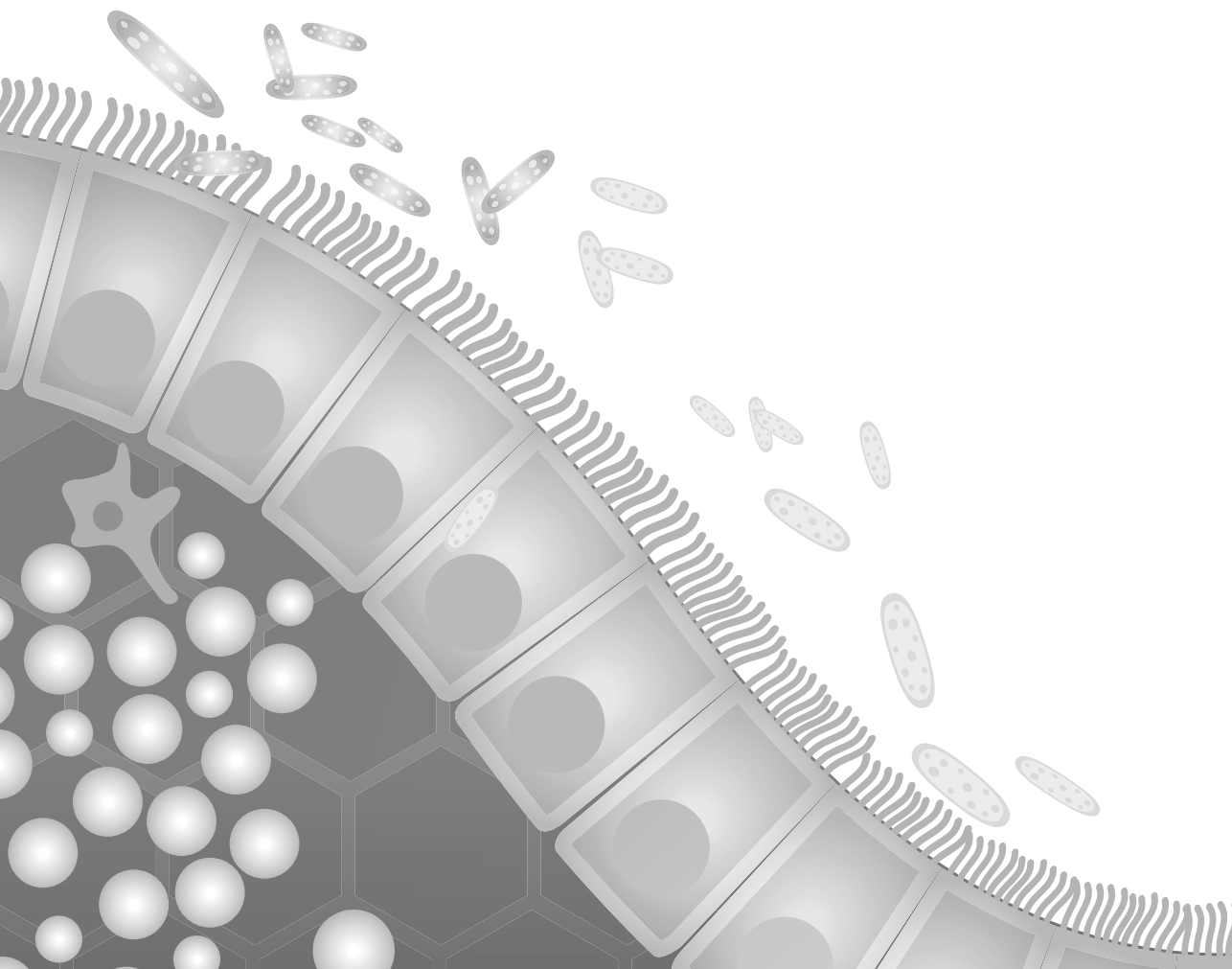

Chapter 2

Immunomodulatory properties of key anaerobic bacteria isolated from the human colon

Nuning Winaris[1,2], Ellen Kranenbarg[1], Eleni Tsompanidou[3,6], Hermi J.M. Harmsen[3], Paul O. Sheridan[4], Alan W. Walker[4], Sylvia H. Duncan[4], Gemma Henderson[5], Jerry M. Wells[1]

[1] Host-Microbe Interactomics Group, Department of Animal Science, Wageningen University & Research, Wageningen, Netherlands

[2] Master Program in Biomedical Sciences, Faculty of Medicine, Universitas Brawijaya, Malang, Indonesia

[3] Department of Medical Microbiology, University of Groningen, University Medical Center Groningen, Groningen, Netherland

[4] Gut Health Group, Rowett Institute, University of Aberdeen, Foresterhill, Aberdeen, Scotland, UK

[5] Human Health Innovation, Chr. Hansen, Hørsholm, Denmark

[6] Winclove Probiotics, Amsterdam, Netherland

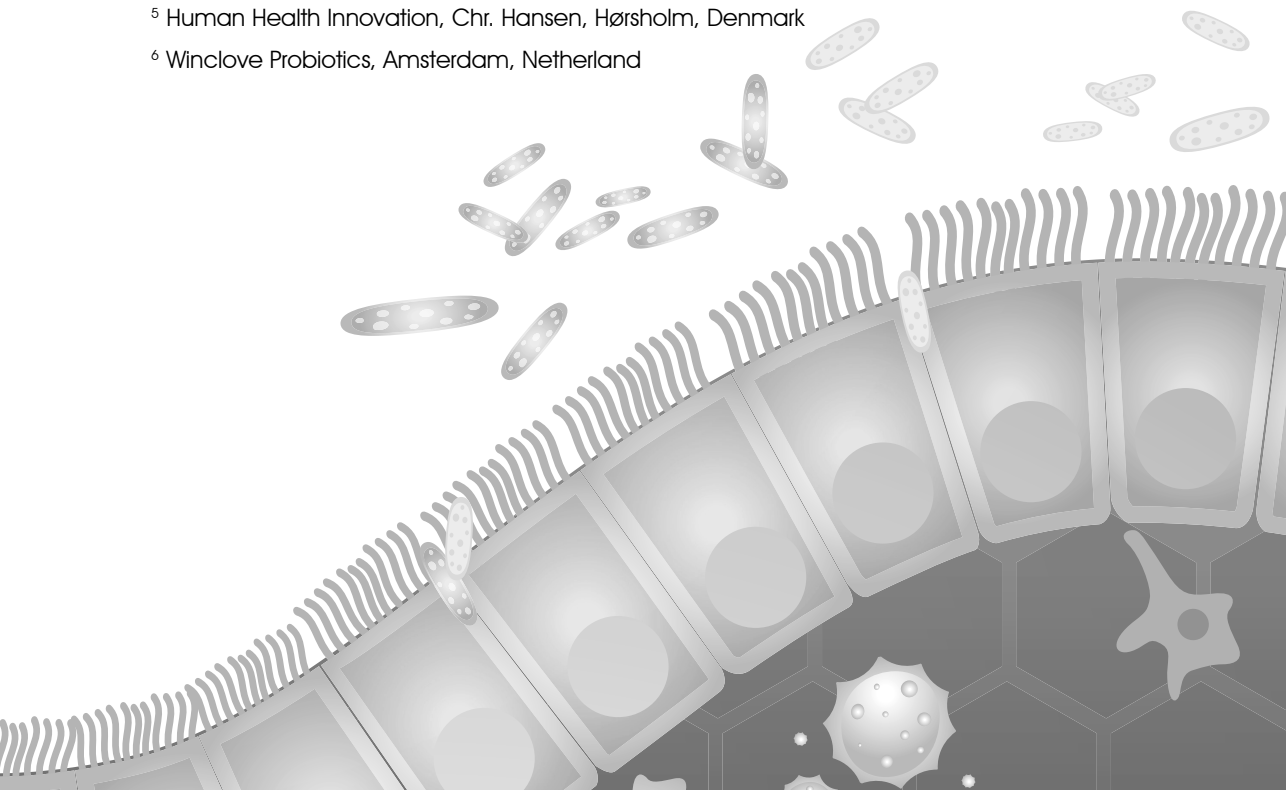

Abstract

The colonic microbiome has been recognized as a potential source of next-generation of probiotics to prevent and treat human disease, including inflammatory bowel disease (IBD). The aim of this study was to evaluate the anti-inflammatory potential of a large strain collection of human colonic anaerobic bacteria isolated from healthy human donors. We used human peripheral blood mononuclear cells (PBMCs) from different donors as a model for evaluating the immunomodulatory effects of the strains and measured the balance between pro-and anti-inflammatory cytokine secretion. Additionally, we devised an assay to test the potential of the strains to modulate cytokine responses by co-stimulation with heat-inactivated bacteria (HIB). We also assessed the capacity of bacterial strains to induce nuclear factor-kappaB (NF-κB) signalling via specific Toll-like receptors (TLRs) reporter cell assays. Moreover, murine macrophage RAW 264.7 cells were used to assess nitric oxide release caused by stimulation with these colonic bacteria. We found that the immune profile of colonic anaerobic bacteria is mostly strain specific and there appear to be no general trends associated with a specific species, although some species may show similar immune profiles. The bacterial strains could be categorised into one of three main immune profiles, namely immunostimulatory, immunomodulatory and immunosuppressive or 'silent' profiles. This research identified new immune phenotypes/profiles of gut bacteria that warrant further study *in vivo*.

Keywords: Next-generation probiotic, colonic anaerobic bacteria, immunomodulation.

INTRODUCTION

The gut microbiota is a complex ecosystem containing symbionts, commensals and sometimes opportunist pathogens, which is influenced both by the diet and human immune system[77]. In the 1990s, the research on gut microbiota was mainly focused on pathogen associated bacteria and how they caused intestinal diseases. However, for the past decade microbiota research has focused on understanding the consequences of the dramatic changes in the microbiota diversity and composition (aka dysbiosis) that occur in different disease states as well as the mechanisms contributing to intestinal homeostasis and health[77, 78].This has led to the concept that culturing and characterisation of abundant and well conserved species of colonic microbiota may lead to the generation of new probiotics to prevent and treat diseases.

Previous studies, focused mainly on species of *Lactobacillus* and *Bifidobacterium,* showed that oral administration of gut bacteria can modulate systemic and mucosal immunity in the host[14-19]. Extracellular polysaccharides (EPS) produced by these *Lactobacillus* and *Bifidobacterium* species were shown to be protective against pathogen invasion in a murine *Citrobacter rodentium* infection model and to attenuate pro-inflammatory cytokine production *in vitro*[79-81]. *Lactobacillus plantarum* was also reported to produce an immunomodulatory serine-threonine rich peptide (STp), which mediates anti-inflammatory effects through modulation of intestinal dendritic cells (DC) function[82, 83].

Strict anaerobes inhabiting the large intestine have been much less studied than the lactic acid bacteria due to difficulties in isolation and growth *in vitro*. Presently, the exploration of gut commensal bacteria in search of novel probiotic candidates, known as next-generation probiotics, is increasing due to their potential beneficial effects in modulating the intestinal immune response of the host[40-42]. Colonic bacteria that can directly attenuate inflammatory responses in immune cells or enhance host mechanisms to regulate inflammation are of considerable interest as new treatments for the management of inflammatory bowel disease (IBD)[43]. Atarashi et al. (2013) reported that oral inoculation of 17 selected Clostridia strains in germ-free mice lead to $CD4^+$ $FOXP3^+$ regulatory T (Treg) cell induction, which plays an important role in maintaining mucosal and systemic homeostasis. This mixture also proved to attenuate clinical symptoms of TNBS-induced colitis[44]. The *Firmicutes* phylum, including species of butyrate-producing bacteria such as *Faecalibacterium prausnitzii*, has shown potential as a novel treatment in IBD[21-23, 45, 84].

There are a limited number of studies investigating screening approaches to identify candidate probiotics to treat inflammatory diseases. Foligne et al. (2007) found a strong correlation between anti -and pro-inflammatory cytokines (IL-10/IL-12 ratio) induced by lactic acid bacteria *in vitro* and their protective capacity in a mouse colitis model[39]. However, there

remains a need for other assays with a conclusive predictive outcome for the selection of immunomodulatory strains to be tested *in vivo.*

The aim of this study was to evaluate the anti-inflammatory potential of a large collection of human colonic anaerobic bacteria, which had been previously cultured from healthy human donors at the Rowett Institute, at the University of Aberdeen in Scotland and the Department of Medical Microbiology, at the University Medical Centre Groningen, the Netherlands. As a model for immune response, we used human peripheral blood mononuclear cells (PBMCs) and measured the balance between pro-and anti-inflammatory cytokine secretion after stimulation with the different strains. Additionally, we devised an assay to test the potential of the strains to modulate cytokine responses by co-stimulation with heat-inactivated bacteria (HIB). We also assessed the capacity of bacterial strains to induce nuclear factor-kappaB (NF-κB) signalling via specific Toll-like receptors (TLRs), using reporter cell assays. Moreover, as oxidative stress has been proposed as a mechanism underlying the pathophysiology of IBD[85], murine macrophage RAW 264.7 cells were used to assess nitric oxide release caused by stimulation with these colonic bacteria.

MATERIALS AND METHODS

Bacterial culture and harvesting

Various isolates of colonic anaerobic bacteria were grown in YCFAGSC, a modified YCFA (yeast, casitone, fatty acids) medium supplemented with additional carbon sources (glucose, soluble starch and cellobiose). The bacterial cultures were grown at 37°C inside an anaerobic chamber (Bactron 3000) containing 90% nitrogen (N_2), 5% hydrogen (H_2) and 5% carbon dioxide (CO_2). The optical density of bacterial cultures was measured at 600 nm using a Spectramax M5 microplate reader (Molecular Devices) and bacteria harvested from 2 ml of culture by centrifugation at 4000 rpm for 10 minutes at RT. The supernatant was filtered through a 0.22 µm MF-Millipore Membrane (Sigma-Aldrich) to remove bacteria and stored at -80°C. Bacterial pellets were resuspended in Roswell Park Memorial Institute (RPMI) 1640 Medium (Thermo Fisher Scientific) containing 15% glycerol and stored at -80°C. Prior to the experiment, the bacterial pellet and supernatant were thawed and diluted to OD 0.1 (600 nm) (equivalent to about 5 x 10^7 bacteria).

Isolation and stimulation of human peripheral blood mononuclear cells (PBMC)

Human peripheral blood mononuclear cells (PBMC) were isolated from blood using Ficoll density centrifugation. The blood was diluted 1:1 with Roswell Park Memorial Institute (RPMI) 1640 Medium (Thermo Fisher Scientific). PBMCs were isolated by density gradient centrifugation on Ficoll-Plaque PLUS (GE healthcare). The diluted plasma was removed and the layer of white blood cells was recovered and washed four times with RPMI. Purified

PBMCs were seeded in 96 well plate (2 x 10^5 cells/well) and rested for one hour in RPMI supplemented with 10% FBS (Invitrogen) and 100 U/ml penicillin/100 µg streptomycin (Sigma-Aldrich) at an atmosphere of 5% CO_2 - 95% O_2 at 37ºC. Subsequently, PBMCs were used for profiling secreted cytokine production in response to the stimulation of various anaerobic bacteria strains. PBMC were stimulated with a ratio of 1:2 cell to bacteria. In some assays heat-inactivated bacteria (HIB), were added as an additional stimulus with a cell to bacteria ratio of 1:20. Then PBMC were incubated for 24 hours at 37ºC in an atmosphere of 5% CO_2, 95% O_2. After incubation, supernatants of PBMC cultures and the cells were harvested for cytokine and viability measurements respectively.

Annexin V/Propidium iodide (PI) viability staining

Annexin V/Propidium Iodide (PI) staining (BD Biosciences) was used to distinguish viable from early and late apoptotic or necrotic cells according to manufacturer's protocol. The cells were analysed using CytoFlex™ Flow Cytometry (Beckman Coulter).

Cytokine measurements

Cytokines were measure using the the Bioplex Pro™ Assay according to manufacturers' recommended protocol. Briefly, magnetically coupled beads (containing the detection antibody) for the different cytokines were premixed in assay buffer and added to flat bottom 96 well plates and washed twice using a magnetic handheld washer. Next, 25 µl of defrosted culture supernatant was mixed with 25 µl of sample buffer, or 50 µl of cytokine standard and incubated with gentle shaking at room temperature for 30 minutes. After incubation, the plate was washed three times and 25 µl of premixed detection antibodies were added and incubated for 30 minutes, with gentle shaking. After incubation, the plate was washed three times and 50 µl of streptavidin-PE was added and incubated at room temperature for 10 minutes, with gentle shaking. After three final washes, the beads were taken up in 75 µl of drive fluid, briefly shaken (700 rpm) and analysed. Samples and standards were measured in the MagPix reader, and analysed using the MAGPIX xPONENT software, Bio-Plex Manager version 5.0. Five cytokines were measured: interleukin 1 beta (IL-1β), interleukin-10 (IL-10), interleukin-12p70 (IL-12p70), interferon gamma (IFN-γ), and tumour necrosis factor alpha (TNF-α).

TLR reporter assay

Human embryonic kidney (HEK293) (Invivogen) were transformed with different human Toll-like receptors (TLR1/2, TLR2 and 2/6) and a NF-κB luciferase reporter construct (Invivogen). These cells were seeded at 6×10^4 cells per well into black, clear bottom 96-well plates in DMEM medium (Invitrogen), supplemented with 100 U/ml penicillin and 100 µg/ml streptomycin (Sigma-Aldrich) and 10% FBS (Invitrogen) and incubated overnight at an atmosphere of 5% CO2 - 95%, O2 at 37ºC. Cells were subsequently incubated for at least 3 hours with different bacterial pellets or TLR agonists as controls (20 ng/ml Pam2PCSK for TLR2 and 2/6; 200 ng/

ml Pam3PCSK for TLR1/2; Invivogen). Medium alone was used as a negative control. After the incubation period half of the medium was aspirated and replaced with Bright glow (Promega), subsequently the plate was vortexed for 5 minutes and the luminescence was measured using a Spectramax M5 microplate reader (Molecular Devices) at 750 ms integration time. Human embryonic kidney HEK293 cells not expressing TLR receptors but harbouring the pNiFty, NF-κB luciferase reporter construct (Invivogen), were used as negative controls in the TLR reporter assays.

Macrophage stimulation

The macrophage cell line RAW 264.7 (ATCC TIB-71) was maintained in Dulbecco's Modified Eagle Medium (DMEM) containing GlutaMAX (Thermo Fisher Scientific) with addition of 100 U/ml penicillin and 100 µg/ml streptomycin (Sigma-Aldrich). Cells (1.5×10^5) were seeded in 96-well culture plates in 200 µl of culture medium without phenol red. Immediately, the different bacterial pellets or immunostimulant lipopolysaccharide (LPS; 1µg/ml) were added to the cells and then incubated for 24 hours at 37°C in 5% CO_2. After incubation, 75 µl of supernatant was harvested and transferred to a new plate for measurement of nitric oxide (NO) using the Griess assay. The viability of the remaining cells was measured using Cell Proliferation Reagent WST-1(Sigma-Aldrich) according to manufacturer's protocol.

Nitrite (Griess) assay

NO produced by activated macrophages was converted to nitrite and measured using the Griess assay. An aliquot of 75 µl culture supernatant from each well was transferred to a new flat-bottomed 96-well plate and combined with 100 µl of 1% sulphanilamide and 100 µl of 0.1% naphthylenediamine (both were prepared in 2.5% phosphoric acid solution). After 5 minutes incubation at room temperature, the nitrite concentration was determined by measuring optical density (OD 540, reference filter 690 nm) using a Spectramax M5 microplate reader (Molecular Devices). Sodium nitrite (Sigma-Aldrich) was used as a standard to calculate NO concentrations in the cell-free medium.

RESULTS

Bacterial pellets and supernatants harvested from the anaerobically grown cultures were tested in various immune assays to evaluate their immunomodulatory properties (**Table 2.1**). Initial results showed that the unconditioned culture medium had an immunomodulatory effect which we hypothesized might be due to presence of short chain fatty acids (SCFA). As SCFA are produced in different amounts by the strains we decided not to test the culture supernatants. The immunomodulatory effects of SCFAs will be further discussed in other chapters of this thesis (**Chapter 3**, **4** and **5**).

Table 2.1. List of colonic bacteria isolated from healthy donors

No.	PHYLUM	SPECIES	ISOLATE ID
1	Firmicutes	*Anaerobutyricum soehngenii* sp. nov.[86]	L2-7
2	Firmicutes	*Anaerobutyricum* sp. nov.[86]	VPI B4-27 (DSM 3353)
3	Firmicutes	*Anaerostipes caccae*	L1-92
4	Firmicutes	*Anaerostipes hadrus*	HTF-920 (F. prau 10)
5	Firmicutes	*Anaerostipes hadrus*	HTF-146
6	Firmicutes	*Anaerostipes hadrus*	HTF-370
7	Firmicutes	*Anaerostipes hadrus*	HTF-412
8	Firmicutes	*Anaerostipes hadrus*	SS2/1
9	Firmicutes	*Anaerostipes hadrus*	HTF-463
10	Firmicutes	*Anaerostipes hadrus*	HTF-774
11	Firmicutes	*Anaerostipes hadrus*	SSC/2
12	Firmicutes	*Anaerostipes hadrus*	HTF-783
13	Bacteroidetes	*Bacteroides dorei*	HTF-641
14	Bacteroidetes	*Bacteroides fragilis*	HTF-786
15	Bacteroidetes	*Bacteroides thetaiotaomicron*	HTF-488
16	Bacteroidetes	*Bacteroides uniformis*	HTF-203
17	Actinobacteria	*Bifidobacterium adolescentis*	L2-32
18	Firmicutes	*Blautia luti*	SR1/5
19	Firmicutes	*Blautia obeum*	A2-162
20	Firmicutes	*Blautia wexlerae*	HTF-A34
21	Firmicutes	*Butyricicoccus-like*	HTF-141
22	Firmicutes	*Butyrivibrio fibrisolvens*	16/4.
23	Firmicutes	*Butyrivibrio* spp.	HTF-01D grB
24	Firmicutes	*Clostridiales* sp.	GM2/1
25	Firmicutes	*Clostridiales* sp.	SS3/4
26	Firmicutes	*Clostridium scindens*	HTF-602
27	Firmicutes	*Coprococcus catus*	GD/7
28	Firmicutes	*Coprococcus comes*	HTF-92A
29	Firmicutes	*Coprococcus comes*	HTF-515
30	Firmicutes	*Coprococcus eutactus*	ART55/1
31	Firmicutes	*Coprococcus eutactus*	L2-50
32	Firmicutes	*Dorea longicatena*	HTF-113
33	Firmicutes	*Dorea longicatena*	HTF-28
34	Firmicutes	*Eubacterium hallii*	HTF-05 A

Continue

Table 2.1. List of colonic bacteria isolated from healthy donors

No.	PHYLUM	SPECIES	ISOLATE ID
35	Firmicutes	*Eubacterium hallii*	HTF-83 D
36	Firmicutes	*Eubacterium hallii*	SL6/1/1
37	Firmicutes	*Eubacterium hallii*	SM6/1
38	Firmicutes	*Eubacterium hallii*	HTF-385
39	Firmicutes	*Eubacterium rectale*	A1-86
40	Firmicutes	*[Eubacterium] rectale*	HTF-171
41	Firmicutes	*[Eubacterium] rectale*	HTF-777
42	Firmicutes	*Eubacterium siraeum*	70/3
43	Firmicutes	*Flavonifractor plautii*	HTF-137
44	Firmicutes	*Flavonifractor plautii*	HTF-589
45	Firmicutes	*Flavonifractor plautii*	HTF-630
46	Firmicutes	*Hungatella hathewayi*	CB (L) FAA B
47	Firmicutes	*Intestinibacter bartlettii*	80/4
48	Firmicutes	*Intestinibacter bartlettii*	80/6
49	Firmicutes	*Intestinibacter bartlettii*	HTF-135 (F. prau 4)
50	Firmicutes	*Intestinibacter bartlettii*	HTF-136 (F. prau 8)
51	Firmicutes	*Lachnospira pectinoshiza*	HTF-314
52	Firmicutes	*Lachnospiraceae* gen. nov. sp. nov	HTF-03
53	Firmicutes	*Lachnospiraceae* sp. nov.	M62/1
54	Firmicutes	*Mitsuokella multiacidus*	HTF-51A gr G
55	Bacteroidetes	*Prevotella copri*	HTF-504
56	Bacteroidetes	*Prevotella copri*	HTF-155
57	Firmicutes	*Roseburia faecis*	HTF-01A gr F
58	Firmicutes	*Roseburia faecis*	HTF-78
59	Firmicutes	*Roseburia faecis*	M6/1
60	Firmicutes	*Roseburia faecis*	M72/1
61	Firmicutes	*Roseburia faecis*	M88/1
62	Firmicutes	*Roseburia hominis*	A2-183
63	Firmicutes	*Roseburia intestinalis*	L1-82
64	Firmicutes	*Roseburia inulinivorans*	A2-194
65	Firmicutes	*Ruminococcus bicirculans*	80/3
66	Firmicutes	*Ruminococcus bromii*	ATCC 27255
67	Firmicutes	*Ruminococcus bromii*	L2-63
68	Firmicutes	*[Ruminococcus] torques*	L2-14

None of the 68 strains belonging to the Firmicutes, Bacteriodetes and Actinobacteria phyla caused cell death when incubated with PBMC. The percentage of viable PBMC was about 70 – 90% after 24 hours of stimulation with either bacterial pellet or bacterial supernatant, which was not significantly different to the unstimulated cells (data not shown). In contrast, bacterial supernatants of some *E. hallii* and *F. plautii* strains significantly reduced viability of PBMCs compared to the control (**Figure 2.1**). As it is known that SCFA production can lower the pH of the medium, we tested cell viability at different pH. The pH of the *E. hallii and F. plautii* supernatants was higher than that which reduces viability (data not shown) suggesting other bacterial metabolites or molecules are detrimental to the cells.

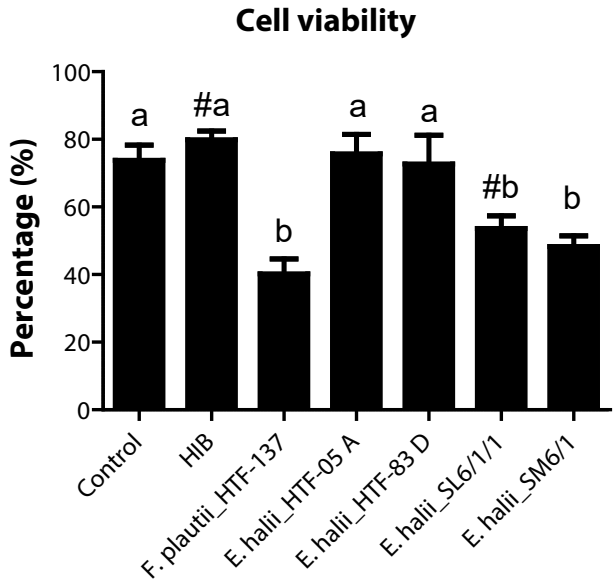

Figure 2.1. Percentage of viable PBMC after stimulation *with E. hallii* and *F. plautii* supernatants for 24 hours. Error bars represent SEM, n= 3 donors. Significant differences among the groups were analysed using non parametric test one-way ANOVA followed by a Tukey post-hoc analysis (*p<0.05, **p<0.01, ***p<0.001). Letters above bars represent statistically significant differences between the groups.

The profile of cytokines secreted by PBMCs stimulated with different bacterial strains was highly strain dependent and not characteristic of a specific species. For example, *A. hadrus* strain HTF-920 (F. prau 10) induced relatively high amounts of IL-10 in PBMCs (162% relative to our positive control HIB) but *A. hadrus* strain SSC/2 induced a relatively low amount of IL-10 secretion (38% relative to HIB). Other strains of this species induced IL-10 secretion in the range 79 - 127 % of the HIB control. Similarly, the amounts of IL-10 induced by the *E. halli* strains ranged between 0.5 - 51% of HIB control. *C. scindens* strain HTF-602 induced the highest concentration of IL-10 (525% relative to HIB), which was equivalent to 12000 pg/

ml and *Anaerobutyricum* sp. nov. strain VPI B4-27 (DSM 3353) the lowest amount of IL-10 secretion (0.5% compared relative to HIB) which was equal to 20 pg/ml (**Figure 2.2A**).

Like IL-10, the amount of IL-12 and TNF-α induced in our PBMC assay was also strain specific. The concentration of IL-12 in the PBMC culture supernatant ranged from 0.11 to 362% relative to the HIB control (0.6 - 4842 pg/ml). The strain which induced the largest amount of IL-12 was *Clostridiales sp.* strain GM2/1, and the strain *B. wexlerae* HTF-A34 induced the lowest amount of IL-12 (**Figure 2.2B**). *B. obeum* strain A2-162 elevated the concentration of TNF-α 8-fold compared relative to HIB, which was equal to 230000 pg/ml. Whereas, *R. bicirculans* strain 80/3 induced the lowest amount of TNF-α secretion of all 68 strains (0.4% of HIB control (262 pg/ml) (**Figure 2.2C**). The amounts of the pro-inflammatory cytokines IL-1β and IFN-γ secreted by PBMCs stimulated with the 68 different bacterial pellets were also measured (**Supplementary figure S2.1**).

The ratio of IL-10 to IL-12 induced by each strain (**Figure 2.3A**) was used to predict the anti-inflammatory capacity of the strain as previously described by Foligne et al. (2007)[39]. *R. faecis* strain M72/1 had the highest IL-10/IL-12 ratio among the 68 tested strains. This strain induced moderate amounts of IL-10 (112%) but very low amounts of IL-12 (0.3%) secretion relative to HIB. *Clostridiales sp.* strain GM2/1 which induced the highest amount of IL-12 secretion, had the lowest IL-10/IL-12 ratio as it induced only a moderate amount of IL-10 (56%). Additionally, the IL-10/TNF-α ratio was examined to make a better prediction of the anti-inflammatory properties of the strains. The ranking of strains according to the IL-10/TNF-α ratio (**Figure 2.3B**) was different to that of the IL-10/IL-12 ratio. *C. comes* strain HTF-515 ranked highest in the IL-10/TNF-α ratio, whereas *A. hadrus* strain HTF-146 had the lowest IL-10 /TNF-α ratio.

Furthermore, to investigate whether the different strains might attenuate an inflammatory response to a bacterial infection, we studied the capacity of the strains to modulate cytokine secretion induced by a bacterial stimulus. Heat-inactivated bacteria (HIB) are known to significantly increase the secretion of both pro- and anti-inflammatory cytokines in PBMCs. In general, the addition of HIB together with the strain hardly altered the cytokine rank order (**Figure 2.4**). We observed that *C. scindens* strain HTF-602, which was previously found to be the strongest inducer of IL-10 (**Figure 2.2A**), was still among the strongest inducers and further increased the IL-10 secretion induced by HIB up to 759% (18143 pg/ml). *I. bartlettii* strain HTF-135 (F. prau 4), one of the strains that induced the lowest amount of IL-10 secretion (**Figure 2.2A**), still induced very low amounts of IL-10 when combined with HIB. Compared to stimulation with HIB alone, this strain attenuated HIB induced IL-10 secretion to 29% (274 pg/ml) (**Figure 2.4A**). The pro-inflammatory cytokines IL-12 and TNF- α were generally increased when the strains were combined with HIB. Concentrations of IL-12 as a result of strain stimulation in combination with HIB ranged between 7 to 266% (101- 3957

pg/ml) relative to HIB stimulation alone. The strongest inducer of IL-12 secretion was *B. luti* strain SR1/5, while *R. faecis* strain M88/1 induced the lowest amount of IL-12 secretion (**Figure 2.4B**). For TNF-α, the concentration measured after stimulation with the strains in combination with HIB ranged between (26 to 1453% (8540 - 855600 pg/ml). *Clostridiales sp.* strain GM2/1 induced the highest level of TNF-α secretion induced whereas *B. fibrisolvens* strain 16/4 showed the lowest induction of TNF-α secretion. Additionally, *B. fibrisolvens* strain 16/4 attenuated the HIB induced TNF-α secretion to about 25% of that induced by HIB alone (**Figure 2.4C**).

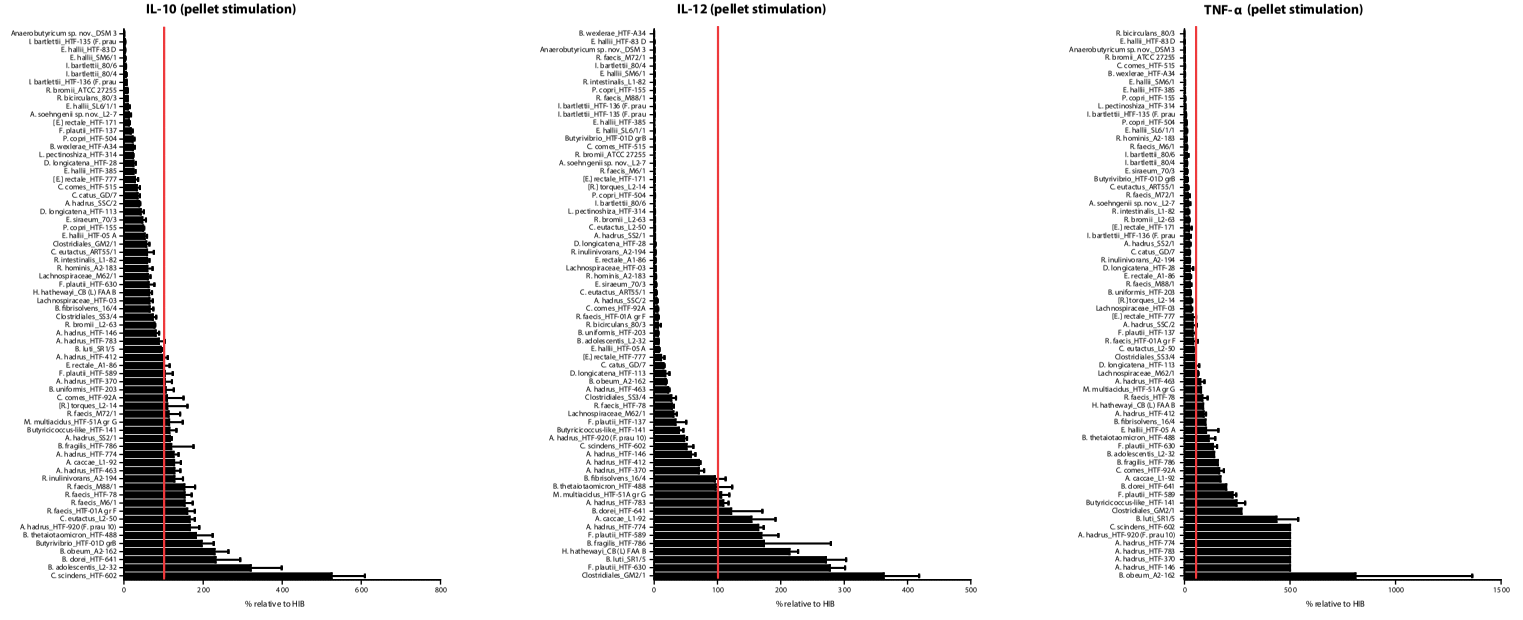

Figure 2.2(A-C). Percentages of **(A)** IL-10, **(B)** IL-12 and **(C)** TNF-α secretion measured in PBMC cultures after 24h incubation with different strains of colonic anaerobic bacteria. Concentrations of IL-10, IL-12 and TNF-α are shown relative to positive control HIB (%). Error bars represent SEM, n = 3 donors. Red line indicates the amount of secreted cytokine induced by the positive control (100%).

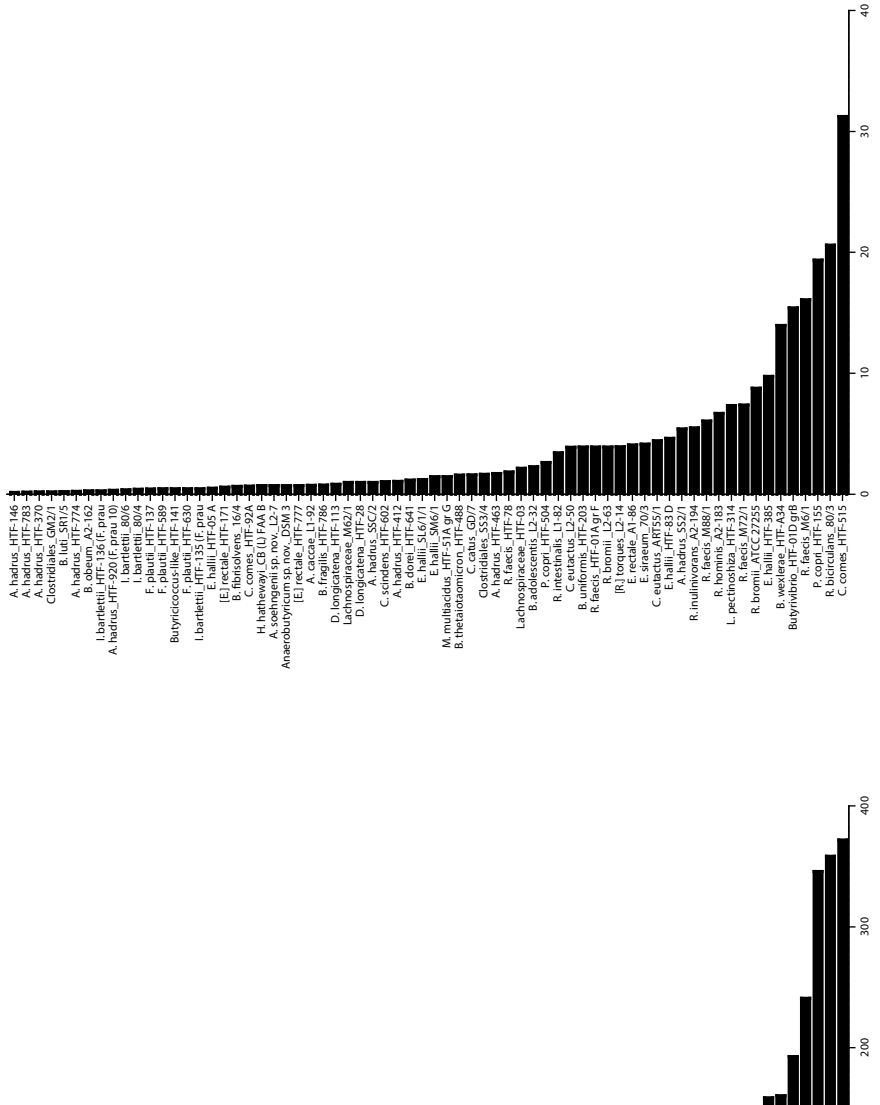

Figure 2.3(A-B). Ratio of IL-10 to IL-12 **(A)** and IL-10 to TNF-α **(B)** secretions in PBMC assays. Secretion of these cytokines compared relative to HIB (100%). n = 3.

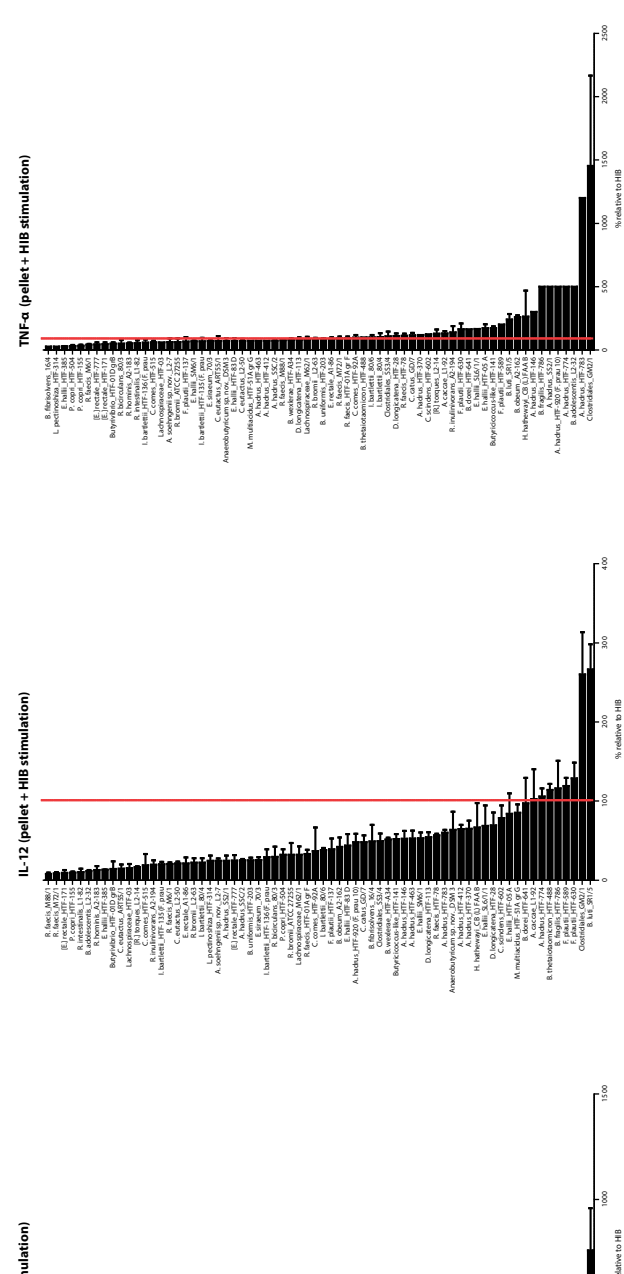

Figure 2.4(A-C). Percentages of **(A)** IL-10, **(B)** IL-12 and **(C)** TNF-α secretion measured in PBMC cultures after 24h incubation with HIB and different strains of colonic anaerobic bacteria simultaneously. Concentrations of IL-10, IL-12 and TNF-α are shown relative to positive control HIB (%). Error bars represent SEM, n = 3 donors. Red line indicates the amount of secreted cytokine induced by the positive control (100%).

To investigate the capacity of colonic anaerobic bacteria to activate the NF-κB signalling pathway via different TLR receptors, a TLR reporter assay was used. The results showed that as with cytokine secretion, also TLR activation was strain specific rather than species specific. The majority of tested strains were able to activate NF-κB signalling pathway via TLR1/2, TLR 2 and TLR2/6, to different extents (**Figure 2.5**). There was no positive correlation between capacity of a strain to active TLR signalling and the amounts of different cytokines secreted in PBMC stimulation assays. For example, strains strongly activating NF-κB signalling such as *E. hallii* HTF-05A and HTF-385, did not induce the largest amount of cytokine secretion in PBMCs. Conversely, some of the strains which had a low capacity to activate NF-κB signalling pathway via TLR receptors, such as *D. longicatena* strain HTF-28 and *F. plautii* strain HTF-137 (**Figure 2.5**), induced significant amounts of cytokine secretion (**Figure 2.2**). Likewise, *E. hallii* strain HTF-83 D, which was one of the strongest NF-κB activators (**Figure 2.5**), induced only low amounts of cytokines (**Figure 2.2**). Additionally, there were some strains that showed a 'silent' profile in terms of cytokine secretion as well as NF-κB activation in TLR assays. For example, *I. bartlettii* strain HTF-135 (F. prau 4) was among the weakest inducers of cytokine secretion (**Figure 2.2**) and NF-κB activation (**Figure 2.5**). Interestingly, *D. longicatena* strain HTF-28 and *I. bartlettii* strain HTF-135 (F. prau 4), which both showed a low capacity to activate NF-κB via TLR signalling, aggregated when grown in culture, most likely as a result of extracellular polymeric substances (EPS) production (**Figure 2.6**).

Furthermore, the strains were tested in HEK239 cells that expressed TLR4 (natural ligand LPS) and TLR5 (natural ligand flagellin). Among the 68 tested strains, only one showed NF-κB activation via TLR4. This strain was identified as *M. multiacidus* strain HTF-51A gr G, which is indeed known as a Gram-negative bacterium. In addition, *R. faecis* strain M72/1, *R. inulinivorans* strain A2-194 and *R. faecis* strain M6/1 highly activated NF-κB signalling pathway via TLR5, suggesting these strains harbour flagella (**Supplementary Figure S2.2**).

Lastly, to assess oxidative stress caused by stimulation with the colonic bacterial strains, nitric oxide (NO) secreted from murine macrophage RAW 264.7 cells was measured (**Figure 2.7**). Similar to cytokine secretion and TLRs findings, the NO secretion level was also found to be strain specific. The highest NO secretion was induced by *P. copri* strain HTF-155, inducing almost the same level (97%) of NO secretion as LPS (100%). The lowest levels of NO secretion were measured after stimulation with *I. bartlettii* strain 80/6 (2%), which also induced low amounts of cytokine secretion (**Figure 2.2**) and weakly induced NF-κB activation via the different TLR reporter assays (**Figure 2.5**).

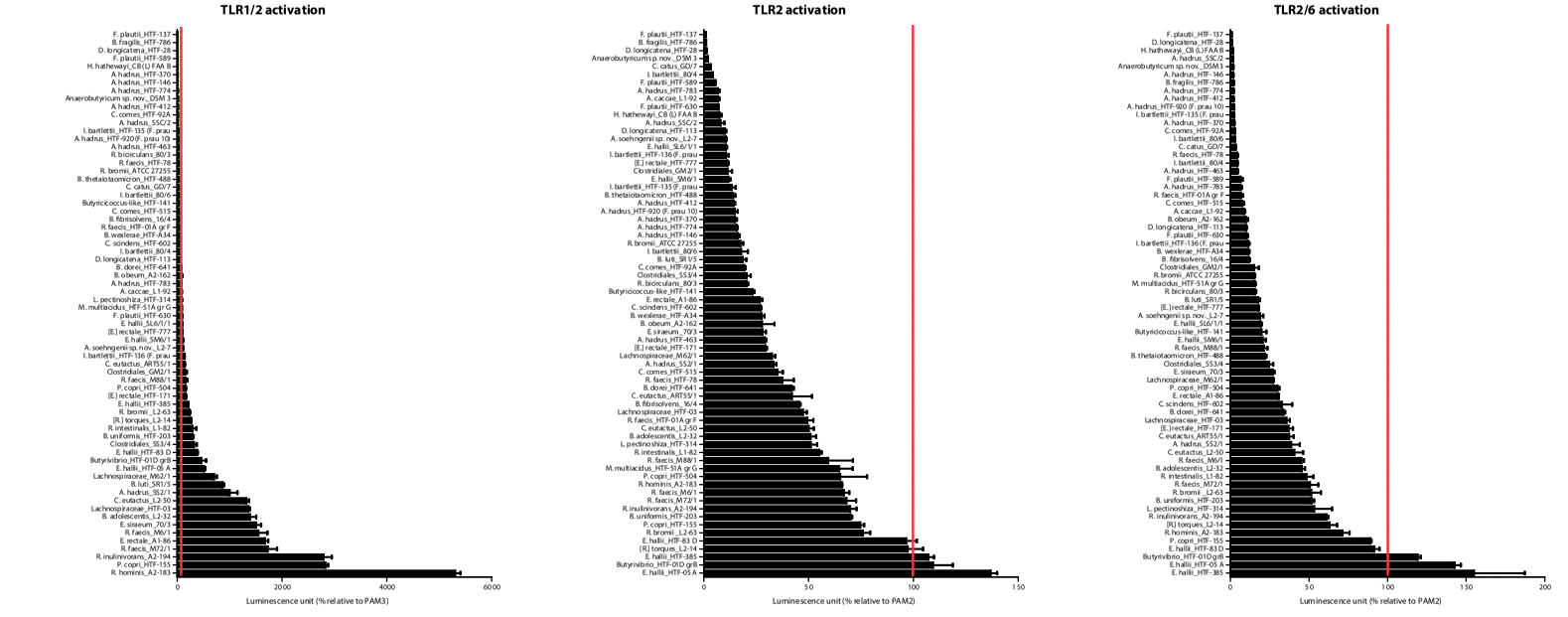

Figure 2.5(A-C). Percentages of **(A)** TLR 1/2 **(B)** TLR 2 and **(C)** TLR 2-6 activation level measured in TLR receptor cell lines after stimulation with different strains of colonic anaerobic bacteria. Activation levels of TLR 1/2, TLR 2 and TLR 2/6 are depicted relative to their respective ligands (%). Error bars represent SEM, n = 3. Red line indicates the activation level induced by the ligands (100%).

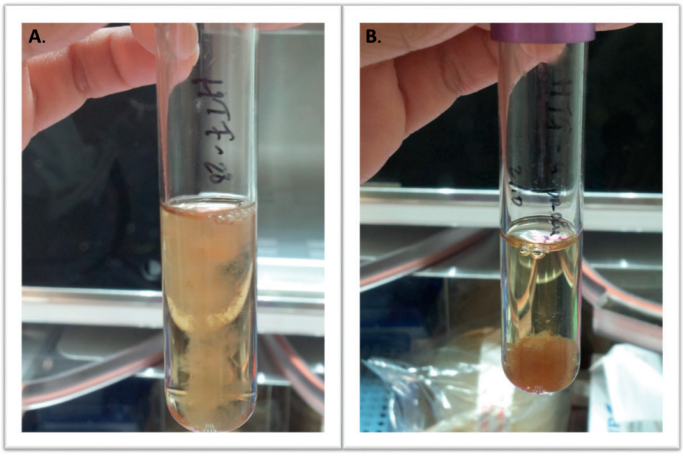

Figure 2.6(A-B). Bacterial culture of **(A)** *D. longicatena* strain HTF-28 **(B)** *I. bartlettii* strain HTF-135 (F. prau 4) grown in anaerobic conditions. These strains aggregate, most likely due to production of EPS.

A heat map table was generated to summarize the immunomodulatory capacity of the colonic anaerobic bacteria tested (**Table 2.2**). Except for IL-10 (marked with asterisk symbol), a gradient of green to red colour was used to mark low to high concentration of cytokine and NO secretion and TLR activation level. For cytokines and NO production, the red colour represents an inflammatory profile whereas the green colour indicates an anti-inflammatory profile. As can be observed from the table, the immunomodulatory capacity among the different colonic anaerobic bacteria is highly diverse. There were no obvious similarities in immune profiles observed among the strains belonging to the same phylogenetic cluster (**Table 2.2**).

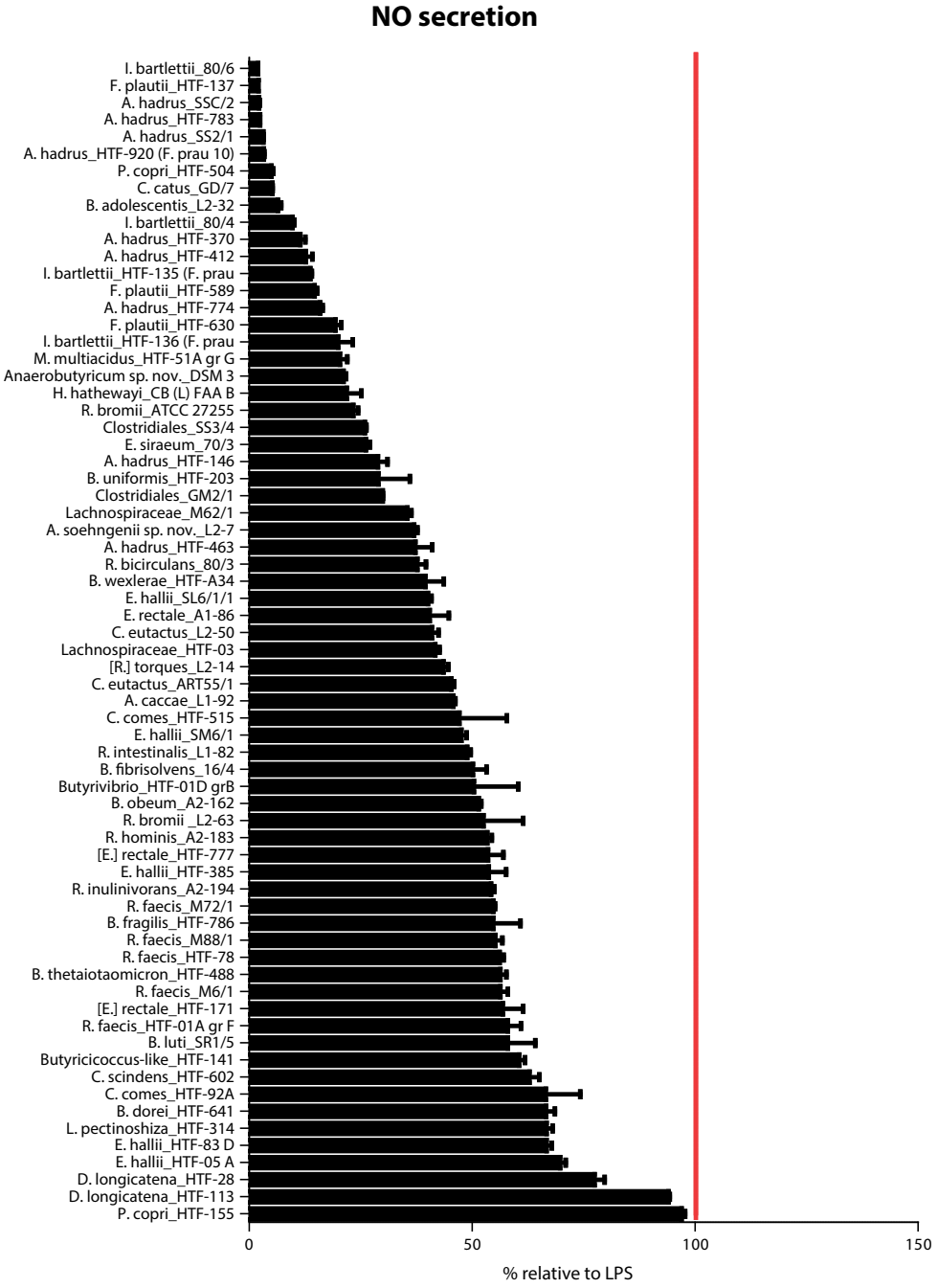

Figure 2.7. Percentages of NO secretion as a result of stimulation of mouse macrophages (RAW 264.7) with various colonic anaerobic bacteria. The concentration of NO is depicted relative to stimulation with 1 µg/ml LPS (100%; depicted by red line). Error bars represent SEM, n = 3.

Table 2.2. Summary of immune profile measured from various immune assays9

No.	PHYLUM	SPECIES	ISOLATE ID	IL-10*	IL-12	TNF-α	IL-10* (+HIB)	IL-12 (+HIB)	TNF-α (+HIB)	IL-10*/IL-12	IL-10*/TNF-α	TLR1/2	TLR2	TLR2/6	TLR4	TLR5	NO
1	Firmicutes	Anaerobutyricum soehngenii sp. nov.	L2-7	12.1	0.6	16.7	80.1	24.4	61.7	19.4	0.7	106.2	10.4	18.9	2.9	0.6	37.0
2	Firmicutes	Eubacterium hallii	VPI B4-27 (DSM 3353)	0.5	0.2	0.7	80.3	63.4	69.5	2.6	0.7	11.5	1.9	1.8	2.9	0.8	21.1
3	Firmicutes	Anaerostipes caccae	L1-92	126.4	153.3	170.3	135.3	102.4	129.6	0.8	0.7	81.4	6.8	8.7	20.8	4.0	45.8
4	Firmicutes	Anaerostipes hadrus	HTF-920 (F. prau 10)	166.7	47.3	500.0	130.5	48.1	500.0	3.5	0.3	19.1	14.7	2.2	20.2	8.5	3.3
5	Firmicutes	Anaerostipes hadrus	HTF-146	79.7	58.0	500.0	85.7	52.3	300.0	1.4	0.2	10.6	16.1	1.8	11.5	7.3	28.9
6	Firmicutes	Anaerostipes hadrus	HTF-370	103.5	70.6	500.0	157.4	64.9	116.9	1.5	0.2	9.4	14.8	2.4	11.6	7.7	11.4
7	Firmicutes	Anaerostipes hadrus	HTF-412	97.9	70.3	90.5	142.8	64.5	72.9	1.4	1.1	11.7	14.3	2.0	12.8	8.6	12.7
8	Firmicutes	Anaerostipes hadrus	SS2/1	116.0	1.1	21.5	205.3	24.5	500.0	104.4	5.4	996.4	33.2	38.6	30.5	3.5	3.2
9	Firmicutes	Anaerostipes hadrus	HTF-463	127.1	21.6	73.9	156.1	52.9	72.0	5.9	1.7	20.4	29.0	4.5	12.2	9.1	37.3
10	Firmicutes	Anaerostipes hadrus	HTF-774	125.6	164.3	500.0	172.1	105.9	500.0	0.8	0.3	10.9	15.6	1.9	13.4	9.4	15.9
11	Firmicutes	Anaerostipes hadrus	SSC/2	38.2	3.5	38.6	109.3	25.0	73.2	11.0	1.0	15.0	7.9	1.7	18.2	6.6	2.2
12	Firmicutes	Anaerostipes hadrus	HTF-783	88.3	109.1	500.0	92.0	60.0	1199.5	0.8	0.2	78.2	6.8	6.5	16.1	2.6	2.4
13	Bacteroidetes	Bacteroides dorei	HTF-641	231.2	121.4	196.9	343.2	97.1	163.8	1.9	1.2	73.6	41.8	33.7	29.6	2.3	66.6
14	Bacteroidetes	Bacteroides fragilis	HTF-786	119.2	173.3	157.4	375.5	116.1	500.0	0.7	0.8	3.2	1.1	1.9	26.2	2.0	54.7
15	Bacteroidetes	Bacteroides thetaiotaomicron	HTF-488	181.9	96.9	114.5	285.2	114.0	97.7	1.9	1.6	30.5	13.9	21.8	46.7	1.6	56.3
16	Bacteroidetes	Bacteroides uniformis	HTF-203	105.6	5.8	27.1	239.1	25.0	85.8	18.2	3.9	294.6	69.9	51.5	18.5	8.7	29.0
17	Actinobacteria	Bifidobacterium adolescentis	L2-32	320.5	6.5	140.2	221.1	11.6	500.0	49.3	2.3	1387.8	50.9	45.3	23.4	3.1	6.5
18	Firmicutes	Blautia luti	SR1/5	93.0	271.3	435.3	74.8	266.3	239.7	0.3	0.2	863.5	18.6	17.5	9.9	3.0	58.0
19	Firmicutes	Blautia obeum	A2-162	228.4	18.4	809.5	243.3	42.2	257.8	12.4	0.3	78.1	27.7	9.8	16.6	7.0	51.5
20	Firmicutes	Blautia wexlerae	HTF-A34	22.3	0.1	1.8	161.4	51.4	78.2	192.9	14.0	45.6	27.6	11.5	11.6	7.8	39.5
21	Firmicutes	Butyricicoccus-like	HTF-141	114.5	38.7	246.7	122.0	52.0	172.5	3.0	0.5	31.5	23.3	19.7	26.6	1.9	60.6
22	Firmicutes	Butyrivibrio fibrisolvens	16/4	64.8	95.7	98.9	91.5	49.1	25.7	0.7	0.7	36.0	45.4	11.7	21.3	8.0	50.2
23	Firmicutes	Butyrivibrio spp.	HTF-01D gr B	196.3	0.5	12.7	296.4	14.2	48.7	358.4	15.4	453.8	109.3	119.1	18.4	29.9	50.4
24	Firmicutes	Clostridiales sp.	GM2/1	56.0	362.4	270.1	112.3	260.0	1452.6	0.2	0.2	150.3	11.3	15.0	19.2	3.5	29.9
25	Firmicutes	Clostridiales sp.	SS3/4	72.8	27.0	44.0	165.3	49.4	107.1	2.7	1.7	318.2	20.3	24.5	19.6	35.5	26.0
26	Firmicutes	Clostridium scindens	HTF-602	524.8	51.1	500.0	759.2	78.7	124.4	10.3	1.0	47.0	27.1	32.6	63.4	1.6	62.9
27	Firmicutes	Coprococcus catus	GD/7	34.4	14.6	21.5	148.6	48.2	115.7	2.4	1.6	31.0	3.2	3.3	18.5	3.0	5.2
28	Firmicutes	Coprococcus comes	HTF-92A	108.8	4.8	163.5	85.7	36.6	96.0	22.6	0.7	13.6	19.4	2.8	13.4	7.7	66.5
29	Firmicutes	Coprococcus comes	HTF-515	31.9	0.6	1.0	205.1	18.6	58.6	56.0	31.2	31.7	35.1	7.5	15.7	8.7	47.1
30	Firmicutes	Coprococcus eutactus	ART 55/1	58.0	3.0	13.1	153.8	14.5	69.5	19.5	4.4	138.2	42.0	37.3	17.8	7.5	45.3
31	Firmicutes	Coprococcus eutactus	L2-50	165.3	1.0	42.5	154.6	21.0	70.0	158.7	3.9	1320.1	49.9	40.7	27.5	3.6	41.0
32	Firmicutes	Dorea longicatena	HTF-113	42.5	17.2	51.8	84.3	54.3	78.2	2.5	0.8	53.1	9.9	9.9	3.5	0.9	94.0
33	Firmicutes	Dorea longicatena	HTF-28	23.6	1.1	24.2	96.6	69.4	110.1	20.8	1.0	5.7	1.3	1.1	3.7	0.7	77.5
34	Firmicutes	Eubacterium hallii	HTF-05 A	52.0	6.9	101.9	183.0	83.9	171.0	7.6	0.5	511.0	136.8	142.6	3.5	3.6	69.7
35	Firmicutes	Eubacterium hallii	HTF-83 D	2.5	0.1	0.5	88.7	43.8	69.7	21.0	4.6	375.5	96.5	91.4	3.7	0.6	66.7
36	Firmicutes	Eubacterium hallii	SL6/1/1	10.1	0.5	8.2	149.4	68.8	165.1	20.8	1.2	92.5	10.4	19.1	2.8	0.5	40.1
37	Firmicutes	Eubacterium hallii	SM6/1	2.5	0.4	1.7	85.4	53.0	66.8	6.9	1.4	104.2	11.7	20.5	2.2	0.6	47.6
38	Firmicutes	Eubacterium hallii	HTF-385	23.7	0.5	2.4	90.9	13.3	27.5	49.6	9.7	208.8	107.1	154.9	28.4	2.0	53.7
39	Firmicutes	Eubacterium rectale	A1-86	99.1	1.6	24.3	178.5	21.1	86.8	61.7	4.1	1669.2	26.6	30.7	10.1	10.9	40.5
40	Firmicutes	[Eubacterium] rectale	HTF-171	12.1	0.6	20.3	48.9	9.3	45.4	18.8	0.6	160.9	29.4	36.9	5.9	0.8	56.9
41	Firmicutes	[Eubacterium] rectale	HTF-777	27.8	10.8	38.2	81.8	24.8	43.1	2.6	0.7	97.0	11.1	17.9	3.8	0.8	53.6
42	Firmicutes	Eubacterium siraeum	70/3	46.2	2.6	11.1	102.3	25.5	69.3	17.6	4.1	1500.4	28.0	27.0	8.8	24.1	26.2
43	Firmicutes	Flavonifractor plautii	HTF-137	17.4	33.6	38.8	72.1	38.9	65.9	0.5	0.4	3.0	1.0	0.7	2.6	0.6	2.1
44	Firmicutes	Flavonifractor plautii	HTF-589	103.5	169.1	226.7	147.4	119.1	199.1	0.6	0.5	7.0	5.4	6.5	31.7	1.6	14.7
45	Firmicutes	Flavonifractor plautii	HTF-630	62.3	277.5	134.1	83.5	128.6	162.9	0.2	0.5	89.2	6.9	10.2	32.3	3.2	19.4
46	Firmicutes	Hungatella hathewayi	CB (L) FAA B	63.5	213.4	88.4	55.5	66.7	262.6	0.3	0.7	7.5	7.4	1.6	20.4	5.6	21.9
47	Firmicutes	Intestinibacter bartlettii	80/4	4.5	0.3	11.1	40.3	22.2	101.1	14.4	0.4	52.0	4.3	4.4	11.8	2.3	9.7
48	Firmicutes	Intestinibacter bartlettii	80/6	3.9	0.7	10.5	81.4	37.9	99.4	5.3	0.4	31.1	17.7	2.8	18.5	7.7	2.0
49	Firmicutes	Intestinibacter bartlettii	HTF-135 (F. prau 4)	2.4	0.5	5.1	29.0	20.2	67.9	5.0	0.5	18.5	13.3	2.3	17.0	7.8	13.7
50	Firmicutes	Intestinibacter bartlettii	HTF-136 (F. prau 8)	6.2	0.5	21.2	35.7	29.3	56.8	13.6	0.3	135.7	10.6	11.3	25.0	3.7	20.0
51	Firmicutes	Lachnospira pectinoshiza	HTF-314	22.3	0.8	3.0	268.4	24.4	26.7	27.9	7.3	84.4	51.0	53.1	28.0	3.2	66.7
52	Firmicutes	Lachnospiraceae gen. nov. sp. nov	HTF-03	63.9	1.7	29.7	224.2	15.1	58.9	37.6	2.2	1355.7	47.2	35.7	13.6	2.3	41.8
53	Firmicutes	Lachnospiraceae sp. nov.	M62/1	60.1	30.3	62.0	84.5	32.2	79.8	2.0	1.0	699.0	32.5	27.2	15.1	3.1	35.5
54	Firmicutes	Mitsuokella multiacidus	HTF-51A gr G	113.7	105.4	78.5	89.2	85.1	71.5	1.1	1.4	85.8	64.5	15.5	114.6	9.8	20.4
55	Bacteroidetes	Prevotella copri	HTF-504	21.4	0.7	8.1	108.0	32.1	29.1	29.8	2.6	157.9	65.0	29.9	18.7	8.7	5.0
56	Bacteroidetes	Prevotella copri	HTF-155	48.0	0.4	2.5	158.0	9.5	33.1	111.1	19.4	2826.7	74.6	89.0	29.7	2.9	97.0
57	Firmicutes	Roseburia faecis	HTF-01A gr F	159.5	5.1	40.9	255.6	33.2	93.2	31.1	3.9	37.3	49.4	6.7	19.4	32.0	58.0
58	Firmicutes	Roseburia faecis	HTF-78	153.4	27.5	83.6	262.6	56.5	112.3	5.6	1.8	25.8	37.4	4.2	20.0	41.9	56.2
59	Firmicutes	Roseburia faecis	M6/1	153.5	0.6	9.5	237.0	20.4	41.5	240.9	16.1	1548.4	66.7	45.1	20.6	83.0	56.3
60	Firmicutes	Roseburia faecis	M72/1	112.7	0.3	15.3	267.8	8.6	89.2	372.0	7.4	1724.4	68.0	50.5	20.6	229.9	54.7
61	Firmicutes	Roseburia faecis	M88/1	152.2	0.4	25.1	303.9	7.8	75.2	345.8	6.1	155.8	59.3	21.3	21.0	39.3	55.2
62	Firmicutes	Roseburia hominis	A2-183	58.7	1.9	8.8	120.7	12.8	51.4	30.2	6.7	5306.5	65.8	71.3	10.0	13.3	53.4
63	Firmicutes	Roseburia intestinalis	L1-82	58.2	0.4	17.0	133.8	10.4	53.4	149.7	3.4	289.8	55.1	48.3	19.7	10.5	48.9
64	Firmicutes	Roseburia inulinivorans	A2-194	127.3	1.4	23.2	354.3	19.5	138.8	92.1	5.5	2790.1	69.7	61.0	21.1	216.4	54.2
65	Firmicutes	Ruminococcus bicirculans	80/3	8.8	5.5	0.4	149.8	29.6	50.4	1.6	20.6	25.4	20.4	15.7	31.6	2.1	37.7
66	Firmicutes	Ruminococcus bromii	ATCC 27255	8.1	0.6	0.9	136.0	32.2	62.5	13.2	8.8	27.0	17.4	15.2	31.1	2.2	23.4
67	Firmicutes	Ruminococcus bromii	L2-63	76.4	1.0	19.5	214.6	22.2	84.7	77.5	3.9	231.3	75.9	51.4	19.0	8.1	52.6
68	Firmicutes	[Ruminococcus] torques	L2-14	109.5	0.7	27.9	250.9	16.5	126.8	160.4	3.9	259.9	97.3	63.1	14.1	7.0	43.6

Red to green indicates high to low amounts of inflammatory cytokine, NO, or TLR-activation. For anti-inflammatory cytokines the colour scale is reversed (indicated by an asterix).

DISCUSSION

In our search for a potential therapeutic (probiotic) candidate for the treatment of IBD, we screened 68 colonic anaerobic strains, obtained from healthy volunteers. Most importantly, we found that that the immune profile resulting from PBMC stimulation and cytokine measurements, the NO secretion by macrophages, as well as the TLR activation was strain specific (**Figures 2.2, 2.3, 2.4, 2.5** and **2.7**). There were also no correlations observed between the induced cytokine production, TLR activation or NO secretion. Most of the tested strains were able to activate the NF-κB signalling pathway through TLR1/2, TLR2 and TLR2/6 albeit to various degrees (**Figure 2.5**). Only one strain activated NF-κB signalling pathway via TLR4 (**Supplementary figure S2.2**), a TLR family member which recognizes lipopolysaccharide (LPS), a microbial component belonging to Gram-negative bacteria[87]. This particular strain, *M. multiacidus* strain HTF-51A gr G, was indeed identified as a Gram-negative bacterium[88]. A few *Roseburia* strains showed strong NF-κB activation via TLR5 (**Supplementary figure 2**) which indicated flagellin recognition[89, 90]. *Roseburia hominis* (A2-183) is indeed a flagellated gut anaerobic bacterium, and a significant decrease of *R. hominis* colonization in the gut of ulcerative colitis patients has recently been reported[91]. Moreover, a recent study of Tamanai-Shacoori showed that *Roseburia* might be used as a biomarker for intestinal health[92].

As most of the strains tested in this study were Gram-positive, their cell wall would consist of peptidoglycan and lipoteichoic acid and therefore we expected all strains to strongly trigger NF-κB signalling. Some strains however, hardly activated NF-κB signalling. This could be a result from extracellular polymeric matrix substances (EPS), which might 'shield' the bacterium and prevent recognition of their molecular patterns[23]. We found that *D. longicatena* strain HTF-28 and *I. bartlettii* strain HTF-135 (F. prau 4), form particular aggregates when cultured, most likely as a result of extracellular polymeric matrix substances (**Figure 2.6**). These strains induced hardly any NF-κB activation via TLR activation. Unexpectedly, even though NF-κB activation is known to trigger cytokine secretion, the capacity of certain bacterial strains to activate NF-κB signalling pathway through TLRs did not positively correlate with cytokine secretion. The above-mentioned *D. longicatena* strain HTF-28 hardly activated NF-κB signalling pathway through TLR activation but nevertheless induced significant amounts of cytokine secretion. A possible explanation for the capacity of HTF-28 to induce cytokine secretion independently from TLR activation could be its ability to activate other receptors that play an important role in activating the innate immune response, such as the nucleotide-binding and oligomerization domain (NOD)-like receptors (NLRs) and/or C-type lectin receptors. Similar to TLRs, NLRs are also known as pattern-recognition receptors. TLRs are transmembrane receptors, while NLRs are cytoplasmic receptors that play a crucial role in the innate immune response by recognizing both microbe-associated molecular patterns (MAMPs) as well as damage-associated molecular patterns (DAMPs)[93]. C-type lectin receptors recognize

carbohydrates, through one or more carbohydrate recognition domains (CRDs). Besides, they can recognize structurally similar C-type lectin-like domains (CTLDs) which do not necessarily have to be carbohydrate ligands[94]. EPS produced by HTF-28 could be recognized by a C-type lectin receptor and thereby activate NF-κB signalling pathway which would lead to inflammatory cytokine production[95]. Bacterial MAMPs can be modified to avoid pattern recognition receptor (PRR) activation. Modified structures of LPS produced by *Bacteroides dorei* (*B. dorei*) avoid detection by TLR4 and NOD receptors[96]. Moreover, modification of bacterial peptidoglycan to escape NOD receptors[97, 98] has been reported as a strategy to avoid PRR activation. It remains to be investigated if strain HTF-28 also expresses modified MAMPs to avoid TLRs or other PRRs activation, however HTF-28 still triggers cytokine secretion, therefore some mechanism of recognition is activated by this strain.

Based on the result of our immune assays, the 68 tested strains were grouped into three different immune profiles. Firstly, the immunostimulatory profile; the strains belonging to this profile, (e.g. *C. scindens* strain HTF-602) showed an immuno-stimulatory capacity by strongly inducing cytokine secretion. These strains were also characterized by induction of relatively high NO secretion, and/or high NF-κB signalling after TLR activation. Although increased IL-10 secretion after stimulation with some of these strains is observed, in general stimulation with these strains is more likely to increase inflammation, rather than to attenuate it. These immunostimulatory strains would therefore not be the first choice for future probiotics.

Secondly, the immunomodulatory profile; some strains, (e.g. *R. faecis* strain M88/1) only induced moderate amounts of cytokine secretion in our PBMCs assay. However, when they were combined together with HIB, to mimic an inflammatory situation, these strains were able to modulate this HIB induced cytokine secretion. HIB is a bacterial stimulus which principally triggers inflammation due to its ability to increase secretion of both anti- and pro-inflammatory cytokines. The immunomodulatory strains were able to reduce the pro-inflammatory cytokines IL-12 and TNF-α, but could at the same time increase secretion of the anti-inflammatory cytokine IL-10. These strains also induced only moderate amounts of NO secretion. Combined, the generally anti-inflammatory cytokine profile and the attenuated NO secretion would likely be beneficial in situations of (excessive) inflammation. These strains therefore could be considered as potential candidates for future probiotics.

Lastly, we observed the immunosuppressive or ‘silent’ profile (e.g. *F. plautii* strain HTF-137); this profile was characterized by a low capacity to induce cytokine secretion, in combination with low NO secretion and/or TLR NF-κB signalling after TLR activation. More importantly, when HIB was added as an immune/inflammatory stimulus, these strains attenuated the resulting pro-inflammatory cytokine response. These strains could be very interesting as probiotic candidates as they would not stimulate inflammatory responses and would attenuate inflammation.

The most desirable immune profile of strains to be used as a therapy for a chronic inflammatory disease in the gut, such as IBD, must include a combination of some criteria such as an induction of a moderate to high IL-10 versus low IL-12 secretions (moderate-high IL-10 to IL-12 ratio) accompanied with induction of a moderate to low TNF-α secretion. Moreover, when there is inflammation, the ideal probiotic strain should have a moderate to high modulatory capacity to increase IL-10 and decrease IL-12 and TNF-α secretion, as well as a low capacity to induce oxidative stress (low NO induction). Some strains, such as *P. copri* strain HTF-504 and *A. hadrus* strain SSC/2, indeed fit the criteria mentioned. However, this does not mean that other unique immune profiles might not be desirable for therapeutic application. For example, the strains that showed an immunosuppressive or 'silent' profile, such as *F. plautii* strain HTF-137, may be interesting to explore further as new therapeutic candidates for chronic inflammatory disease such as IBD. Such strains could maintain an anti-inflammatory status in the gut by allowing low secretion of cytokines and NO during remission, and decrease the inflammation by attenuating pro-inflammatory cytokine secretion during the 'flare-up' state of IBD. As we observed from the heat map (**Table 2.2**), most of tested strains within a certain species showed different immune profiles. However, some species showed similar pattern of immune profile, for all the strains tested, for example the *E. hallii* and *I. bartlettii* species. These species showed similar ranges of cytokine and NO secretion, as well as NF-κB signaling via TLR activation, with only one or two exceptions. It therefore remains paramount to investigate each strain individually to determine its immunomodulatory capacities, as phylogenetic similarities do not predict phenotypic properties.

CONCLUDING REMARKS

To conclude, in this study we found that the immune profile of colonic anaerobic bacteria is mostly strain specific and there appear to be no general trends associated with a specific species, although some species may show similar immune profiles. We identified three different types of immune profiles which could theoretically be used to select anti-inflammatory probiotics. The three types were immunostimulatory, immunomodulatory and immunosuppressive or 'silent' profiles. We also found some strains meet the criteria for a potential therapeutic candidate for IBD treatment. This work identified new immune phenotypes/profiles of gut bacteria warrant further study *in vivo*. In the future we aim to test these immunomodulatory predictions in an *in vivo* mouse model of IBD.

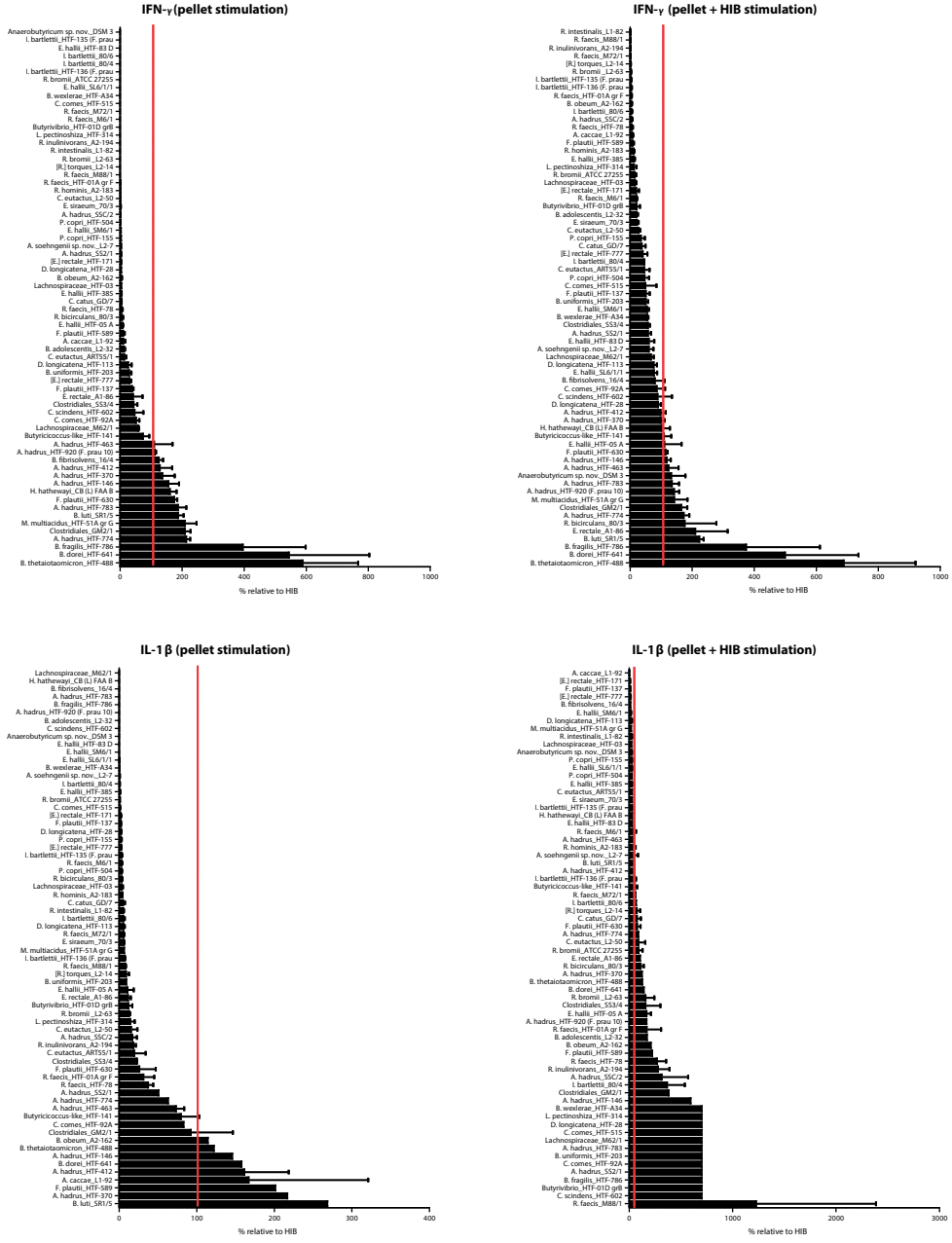

Supplementary figure S2.1. Percentages of IFN-γ and IL-1β cytokines secretion measured in PBMC cultures after 24 hours incubation with different strains of colonic anaerobic bacteria, with or withouth HIB stimulation. Concentrations of IFN-γ and IL-1β are shown relative to positive control HIB (%). Error bars represent SEM, n = 3 donors. Red line indicates the amount of secreted cytokine induced by the positive control (100%).

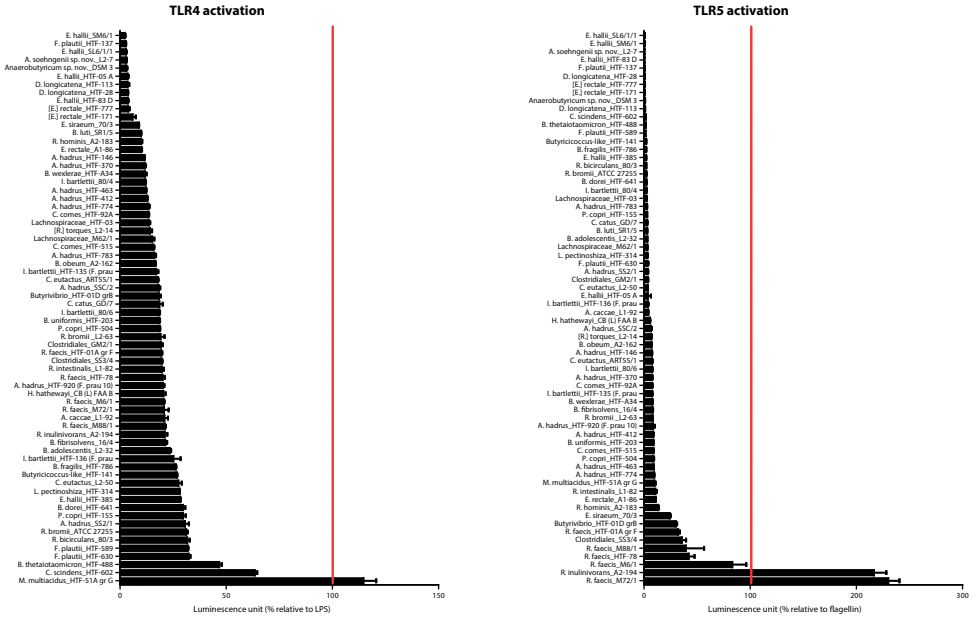

Supplementary figure S2.2. Percentages of TLR4 and TLR5 activation level measured in TLR receptor cell lines after stimulation with different strains of colonic anaerobic bacteria. Activation levels of TLR4 and TLR5 are depicted relative to their respective ligands (%). Error bars represent SEM, n = 3. Red line indicates the activation level induced by the cognate TLR ligands (100%).

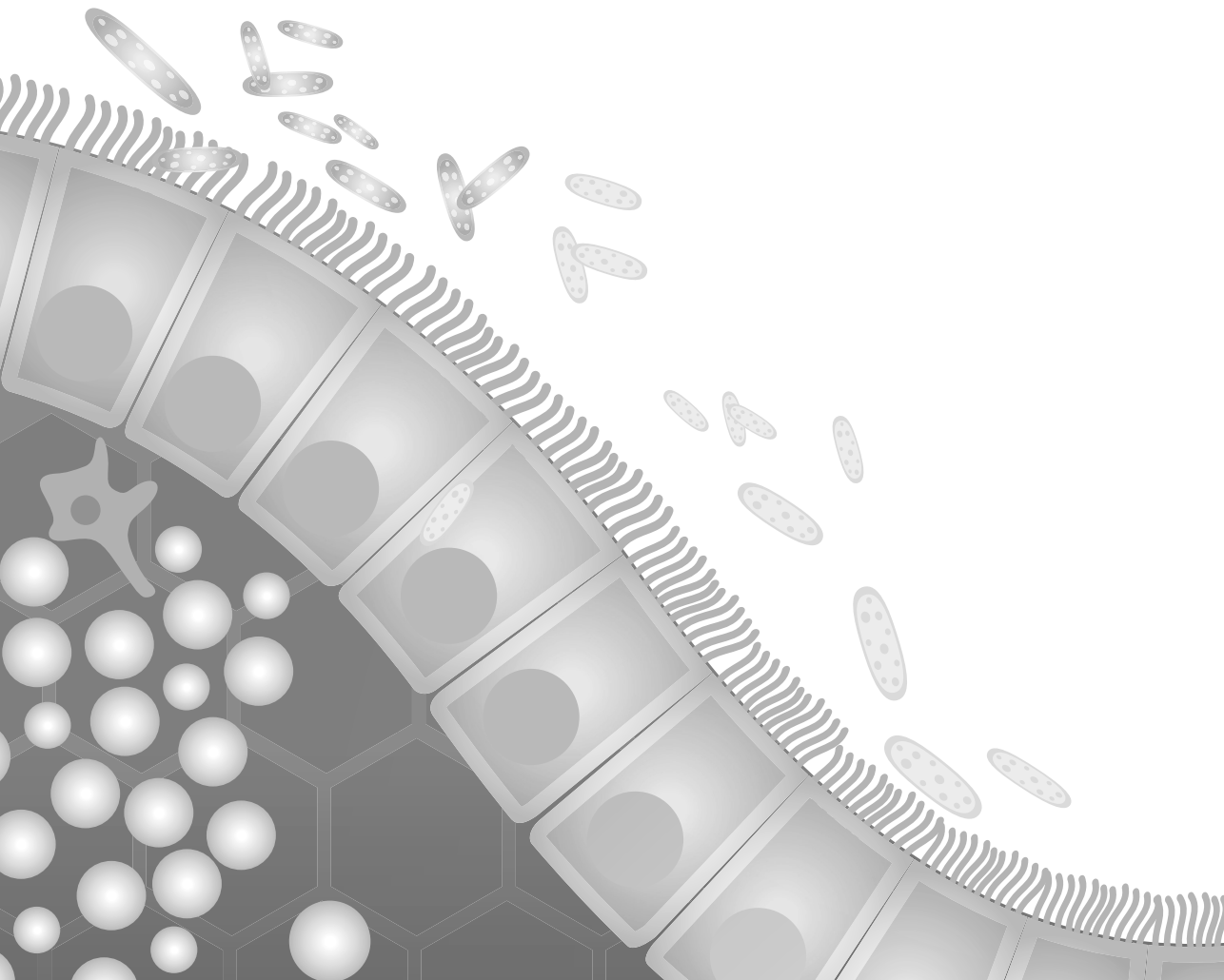

Chapter 3

Immunomodulatory capacities of a collection of *Faecalibacterium prausnitzii* strains

Nuning Winaris[1,2], Ellen Kranenbarg[1], Eleni Tsompanidou[3,6], Hermi J.M. Harmsen[3], Paul O. Sheridan[4], Alan W. Walker[4], Sylvia H. Duncan[4], Gemma Henderson[5], Jerry M. Wells[1]

[1] Host-Microbe Interactomics Group, Department of Animal Science, Wageningen University & Research, Wageningen, Netherlands

[2] Master Program in Biomedical Sciences, Faculty of Medicine, Universitas Brawijaya, Malang, Indonesia

[3] Department of Medical Microbiology, University of Groningen, University Medical Center Groningen, Groningen, Netherland

[4] Gut Health Group, Rowett Institute, University of Aberdeen, Foresterhill, Aberdeen, Scotland, UK

[5] Human Health Innovation, Chr. Hansen, Hørsholm, Denmark

[6] Winclove Probiotics, Amsterdam, Netherland

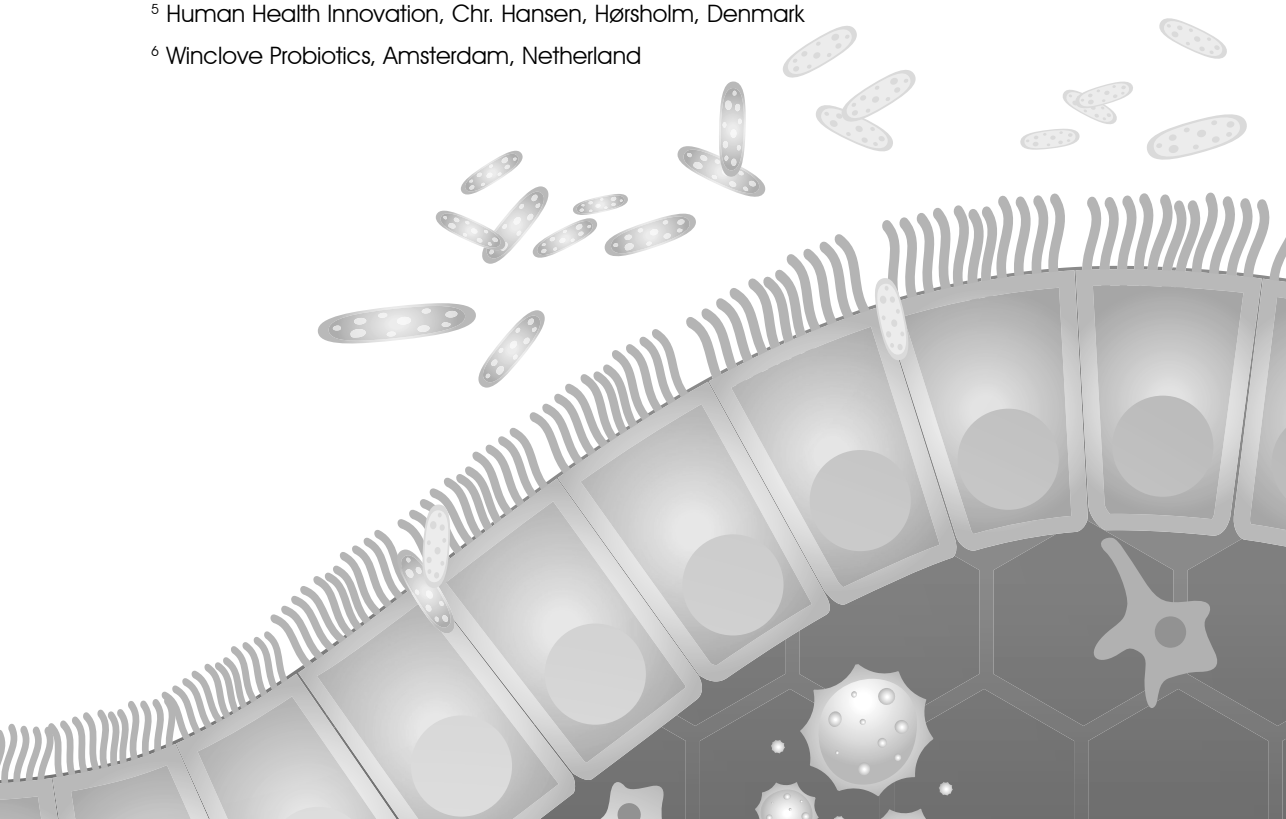

Abstract

Faecalibacterium prausnitzii has been reported as a promising probiotic for the treatment and prevention of inflammatory bowel disease. However, it is not known whether different strains or phylogenetic clades of *F. prausnitzii* have different immunomodulatory properties linked to evolutionary differences in the genome. Here we describe the immunomodulatory properties of a unique collection of 26 novel and two previously described strains of *F. prausnitzii* using various immune assays *in vitro*. Comparison of the sequenced genomes of the 28 strains revealed distinct phylogenetic clusters. *F. prausnitzii* strains were incubated with isolated human peripheral blood mononuclear cells (PBMC) with and without an additional stimulus and the amounts of secreted cytokines measured in the culture supernatant after 24 hours. We also measured the capacity of each strain to signal through Toll-like receptors (TLR) using luciferase reporter assays. Additionally, nitric oxide (NO) was measured after incubation of the strains with murine macrophage RAW 264.7 cells as an indicator of macrophage activation. The strains fell into one of three immunomodulatory categories: immue-stimulatory, immunomodulatory and 'silent' (inhibitory) response profiles. The immune profiles of the strains were not correlated with a distinct phylogenetic cluster. Future research will be aimed at establishing the potential anti-inflammatory effects of selected strains in a mouse colitis model.

Keywords: *Faecalibacterium prausnitzii*, immune profiles, anti-inflammatory

INTRODUCTION

Faecalibacterium prausnitzii (*F. prausnitzii*) is one of the most abundant species found the human faecal microbiota[99]. Reduced abundance has been linked to as Crohn's disease (CD) and ulcerative colitis (UC), two forms of human inflammatory bowel disease (IBD)[20, 45, 100]. *F. prausnitzii* produces butyrate which is an important energy source for enterocytes, linked to the induction of regulatory T cells in the colon[26, 44, 68] and anti-inflammatory effects in the intestine[20, 22]. Other anti-inflammatory mechanisms of *F. prausnitzii* have also been reported in the literature. *F. prausnitzii* strains have a high capacity to induce IL-10 in human and murine dendritic cells *in vitro* and modulate T cell responses *in vivo*[21]. The culture supernatant of *F. prausnitzii* strain A2-165 was also reported to attenuate severity of colitis in mouse models of relapsing colitis[22, 84]. Recently several peptides present in *F. prausnitzii* culture supernatants were shown to attenuate IL-1β induced production of IL-8 in Caco-2 epithelial cells *in vitro*. The peptides were derived from a single a 15 kDa protein, which attenuated activation of the nuclear factor (NF)-κB pathway when transfected into mammalian cells[100].

Recently *F. prausnitzii* strain HTF-F was shown to produce an extracellular polymeric matrix (EPM), that may play a role in biofilm formation and colonization[23]. The EPM was shown to modulate IL-12 and IL-10 cytokine production in antigen presenting cells, suggesting that it contributes to anti-inflammatory effects. Oral administration of strain HTF-F and to a lesser extent even the EPM alone attenuated the severity of disease in a mouse dextran sodium sulphate (DSS)-induced colitis model[23]. Overall, these findings suggest that *F. prausnitzii* strains can differ in their capacity to attenuate colitis and might possess different properties influencing gut colonization and survival, as well as different mechanisms to attenuate inflammation.

F. prausnitzii are generally regarded as extremely oxygen sensitive (EOS) bacteria with death occurring within minutes after exposure to atmospheric levels of oxygen. *F. prausnitzii* has been shown to shuttle electrons to oxygen through an extracellular electron transport chain utilizing riboflavin[101], which may allow *F. prausnitzii* to survive under low oxygen tension. This could be important for survival in an inflamed gut where oxygen tension may increase due to epithelial damage and production of reactive oxygen species by inflammatory cells. Riboflavin is not secreted by *F. prausnitzii* so it depends on its production by other members of the microbiota. Therefore, oral administration of riboflavin or other antioxidants may help promote survival of *F. prausnitzii* in therapeutic applications[101].

Given the interest and potential of using *F. prausnitzii* strains as next generation probiotics we investigated the immunomodulatory properties of a unique collection of 28 different strains from healthy human donors. Comparison of the sequenced genomes of the 28

strains revealed distinct phylogenetic clusters. The aim was to investigate whether strains of different phylogenetic clades possessed distinct immunomodulatory characteristics, linked to evolutionary differences in the genome. *F. prausnitzii* strains were incubated with isolated human peripheral blood mononuclear cells (PBMC) with and without an additional stimulus and the amounts of secreted cytokines measured in the culture supernatant after 24 hours. We also measured the capacity of each strain to signal through Toll-like receptors (TLR) using luciferase reporter assays. Additionally, nitric oxide (NO) was measured after incubation of the strains with murine macrophage RAW 264.7 cells as an indicator of macrophage activation.

MATERIALS AND METHODS

Bacterial culture and harvesting

Various isolates of *F. prausnitzii* strains were grown in YCFAGSC, a modified YCFA (yeast, casitone, fatty acids) medium supplemented with additional carbon sources (glucose, soluble starch and cellobiose). The bacterial cultures were grown at 37°C inside an anaerobic chamber (Bactron 3000) containing 90% nitrogen (N_2), 5% hydrogen (H_2) and 5% carbon dioxide (CO_2). The optical density of bacterial cultures was measured at 600 nm using a Spectramax M5 microplate reader (Molecular Devices) and bacteria harvested from 2 ml of culture by centrifugation at 4000 rpm for 10 minutes at RT. The supernatant was filtered through a 0.22 µm MF-Millipore Membrane (Sigma-Aldrich) to remove bacteria and stored at -80°C. Bacterial pellets were resuspended in Roswell Park Memorial Institute (RPMI) 1640 Medium (Thermo Fisher Scientific) containing 15% glycerol and stored at -80°C. Prior to the experiment, the bacterial pellet and supernatant were thawed and diluted to OD 0.1 (600 nm) (equivalent to about 5 x 10^7 bacteria).

Isolation and stimulation of human peripheral blood mononuclear cells (PBMC)

Human peripheral blood mononuclear cells (PBMC) were isolated from blood using Ficoll density centrifugation. The blood was diluted 1:1 with Roswell Park Memorial Institute (RPMI) 1640 Medium (Thermo Fisher Scientific). PBMCs were isolated by density gradient centrifugation on Ficoll-Plaque PLUS (GE healthcare). The diluted plasma was removed and the layer of white blood cells was recovered and washed four times with RPMI. Purified PBMCs were seeded in 96 well plate (2 x 10^5 cells/well) and rested for one hour in RPMI supplemented with 10% FBS (Invitrogen) and 100 U/ml penicillin/100 µg streptomycin (Sigma-Aldrich) at an atmosphere of 5% CO_2 - 95% O_2 at 37ºC. Subsequently, PBMCs were used for profiling secreted cytokine production in response to the stimulation of various *F. prausnitzii* strains. PBMC were stimulated with a ratio of 1:2 cell to bacteria. In some assays heat-inactivated bacteria (HIB), were added as an additional stimulus with a cell to bacteria ratio of 1:20. Then PBMC were incubated for 24 hours at 37ºC in an atmosphere of 5% CO_2,

95% O_2. After incubation, supernatants of PBMC cultures and the cells were harvested for cytokine and viability measurements respectively.

Annexin V/Propidium iodide (PI) viability staining

Annexin V/Propidium Iodide (PI) staining (BD Biosciences) was used to distinguish viable from early and late apoptotic or necrotic cells according to manufacturer's protocol. The cells were analysed using CytoFlex™ Flow Cytometry (Beckman Coulter).

Cytokine measurements

Cytokines were measure using the the Bioplex Pro™ Assay according to manufacturers' recommended protocol. Briefly, magnetically coupled beads (containing the detection antibody) for the different cytokines were premixed in assay buffer and added to flat bottom 96 well plates and washed twice using a magnetic handheld washer. Next, 25 µl of defrosted culture supernatant was mixed with 25 µl of sample buffer, or 50 µl of cytokine standard and incubated with gentle shaking at room temperature for 30 minutes. After incubation, the plate was washed three times and 25 µl of premixed detection antibodies were added and incubated for 30 minutes, with gentle shaking. After incubation, the plate was washed three times and 50 µl of streptavidin-PE was added and incubated at room temperature for 10 minutes, with gentle shaking. After three final washes, the beads were taken up in 75 µl of drive fluid, briefly shaken (700 rpm) and analysed. Samples and standards were measured in the MagPix reader, and analysed using the MAGPIX xPONENT software, Bio-Plex Manager version 5.0. Five cytokines were measured: interleukin 1 beta (IL-1β), interleukin-10 (IL-10), interleukin-12p70 (IL-12p70), interferon gamma (IFN-γ), and tumour necrosis factor alpha (TNF-α).

TLR reporter assay

Human embryonic kidney (HEK293) (Invivogen) were transformed with different human Toll-like receptors (TLR1/2, TLR2 and 2/6) and a NF-κB luciferase reporter construct (Invivogen). These cells were seeded at 6×10^4 cells per well into black, clear bottom 96-well plates in DMEM medium (Invitrogen), supplemented with 100 U/ml penicillin and 100 µg/ml streptomycin (Sigma-Aldrich) and 10% FBS (Invitrogen) and incubated overnight at an atmosphere of 5% CO2 - 95%, O2 at 37ºC. Cells were subsequently incubated for at least 3 hours with different bacterial pellets or TLR agonists as controls (20 ng/ml Pam2PCSK for TLR2 and 2/6; 200 ng/ml Pam3PCSK for TLR1/2; Invivogen). Medium alone was used as a negative control. After the incubation period half of the medium was aspirated and replaced with Bright glow (Promega), subsequently the plate was vortexed for 5 minutes and the luminescence was measured using a Spectramax M5 microplate reader (Molecular Devices) at 750 ms integration time. Human embryonic kidney HEK293 cells not expressing TLR receptors but harbouring the pNiFty, NF-κB luciferase reporter construct (Invivogen), were used as negative controls in the TLR reporter assays.

Macrophage stimulation

The macrophage cell line RAW 264.7 (ATCC TIB-71) was maintained in Dulbecco's Modified Eagle Medium (DMEM) containing GlutaMAX (Thermo Fisher Scientific) with addition of 100 U/ml penicillin and 100 µg/ml streptomycin (Sigma-Aldrich). Cells (1.5 x 10^5) were seeded in 96-well culture plates in 200 µl of culture medium without phenol red. Immediately, the different bacterial pellets or immunostimulant lipopolysaccharide (LPS; 1µg/ml) were added to the cells and then incubated for 24 hours at 37°C in 5% CO_2. After incubation, 75 µl of supernatant was harvested and transferred to a new plate for measurement of nitric oxide (NO) using the Griess assay. The viability of the remaining cells was measured using Cell Proliferation Reagent WST-1(Sigma-Aldrich) according to manufacturer's protocol.

Nitrite (Griess) assay

NO produced by activated macrophages was converted to nitrite and measured using the Griess assay. An aliquot of 75 µl culture supernatant from each well was transferred to a new flat-bottomed 96-well plate and combined with 100 µl of 1% sulphanilamide and 100 µl of 0.1% naphthylenediamine (both were prepared in 2.5% phosphoric acid solution). After 5 minutes incubation at room temperature, the nitrite concentration was determined by measuring optical density (OD 540, reference filter 690 nm) using a Spectramax M5 microplate reader (Molecular Devices). Sodium nitrite (Sigma-Aldrich) was used as a standard to calculate NO concentrations in the cell-free medium.

RESULTS

Phylogenetic clustering

Phylogenetic clustering of 72 *F. prausnitzii* strains was created based on their genome sequences (**Figure 3.1.**) [**Collaborative *F. prausnitzii* manuscript in preparation**]. The colour code in this phylogenetic tree reflects the different phylogenetic clusters of *F. prausnitzii* and was used in other graphs in this chapter to identify the clusters (A to L). In this study we investigated the immunomodulatory properties of 28 strains, representing 8 of the 12 different phylogenetic clusters (**Figure 3.1**).

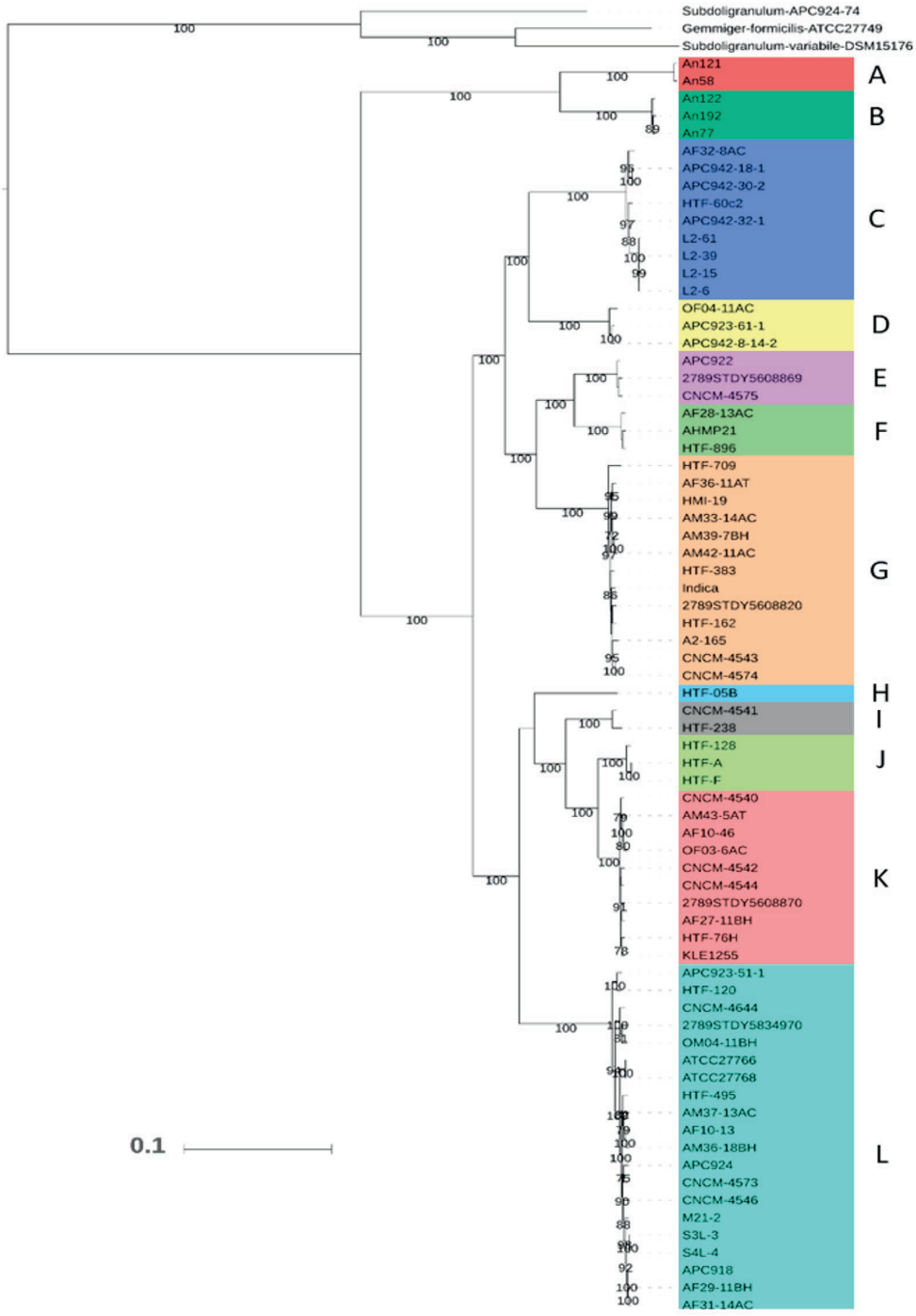

Figure 3.1. Genomic diversity of *F. prausnitzii* strains. Phylogenetic clustering of 72 *F. prausnitzii* strains based their genomic sequences. Different colours represent different clusters which are indicated by alphabetic order (A-L).

Cytokine profiling in PBMC

Similar CFUs of each *F. prausnitzii* strain, suspended in RPMI were incubated with human PBMCs from three separate donors. After 24 hours incubation the secreted cytokines in the supernatant were measured by multiplex bead-capture assays (Magpix Luminex). As the amount of secreted cytokine can vary considerably between donors we included stimulation with a standard frozen inoculum of heat-inactivated bacterium (HIB) to facilitate normalisation between assays.

There were considerable differences in amounts of secreted cytokine induced by the bacterial pellets of the different *F. prausnitzii* strains. For example, some strains induced less than 5 pg/ml IL-10 secretion, whereas other strains induced up to 4362 pg/ml suggesting that the capacity to induce high amounts of IL-10 in PBMCs is strain dependent and high IL-10 production is not a conserved feature of the species (**Figure 3.2A**). Most (27 out of 28) of the *F. prausnitzii* strains tested elicited small amounts of IL-12 (depending on donor) in the range of (1 - 12 pg/ml), which was less than 4% of the levels elicited by the control stimulus (**Figure 3.2B**). The exception was strain S3L/3, which produced relatively high amounts of IL-12 (337 pg/ml), which was comparable to the positive control (HIB).

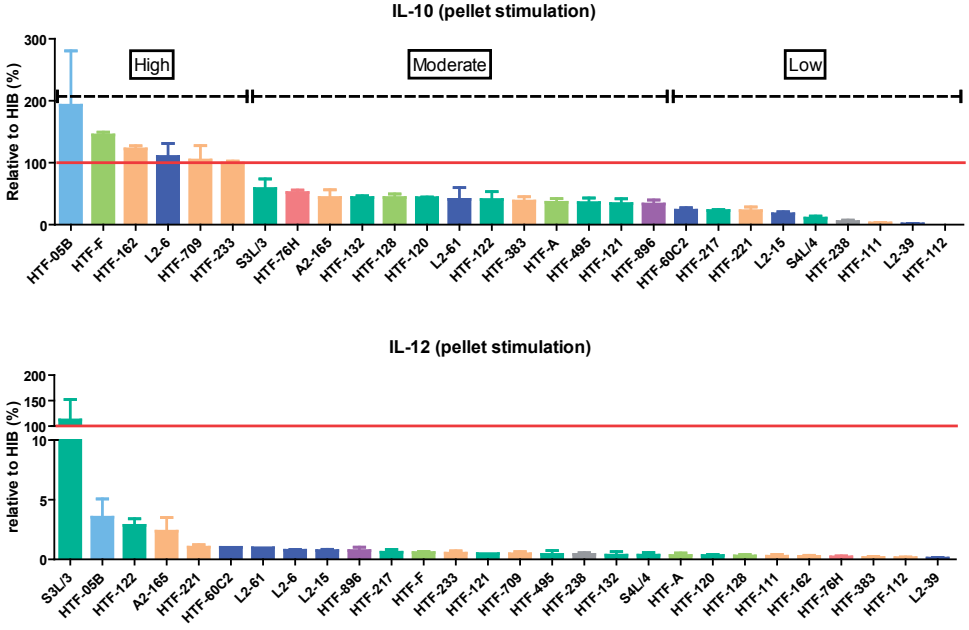

Figure 3.2A & B. Percentages of IL-10 (A) and IL-12 (B) secretion measured from PBMCs after 24 hours incubation with different strains of *F. prausnitzii*. Concentrations of IL-10 and IL-12 are shown relative to the positive control HIB (%). Error bars represent SEM, n = 3 donors. Red line indicates the amount of secreted cytokine induced by the positive control (100%). Bar colours indicate the phylogenetic cluster of each strain.

As the induction of high IL-10/IL-12 cytokine ratios has been suggested to correlate with protective effects of probiotics in a mouse colitis model[39], we calculated the ratio between the anti-inflammatory IL-10 and the pro-inflammatory IL-12 with the lowest value of IL-12 being nominally 1.06 pg/ml (**Figure 3.2C**). IL-10 is known to have a suppressive effect on IL-12 production so it was surprising to find the highest inducer of IL-10, strain HTF-05B, also induced high amounts of secreted IL-12, resulting in a low ratio for IL-10/IL-12. Strain S3L/3, which induced moderate amounts of IL-10 but the highest amount of IL-12, ranked last.

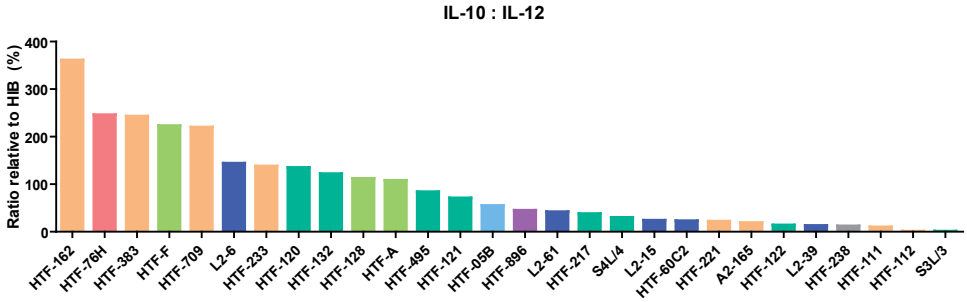

Figure 3.2C. Ratio of secreted IL-10 to IL-12 in PBMCs assays. The ratios were obtained from percentage of IL-10 vs. IL-12 secretions relative to HIB. Error bars represent SEM, n = 3 donors. Bar colours indicate phylogenetic clusters of the strain.

The 28 strains varied considerably in their capacity to induce TNF-α ranging from 88 - 185286 pg/ml (**Figure 3.2D**), but there was no correlation between capacity of a strain to elicit high amounts of IL-10 and high amounts of TNF-α. Strain HTF-05B had a unique immune profile, inducing the highest amounts of IL-10 and TNF-α and the second highest amounts of IL-12. This strain was also a strong inducer of IL-1β and IFN-γ (**Supplementary Figure 3.1**). Interestingly, a few strains, in particular HTF-112, L2-39, HTF-238 and HTF-111, induced low or undetectable amounts of all cytokines.

As the amount of secreted IL-12 was low (1 - 12 pg/ml), the IL-10 to IL-12 ratio reflected more on the amount of IL-10. Therefore, we also calculated the IL-10/TNF-α ratio. The ranking of strains according to the IL-10/TNF-α ratio was different to that of the IL-10/IL-12 ratio (**Figure 3.2C**). Neither of these ratios correlated with the *F. pausnitzii* phylogenetic cluster (**Figure 3.2E**).

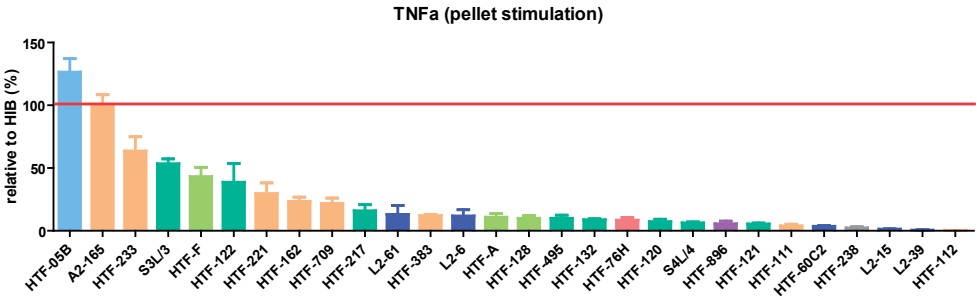

Figure 3.2D. Percentages of TNFα secretion as a result of stimulation of PBMCs with various *F. prausnitzii* strains. Concentration of TNF-α is shown relative to positive control HIB. Error bars represent SEM, n = 3 donors. Red line indicates the positive control (100%). Bar colours indicate phylogenetic clusters of the strains.

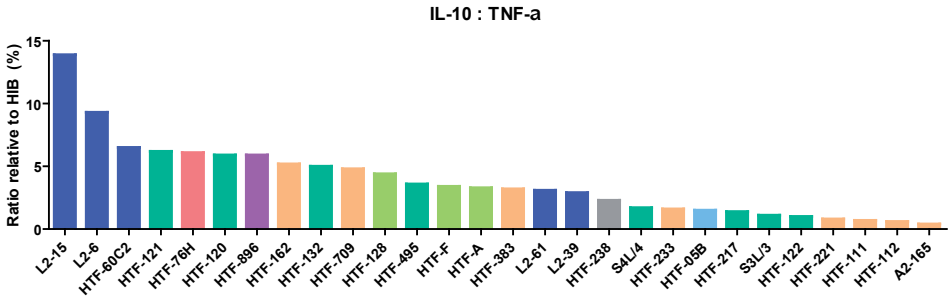

Figure 3.2E. Ratio of IL-10/TNF-α based on PBMCs screening. The ratios were obtained from percentage of IL-10 vs. TNF-α secretions relative to HIB. Error bars represent SEM, n = 3 donors. Bar colours indicates phylogenetic clusters of the strains.

TLR signalling

All 28 *F. prausnitzii* strains activated NF-κB-mediated reporter gene expression in the TLR2/6 and TLR2 reporter assays, but their capacity to induce expression of luciferase (an arbitrary measure of NF-kB activation) was highly strain dependent (**Figure 3.3A** and **3B**). However, as expected, none of the strains activated TLR5 (flagellin) or TLR4 (LPS) signalling (data not shown). Several strains did not induce NF-κB activation in control cells containing only the pNIFTY reporter construct (data not shown). Interestingly, the amounts of cytokines induced in PBMCs by a particular strain did not correlate with the capacity of the same strain to activate the NF-κB pathway through TLR signalling pathways, suggesting that other MAMPs and/or strain properties influence the cell's inflammatory response. Indeed, even though HTF-112 was the strongest activator of the NF-κB inflammatory pathway in HEK reporter cells, stimulation of PBMCs with this particular strain hardly induced any cytokine secretion (**Figure 3.2**).

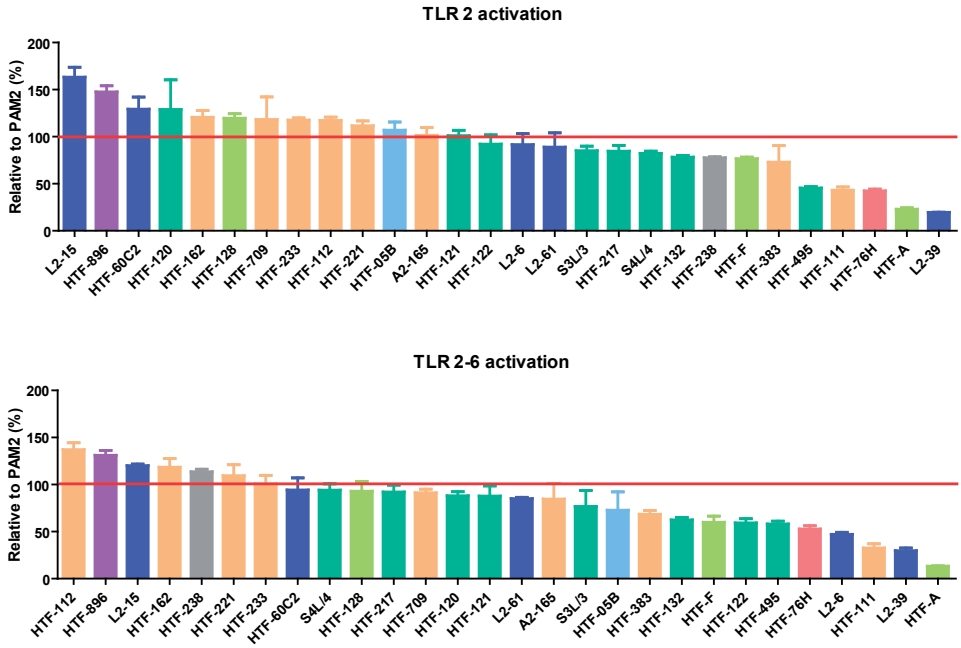

Figure 3.3A & B. Percentages of (A) TLR 2 and (B) TLR 2/6 activation level as a result of stimulation of TLR receptor cell lines with different *F. prausnitzii* strains. Activation levels of TLR 2 and 2/6 are depicted relative to the TLR2/6 agonist PAM2 (%). Error bars represent SEM, n = 3. Bar colours indicate phylogenetic cluster of the strains.

Immunomodulatory activity

To investigate the potential of the *F. prausnitzii* strains to modulate immune responses in PBMC we included heat-inactivated bacteria (HIB) as an innate stimulus. HIB induced secretion of all cytokines measured in our PBMC culture supernatant. For example, IL-10 increased from 5 pg/ml in supernatant of unstimulated PBMCs to 2000 pg/ml after addition of HIB (depending on the donor). Most *F. prausnitzii* strains either increased or had no significant effect on levels of secreted IL-10 by HIB stimulated PBMCs. A few strains, including HTF-112, HTF-60C2 and L2-39 decreased HIB induced IL-10 secretion (**Figure 3.4A**). Interestingly, all *F. prausnitzii* strains attenuated HIB induced IL-12 secretion (**Figure 3.4B**), whereas about half the strains were able to attenuate HIB induced TNFα secretion (**Figure 3.4C**).

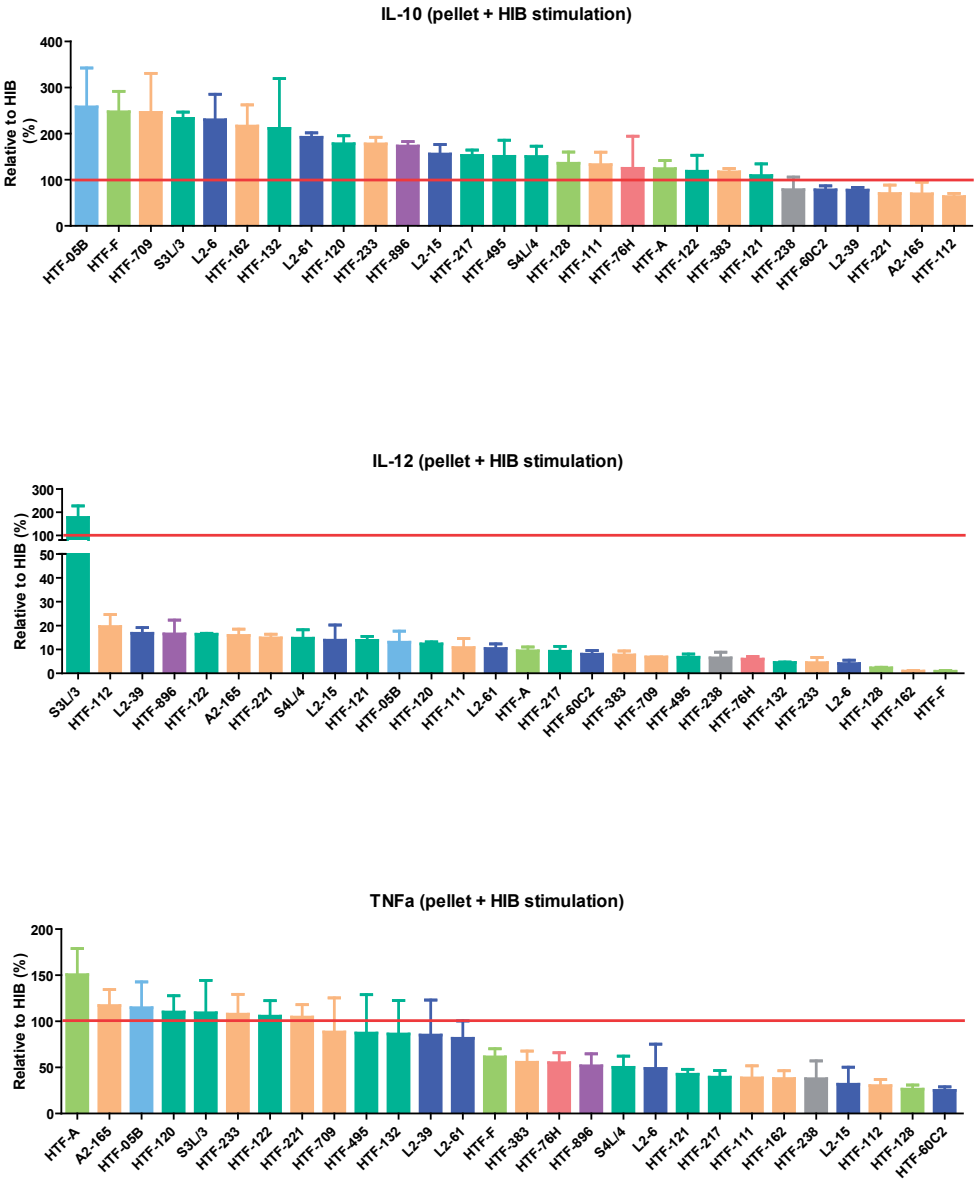

Figure 3.4A-C. Percentages of IL-10 (A), IL-12 (B) and TNF-α (C) secretion as a result of PBMC stimulation with HIB and different *F. prausnitzii* strains relative to HIB stimulation alone (red line 100%). Error bars represent SEM, n - 3 donors. Bar colours indicate phylogenetic clusters of the strains.

Nitric oxide production by RAW 264.7 cells stimulated with different *F. prausnitzii* strains

The levels of NO secretion after bacterial stimulation were compared to NO secretion as a result of (1 µg/ml) LPS stimulus. Addition of various *F. prausnitzii* strains, resulted in different levels of NO production by RAW 264.7 cells (range between 3 to 85 µM) (**Figure 3.5.**). Interestingly, there was no correlation observed between strains that induced high levels of cytokine secretion (**Figure 3.2.**) and strains that strongly induced NO (**Figure 3.5.**). Although there were some exceptions, for example strain HTF-05B, which strongly induced IL-10 and TNF-α secretion, also induced the highest levels of NO. Conversely, HTF-111, which only induced low amounts of IL-10 and TNF-α secretion, also induced the lowest amount of NO. To investigate if strains would be capable of attenuating LPS induced NO secretion, a combination of LPS with bacterial pellet was added to the macrophages. However, none of the investigated strains attenuated LPS induced NO secretion (data not shown).

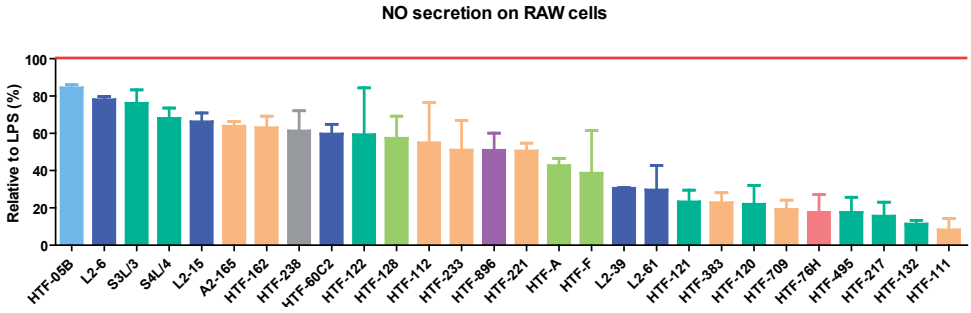

Figure 3.5. Percentages of NO secretion as a result mouse macrophage (RAW 264.7) stimulation with various F. prausnitzii strains. Concentration of NO is depicted relative to stimulation with LPS (100%) shown by red line. Error bars represent SEM, n = 3. Bar colours indicate phylogenetic clusters of the strains.

A heat map table was used to summarize the immunomodulatory capacity of each *F. prausnitzii* strain (**Table 3.1**). Except for IL-10 (marked with asterisk symbol), a gradient of green to red colour was used to mark low to high concentration or activation level measured in cytokines, NO and TLR. For cytokines and NO production, the red colour represents an inflammatory profile whereas the green indicates an anti-inflammatory profile. As can be observed from the table, the immunomodulatory capacity among *F. prausnitzii* strains is highly diverse. There were no similarities of immune profile observed among the strains belonging to the same phylogenetic cluster (**Table 3.1**).

Table 3.1. Summary of immune profile measured from various immune assays

Cluster	Strain	IL-10*	IL-12	TNF-α	IL-10* (+HIB)	IL-12 (+HIB)	TNF-α (+HIB)	IL-10*/IL-12	IL-10*/TNF-α	TLR2	TLR2/6	NO
C	L2-6	110.2	0.8	11.8	230.1	4.1	48.8	143.6	9.3	91.6	47.0	78.0
C	L2-61	41.0	1.0	13.1	192.1	10.4	81.7	42.3	3.1	89.0	85.0	29.6
C	HTF-60C2	23.5	1.0	3.6	78.3	8.0	25.2	23.2	6.5	129.3	94.2	59.6
C	L2-15	17.5	0.7	1.3	155.9	13.8	31.8	23.6	13.9	163.2	120.1	66.2
C	L2-39	1.5	0.1	0.5	77.5	16.7	85.0	13.4	2.9	19.6	29.7	30.5
E	HTF-896	33.3	0.7	5.6	173.1	16.5	51.7	45.2	5.9	147.6	131.0	50.8
G	HTF-162	122.3	0.3	23.5	216.4	0.9	37.9	360.6	5.2	120.6	118.4	63.0
G	HTF-709	104.5	0.5	21.8	246.1	6.8	88.5	219.9	4.8	118.2	91.2	19.2
G	HTF-233	99.5	0.5	63.5	177.8	4.5	107.8	138.2	1.6	117.6	100.5	51.0
G	A2-165	44.0	2.4	100.8	69.6	15.9	117.1	18.6	0.4	101.5	84.6	63.9
G	HTF-383	38.2	0.2	12.0	117.1	7.7	55.5	243.1	3.2	72.9	68.5	22.8
G	HTF-221	22.7	1.0	29.7	70.2	14.9	104.6	22.2	0.8	111.6	109.5	50.5
G	HTF-111	2.8	0.3	3.9	132.9	10.8	38.6	10.2	0.7	43.0	32.6	8.2
G	HTF-112	0.1	0.1	0.2	63.4	19.6	30.3	0.7	0.6	117.3	137.0	54.9
H	HTF-05B	193.0	3.5	126.5	258.0	13.0	114.8	54.6	1.5	106.9	72.7	84.4
I	HTF-238	5.2	0.4	2.3	78.5	6.5	37.8	12.3	2.3	77.6	113.6	61.3
J	HTF-F	144.9	0.6	43.2	247.4	0.9	61.5	223.1	3.4	76.6	59.9	38.6
J	HTF-128	43.8	0.3	9.9	135.8	2.3	26.5	111.5	4.4	119.6	93.0	57.4
J	HTF-A	36.0	0.3	10.9	124.2	9.4	150.5	107.9	3.3	23.0	13.2	42.7
K	HTF-76H	51.8	0.2	8.5	124.8	5.9	55.2	245.9	6.1	42.4	52.8	17.7
L	S3L/3	58.3	112.1	53.4	233.1	177.6	109.3	0.5	1.1	85.0	76.7	76.1
L	HTF-132	43.8	0.4	8.8	211.5	4.5	86.2	122.5	5.0	78.3	62.4	11.4
L	HTF-120	43.7	0.3	7.4	178.1	12.3	110.0	135.3	5.9	129.0	88.0	22.0
L	HTF-122	40.6	2.9	38.7	118.5	16.4	105.6	14.2	1.0	92.1	59.3	59.3
L	HTF-495	35.7	0.4	9.9	150.7	6.7	87.2	84.1	3.6	45.3	58.1	17.6
L	HTF-121	34.1	0.5	5.5	109.3	13.8	42.6	71.4	6.2	101.1	87.8	23.3
L	HTF-217	23.0	0.6	15.9	152.9	9.2	39.4	38.2	1.4	84.6	92.1	15.7
L	S4L/4	10.5	0.4	6.4	150.4	14.7	50.0	30.1	1.7	82.3	94.1	68.0

Red to green indicates high to low amounts of inflammatory cytokine, NO, or TLR-activation. For anti-inflammatory cytokines the colour scale is reversed (indicated by an asterix).

DISCUSSION

Previously, *F. prausnitzii* strains were reported to have a high capacity to induce IL-10 and little or no IL-12 in human and murine dendritic cells[21-23]. By using a large collection of human strains from different phylogenetic clusters we showed that induction of IL-10 secretion in PBMCs in fact varies considerably (5 - 4362 pg/ml) depending on the strain although strains A2-165 and HTF-F, which were previously studied in mouse models of colitis do indeed have high IL-10/IL-12 ratios (**Figure 3.2A**). In agreement with previous literature, all 28 strains (with the exception of strain S3L/3) induced very low IL-12 secretion (1 - 12 pg/ml). Therefore, the IL-10/IL-12 ratios mostly reflect the induction of IL-10 secretion by the strains (**Figure 3.2B**). In a previous study, high IL-10 to IL-12 ratios measured in PBMC assays correlated with a better protective capacity of lactic acid bacteria in mice colitis model[39]. IL-12 has a pivotal role in the generation of the Th1-dominant immune responses which are associated with Crohn's disease[102]. IL-12 generates a positive feedback by inducing IFN-γ secretion from natural killer (NK) and T cells which in turn leads to IFN-γ enhancement of IL-12 secretion by monocytes and polymorphonuclear cells[103]. In an *in vivo* model of mucosal tolerance induction to ovalbumin, intranasal administration of *F. prausnitzii* strain A2-165 with ovalbumin induced an approximately three-fold reduction in the percentage of ova-specific IFN-γ secreting cells which is consistent with the high IL-10 to IL-12 ratio elicited by this strain and its predicted influence on Th1 immune responses[21]. Furthermore, strain A2-165 was previously shown to protect against colitis in a TNBS/DNBS model of chronic relapsing colitis, where Th1 responses to haptenized host proteins drives inflammation and damage to the mucosa[21].

In this *in vitro* study we demonstrated that the immunomodulatory capacity among *F. prausnitzii* strains is highly diverse. There were no correlations observed between the phylogenetic cluster of the strains and their immune phenotype (**Table 3.1**). This interesting finding suggested that the immuno-phenotypes of *F. praunitzii* strains are strain specific and not linked to evolutionary differences in the genome.

Strain HTF-F is still among the strains that induced the highest IL-10/IL-12 ratios, but strains HTF-76H, HTF-383 and HTF-709 are quite comparable. Strain HTF-162 is even capable of inducing higher IL-10/IL-12 ratios and might therefore be an interesting candidate for further investigations (**Figure 3.2C)**.

However, IBD is also characterized by high levels of pro-inflammatory cytokines other than IL-12. We found TNF-α to be induced in higher amounts than IL-12 and therefore a potentially more useful predictor of immunomodulatory capacity than IL-12. Interestingly, although A2-165 and HTF-F both have been shown to have positive effects in animal colitis models, they both triggered quite high levels of the pro-inflammatory TNF-α. Both A2-165 and HTF-F are

among the 5 highest TNF-α inducers, with A2-165 only to be surpassed by HTF-05B (**Figure 3.2D**). In fact, HTF-05B appeared to have a quite unique immuno-stimulatory profile, as it induced very high or the highest level of each cytokine we measured. We would therefore assume that this strain would probably exacerbate any inflammatory disease. However, it would be interesting to test this hypothesis to see if *in vitro* results are predictive of *in vivo* outcomes.

Besides the immuno-stimulatory profile, some *F. prausnitzii* strains seem to have 'silent' or inhibitory immune profiles. Strains HTF-111 and HTF-112 consistently induced low amounts of IL-10, IL-12 and TNF-α in our PBMC assay. They were also among the strains that induced the lowest amounts of IFN-γ and IL-1β (**Supplementary Figure S3.1**).

Interestingly, the rank order among the strains based on the IL-10/TNF-α ratio is quite different compared to IL-10/IL-12 ratio. Strain L2-15 for example, which secreted low amounts of IL-10 and TNF-α had the highest IL-10/TNF-α ratio (**Figure 3.2E**), whereas the IL-10/IL-12 ratio was only moderate (**Figure 3.2C)**. Interestingly, the immunomodulatory strain A2-165, which secreted moderate amounts of IL-10 but high amounts of TNF-α, came in last in the IL-10/TNF-α ratio ranking order. However, the immuno-stimulatory strain HTF-05B, which secreted high amount of IL-10 and TNF-α, also had a very low IL-10/TNF-α ratio. Surprisingly however, for both the IL-10/IL-12 and the IL-10-/TNF-α ratios no correlation can be found between the immune phenotype and the strain phylogenetic clusters. Therefore it remains paramount to investigate the anti-inflammatory potential of each candidate probiotic strain.

Although it is informative to investigate the cytokine profiles each strain induces, the effect they elicit in an ongoing 'inflamed' situation is perhaps far more important. As IBD is characterized by a high bacterial load and a leaky gut we also investigated the immunomodulatory properties of the *F. prausnitzii* strains in combination with a heat inactivated bacterium (HIB), which strongly induced both pro- and anti-inflammatory cytokine secretion by PBMCs.

When we combined HIB with our immuno-stimulatory strain HTF-05B, we found that this strain further increased IL-10 secretion (**Figure 3.4A**), whereas the TNF-α secretion remained comparable to the levels induced by HIB only (**Figure 3.4C**). This higher level of IL-10 secretion might have beneficial effects, but as it is still accompanied by secretion of high levels of pro-inflammatory cytokines, the overall effect might not be optimal. Strain HTF-F also further increased the HIB induced IL-10 secretion, but was accompanied by a concomitant decrease of the HIB induced TNF-α secretion. This attenuated pro-inflammatory cytokine secretion combined with an increased anti-inflammatory cytokine secretion, might therefore account for the beneficial effects seen in mouse colitis models[23].

However, the 'silent' or inhibitory strains might also prove to have therapeutic potential. Although they do not affect the HIB induced IL-10 secretion levels, they are able to reduce the HIB induced TNF-α secretion. This unique signature of immune profile is a new finding for *F. prausnitzii* strains and might lead to new therapeutic strains. As these strains do not induce much cytokine secretion without additional stimuli present, they would not have an effect when a patient is in remission. However, when the inflammation flares up, strains with this unique signature are expected to dampen the inflammation by lowering pro-inflammatory cytokine secretion while maintaining a sufficient level of the anti-inflammatory cytokine IL-10, promoting immune homeostasis.

F. prausnitzii strains are Gram-positive bacteria and were therefore expected to activate NF-κB signaling pathway mainly via the TLR2 receptor which will result, among others, in cytokine production. Indeed all strains tested triggered TLR2 activation (**Figure 3.3**). Interestingly, the capacity to induce TLR activation was highly variable among the different strains. Moreover, there was no correlation between the level of cytokine secretion induced by the strains and their capacity to induce TLR2 activation. This result suggested that immune responses elicited by *F. prausnitzii* strains were affected by other unknown factors and not based solely on their capacity to activate TLR signalling. Strain HTF-112 was the strongest activator of the NF-κB inflammatory pathway in HEK reporter cells, whereas stimulation of PBMCs with this particular strain hardly induced any cytokine secretion (**Figure 3.2**). This suggests that strain HTF-112 has a specific mechanism to prevent cytokine secretion, even after the NF-κB pathway is activated.

Intestinal inflammation is intimately related to formation of reactive intermediates, including reactive oxygen and nitrogen species (ROS/RNS). Excessive production of either NO or ROS is detrimental to the host because of collateral damage to neighbouring cells. Oxidative stress has been proposed as a mechanism underlying the pathophysiology of IBD[55-57]. In this study we found that the novel *F. prausnitzii* strains induced different amount of NO in RAW 264.7 cell lines (**Figure 3.5**). Again we found that there was no correlation observed between the NO response in the tested macrophage cell lines and strain phylogenetic cluster, suggesting once more that the immunomodulatory properties of the novel strains are strain-specific.

Overall, the NO response as a result from stimulation with pellet of the *F. prausnitzii* strains was lower than the LPS (1 μg/ml) stimulation. This would suggest that these bacteria themselves do not induce high levels of oxidative stress response in host cells. Phagocytosis may involve in low induction of NO due to the presence of these bacteria, as this mechanism does not activate the signal for the induction of NO synthase activity in macrophages[104]. We also tested whether the *F. prausnitzii* strains would be capable of attenuating LPS induced NO production, and as such attenuate the effects of inflammation which are seen

in IBD. However, the tested strains were not able to reduce the inflammatory status of the macrophages as measured by their NO secretion (data not shown).

IL-10 is known to antagonise the function of IFN-γ by modulating the mechanism of NO synthesis in the murine macrophage cell line J774[104]. Further studies are therefore needed to investigate whether the strains that secreted high amount of IL-10 in our human PBMC assay were indeed among the lowest producers of NO and IFN-γ in murine macrophages. Only then, we can propose that IL-10 does indeed suppresses NO production which may lead to attenuation of IFN-γ in macrophages.

CONCLUDING REMARKS

The effort on exploiting the immuno-modulatory capacity of *F. prausnitzii* strains has steadily progressed over the past decade. However, the anti-inflammatory mechanisms have not been completely elucidated. In this study of 26 novel and two previously described strains, we conclude that each *F. prausnitzii* strain has specific immuno-modulatory properties. Based on our *in vitro* study, their capacities to induce immune responses, via activation of TLR signalling, or induction of cytokine or NO secretion, are not correlated with the phylogenetic clustering of the strains. In depth genomic analysis is warranted to discover putative signature genes linked to their immunomodulatory properties. The most interesting finding in this study is the discovery of three different signature immune profiles. The first is an immuno-stimulatory profile, as represented by HTF-05B, which is characterized by a strong induction of all cytokines investigated. The second is an immunomodulatory profile (for example HTF-F and HTF-162) which induced the secretion of the anti-inflammatory IL-10, but not of pro-inflammatory IL-12, and is suggested to be beneficial to treat inflammatory bowel diseases. The third and newly discovered 'silent' or inhibitory profile as represented by HTF-111 and HTF-112, which hardly induced any cytokine secretion in PBMCs. However, when inflammation is triggered, these strains are capable to attenuate the resulting pro-inflammatory cytokine secretion. This might prove valuable for IBD treatment, as these strains would not interfere during remission, but only during the inflammatory state of the disease. The new immune phenotypes of *F. prausnitzii* identified here, warrant further study *in vivo*.

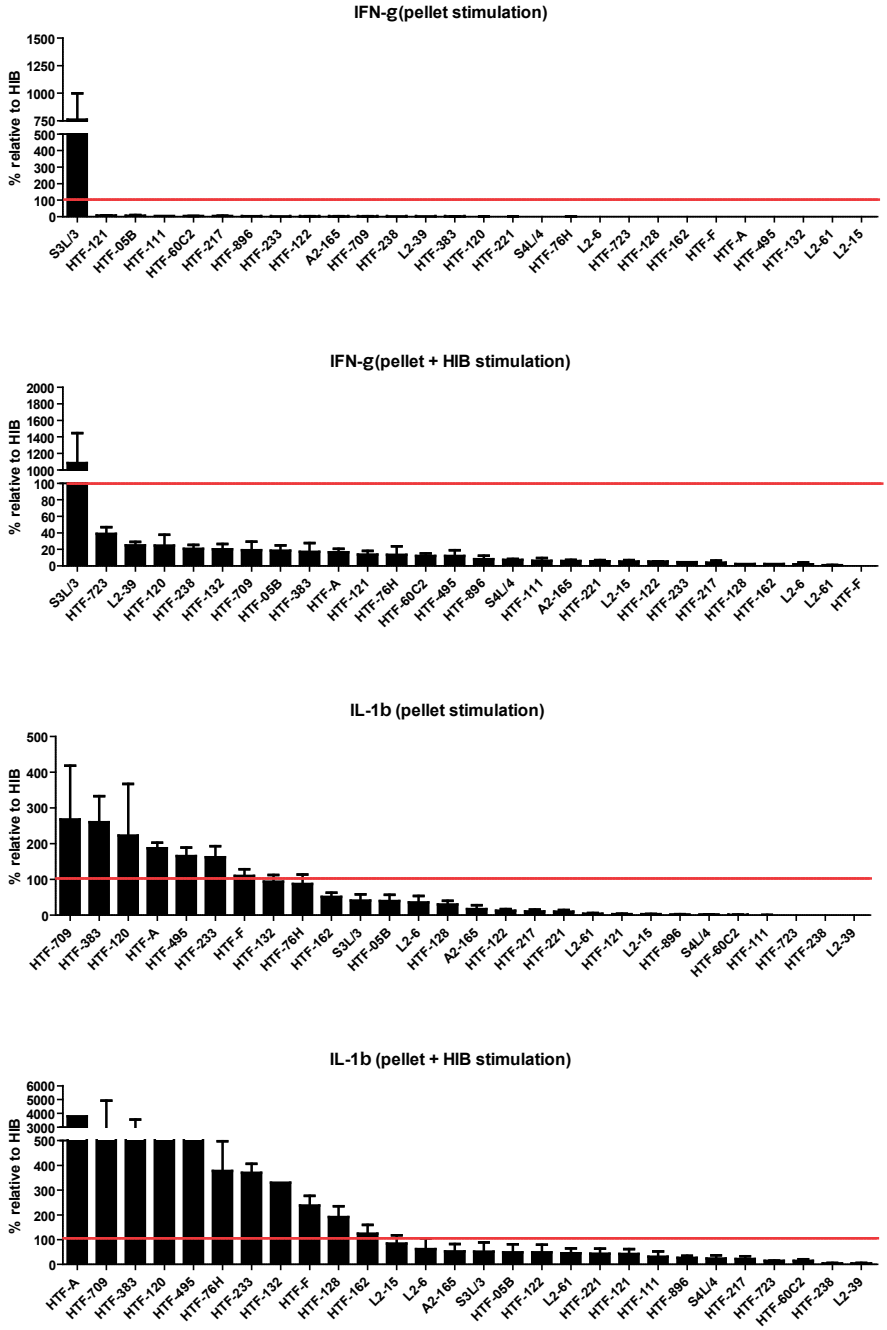

Supplementary Figure S3.1. Percentages of IFN-γ and IL-1β cytokines secretion measured in PBMC cultures after 24 hours incubation with different strains of *F. prausnitzii* strains, with or withouth HIB stimulation. Concentrations of IFN-γ and IL-1β are shown relative to positive control HIB (%). Error bars represent SEM, n = 3 donors. Red line indicates the amount of secreted cytokine induced by the positive control (100%)

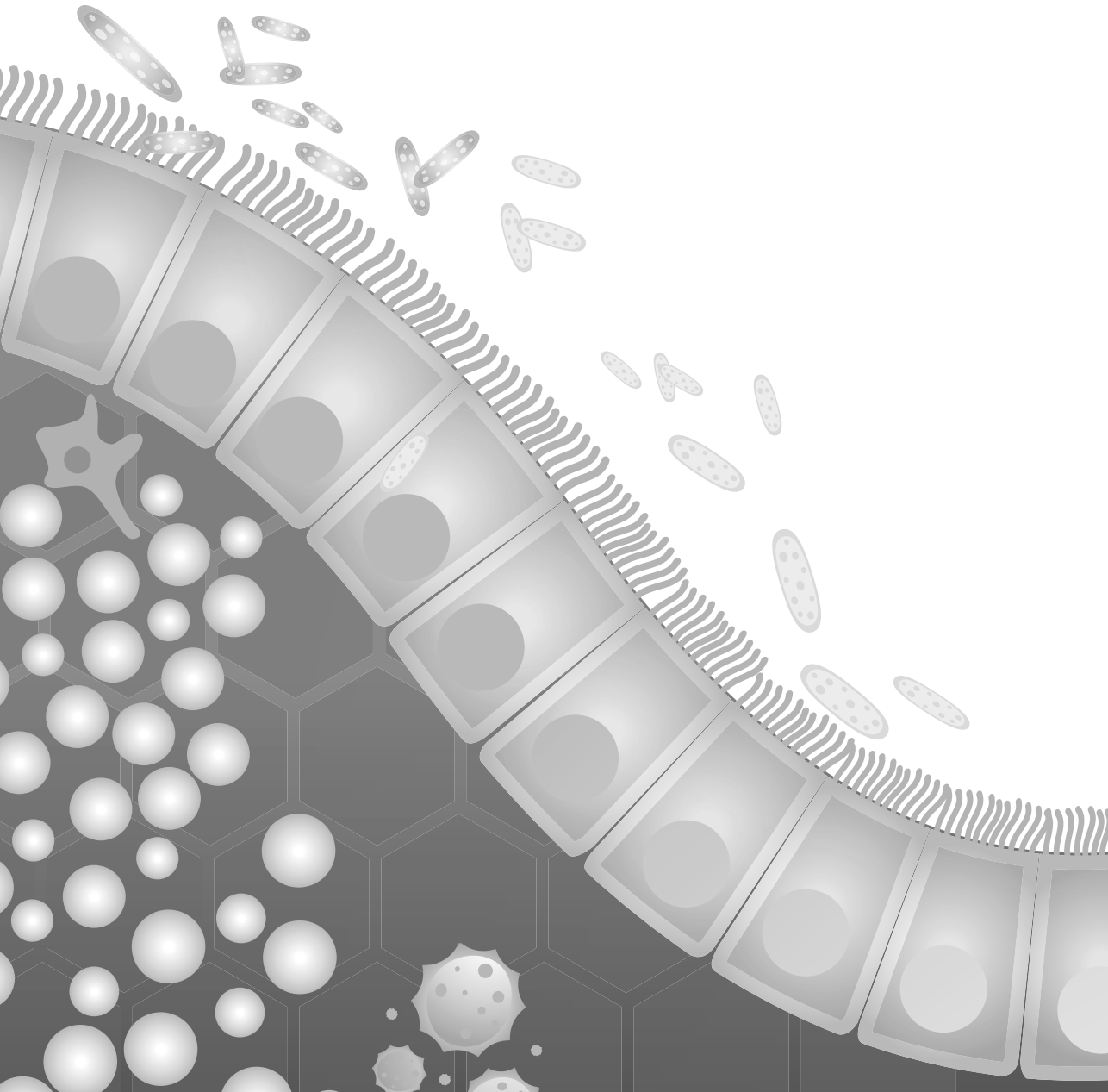

Chapter 4

Butyrate and acetate maintain an anti-inflammatory status in the gut through distinct mechanisms

Nuning Winaris[1,2], Ellen Kranenbarg[1], Jerry M. Wells[1]

[1] Host-Microbe Interactomics Group, Department of Animal Science, Wageningen University & Research, Wageningen, Netherlands

[2] Master Program in Biomedical Sciences, Faculty of Medicine, Universitas Brawijaya, Malang, Indonesia

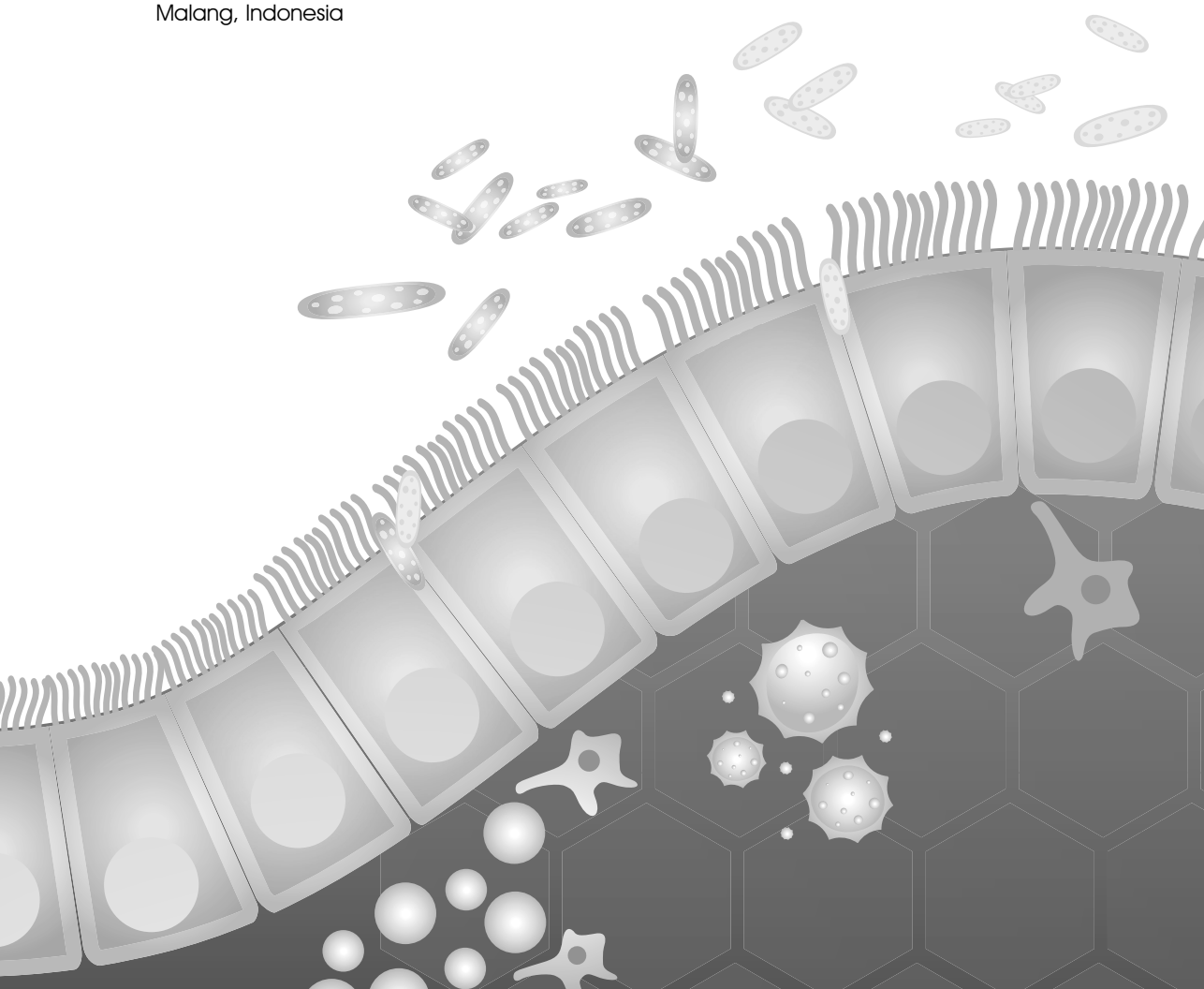

Abstract

Intestinal delivery of short-chain fatty acids (SCFAs) has been proposed as new approach for the management of inflammatory bowel disease (IBD). Butyrate has long been considered an anti-inflammatory molecule and was shown to induce regulatory T cells in the colon of mice, which are important for the regulation of inflammation. Acetate, which is present at highest concentration in the intestinal lumen and blood circulation, was shown to protect mice against colitis induced by 2,4,6-trinitrobenzene sulphonic acid (TNBS). The mechanisms by which different SCFA contribute to immune homeostasis in the gut are not fully understood but are important for future strategies to prevent or treat IBD. The aim of this study was to investigate the effects of acetate and butyrate on immune cell function and gain a better understanding of their mechanisms *in vitro*. Butyric and acetic acids were incubated with peripheral blood mononuclear cells (PBMCs) and $CD14^+$ monocytes in the presence or absence of aheat-inactivated bacterial stimulus for 24 hours to determine the effect on production of pro and anti-inflammatory cytokines. Concentrations of 1 to 5 mM of butyrate or acetate did not induce cytokine production in cultured PBMCs. However, butyrate strongly decreased pro-inflammatory cytokine secretion that was induced by a bacterial stimulus. Surprisingly, in our study we showed that butyrate also decreased secretion of the anti-inflammatory cytokine interleukin-10 (IL-10) and reduced the viability of PBMCs in a dose dependent manner. Acetate also decreased pro-inflammatory cytokine secretion in PBMCs in a concentration-dependent fashion but had not effect on production of anti-inflammatory IL-10 or cell viability. The anti-inflammatory effects of SCFA were independent of SCFA G protein-coupled receptor signalling. We conclude that SCFA produced by colonic bacteria play an important role in maintaining an anti-inflammatory tone in the intestinal mucosa. Acetate appears to mediate anti-inflammatory effects via a different mechanism to butyrate, a known inhibitor of class 1 histone deacetylases.

Keywords: short-chain fatty acids, anti-inflammatory, gut health.

INTRODUCTION

The anaerobic fermentation of non-digestible dietary fibre by colonic microbiota produces short-chain fatty acids, the most abundant being acetate, butyrate and propionate. Depending on the nature of fibers consumed, the concentration of SCFAs in the proximal colon ranges from 70 to 140 mM, and from 20 to 70 mM in the distal colon[58, 59]. Butyrate is used by colonocytes as an energy source and small amounts are found in the portal vein[60]. Acetate and propionate are transported across the basolateral membrane of the colonocytes mediated by an unknown HCO_3^- exchanger, most likely monocarboxylate transporter (MCT) 4 or 5[105]. Transported SCFAs then reach the liver and blood circulation through the portal vein. Acetate concentrations in the plasma and serum are around 50 to 100 µmol/L, whereas these are only 0.5 to 10 µmol/L for butyrate and propionate[59, 60]. The concentrations are anticipated to be much higher in the lamina propria and portal vein.

SCFAs are well-known to play an important role in maintaining barrier protection and regulate the inflammation status in the gut[63]. In addition to local effects on the gastrointestinal mucosal immune function, SCFAs may reach remote organs and modulate immune responses. SCFA are known to modulate several cellular process including gene expression, chemotaxis, differentiation and apoptosis. SCFA may activate signalling pathways through activation of G protein-coupled receptors (GPCRs) for SCFA. Additionally, butyrate and propionate can alter chromatin structure and gene expression through inhibition of histone deacetylases (HDACs), as well as affecting and stabilization of hypoxia-inducible factor (HIF)[64-67].

Several studies report anti-inflammatory activities of butyrate and studies in mice showed its crucial role in the induction of inducible regulatory T cells (Treg) in the colon[26, 68]. The SCFA receptor GPCR43, also known as free fatty acid receptor 2 (FFAR2), plays an important role in regulation of inflammation[69] and mice lacking this receptor exhibit more severe inflammatory responses in disease models[70]. Other SCFA receptors such as GPCR41 (FFAR3), GPCR109a (HCA2) and olfactory receptor-78 (Olfr-78) are known to mediate the effect of SCFAs on leukocyte and epithelial cells (IECs)[72, 106]. These findings support the concept of utilizing viable butyrate-producing bacteria like *Faecalibacterium prausnitzii* (*F. prausnitzii*) to maintain homeostasis and promote anti-inflammatory mechanisms in the host[22].

Besides the anti-inflammatory mechanisms of butyrate in the gut, it can also suppress proliferation of stem/progenitor cells by inhibiting HDAC and increase promotor activity for the negative cell-cycle regulator Foxo3[73]. Moreover, butyrate induced apoptosis in a colonic tumour cell line[74]. In contrast, acetate, which is present in higher concentrations in the large intestine and blood compared to butyrate or propionate, might be a better candidate as an anti-inflammatory compound. Acetate is reported to suppress interleukin (IL-8) production

in IECs of colonic mucosa, suggesting its capacity to protect the intestinal barrier[75]. Furthermore, administration of acetate effectively attenuated inflammation in mouse models of trinitrobenzenesulfonic acid (TNBS)-induced colitis and dinitrofluorobenzene-induced dermatitis[76]. In another mouse model, Thornburn et al. (2015) proved that maternal intake of acetate attenuates induced allergic airways disease (AAD) in the offspring[59]. This evidence suggests that there appears to be a significant role for SCFAs other than butyrate in mediating anti-inflammatory effects in the gut.

The aim of this study was to investigate the mechanism of the SCFAs acetate and butyrate in mediating anti-inflammatory effects on immune cells in the lamina propia. For this, we tested and compared the immune-modulating capacity of both butyrate and acetate on PBMCs, by measuring their cytokine responses as a model for leukocytes in the intestinal mucosa. Monocyte-derived dendritic cell (MDDCs) which are known to express GPCRs were also used to study the intracellular mechanisms of the SCFAs butyrate and acetate in mediating the immune response. In addition, detection of histone acetylation as a result of acetate and butyrate stimulation of PBMCs was performed in order gain insights into the potential role of epigenetic effects in immunomodulation.

MATERIAL AND METHODS

Isolation of peripheral blood mononuclear cells (PBMC) and SCFA stimulation

PBMCs were isolated from human blood donors from Sanquin blood Bank in Nijmegen, The Netherlands. Human blood was diluted 1:1 with Roswell Park Memorial Institute (RPMI) 1640 media (Thermo Fisher Scientific), then 25 ml of diluted blood loaded carefully on top of a 12.5 ml of Ficoll-paque (17-1440-02, Amersham). The leukocytes were isolated by centrifugation at 200 x g, 5 minutes (without brake) room temperature (RT), and then immediately 500 x g for 15 minutes without brake at RT. After centrifugation, the buffy coat (PBMCs /leukocyte layer) was collected and washed by centrifugation 200 x g for 7 minutes in RPMI. PBMCs were then plated in RPMI 1640 containing 10% foetal calf serum (Thermo Fisher Scientific) and 1% v/v penicillin, streptomycin (Invitrogen) in 96 well plate ($2x10^5$ cells/well) and stimulated with different SCFAs, with or without heat-inactivated bacteria as co-stimulation, followed by 24 hours incubation at 37°C, 5% CO2. After incubation, PBMC and culture supernatants were collected for viability and cytokine measurements respectively.

Annexin V/Propidium iodide (PI) viability staining

Annexin V/Propidium Iodide (PI) staining (BD Biosciences) was used to distinguish viable from early and late apoptotic or necrotic cells according to manufacturer's protocol. The cells were analysed using CytoFlex™ Flow Cytometry (Beckman Coulter).

Measurement of secreted cytokines from stimulated PBMCs

Major human inflammatory markers including the anti-inflammatory cytokine interleukin-10 (IL-10), and some pro-inflammatory cytokines such as interleukin-1 beta (IL-1B), interleukin-12p70 (IL-12p70), interleukin-6 (IL-6), interferon gamma (IFN-γ) and tumour necrosis factor (TNF-α) were measured to investigate the immunomodulatory effect of SCFAs on PBMCs. Cytokines were detected according to Bio-Plex Pro™ Human Cytokine Standard 27-Plex, Group I (BIO-RAD) kit, and their concentration was measured by using MAGPIX system (Luminex™) according to the manufacturer's recommended protocol.

Extraction and detection of histone H3 from Human PBMCs

Extraction and detection of histone H3 from human PBMCs was performed by using Histone Extraction Kit (Abcam, ab113476) followed by Histone H3 Total Acetylation Detection Fast Kit (Abcam, ab131561). These assays were performed according to the manufacturer's protocol.

Differentiation and maturation of monocyte-derived dendritic cells (MDDCs)

Human PBMCs were isolated according to our protocol mentioned above. CD14+ monocytes were then isolated using magnetic cell sorting with BD iMag CD14+ magnetic particle microbeads according to the manufacturer's protocol (Becton Dickinson). To generate MDDCs approximately 10^6 $CD14^+$ cells/ml were cultivated in 96 well plates. The cells were cultured in RPMI 1640 containing 10% v/v foetal calf serum (Thermo Fisher Scientific) and 1% v/v penicillin, streptomycin (Invitrogen), 50 ng/mL IL-4 (R&D System) and 50 ng/mL granulocyte macrophage-colony stimulating factor (GM-CSF) (R&D System). At day 3 and 6, half of medium was refreshed.

GPCR inhibitor assay

On day 6 monocyte-derived dendritic cells (MDDCs) were stimulated with pharmacological inhibitors of G protein receptors (GPCRs) recognising SCFA. One hour after adding the GPCR inhibitors, heat-inactivated bacteria (HIB) together with/without SCFAs were added to MDDCs in culture and incubated for 48 hours to stimulate cytokine secretion. MDDCs culture supernatant was harvested after 48 hours to measure secreted cytokines IL-10, IL-12p70, TNF-α, IL-6 and IFN-γ using Bio-Plex Pro™ Human Cytokine Standard 27-Plex, Group I (BIO-RAD) kit, and MAGPIX system (Luminex™).

TLR reporter assay

Human embryonic kidney (HEK293) (Invivogen) were transformed with different human Toll-like receptors (TLR1/2, TLR2 and 2/6, TLR4 and TLR5) and a NF-κB luciferase reporter construct (Invivogen). These cells were seeded at 6×10^4 cells per well into black, clear bottom 96-well plates in DMEM medium (Invitrogen), supplemented with 100 U/ml penicillin and 100 µg/ml streptomycin (Sigma Aldrich) and 10% FBS (Invitrogen) and incubated overnight at 37°C and 5% CO_2. Cells were stimulated with SCFAs or Trichostatin A (TSA; a class I and II HDAC inhibitor;

Sigma) for 1 hour and then stimulated with specific TLR ligands; 2.5 ng/ml Pam2PCSK (Pam2) (Invivogen), 200 ng/ml Pam3PCSK (Pam3) (Invivogen), 1 µg/ml lipopolysaccharides (LPS) (Sigma Aldrich), 50 ng/ml Flagellin (Invivogen) or with medium alone (negative control). The stimulated cells were then incubated for at least 3 hours. After this incubation period half of the medium was replaced with Bright glow (Promega), the plate was vortexed for 5 minutes and the luminescence was measured using a Spectramax M5 microplate reader (Molecular Devices) at 750 ms integration time. Human embryonic kidney HEK293 cells not expressing TLR receptors but harbouring pNIFTY, a NF-κB luciferase reporter construct (Invivogen) were used as a negative control in the TLR reporter assays.

Statistical analysis

The statistical analyses were performed by using GraphPad Prism® software (version 5, GraphPad Software, Inc). Results are shown as mean (± SEM). Significant differences among the treatment groups were analysed using non parametric test one-way ANOVA followed by a Tukey post hoc analysis (*$p<0.05$, **$p<0.01$, ***$p<0.001$). Letters above bars represent statistically significant differences between the treatment groups. Each graph bar with the same letter is not statistically different. Hashtag symbol (#) represent statistically significant differences between the treatment groups which have the same symbol.

RESULTS

Increasing concentrations of butyrate induce death of PBMC

PBMCs were incubated with different concentrations of acetate and butyrate to test their potential toxicity. In our study, PBMC preparations typically had between 70 - 90% of viable cells. Butyrate decreased PBMC viability in a concentration dependent manner, with some variability between PBMCs of different donors (**Figure 4.1**). In a separate experiment 5 mM butyrate decreased cell viability by up to 50% (data not shown). As acetate and butyrate are known to decrease the pH of cell culture medium, we also tested the effect of pH on cell viability and found that pH values above 6.8, which was the case for the concentration of SCFAs used for our stimulations, did not induce cell death (data not shown).

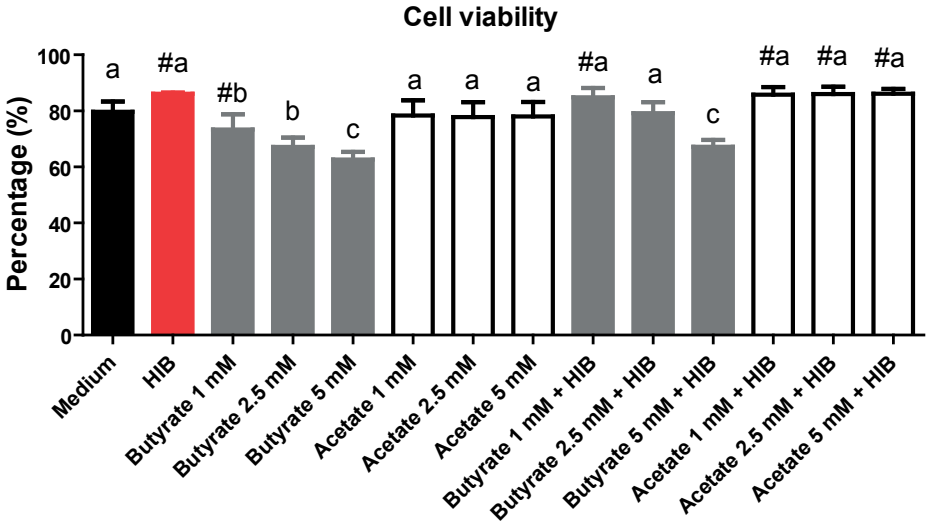

Figure 4.1. Cell Viability measured from stimulated PBMC. Percentage of cell viability measured in 3 different donors as a result of PBMC stimulation for 24 hours with various concentrations of butyrate and acetate. Error bars represent SEM.

Butyrate and acetate

We investigated the potential of butyrate and acetate to induce cytokine secretion in PBMCs or modulate cytokine responses to bacterial stimulation. Neither acetate or butyrate alone at a concentration of 1 mM induced pro- or anti-inflammatory cytokine secretion in PBMCs compared to controls (**Figure 4.2A-E**). However, when SCFAs are combined with heat-inactivated bacteria (HIB), we could clearly observe altered secretion of the pro- and anti-inflammatory cytokines. Butyrate significantly attenuated pro-inflammatory cytokine secretion stimulated by HIB (**Figure 4.3B-E**). Addition of 1 mM butyrate decreased secretion of pro-inflammatory and the anti-inflammatory cytokine IL-10 secretion (**Figure 4.2A**). In contrast, IL-10 secretion was unaffected by addition of 1 mM acetate. Although 1 mM acetate was less potent in attenuating pro-inflammatory cytokine secretion stimulated by HIB, we observed a trend towards decreased IL-12 and IFN-γ secretion (**Figure 4.3B&E**).

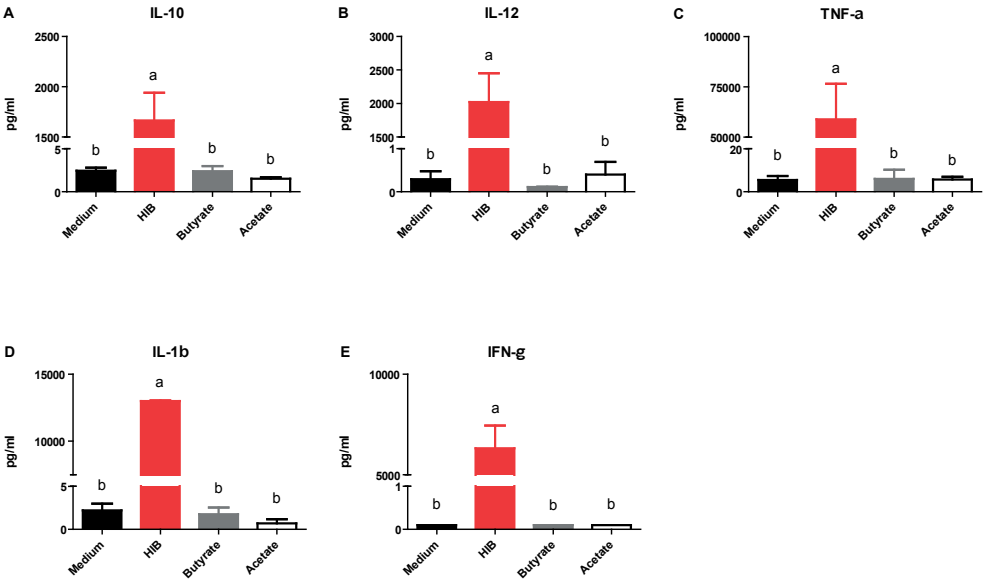

Figure 4.2(A-E). Butyrate and acetate do not induce pro & anti-inflammatory cytokines secretion on PBMC.Secretion of **(A)** IL-10, **(B)** IL-12, **(C)** TNF-α, **(D)** IL-1β and **(E)** IFN-γ by PBMCs as a result of 1 mM acetate or butyrate stimulation for 24 hours. Error bars represent SEM, n = 3 donors.

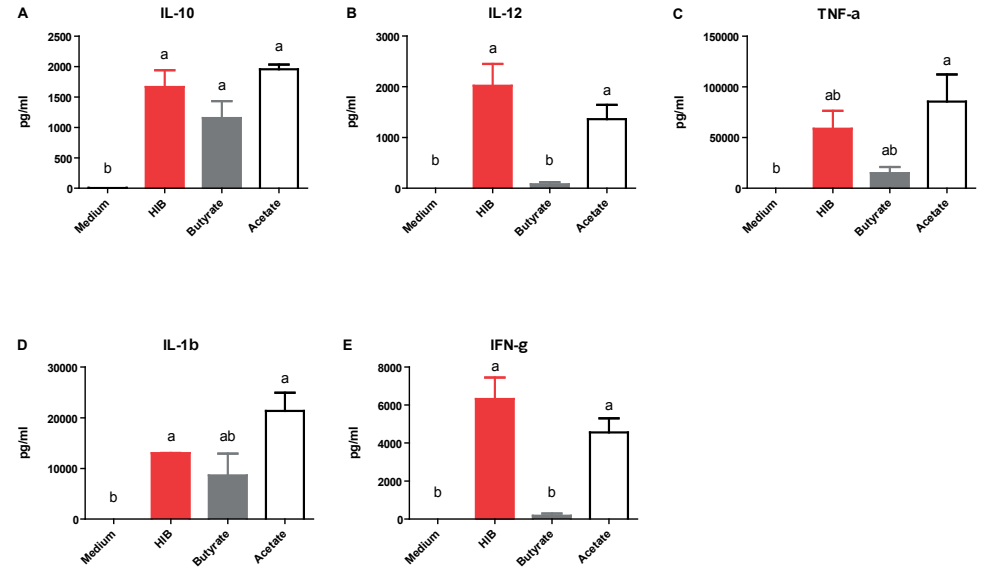

Figure 4.3(A-E). SCFAs modulate pro- and anti-inflammatory cytokines secretion induced by bacterial stimulus (HIB). Secretion of **(A)** IL-10, **(B)** IL-12, **(C)** TNF-α, **(D)** IL-1β and **(E)** IFN-γ by PBMCs as a result of HIB and 1 mM acetate/butyrate stimulation for 24 hours. Error bars represent SEM, n = 3 donors.

Butyrate attenuates secretion of IL-10 in a dose-dependent manner

In order to verify the effect of butyrate on mitigating HIB induced IL-10 secretion, a titration experiment was performed on PBMCs. The results showed that butyrate attenuated HIB induced IL-10 and pro-inflammatory cytokine secretion in dose-dependent manner. In contrast, increasing concentrations of acetate did not affect HIB induced IL-10 secretion, whereas they were able to reduce pro-inflammatory cytokine secretion (**Figure 4.4A-D**). As in previous experiments, acetate and butyrate alone did not induce cytokine secretion (data not shown).

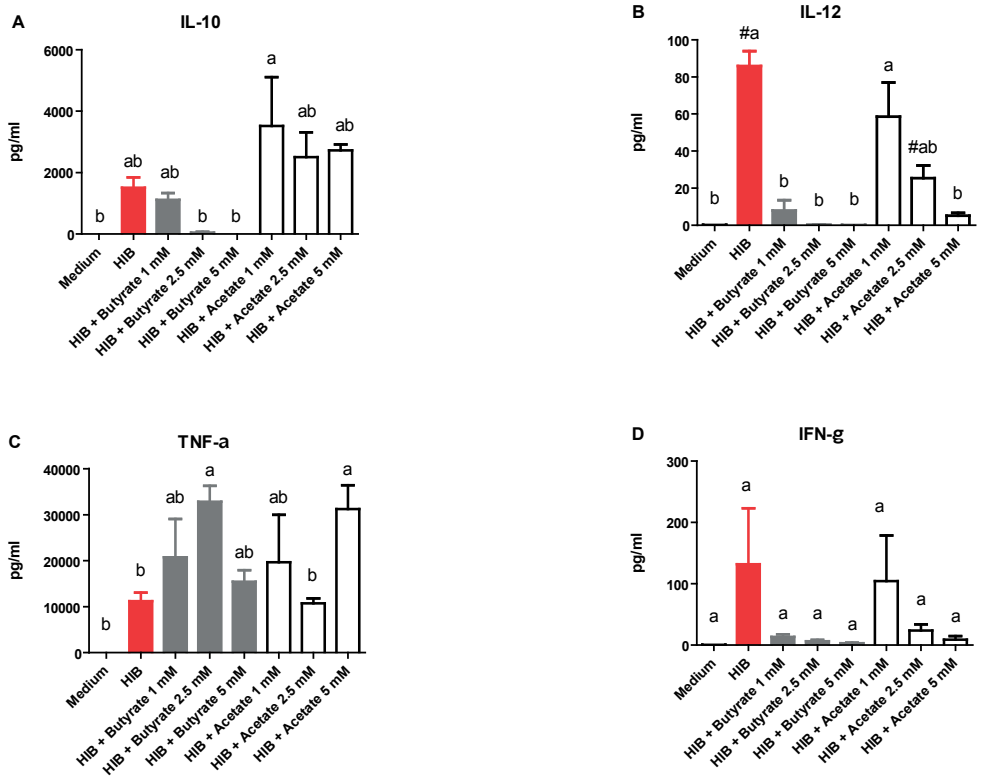

Figure 4.4(A-D). Butyrate is reducing IL-10 induced by bacterial stimulus (HIB) in dose dependent manner. Secretion of **(A)** IL-10, **(B)** IL-12, **(C)** TNF-α and **(D)** IFN-γ by PBMCs as a result of stimulation with HIB and various concentrations of acetate/butyrate stimulations for 24 hours. Error bars represent SEM, n = 3 donors.

Effects of acetate and butyrate on secretion of IL-10 and IL-12 in human CD14⁺ Monocytes

As monocytes are known as important target of SCFA, we investigated the effect of acetate and butyrate on CD14+ monocytes. Compared to PBMCs, which was a mixed cell population, the immune modulatory effects of acetate and butyrate were more strongly demonstrated by CD14⁺ monocytes, which was ≥95% pure (data not shown). As was seen with the PBMCs,

1 mM of butyrate was able to significantly reduce HIB induced IL-10 secretion. In contrast, 2.5 mM acetate did not affect IL-10 secretion by monocytes. Our results also showed a trend in attenuated HIB induced IL-12 secretion by acetate and butyrate, though the results were statistically not significant due to high variation among the donors. As expected, monocytes secreted only low levels of IFN-γ (**Figure 4.5A-F**). Importantly, viability of the cells did not differ among the treatments, suggesting the concentration of SCFAs used was not toxic for the monocytes (data not shown).

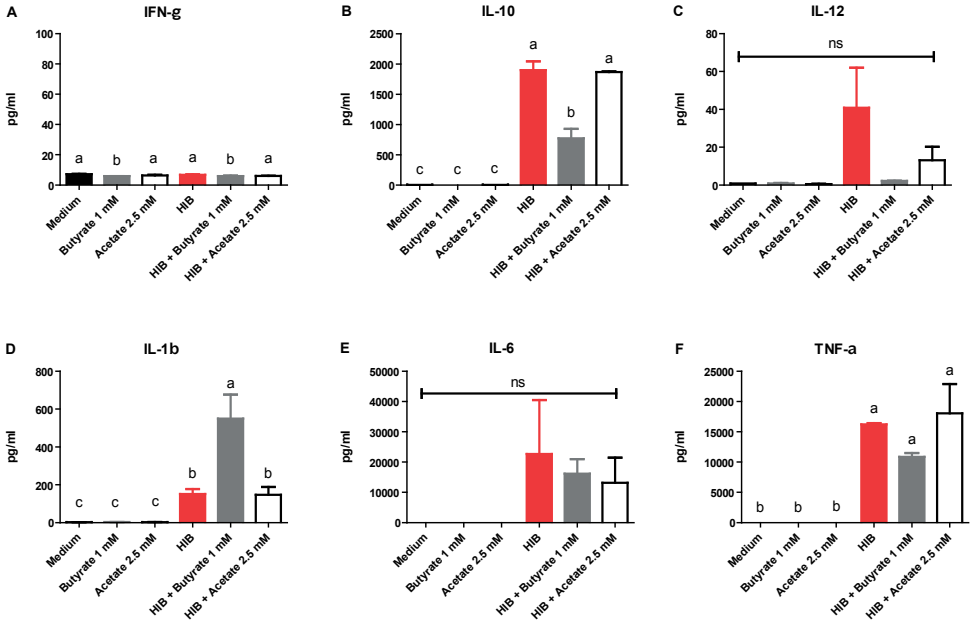

Figure 4.5(A-F). Cytokines modulation induced by acetate and butyrate on human CD14⁺ Monocyte Secretion of **(A)** IFN-γ, **(B)** IL-10, **(C)** IL-12, **(D)** IL-1β, (E) IL-6 and **(F)** TNF-α measured in CD14⁺ monocytes after stimulation with acetate and butyrate with and without the presence of HIB for 24 hours. Error bars represent SEM, n = 3 donors.

Butyrate and acetate modulate immune responses in monocyte-derived dendritic cells (MDDCs) through a G protein-coupled receptor (GPCR) independent mechanism

To investigate the mechanism of the immune modulatory responses induced by butyrate and acetate, we focused on the GPCRs as these are known receptors of SCFAs. MDDCs were used to study butyrate and acetate effects on GPCR signalling pathways. GPCR signaling in MDDCs was inhibited using Pertussis toxin (PTX) or specific inhibitors of G proteins Gi, Go and Gt and U73122 (Gq inhibitor). We showed that the effect of butyrate in attenuating pro and anti-inflammatory cytokine secretion elicited by HIB was not blocked by specific inhibitors

PTX and U73122, suggesting that the immunomodulatory capacity of butyrate was GPCR-independent (**Figure 4.6A-E**).

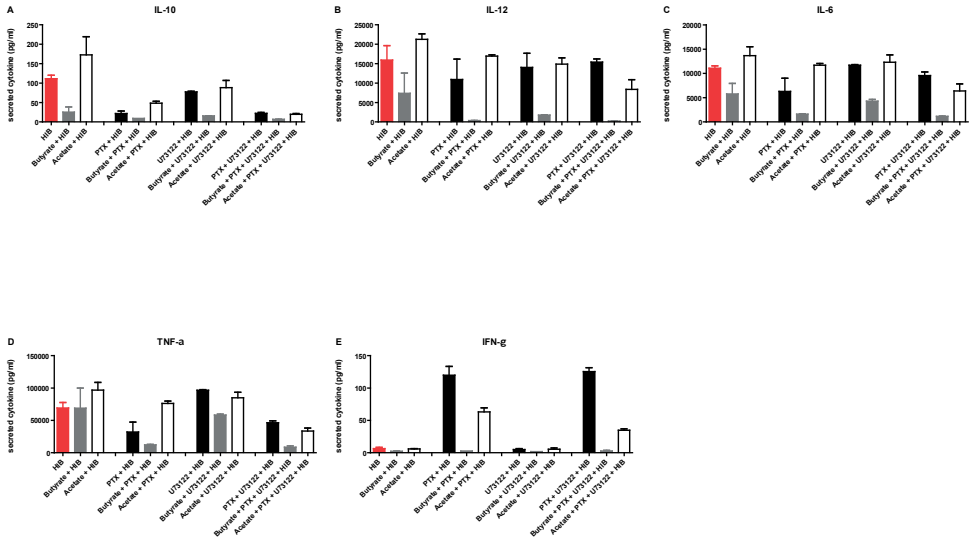

Figure 4.6. Butyrate modulates immune responses in MDDCs through GPR-independent mechanism. Cytokine secretion **(A)** IL-10, **(B)** IL-12, **(C)** IL-6, **(D)** TNF-α and **(E)** IFN-γ measured in MDDCs as a result of HIB stimulation in combination with butyrate/acetate and GPCR inhibitors for 24 hours. Other donors were tested and results were similar (data not shown).

Butyrate increased histone H3 acetylation of PBMCs and monocytes

To study the effect of butyrate and acetate on histone acetylation activity PBMCs were stimulated with butyrate and acetate for 5 hours, and after isolation of the histone proteins, total histone H3 acetylation was detected by using a histone acetylation detection kit. In this experiment Trichostatin A (TSA), a prototypical pan-histone deacetylase enzyme (pan-HDAC) inhibitor was used as positive control. Indeed, TSA at a concentration of 200 nM was able to increase histone H3 acetylation (see **Figure 4.7A**), confirming its reported inhibition of HDAC. The results showed that higher concentrations of butyrate increased histone H3 acetylation, while no significant affects were observed with acetate(**Figure 4.7A**).

To see if these acetylation effects were indicative of a more general mechanism of SFCA induced immune regulation, we also tested freshly isolated monocytes. Western blotting was used to detect the total amount of histone acetylation present in the monocyte samples. Our results showed that the amount of histone acetylation increased after 24 hours of 1 mM butyrate stimulation. Stimulation with 2.5 mM of acetate slightly increased total histone acetylation in monocytes. When acetate was combined with HIB, the total histone acetylation

increased noticeably. However, the effect became less visible when HIB was combined with butyrate(**Figure 4.7B**).

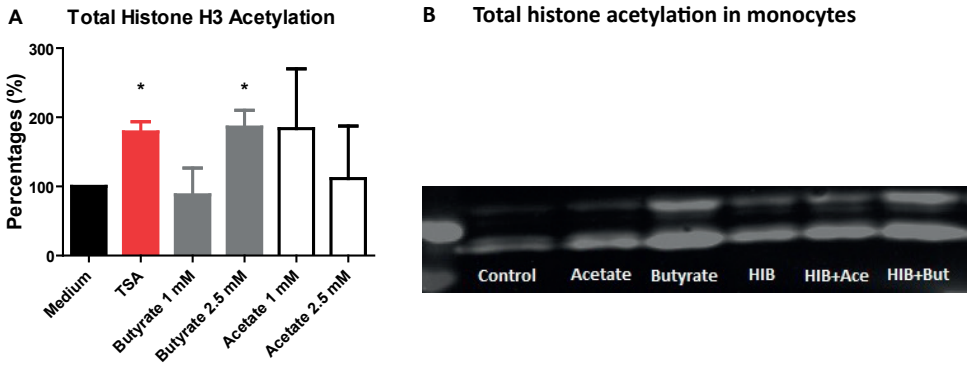

Figure 4.7(A-B). (A) Percentages of total histone H3 acetylation in PBMCs detected 5 hours after butyrate and acetate stimulation. Error bars represent SEM, n = 3 donors **(B)** Western-blot of total histone acetylation detected from monocyte samples 24 hours after stimulation with 2.5 mM acetate and 1 mM butyrate, with or without HIB.

Different mechanisms of NF-κB activation are mediated by acetate and butyrate

Activation of NF-κB is key in initiating cytokine secretion by immune cells. In this study we performed SCFA stimulation of HEK293 which expressed various kind of TLRs in order to investigate the effect of SCFA on NF-κB activation mediated by TLRs. We observed that acetate and butyrate, as well as TSA, suppressed NF-κB activation induced by respective ligands of TLR1/2, TLR2 and TLR2/6 or TNF-α stimulant. Conversely, the opposite response was observed in TLR4 and TLR 5 cells, where butyrate and TSA, but not acetate, enhanced NF-κB activation induced by respective ligands and TNF-α stimulant (**Figure 4.8**). These effects of the SCFAs were seen if we added the SCFA simultaneously with the ligands or TNF-α, as well as if we stimulated the cells with SCFAs one hour before addition of ligands or TNF-α (data not shown). Additionally, we used both the Na-acetate and Na-butyrate salts to obtain the same acetate and butyrate concentrations in our assay and found similar results (data not shown).

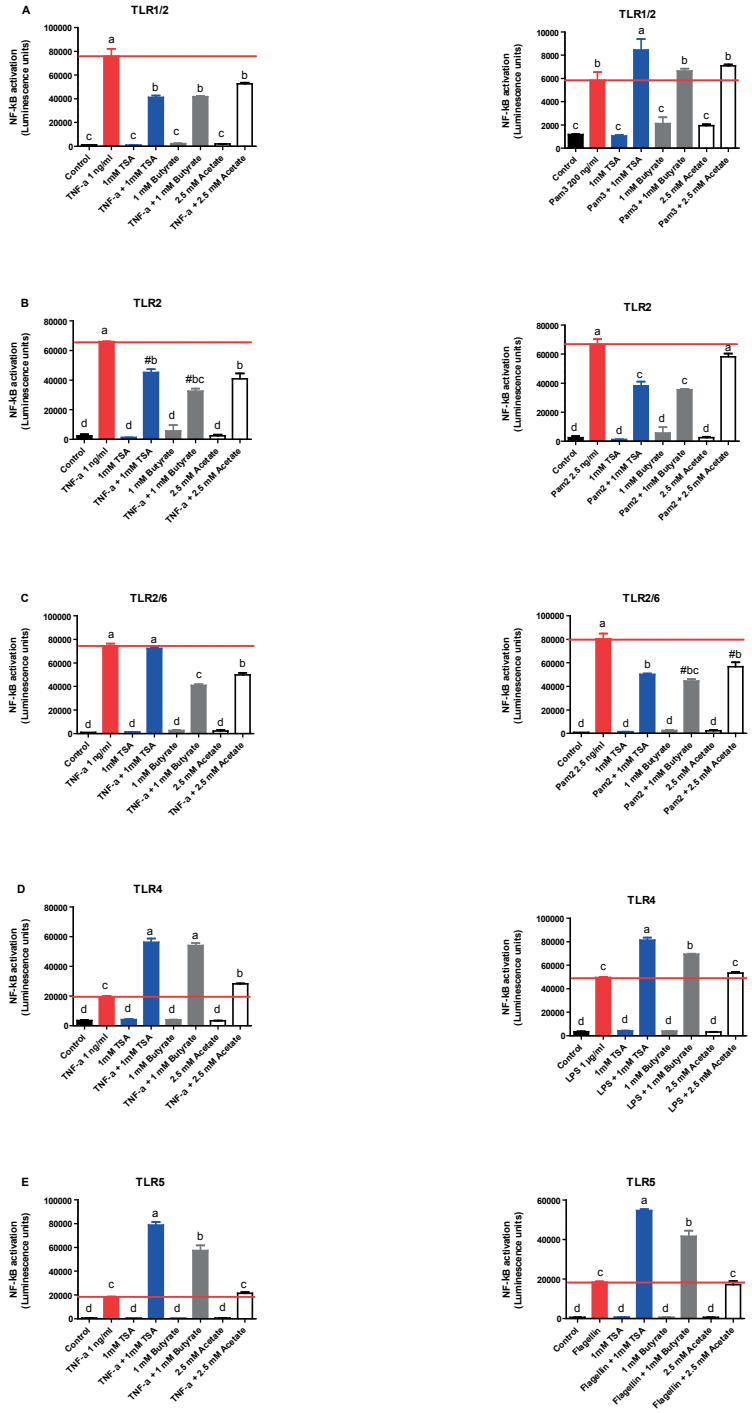

Figure 4.8(A-E). NF-κB activation mediated by **(A)** TLR1/2, **(B)** TLR2, **(C)** TLR2/6, **(D)** TLR4 and **(E)** TLR5. Activation level measured as a result of stimulation with TNF-α (left) or respective ligands (right), with or without additional SCFA/TSA. Red line indicates activation level induced by ligands or TNF-α stimulant.

DISCUSSION

Modulation of the immune response by SCFAs has been known to play an important role in maintaining an anti-inflammatory status in the gut. However, the mechanisms of immunomodulation by SCFA are not yet fully understood. Correa et al., (2016) stated that there are several factors that contribute to the immunomodulatory effects of SCFAs. Depending on the type of cell used, conditions, environment and also the type of stimulation; SCFAs can act both as pro- or anti-inflammatory compounds[58].

Butyrate is mostly taken up and metabolised by intestinal epithelial cells (IECs), whereas acetate is transported through IECs and finally enters the blood circulation via the portal vein to reach concentrations up to 250 uM in humans and mice[105]. Therefore the concentration of acetate may be sufficiently high in the lamina propria and venous serum to have effects on immune and tissue cells as suggested by recent studies in mice[59]. In this study we focused on acetate, a SCFA that is present in higher concentrations in the blood compared to butyrate.

One of the most interesting findings in our study is that acetate and butyrate (as well as other SCFAs) do not trigger an immune response when using concentrations that are even higher than normally observed in serum[107]. However, when immune homeostasis is disrupted by inflammation, SCFAs will modulate cytokine secretion in activated immune cells e.g. PBMCs, monocytes and DCs. In this study we used HIB, heat inactivated bacteria which trigger a strong immune response, resulting in secretion of both anti and pro-inflammatory cytokines in our immune assays. The capability of acetate in maintaining secretion of high levels of anti-inflammatory cytokine IL-10, as well as gradually dampening secretion of pro-inflammatory cytokines, is the key finding, that sets its beneficial effects apart from butyrate. High concentrations of acetate do not affect IL-10 secretion, yet effectively reduce pro-inflammatory cytokine secretion, particularly IL-12.

The IL-10/IL-12 ratio has been used to predict anti-inflammatory properties of probiotics *in vitro* and *in vivo* and an high IL-10/IL-12 ratio *in vitro* profile is predictive of a positive outcome in inflammatory diseases *in vivo*[39, 108]. The fact that acetate does not decrease IL-10 secretion, whereas butyrate does, could be paramount. IL-10 plays important role in maintaining an anti-inflammatory status by inhibition of IL-12 produced by activated DCs and macrophages. IL-12 is a critical stimulus for IFN-γ, the key player in innate and adaptive cell-mediated immune reactions against intracellular microbes, and IL-10 functions to suppress those reactions. IL-10 is also known to inhibit T cell activation and terminate cell-mediated immune reactions by downregulating the expression of co-stimulators and class II MHC molecules on DCs and macrophages[109]. To emphasise the important role of IL-10, Kuhn et al. (1993) conducted a study using knockout mice with an IL-10 gene deletion which led to

high susceptibility to spontaneous colitis[110-113]. Similarly, a mutation in the IL-10 receptor is known to result in severe colitis that develops in early life[114].

It is generally known that SCFAs activate GPCRs signalling pathways in order to modify several cellular processes such as gene expression, differentiation, proliferation and apoptosis[Correa et al., 2015]. GPR109a for example, is known to be involved in maintaining the balance between pro- and anti-inflammatory $CD4^+$ T cells. Singh et al. (2014) reported that incubation of macrophages and DCs with butyrate or niacin (agonist of GPR109a) lead to an increased expression of *Il-10* and *Aldh1a1* genes which contributed to differentiation of naive T cells to T regulatory (Treg) lymphocytes[115]. However, in our study we proved that butyrate modulated the immune response independent of SCFA induced GPCR signaling, as inhibitors used to block GPCRs expressed in MDDCs failed to block the SCFA induced effects on cytokines production. This result suggests that butyrate might activate other receptors expressed in MDDC which also lead to NF-κβ activation. Other receptors, such as Olfr-78, which is known to be expressed on leukocytes and IECs, are also reported to mediate the effect of SCFA in modification of several cellular process[106]. However, it remains to be investigated whether this receptor is also expressed on DCs and is thereby able to modulate cytokine production.
Inhibition of histone deacetylases (HDACs) which leads to enhancement of histone acetylation is often used to explain epigenetic effects of the SCFA butyrate on immune and epithelial cells, suggesting its role in regulating gene transcription[116, 117]. Indeed we found that butyrate increased the histone acetylation, most likely as a result of its inhibition of HDACs (**Figure 4.7**). In contrast, acetate showed less potent effects on inhibition of histone deacetylases (HDACs). This could suggest that acetate utilizes other molecular mechanisms to modulate anti -and pro-inflammatory cytokine secretion from immune cells. Inhibition of HDACs has been previously proposed as a molecular mechanism responsible for NF-κB activation mediated by TLRs[117]. In their study, Lin et al. (2015) suggested that butyrate and propionate suppressed HDAC leading to increased histone acetylation of NF-κB subunit p65 and increased NF-κB transcriptional activity. They demonstrated that butyrate and propionate enhanced NF-κB activation induced by respective ligands of TLR 2/1, TLR4, TLR5 and TLR9[117]. In contrast, our study showed that butyrate and TSA (inhibitor of HDAC), suppressed ligand induced NF-κB activation in TLR1/2, TLR 2 and TLR2/6 expressing HEK293 cells as well as the response to TNF-α. However, TLR4 and TLR5-mediated NF-κB signaling was induced by both butyrate and TSA. Interestingly, this increase of NF-κB signalling via TLR4 and TLR5 activation was not observed after stimulation with acetate, which might reflect another immuno-modulatory effect of acetate. Above mentioned findings indicate that NF-κB signalling mediated by TLR activation is complex. This is also reflected by the fact that the mechanism of NF-κB signalling activated by TLR1/2, TLR2 and TLR2/6 uses different adapter proteins compared to TLR4 and TLR5[46].

CONCLUDING REMARKS

The concept of bacterial-based metabolite treatment has been developing rapidly over the past few years. SCFAs have been some of the “well-known, yet still hard to explain” bacterial metabolites that have been studied for years. Many studies demonstrated the beneficial effect of SCFAs, yet inconsistency of the results and as of yet undiscovered mechanisms of function are often limiting their therapeutic application. Based on our study we conclude that acetate has a concentration-dependent immunomodulatory effect on cytokine secretion by immune cells. It can selectively inhibit inflammation induced pro-inflammatory IL-12, while not affecting the beneficial anti-inflammatory IL-10. This would lead to a more favourable IL-10/IL-12 ratio and a skewing of the immune response into a more regulatory and ‘damage repair’ mode which would be beneficial in inflammatory diseases. Future research should focus on the effect on histone acetylation, a mechanism that is often used to explain epigenetic effect of SCFAs.

ACKNOWLEDGEMENT

The authors would like to thank Bart Lagerwaard for his help with the Western-blotting experiment.

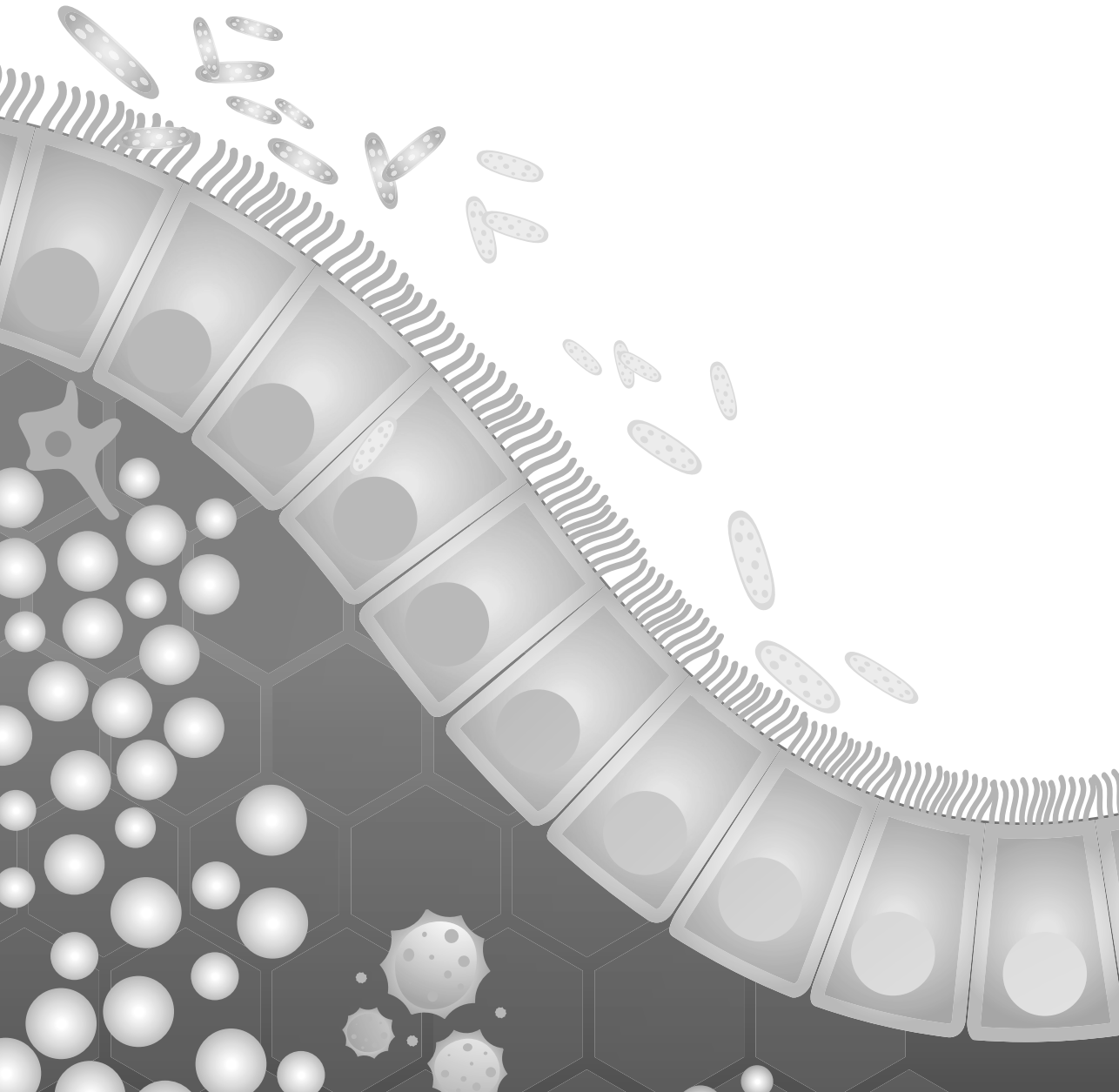

Chapter 5

Transcriptomic studies reveal new insights into the immunomodulatory mechanisms of short-chain fatty acids

Nuning Winaris[1,2], Ellen Kranenbarg[1], Jerry M. Wells[1]

[1] Host-Microbe Interactomics Group, Department of Animal Science, Wageningen University & Research, Wageningen, Netherlands

[2] Master Program in Biomedical Sciences, Faculty of Medicine, Universitas Brawijaya, Malang, Indonesia

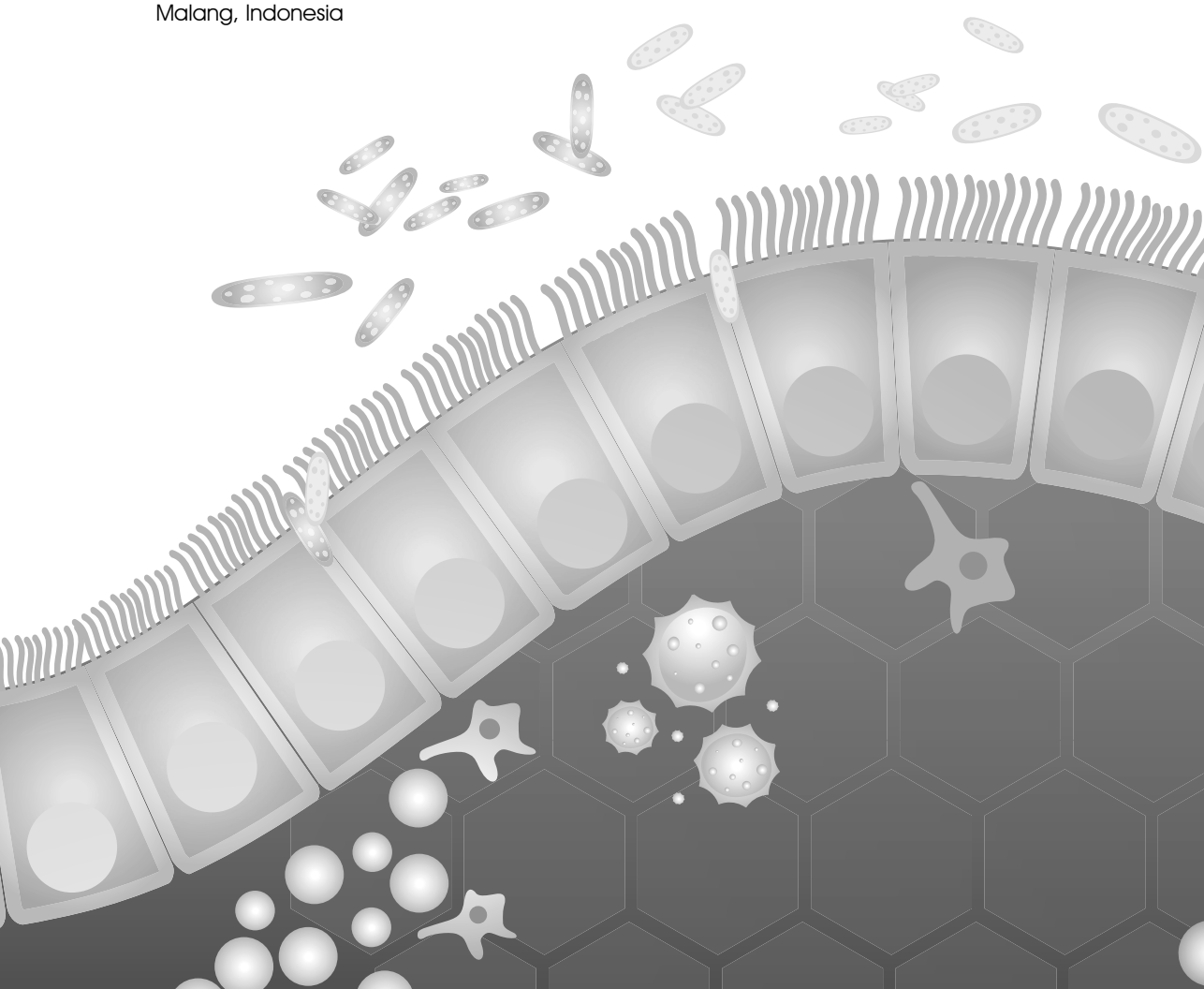

Abstract

Short-chain fatty acids (SCFA) are reported to influence several cellular processes, including differentiation, proliferation and apoptosis, although the mechanisms have yet to be fully explained. A previous study demonstrated an effect of SCFA on the transcriptome of monocyte-derived dendritic cells. However, that study gave little attention to the effects of acetate on the immune response. Here we investigated the mechanism by which acetate and butyrate modulate cytokine secretion in CD14+ monocytes using transcriptomics in absence and presence of heat-activated bacteria (HIB). The anti-inflammatory mechanisms of acetate and butyrate were associated with distinct transcriptomic signatures. Acetate had less effect than butyrate on gene expression and canonical pathway activation. When combined with HIB, acetate was able to modulate cytokine production, particularly IL-10, mainly via the interferon signalling pathway and TLR signalling pathway. On the other hand, butyrate suppressed HIB-induced IL-10 secretion, mediated through the IL-10, NF-κB and TLR signalling pathways. Moreover, 1 mM butyrate decreased cell viability of the monocytes and regulated stress related-responses of the cells as well as many disease-related pathways. Our findings highlight the differential molecular mechanisms of acetate and butyrate in modulating the immune response of the host and support our hypothesis that acetate might be a better candidate for future anti-inflammatory treatments.

Keywords: SCFA, transcriptomic, CD14+ monocytes, anti-inflammatory

INTRODUCTION

Short-chain fatty acids such as butyrate, propionate and acetate are produced by microbial fermentation in the intestine and have been reported to affect many cellular processes including chemotaxis, differentiation, proliferation and apoptosis. SCFA have been proposed to modulate host responses via G protein coupled receptors (GPCRs) for SCFA and via epigenetic mechanisms[64, 66, 67] which contribute to intestinal homeostasis[118-120].

Previous studies on the anti-inflammatory effects of SCFA[70, 121, 122], have focused mainly on butyrate, and to a lesser extent on propionate[123, 124] and acetate[59, 76]. Butyrate, and propionate have immunosuppressive effects on chemokine and cytokine secretion *in vitro*[67, 125-127], with butyrate often having stronger suppressive effects than propionate. One study on acetate described it less potent than butyrate in supressing cytokine and chemokine secretion induced by lipopolysaccharides (LPS) in human monocytes[125]. *In vivo* butyrate induced regulatory T cells in the colon of mice, which is important for the regulation of inflammation[26, 68, 128]. Butyrate has also been shown to attenuate colitis in mouse models[129].

Ishiguro et al., (2007) demonstrated that acetate inhibits nuclear factor of activated T-cells (NFAT), a transcription factor other than NF-κB which plays an important role in regulating the activation of T cells, by interfering with the interaction between NFAT and importin β1 in T cells. NFAT plays an important role in the pathogenesis of inflammatory disorders such as inflammatory bowel disease (IBD). Therefore investigating the effect of acetate on regulating the molecular mechanism of NFAT in T cells may lead us to novel therapeutic applications of acetate against IBD or other inflammatory diseases. Additionally, they also showed that intraperitoneal administration of acetate attenuated disease symptoms in a TNBS-induced mouse model of colitis[76]. Recently, Thornburn et al. (2015) showed that maternal intake of acetate in the drinking water protected the offspring against allergic airways disease (AAD) [59]. Together these studies provide evidence that acetate plays an important role preventing immune-related diseases.

Nastasi et al. (2015) investigated the effect of acetate, butyrate and propionate exposure on the transcriptome of monocyte-derived dendritic cells (MDDC) and showed that butyrate and propionate had a much larger effect on gene expression than acetate. Butyrate and propionate were suggested to regulate leukocyte trafficking by suppressing expression of several chemokines. Additionally butyrate and propionate inhibited expression of LPS-induced cytokines IL-6 and IL-12[130]. However, this paper offered little attention to the effects of acetate on the immune response.

In this study, we demonstrate that acetate (2.5 mM) did not reduce secretion of IL-10 secretion in $CD14^+$ monocytes stimulated with heat-inactivated bacteria (HIB), but significantly decreased pro-inflammatory IL-12 cytokine secretion. However, butyrate decreased secretion of all cytokines induced by HIB in a dose dependent manner. We investigated the mechanism by which acetate and butyrate modulate cytokine secretion in $CD14^+$ monocytes using transcriptomics to gain an insight into pathway regulation in absence and presence of immune stimulation with heat-activated bacteria (HIB).

MATERIALS AND METHODS

Isolation and purification of $CD14^+$ monocytes

Peripheral blood mononuclear cells (PBMCs) were isolated from human blood donors obtained from Sanquin blood Bank in Nijmegen, The Netherlands. Human blood was diluted 1:1 with Roswell Park Memorial Institute (RPMI) 1640 media (Thermo Fisher Scientific) and 25 ml dripped carefully onto 12.5 ml Ficoll-paque (17-1440-02, Amersham). Leukocytes were isolated by centrifugation at 200 x g, 5 minutes (without braking) room temperature (RT), followed immediately by centrifugation at 500 x g 15 minutes (without braking) at RT. After centrifugation, the buffy coat layer, containing the PBMCs was collected and washed by centrifugation 200 x g for 7 minutes in RPMI. $CD14^+$ monocytes were then isolated using magnetic cell sorting with BD iMag $CD14^+$ magnetic particle microbeads according to the manufacturer's protocol (Becton Dickinson). The $CD14^+$ purified monocytes were plated in RPMI 1640 containing 10% foetal calf serum (Thermo Fisher Scientific), 1% v/v penicillin, streptomycin (Invitrogen) in a 96 well plate ($2x10^5$ cells/well) and rested overnight prior to carrying out the experiments with SCFA. The $CD14^+$ purified monocytes were stimulated with different SCFAs, with or without heat-inactivated bacteria as co-stimulation and incubated 37°C, 5% CO2 for 5 or 24 hours. Supernatant from stimulated cells was harvested for measurement of cytokines and stored at -20°C until analysis. The remaining cells were used for a viability assay.

Harvesting and RNA isolation protocol

The $CD14^+$ monocytes were incubated with non-toxic concentrations of acetate (2.5 mM) and butyrate (1 mM) for 1 hour, followed by addition of heat-inactivated bacteria (HIB), or medium control and incubated for 5 h at 37°C, 5% CO_2. After incubation, the monocytes were centrifuged for 10 min at 300 x g at RT and then washed in PBS using the centrifugation protocol described above. The supernatant was then carefully removed and lysis buffer (Qiagen) added to lyse the monocytes. Total RNA was immediately extracted according to the manufacturer's protocol (RNEasy mini-kit, Qiagen). Total RNA concentrations were measured using Qubit 4 Fluorometer (Invitrogen) and RNA quality (230/260 and 260/280 ratios) was checked with a DeNovix spectrophotometer.

mRNA sequencing and transcriptomic analysis

Total RNA samples from acetate, butyrate, or medium-treated monocytes were sequenced on an Illumina sequencing system by Novogene. Quality checks were then performed for the output reads (sequences) using a CLC Genomic Workbench (QIAGEN). Reads were mapped to the human genome reference (GRCh38.p13, Gene bank), and subsequently processed for further downstream analysis. Differential analysis was performed using the CLC Genomic Workbench (QIAGEN) with $P < 0.05$ and $FDR < 0.05$ for determination of significant differences. Gene ontology and pathway integration were performed by ingenuity pathway analysis (IPA).

Annexin V/Propidium iodide (PI) staining for cell viability

Annexin V/Propidium Iodide (PI) staining (BD Biosciences) was used to distinguish viable from early and late apoptotic or necrotic cells according to manufacturer's protocol. The cells were analysed using CytoFlex™ Flow Cytometry (Beckman Coulter).

Measurement of secreted cytokines from stimulated CD14$^+$ monocytes

Human anti-inflammatory cytokine interleukin-10 (IL-10), and pro-inflammatory cytokines interleukin-1 beta (IL-1B), interleukin-12p70 (IL-12p70), interleukin-6 (IL-6), interferon gamma (IFN-γ) and tumour necrosis factor (TNF-α) were measured in culture supernatants to investigate the immunomodulatory effect of SCFAs on CD14$^+$ monocytes. Culture supernatant from stimulated CD14$^+$ monocytes was harvested after 5 and 24 hours incubation to measure the secreted amount of each cytokine. Cytokines were detected using multiplex ELISA; a Bio-Plex Pro™ Human Cytokine Standard 27-Plex, Group I (BIO-RAD) kit, and their concentration was measured by using a MAGPIX system (Luminex™) according to the manufacturer's recommended protocol.

RESULTS

CD14$^+$ monocytes were pre-treated with 1 mM butyrate or 2.5 mM acetate and after 1 hour, an additional HIB stimulus was added and RNA was isolated after 5 hours for RNAseq. Principle component analysis (PCA) of gene expression data was used to examine the variability between the samples (**Figure 5.1A**). We observed that samples from the same treatment group clustered closely together with exception of one HIB stimulated sample. Monocytes exposed to acetate clustered closer to the control samples (RPMI medium) than the butyrate-treated samples indicating a stronger treatment effect for butyrate treated cells. Similarly, butyrate had a much stronger treatment effect than acetate when combined with the HIB stimulus.

A clustered heat map (double dendrogram) showing similarity of differentially expressed genes among the different treatments was generated (**Figure 5.1B**). This clustered heat map

dendrogram, also showed the differences between control and SCFA treated groups and revealed that butyrate had a stronger treatment effect than acetate with or without the HIB stimulus (**Figure 5.1B**).

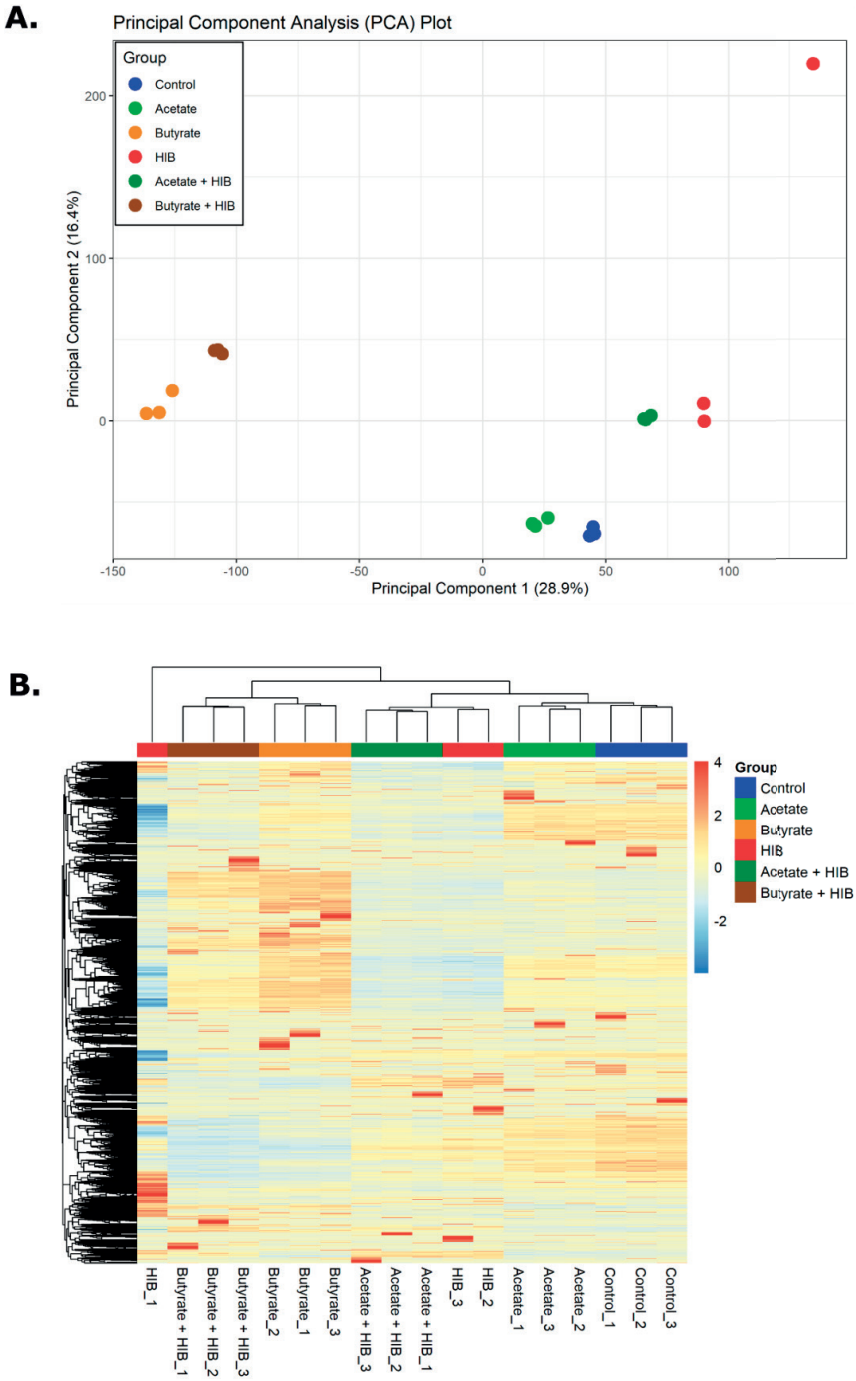

Figure 5.1. **(A)** Principle component analysis (PCA) plot showing the clustering of samples based on the different treatments; **(B)** The overall results of RPKM cluster analysis, clustered using the log10(RPKM+1) value. Red denotes genes with high expression levels, and blue denotes genes with low expression levels. The colour ranges from red to blue representing the log10(RPKM+1) value from high to low.

The number of genes significantly up- or down regulated due to the different treatments and the number of regulated genes in common between treatments are shown in Venn diagrams (**Figure 5.2A**). Butyrate alone elicited a larger number of upregulated (3522 vs. 71) and downregulated (3551 vs. 62) genes compared to acetate (FDR $p < 0.05$). The number of differentially expressed genes (up and downregulation) in acetate and butyrate treated groups was further increased by addition of HIB. Samples treated with HIB only, resulted in a large number of upregulated (2251) and downregulated (2461) genes compared to the medium control, although this number was considerably smaller compared to the effect of butyrate exposure (**Figure 5.2A left & right**) as observed in the Volcano plots (**Figure 5.2B-C**).

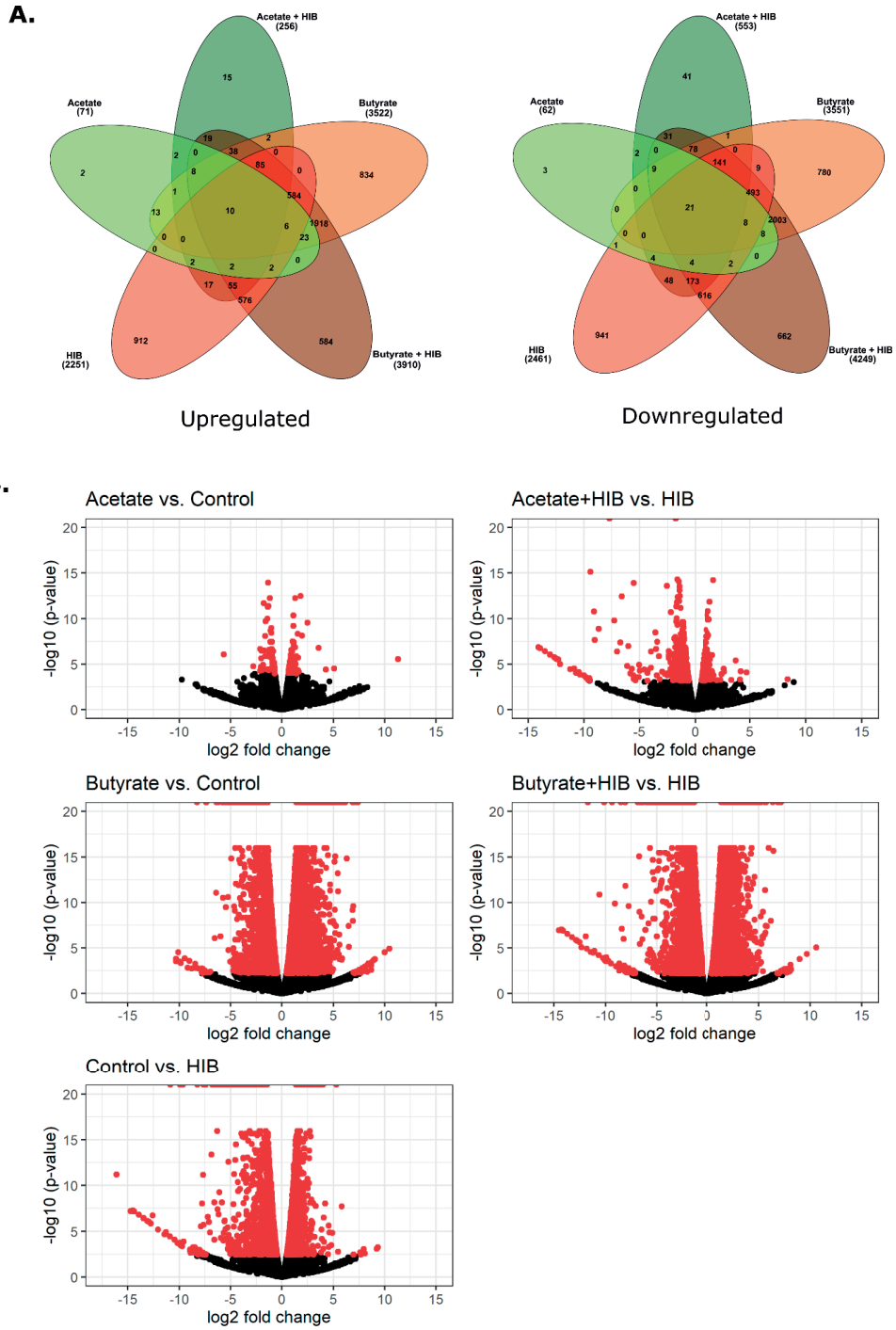

Figure 5.2. **(A)** Venn diagram representing the number of upregulated genes (left) and downregulated (right) genes; **(B)** Volcano plot of differentially expressed genes compared to medium control (left), HIB (right) and control vs. HIB (left-below). Red colour indicates genes with a false discovery rate (FDR) p< 0.05.

Further downstream analysis was performed on the list of differentially expressed genes due to treatment with acetate or butyrate. Based on FDR $p < 0.05$ or $p < 0.05$ for differential expression approximately 800 differentially expressed genes were selected from each treatment group and analysed by IPA. Acetate treatment regulated 120 canonical pathways, whereas butyrate regulated 211 canonical pathways (cut-off –log(p-value) 1.3) (data not shown). For butyrate not only was a larger number of canonical pathways differentially regulated, but also the probability of this regulation was larger (–log(p-value) up to 6.88). The top 40 canonical pathways induced by acetate and butyrate treatments with and without addition of HIB are shown in **Figure 5.3**. Interestingly, the addition of HIB to monocytes treated with either acetate or butyrate resulted in a smaller number of activated canonical pathways than stimulation with either butyrate or acetate alone. For example, the combination of acetate and HIB led to activation of 69 canonical pathways, while the combination of butyrate and HIB resulted in activation of 184 canonical pathways. The rank order of the top canonical pathways also changed due to HIB stimulation.

Among the top 40 canonical pathways differentially regulated by acetate or butyrate, we observed that acetate altered more cellular metabolic processes than butyrate (**Figure 5.3**). There were several immune-related pathways regulated due to acetate treatment. Some pathways, for example interferon signalling was more strongly regulated by addition of HIB to acetate treated monocytes. This pathway, which was only slightly activated in acetate treated monocytes, increased more than 3-fold in the presence of HIB (**Figure 5.3**). On the other hand, butyrate treatment alone induced a larger number of immune -related pathways (18 vs. 12, including NF-κB signalling) compared to acetate (**Figure 5.3**), as well as some stress response-related pathways, such as the NRF2 mediated oxidative stress response pathway. We observed that combination of butyrate with HIB affected expression of other pathways altering the rank order of canonical pathways compared to butyrate treated monocytes (**Figure 5.3**). Several G protein-coupled receptors (GPCRs) signalling pathways were induced both in acetate and butyrate treatment groups (**Figure 5.3A & C**), but none of these were cognate receptors for SCFA. Butyrate treatment changed the expression of several important genes encoding kinases (*PI3K*, *PKC*) and regulators involved in GPCR signalling (**Table 5.5**).

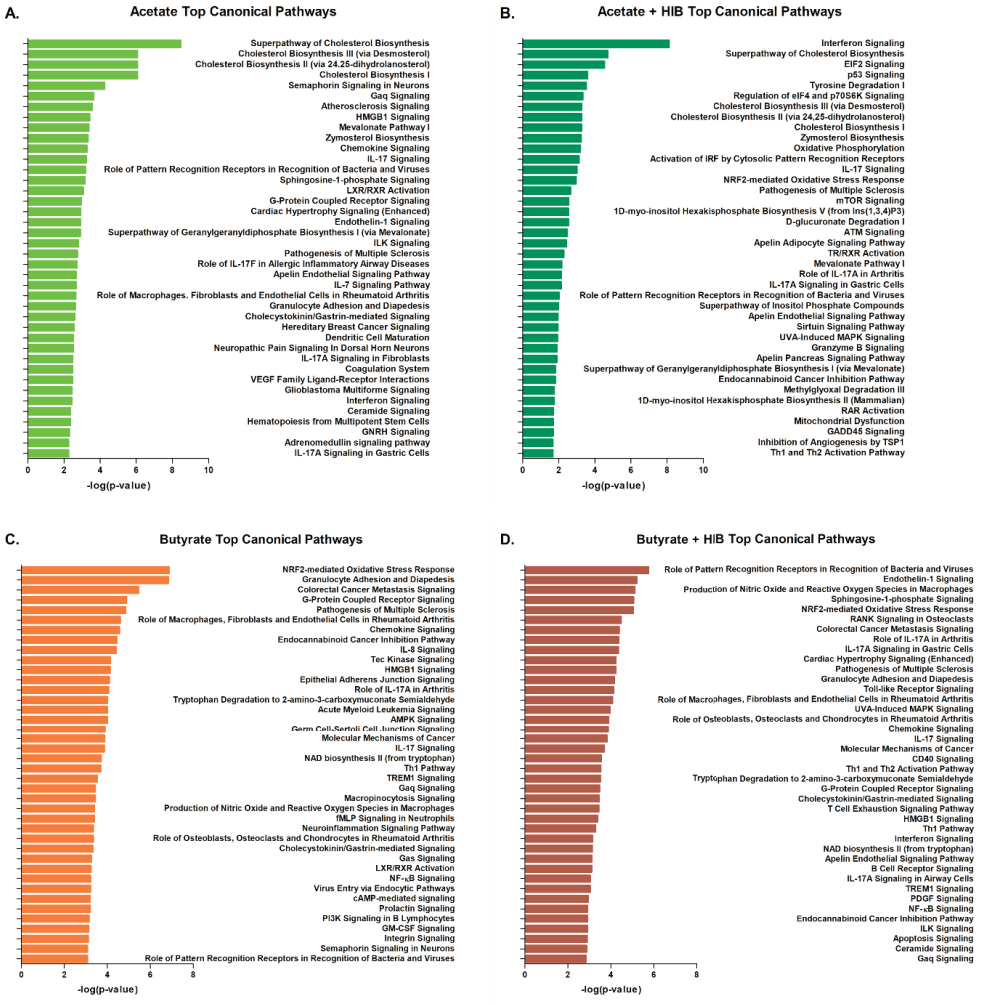

Figure 5.3. Ingenuity pathway analysis (IPA). The top 40 canonical pathways activated by different treatments **(A)** 2.5 mM acetate; **(B)** 2 mM acetate in combination with HIB; **(C)** 1 mM butyrate and **(D)** 1 mM butyrate in combination with HIB. The -log (p-value) is indicated for each significantly regulated pathway.

Immune response-related pathways, which might contribute to the acetate and butyrate modulation of cytokine secretion induced by HIB stimulation were examined in more detail (**Tables 5.1 - 5**). Many of the genes in the interferon-signalling pathway were downregulated after stimulation with acetate and HIB (**Table 5.1**). Genes in the IL-10 and NF-κB signalling pathways were regulated by butyrate and HIB (**Table 5.2 & 3)**. In the NF-κB pathway the RELB subunit of NF-kB was strongly downregulated (-5.35) by butyrate in the presence of HIB, as was TLR2 (-3.219). However, TLR5,7 and 8 were upregulated as were genes for MAPK kinases. Some of these genes are also present in the IL-10 signalling pathway. In addition we found that chemokine receptors CCR1 and CCR5, which are positively regulated by IL-10, were strongly

downregulated (-3.2 and -20.7) (**Table 5.2**). In the TLR signalling pathway, butyrate and HIB regulate the same genes as mentioned above, but in addition IL-12B, IL-36G and its receptor antagonist IL-36RA were strongly downregulated (-14.5 and -87.6 respectively). In this pathway acetate downregulated MAPK11 but upregulated MAPK14 expression (**Table 5.3**).

Table 5.1. Regulation of interferon signalling pathway (acetate + HIB vs. HIB)

Symbol	Entrez Gene Name	Type(s)	Expr Fold Change
IFI6	interferon alpha inducible protein 6	other	-3.196
IFI35	interferon induced protein 35	other	-3.25
IFIT1	interferon induced protein with tetratricopeptide repeats 1	other	-3.024
IFIT3	interferon induced protein with tetratricopeptide repeats 3	other	-2.672
IFITM3	interferon induced transmembrane protein 3	other	-2.393
IFNAR2	interferon alpha and beta receptor subunit 2	transmembrane receptor	1.602
IRF9	interferon regulatory factor 9	transcription regulator	-1.658
ISG15	ISG15 ubiquitin-like modifier	other	-5.883
MX1	MX dynamin like GTPase 1	enzyme	-2.219
OAS1	2'-5'-oligoadenylate synthetase 1	enzyme	-2.655
SOCS1	suppressor of cytokine signaling 1	other	-1.914

Table 5.2. Regulation of the IL-10 signalling pathway (butyrate + HIB vs. HIB)

Symbol	Entrez Gene Name	Type(s)	Expr Fold Change
CCR1	C-C motif chemokine receptor 1	G-protein coupled receptor	-3.188
CCR5	C-C motif chemokine receptor 5 (genepseudogene)	G-protein coupled receptor	-20.719
CD14	CD14 molecule	transmembrane receptor	-7.182
FOS	Fos proto-oncogene, AP-1 transcription factor subunit	transcription regulator	8.54
IL36G	interleukin 36 gamma	cytokine	-14.542
IL36RN	interleukin 36 receptor antagonist	cytokine	-87.578
JUN	Jun proto-oncogene, AP-1 transcription factor subunit	transcription regulator	-2.898
MAP3K14	mitogen-activated protein kinase kinase kinase 14	kinase	4.048
MAPK14	mitogen-activated protein kinase 14	kinase	2.976
NFKBIB	NFKB inhibitor beta	transcription regulator	-3.825

Table 5.3. Regulation of NF-κB signalling pathway (butyrate + HIB vs. HIB)

Symbol	Entrez Gene Name	Type(s)	Expr Fold Change
EIF2AK2	eukaryotic translation initiation factor 2 alpha kinase 2	kinase	-4.836
IGF1R	insulin like growth factor 1 receptor	transmembrane receptor	3.62
IL36G	interleukin 36 gamma	cytokine	-14.542
IL36RN	interleukin 36 receptor antagonist	cytokine	-87.578
INSR	insulin receptor	kinase	3.393
MAP3K3	mitogen-activated protein kinase kinase kinase 3	kinase	3.238
MAP3K14	mitogen-activated protein kinase kinase kinase 14	kinase	4.048
NFKBIB	NFKB inhibitor beta	transcription regulator	-3.825
NRAS	NRAS proto-oncogene, GTPase	enzyme	-3.164
PIK3CD	phosphatidylinositol-4,5-bisphosphate 3-kinase catalytic subunit delta	kinase	8.469
PIK3CG	phosphatidylinositol-4,5-bisphosphate 3-kinase catalytic subunit gamma	kinase	4.919
PIK3R2	phosphoinositide-3-kinase regulatory subunit 2	kinase	10.482
PRKACA	protein kinase cAMP-activated catalytic subunit alpha	kinase	3.256
RELB	RELB proto-oncogene, NF-kB subunit	transcription regulator	-5.35
TDP2	tyrosyl-DNA phosphodiesterase 2	transcription regulator	-8.773
TLR2	toll like receptor 2	transmembrane receptor	-3.219
TLR5	toll like receptor 5	transmembrane receptor	7.643
TLR7	toll like receptor 7	transmembrane receptor	23.872
TLR8	toll like receptor 8	transmembrane receptor	6.727
TNFRSF11A	TNF receptor superfamily member 11a	transmembrane receptor	8.542
TNFRSF1B	TNF receptor superfamily member 1B	transmembrane receptor	3.176

Table 5.4. Regulation of TLR signalling pathway (acetate + HIB vs. butyrate + HIB)

Symbol	Entrez Gene Name	Type(s)	Expr Fold Change	Expr Fold Change2
			Acetate + HIB	Butyrate + HIB
ELK1	ETS transcription factor ELK1	transcription regulator	1.599	
MAPK11	mitogen-activated protein kinase 11	kinase	-3.152	
MAPK14	mitogen-activated protein kinase 14	kinase	1.839	
PPARA	peroxisome proliferator activated receptor alpha	ligand-dependent nuclear receptor	1.913	
TLR5	toll like receptor 5	transmembrane receptor	1.735	7.643
TLR8	toll like receptor 8	transmembrane receptor	1.676	6.727
CD14	CD14 molecule	transmembrane receptor		-7.182
EIF2AK2	eukaryotic translation initiation factor 2 alpha kinase 2	kinase		-4.836
FOS	Fos proto-oncogene, AP-1 transcription factor subunit	transcription regulator		8.54
IL12B	interleukin 12B	cytokine		-47.307
IL36G	interleukin 36 gamma	cytokine		-14.542
IL36RN	interleukin 36 receptor antagonist	cytokine		-87.578
JUN	Jun proto-oncogene, AP-1 transcription factor subunit	transcription regulator		-2.898
MAP3K14	mitogen-activated protein kinase kinase kinase 14	kinase		4.048
MAPK14	mitogen-activated protein kinase 14	kinase		2.976
TLR2	toll like receptor 2	transmembrane receptor		-3.219
TLR7	toll like receptor 7	transmembrane receptor		23.872
TRAF4	TNF receptor associated factor 4	other		4.458

Table 5.5. Regulation of GPCR signalling pathway (all treatments)

Symbol	Entrez Gene Name	Type(s)	Expr Fold Change	Expr Fold Change2	Expr Fold Change3	Expr Fold Change4
			Acetate	Acetate + HIB	Butyrate	Butyrate + HIB
ADCY9	adenylate cyclase 9	enzyme				-3.252
ADORA2A	adenosine A2a receptor	G-protein coupled receptor				-4.16
AVPR2	arginine vasopressin receptor 2	G-protein coupled receptor	3.169			
ADRB2	adrenoceptor beta 2	G-protein coupled receptor			23.084	11.26
APEX1	apurinicapyrimidinic endodeoxyribonuclease 1	enzyme			3.016	
CAMK2G	calciumcalmodulin dependent protein kinase II gamma	kinase	1.38		10.022	11.373
CREB5	cAMP responsive element binding protein 5	transcription regulator	-1.675			
CREBBP	CREB binding protein	transcription regulator			-4.019	
DUSP4	dual specificity phosphatase 4	phosphatase				-5.101
FPR1	formyl peptide receptor 1	G-protein coupled receptor	1.404		5.872	3.16
FPR2	formyl peptide receptor 2	G-protein coupled receptor	1.538		9.161	5.908
GDE1	glycerophosphodiester phosphodiesterase 1	enzyme	1.395		3.101	5.028
GNA11	G protein subunit alpha 11	enzyme	1.475		4.822	10.716
HCAR2	hydroxycarboxylic acid receptor 2	G-protein coupled receptor			3.665	3.569
HCAR3	hydroxycarboxylic acid receptor 3	other			4.051	4.063
HRH1	histamine receptor H1	G-protein coupled receptor	1.666			
HRH2	histamine receptor H2	G-protein coupled receptor			6.708	10.596
LPAR1	lysophosphatidic acid receptor 1	G-protein coupled receptor	-1.399		-13.496	-15.306
MAPK3	mitogen-activated protein kinase 3	kinase	1.557			
MRAS	muscle RAS oncogene homolog	enzyme			-2.788	
NAPEPLD	N-acyl phosphatidylethanolamine phospholipase D	enzyme	-1.766			
NFKBIB	NFKB inhibitor beta	transcription regulator				-3.825
NRAS	NRAS proto-oncogene, GTPase	enzyme			-3.387	-3.164
PDE7A	phosphodiesterase 7A	enzyme			-3.838	-3.881
PIK3CD	phosphatidylinositol-4,5-bisphosphate 3-kinase catalytic subunit delta	kinase	1.402		8.107	8.469
PIK3CG	phosphatidylinositol-4,5-bisphosphate 3-kinase catalytic subunit gamma	kinase			3.956	4.919
PIK3R2	phosphoinositide-3-kinase regulatory subunit 2	kinase	1.616		5.453	10.482
PLCB1	phospholipase C beta 1	enzyme	-2.055			
PLCB3	phospholipase C beta 3	enzyme	1.604			2.941
PRKACA	protein kinase cAMP-activated catalytic subunit alpha	kinase	1.352		2.721	3.256
PRKCA	protein kinase C alpha	kinase			4.404	4.296
PTGER4	prostaglandin E receptor 4	G-protein coupled receptor			2.822	
PTK2B	protein tyrosine kinase 2 beta	kinase	1.376		3.807	3.592
RASGRP1	RAS guanyl releasing protein 1	other				-6.209
RGS2	regulator of G protein signaling 2	other			4.554	8.704
RGS10	regulator of G protein signaling 10	other				-5.076
RGS14	regulator of G protein signaling 14	other			3.262	6.289
RGS18	regulator of G protein signaling 18	other				5.055
S1PR3	sphingosine-1-phosphate receptor 3	G-protein coupled receptor	1.483		7.938	4.914
SRC	SRC proto-oncogene, non-receptor tyrosine kinase	kinase			-3.325	
TDP2	tyrosyl-DNA phosphodiesterase 2	transcription regulator			-8.142	-8.773
XCR1	X-C motif chemokine receptor 1	G-protein coupled receptor			-6.343	

To investigate the immunomodulatory effect of SCFA on monocytes, we measured secreted cytokines after 5 and 24 hours. Stimulation with SCFA alone did not result in cytokine secretion at either 5 or 24 hours, whereas stimulation with heat-inactivated bacteria (HIB) strongly induced both pro-and anti-inflammatory cytokines. Cytokines accumulated in the supernatant over time, which is reflected by the lower levels of IL-10, IL-12 and IFN-γ secretion

after 5 hours of stimulation compared to the levels detected after 24 hours (**Figure 5.4 & 5**). As described in **Chapter 4**, acetate increased HIB-induced IL-10 production after 24 hours, whereas butyrate had the opposite effect and decreased IL-10 secretion. After 24 hours, both acetate and butyrate decreased HIB induced secretion of pro-inflammatory cytokines IL-12 and IL-1β, although acetate to a lesser extent. Butyrate was also able to decrease HIB induced TNF-α secretion (**Figure 5. 5**).

There were no significant differences observed in the viability of monocytes stimulated with HIB or HIB together with acetate or butyrate after 24 hours (data not shown).

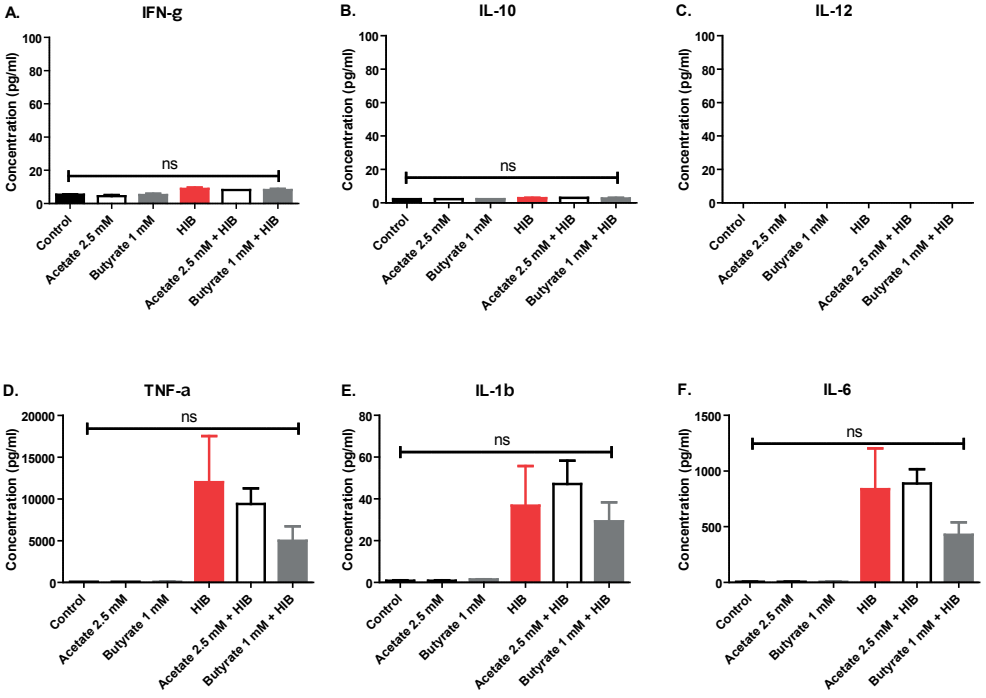

Figure 5.4(A-F). Cytokine secretion profile of $CD14^{+}$ monocytes exposed to 2.5 mM acetate or 1 mM butyrate with or without co-stimulation with HIB for 5 hours. Error bars represent SEM, n = 2 technical duplicates from 1 donor; One-way ANOVA with Tukey post hoc test; * $p < 0.05$, ** $p < 0.01$, *** $p < 0.001$.

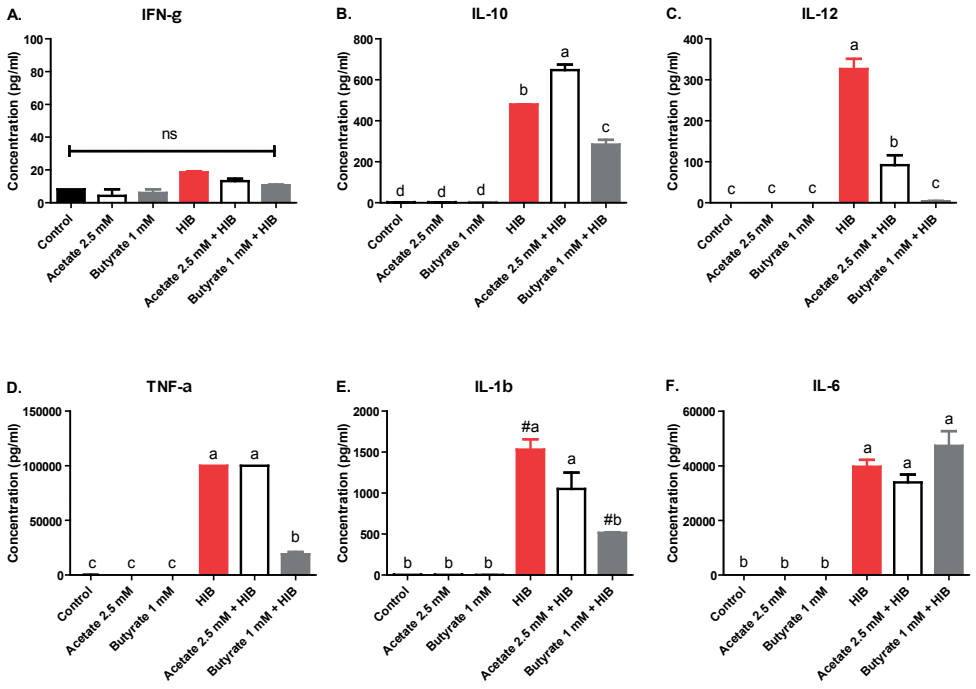

Figure 5.5(A-F). Cytokine secretion profile of CD14⁺ monocytes exposed to 2.5 mM acetate or 1 mM butyrate with or without co-stimulation with HIB for 24 hours. Error bars represent SEM, n = 2 technical duplicates from 1 donor; One-way ANOVA with Tukey post hoc test; * $p < 0.05$, ** $p < 0.01$, *** $p < 0.001$.

DISCUSSION

The role of SCFA in modulation of cytokine secretion of monocyte has been reported previously by Cox et al., (2009). They reported that individual SCFA (acetate, butyrate, formate and propionate) exposure for 22 hours led to attenuation of IL-10 and C-C Motif Chemokine Ligand 2 or monocyte chemoattractant protein-1(CCL2/MCP-1) cytokine/chemokine production induced by LPS (100 ng/ml) in a dose dependent manner (0.2 – 20 mmol/L SCFA concentration). In contrast to our own results with butyrate, there was no attenuation of LPS-induced pro-inflammatory cytokines IL-1β, IL-2, IL-6, IL-8, IL-12, IFN-γ, TNF-α[125]. This may be due to the different stimulus. Butyrate downregulated TLR2, which is the key receptor for recognition of HIB, a Gram-positive bacterium. As this was the only TLR which was downregulated (in fact others were upregulated) we predict that it will have a strong effect on HIB stimulation, but not on LPS stimulation which was used by Cox et al. (2009)[125]. Cox et al., (2009) reported decreased secretion of IL-10 after acetate stimulation which contradicts our own findings[125]. However, this was only observed when acetate was

used in much higher concentrations (20 mM), which is not physiological and might have reduced cell viability.

Acetate and butyrate alone did not induce cytokine secretion by $CD14^+$ monocytes. This result was reflected by the acetate transcriptomic analysis, as we observed that in acetate treated monocytes, the number of differentially expressed genes was low compared to medium control. This finding suggested that acetate induced few changes in gene expression. Indeed only cellular metabolism and a few immune response-related pathways were induced by acetate. However, when HIB was added, many more genes were differentially regulated as a result of acetate exposure. The monocytes also responded differently, modulating cytokine secretion, mainly via the interferon signalling pathway (**Table 5.1**). Hu et al., (2006) reported that IFN-γ ameliorates induction of TNF-α by TLR ligands, immune complexes, and zymosan by suppressing IL-10 production and thereby interrupting STAT3-mediated feedback inhibition[131]. In our study, the presence of acetate in combination with HIB led to downregulation of many genes, and interferon-induced factors suggesting suppression of IFN-γ signalling, which would indirectly increase production of IL-10.

On the other hand, exposure of $CD14^+$ monocytes to butyrate alone altered gene expression dramatically and activated more canonical pathways compared to acetate. Interestingly, this dramatic change did not affect cytokine secretion, samples exposed to butyrate alone had low cytokine secretion. A possible explanation is that butyrate mainly evoked stress response-related pathways, such as the NRF2 mediated oxidative stress response. Even though some immune response-related pathways, such as the NF-κB signalling pathway, were also activated by butyrate alone, those pathways did not lead to cytokine secretion (**Figure 5.5**). Although we observed that 1 mM concentration of butyrate reduced cell viability after 24 hours, which might result in lower cytokine secretion as there would be fewer cells, this was not seen for acetate. Acetate did not affect viability, but still no detectable cytokine levels were measured. More importantly, cell viability was not affected after simultaneous stimulation with HIB and butyrate, so the decreased cytokine secretion compared to samples stimulated with HIB only cannot be a result of decreased cell viability. Furthermore, treatment with a combination of HIB and butyrate induced the activation of many immune-response related pathways such as the IL-10 and NF-κB signalling pathways (**Table 5.2 & 3**). These pathways are known to play an important role in modulation of cytokine production[132, 133].

Similar to the combined acetate and HIB treatment, the butyrate and HIB combination also regulated the TLR signalling pathway, but more significantly log(p-value) 4.13, compared to acetate and HIB (log(p-value) 1.49) (**Figure 5.3D**; **Table 5.4**). The TLR signalling pathway leads to activation of the NF-κB transcription factor and cytokine secretion[46, 134]. Although both acetate and butyrate regulated the TLR signalling pathway, we observed that they had different effects. Acetate only regulated a small number of genes in the TLR signalling pathway.

Whereas butyrate regulating a larger set of genes involved in TLR signalling compared to acetate. Only two differentially expressed genes (TLR 5 & TLR8), were shared between acetate and butyrate in the TLR signalling pathway. This was also observed in the GPCR signalling pathway, although the number of genes shared among the treatments (except for acetate and HIB treatment) are greater compared to the TLR signalling pathway.

CONCLUDING REMARKS

To conclude, acetate and butyrate modulate the host's immune response through distinct mechanisms. Butyrate, which is well known as an anti-inflammatory molecule, suppressed secretion of both anti- and pro-inflammatory cytokines by $CD14^+$ monocytes. In contrast, acetate elevated secretion of the anti-inflammatory cytokine IL-10 while it attenuated pro-inflammatory cytokine IL-12 and IL-1β secretion. The effect elicited by acetate could be more favourable compared to butyrate in case of combating a chronic inflammatory disease in the gut. The result of transcriptomic analysis revealed that acetate evoked only small changes in gene expression levels as well as canonical pathway activation compared to butyrate. However, when combined with HIB, acetate was able to modulate cytokine production, particularly IL-10, mainly via the interferon signalling pathway and TLR signalling pathway. On the other hand butyrate suppressed HIB-induced IL-10 secretion, mediated through the IL-10, NF-κB and TLR signalling pathways. Moreover, 1 mM butyrate decreased cell viability of the monocytes and regulated stress related-responses of the cells as well as many disease-related pathways. Our findings highlight the differential molecular mechanisms of acetate and butyrate in modulating the immune response of the host and support our hypothesis that acetate might be a better candidate for future anti-inflammatory treatments.

ACKNOWLEDGEMENT

The authors would like to thank Berdien van Olst for her help in some graphical visualisation of transcriptomic data.

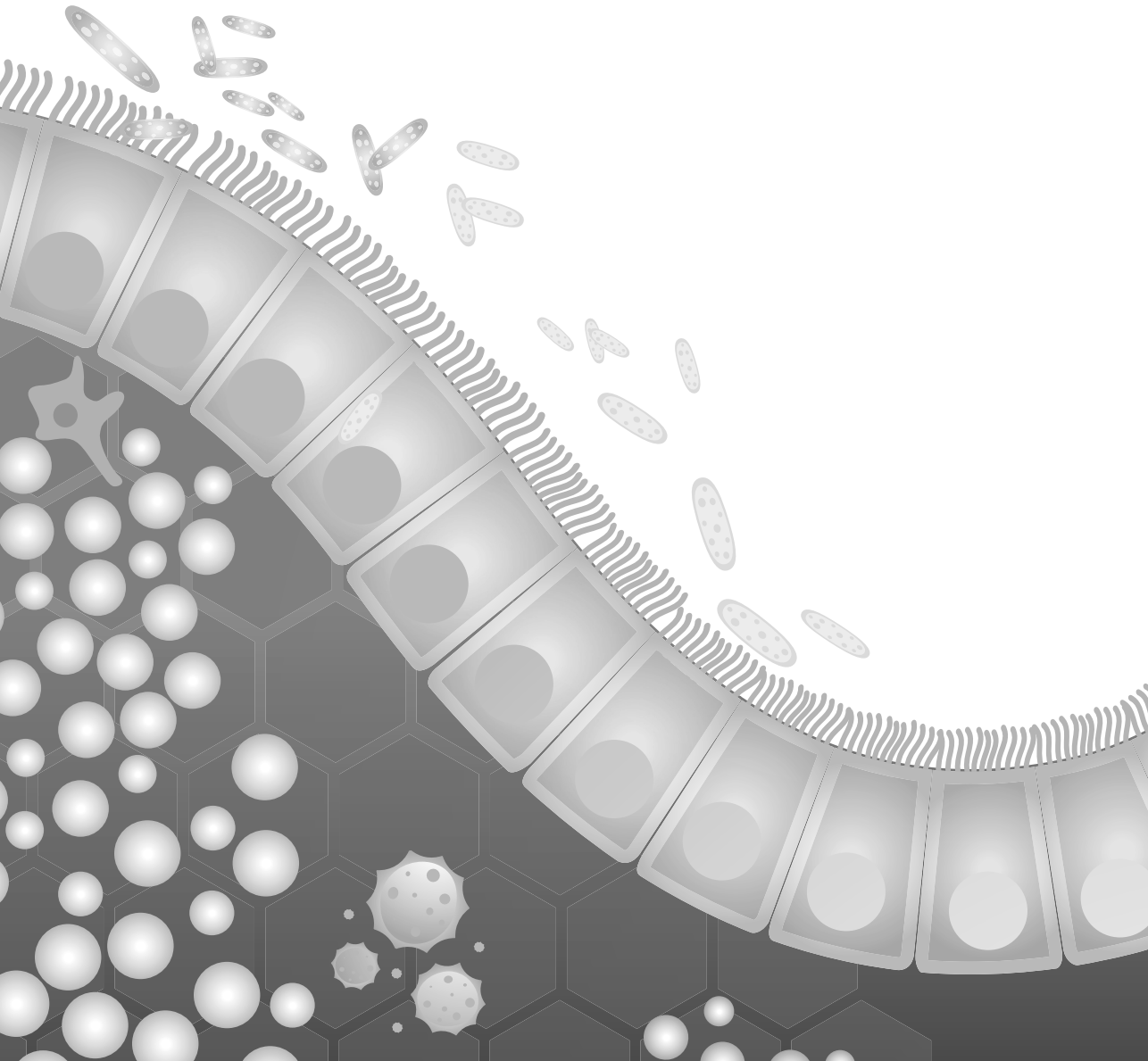

Chapter 6

Transcriptional responses of porcine intestinal organoids exposed to acetate and butyrate

Nuning Winaris*[1,2], Bart van der Hee*[1], Ellen Kranenbarg[1], Jerry M. Wells[1]

[1] Host-Microbe Interactomics Group, Department of Animal Science, Wageningen University & Research, Wageningen, Netherlands

[2] Master Program in Biomedical Sciences, Faculty of Medicine, Universitas Brawijaya, Malang, Indonesia

*Contributed equally

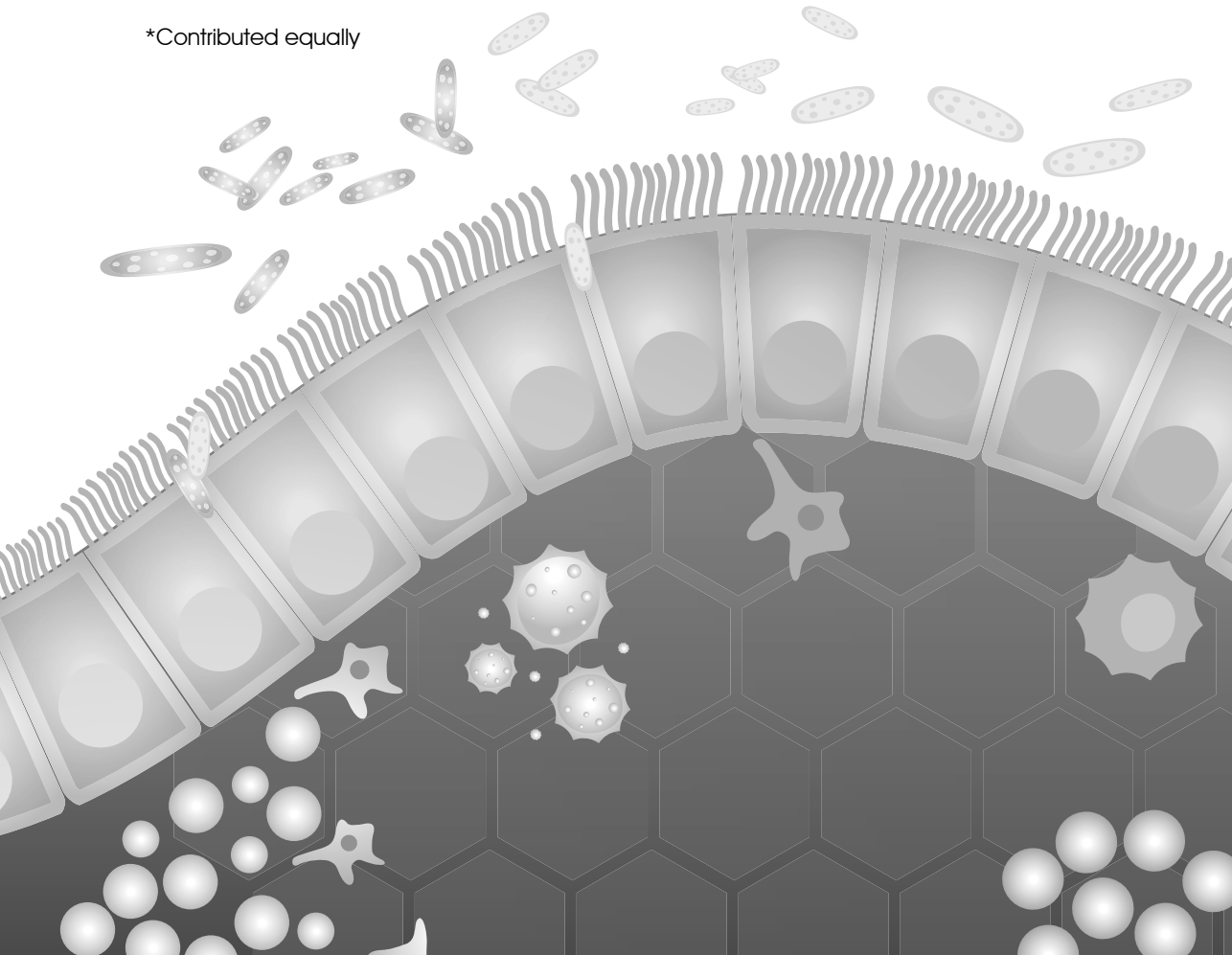

Abstract

Short-chain fatty acids (SCFA), such as butyrate, acetate, and propionate, have been reported to reduce the risk of gastrointestinal disorders. A previous study reported that incubation of ileum organoids with bacterial culture supernatant of *Akkermansia muciniphila* and *Faecalibacterium prausnitzii* (which contained different SCFA), as well as individual SCFA affected the expression of metabolic cellular growth and cell survival pathways. However, these results are difficult to interpret because of the mixture of SCFA and other metabolites present in the bacterial culture supernatants. Furthermore, the combined concentration of SCFAs used was high and possible toxicity was not assessed. In this study we aimed to investigate the effects of non-toxic concentrations of acetate and butyrate on gene expression in 3D organoid cultures in order to gain more insight into their transcriptional effects on epithelial functions. Porcine 3D ileal organoids were exposed to non-toxic concentration of butyrate and acetate for 5 hours or buffer control and RNA was purified for RNA sequencing. Differentially expressed genes and pathways were identified using various bioinformatics software. Butyrate treatment induced the largest set of differentially expressed genes (DEG) compared to acetate. The top canonical pathways activated by acetate treatment mostly related to cellular processes-related pathways, whereas butyrate evoked many cell-cycle related pathways. Moreover, butyrate was predicted to reduce cell proliferation through inhibition of histone deacetylase 3 (HDAC3). In contrast, the effect of acetate on histone 3 acetylation is still unclear. These results reveal that acetate and butyrate regulate different intestinal epithelial functions.

Keywords: porcine ileal organoids, transcriptomic, epithelial function

INTRODUCTION

Commensal bacteria in the gut produce short-chain fatty acids (SCFA), such as butyrate, acetate, and propionate, which have been demonstrated to reduce the risk of gastrointestinal disorders[135, 136]. Total SCFA concentrations in the terminal ileum are estimated to be 13 ± 6 mmol/kg content but much higher in the caecum (131 ± 9 mmol/kg content) and descending colon (80 ± 11 mmol/kg content)[62, 137]. In all parts of the colon acetate was found to be at least 2-fold higher in concentration than propionate or butyrate. A study on individuals in sudden death cases revealed that in the ascending colon, where most saccharolytic fermentation occurs, the concentrations of acetate, propionate and butyrate in mmol/kg content were found to be 63.4 ± 6.8, 26.7 ± 4.0 and 24.5± 4.2 respectively[137].

SCFA can be passively taken up by epithelial cells but in greater amounts by active transport via monocarboxylate transporter 1 (MCT-1) and SMCT-1[61]. Most butyrate is oxidized and used as fuel for colonocytes, deriving 60–70% of their energy supply from SCFA oxidation[138]. The remaining SCFA are transported out of the cell across the basolateral membrane via an unknown HCO_3^- exchanger, most likely monocarboxylate transporter (MCT) 4 or 5[61, 139]. Here SCFA can enter the blood vessels and circulation via the portal vein[138]. The liver clears the major part of propionate and butyrate from the portal circulation but acetate can reach 200 µM in venous serum of humans and pigs[140].

SCFA can also interact with G-protein-couple receptors GPR41 and GPR43 on intestinal epithelial cells, which is important for immune homeostasis in the intestine[141]. SCFA have been reported to induce the expression of vitamin A–converting enzyme RALDH1 in intestinal epithelial cells *in vivo* and *in vitro*, which has been linked to increased numbers of intestinal regulatory T cells and a higher production of luminal IgA[142, 143]. SCFA have also been reported to down-regulate LPS-stimulated IL-8 secretion in different intestinal cancer cell lines[142]. Butyrate has been reported to maintain and/or increase transepithelial electrical resistance (TEER) in human intestinal cell lines Caco-2 and T84, through induction of genes encoding tight-junctions (TJ) components and protein reassembly regulated by transcription factors Signal Transducer and Activator of Transcription 3 (STAT3) and Specificity Protein 1 (SP1)[144-147].

Lukovac et al. (2014) reported that 3 hours incubation of ileum organoids with bacterial culture supernatant of *Akkermansia muciniphila* (containing 3.65 mM acetate and 7.14 mM propionate), *Faecalibacterium prausnitzii* (1.51 mM acetate, 5.51 mM formate, 7.06 mM propionate, and 8.03 mM butyrate), as well as 5 mM concentration of individual SCFA led to altered expression of metabolic cellular growth and cell survival pathways[135]. These results are difficult to interpret because of the mixture of SCFA and other metabolites present in the bacterial culture supernatants. Furthermore, the combined concentration of SCFA is high and

possible toxicity was not assessed. Recently, Kaiko et al., showed that 1mM butyrate inhibits proliferation of intestinal stem cells and that higher concentrations 1-3 mM cause stem cell apoptosis[73].

The aim of this paper was to investigate the effects of non-toxic concentrations of acetate and butyrate on gene expression in 3D organoid cultures in order to gain more insight into their transcriptional effects on epithelial functions. Porcine 3D ileal organoids were exposed to non-toxic concentration of butyrate and acetate for 5 hours or buffer control and RNA was purified for RNA sequencing. Differentially expressed genes and pathways were identified using bioinformatics tools.

MATERIALS AND METHODS

Porcine Ileum 3D organoids culture

Ileum organoids were generated from intestinal tissue of two 5-month-old slaughter pigs, according to the procedure described by Sato and colleagues[148, 149]. Porcine ileal organoids were grown in basal culture medium that was refreshed every two days (BCM: DMEM/F12 (Gibco), supplemented with 100 µg/ml primocin (Invivogen), 10 mM HEPES (HyClone), 1 × B-27 (Gibco), 1.25 mM N-acetylcysteine (Sigma-Aldrich), 50 ng/ml human epidermal growth factor (R&D systems), 15 nM gastrin, 10 mM nicotinamide, 10 µM p38 MAPK inhibitor (Sigma-Aldrich), 600 nM TGFβ receptor inhibitor A83-01, and conditioned media for recombinant Noggin (15% v/v), Spondin (15% v/v), and Wnt3A (30% v/v) (provided by Dr Kuo and the Hubrecht Institute). Organoids were passaged by enzymatic dissociation at a 1 : 5 ratio every 5 days using TrypLE Express (Thermo Fisher) and plating in fresh Matrigel matrix droplets (Basement Membrane, Growth factor reduced, REF 356231, Corning).

Viability test different concentration of SCFA

The 3-dimensional organoids were cultured in single 5 µl Matrigel droplets in 24-well plates (9 replicates per treatment) for 5 days. Organoids were stimulated for 5 hours with non-toxic concentrations of butyrate (1 mM) and acetate (2.5 mM). The Cell Proliferation Reagent WST-1 (Sigma-aldrich) was added to the well after 5 hours incubation. Absorbance was then measured using a Spectramax M5 microplate reader (Molecular Devices) at 450/690 nm.

SCFA exposure and RNA isolation from 3D organoids

Initially the potential toxicity of acetate and butyrate exposure to 3D organoids was tested using Cell Proliferation Reagent WST-1 (Sigma-aldrich) to determine which concentrations to use for the transcriptomics study. Triplicate wells containing 3D ileum organoids in Matrigel were incubated with 2.5 mM acetate, 1 mM butyrate or medium control for 5 hours at 37°C. After incubation, the medium was removed and 1 ml ice-cold DMEM/F12 was added to each

well, the organoid suspension transferred to 15 ml tubes on ice (Falcon) and then centrifuged 5 min at 300 x g at 4°C to recover the organoids. The supernatant was then carefully removed and lysis buffer (Qiagen) was added to lyse the organoids. Total RNA was extracted immediately according to the manufacturer's recommended protocol (RNEasy mini-kit, Qiagen). Total RNA concentrations were measured using a Qubit 4 Fluorometer (Invitrogen) and RNA quality (230/260 and 260/280 ratios) was checked with a DeNovix spectrophotometer.

mRNA sequencing and transcriptomic analysis

Library preparations were performed using total RNA extracted from acetate, butyrate, or medium-treated organoids and then sequenced on an Illumina sequencing system by Novogene (Hong Kong). The sequencing reads were checked for quality using CLC Genomic Workbench (QIAGEN) and FastQC[150] and mapped to the Sus scrofa 11.1 reference genome (Ensembl, [151], see **Supplementary Table S6.1**), and processed as previously described[152] for further downstream analysis.

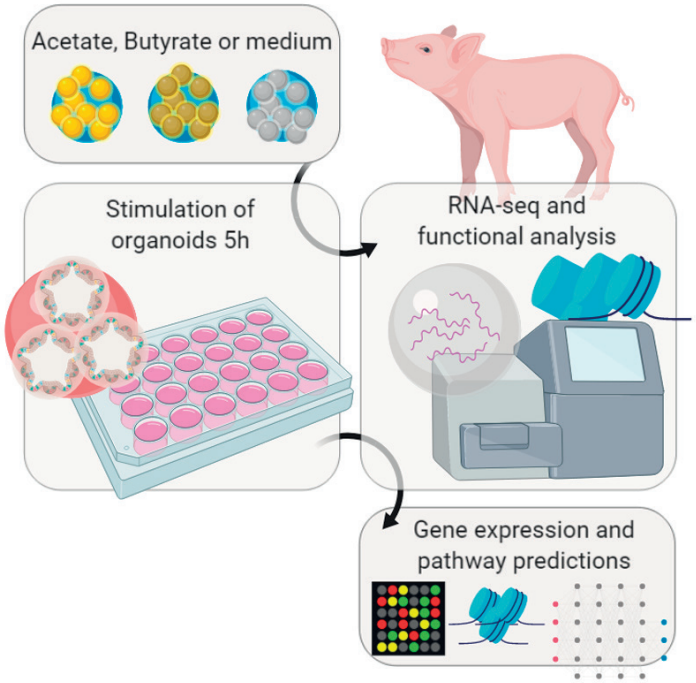

Figure 6.1. Schematic diagram of experimental setup. Ileum organoids were incubated with acetate, butyrate or medium control for 5 hours, followed by RNA extraction and library preparation. RNA sequencing was then performed, and the results were analysed using various bioinformatics tools.

Differentially expressed genes (DEG) were identified using CLC with a probability (P) value < 0.05 and false discovery rate (FDR) < 0.05 for determination of significant differences. Gene ontology and pathway integration of DEG were analysed using Ingenuity pathway analysis (IPA). To utilise the IPA database, unknown *Sus scrofa* identifiers were re-annotated to their human homologues using g:profiler[153]. Schematic diagram of this experimental setup is shown in **Figure 6.1.**

Extraction and detection of histone H3 total acetylation

The same batch of 3D ileum organoid culture were also used for extraction and detection of histone H3 acetylation. Histones were extracted from organoids using a Histone Extraction Kit (ab113476, Abcam) according to manufacturer's protocol. Extracted histones were then aliquoted and stored at -80 °C for further use. Total concentrations of histone proteins were determined using the Bradford protein assay with Coomassie Protein Assay Reagent (Thermo Scientific). 2 µg protein was used for histone H3 acetylation detection with a fluorometric-based assay using Histone H3 Total Acetylation Detection Fast Kit (ab131581, Abcam).

RESULTS AND DISCUSSION

Viability of organoids exposed to acetate and butyrate

Organoids were incubated with acetate (2.5 mM) or butyrate (1 mM) or buffer alone as a control to evaluate their potential toxicity. The viability assay measures conversion of the WST-1 dye into a coloured product by mitochondrial dehydrogenase enzymes. Microscopic examination suggested the large variability in WST-1 conversion between replicates was due to different numbers of organoids per well and thus total cell numbers. Stimulating organoids with non-toxic concentrations of SCFA did not show profound effects on the ability to convert WST-1 to formazan compared to the medium control **(Figure 6.2)**.

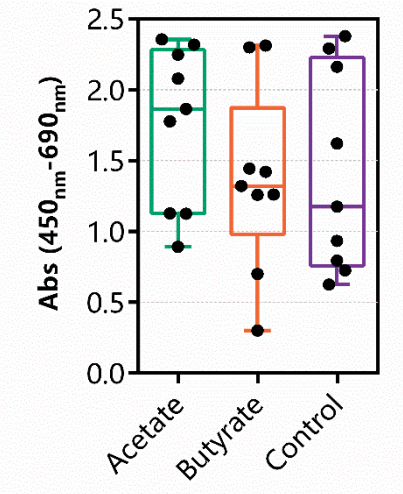

Figure 6.2. WST-1 assay for cell viability of 3D organoids incubated for 5 hours with 2.5 mM acetate, 1 mM butyrate or buffer control. Error bars represent Min to Max, n = 9 per group.

Differentially expressed genes induced by SCFAs acetate and butyrate

A projection scatter plot of principal component analysis (PCA) showed that organoid samples treated with acetate mainly clustered together, one of which was close to the untreated (control) samples, indicating low variation between the two groups. Moreover, the close scatter of this acetate sample was also not due to large differences in the number of reads or mapping efficiency. In contrast, organoids treated with butyrate were clustered furthest away from the control and acetate group **(Figure 6.3A)**. An expression correlation matrix showed good correlation between replicates of the butyrate-treated organoids and replicates of the untreated organoid samples. Higher variation was evident in expression profiles of the acetate-treated organoid samples **(Figure 6.3B)**. The differentially expressed genes (DEG) (log2 cut off 1.5-fold change and $p < 0.05$) induced by butyrate or acetate exposure of organoids compared to untreated organoid controls are shown in Volcano plots **(Figure 6.3C)**. Butyrate-treatment induced the largest set of DEG when $p < 0.05$ (9776 genes, 4841 up/4935 down), whereas acetate had significantly less DEG (1492 genes, 661 up/831 down). Differentially expressed gene expression values are visualized for acetate (**Figure 6.3D**) and butyrate (**Figure 6.3E**). Both treatments had a substantial amount of DEG in common (1173, **Figure 6.3F-left**), but heatmap clustering shows the same sample variability observed in the projection scatter plot for acetate (**Figure 6.3F-right**). Moreover, when the data was adjusted for FDR < 0.05, the amount of DEG by butyrate slightly decreased (8989 genes, 4400 up/4589 down), whereas DEG numbers in acetate-treated organoids dropped substantially (17 genes, 13 up, down).

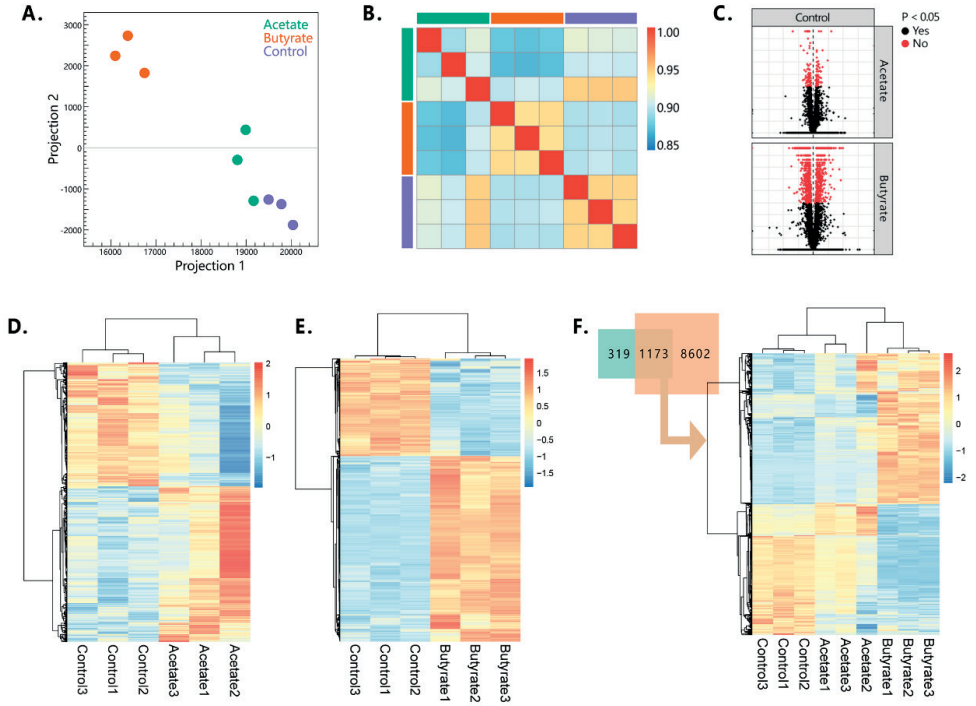

Figure 6.3 (A-F). (A) Projection scatter plot of principal component analysis clustering organoids treated with acetate, butyrate, or medium control. **(B)** Expression correlation matrix for organoids treated with acetate, butyrate, or medium control shows strong separation of butyrate, and variable expression patterns in acetate treated samples. **(C)** Volcano plots showing the comparison of differentially expressed genes induced by acetate and butyrate (red: $p < 0.05$). Heat map showing clustering dendrogram of differentially expressed genes when treated with Acetate **(D)** or Butyrate **(E)** when p-value < 0.05. **(F)** All DEG from control were compared between acetate and butyrate and showed 1173 overlapping genes and were visualized in a heatmap to show actual expression values (right).

Ingenuity Pathway Analysis (IPA) of differentially expressed genes

IPA analysis was used to generate a list of the top canonical pathways (**Figure 6.4**), predicted upstream regulators, and biological functions. This is a tool which categorises genes with significantly altered expression according to their molecular and cellular functions (**Table 6.1**). For both acetate and butyrate, the top regulated molecular and cellular functions were Cell Death and Survival, Cellular Assembly and Organization, and Cellular Function and Maintenance (**Table 6.1**). Functions regulated only by butyrate were Gene Expression and Cell Cycle and only by acetate were Cellular Movement and Cellular Development.

Table 6.1. IPA analysis of Molecular and Cellular Functions affected by SCFA exposure.

Comparison	Molecular and Cellular Functions
Acetate vs. control	Cell Death and Survival, Cellular Movement, Cellular Assembly and Organization, Cellular Function and Maintenance, Cellular Development
Butyrate vs. control	Gene Expression, Cell Death and Survival, Cell Cycle, Cellular Assembly and Organization, Cellular Function and Maintenance

IPA listed 57 significantly regulated canonical pathways ($p < 0.05$, threshold of 1.3) as a result of butyrate exposure and 51 as a result of acetate treatment. The top pathways regulated by acetate were Sirtuin Signaling Pathway, a complex pathway involved in many cellular processes including apoptosis and inflammation, and Signaling by Rho Family GTPases, a pathway related to cell to cell movement (**Figure 6.4A**). The top canonical pathway regulated by butyrate was High Mobility Group Box 1 (*HMGB1*) Signalling Pathway. The high-mobility group box-1 (HMGB1) protein is a DNA-binding nuclear protein, present in almost all eukaryotic cells that can activate a series of signaling components, including mitogen-activated protein kinases (MAPKs) and AKT, which play an important role in proliferation and inflammation[154]. This top pathway may be linked to many other cell cycle and cancer pathways regulated by butyrate (**Figure 6.4B**). Cell stress related pathways such as the unfolded protein response, autophagy and Nuclear Factor Erythroid 2-related Factor 2 (NRF2)-mediated oxidative stress pathway were regulated by butyrate but not acetate.

Figure 6.4 (A-B). Ingenuity Pathway Analysis (IPA). The top canonical pathways expressed in ileum organoids as a result of acetate and butyrate exposure for 5 hours. **(A)** Top canonical pathways activated by 2.5 mM acetate exposure. **(B)** Top canonical pathways activated by 1 mM butyrate exposure.

Some of the top canonical pathways were examined in more detail to give more insights into the genes induced by acetate and butyrate treatment (**Table 6.2-6**). Acetate was predicted to upregulate the Sirtuin signalling pathway, including 3 genes which could have epigenetic effects, namely *H1F0*, *SIRT6* and *KAT2A*. Histone *H1F0* is one of the main chromatin proteins which plays an important role in organizing eukaryotic DNA into a compact structure (**Table 6.2 and Supplementary Figure S6.1**). Histone *H1F0*, is devoid of enzymatic activity and binds nucleosomes without apparent DNA sequence specificity leading to changes in the architecture of chromatin[155]. *SIRT6*, which was upregulated, is an NAD^+-dependent deacetylase of histones and regulating multiple processes including DNA stability and repair[156]. *KAT2A*, a lysine acetyltransferase with demonstrated activity on histone variant H2A.Z, was downregulated. Posttranslational modifications such as acetylation and ubiquitination of H2A.Z, as well as its specific binding partners, is a central player in the control of gene expression[157]. These findings could explain why acetate has such a broad effect on many different types of pathways.

The second top canonical pathway, predicted to be upregulated by acetate, was the Rho Family GTPases signalling pathway in which *ACTA1* and *ACTC1*, were highly upregulated (**Table 6.3**). The reasons for this are not clear but may indicate remodelling of the actin cytoskeleton.

Butyrate was predicted to regulate cell cycle-related pathways e.g. by down regulating cyclin genes *CCNB2* in the G2/M DNA Damage Checkpoint pathway and *CCND1* (**Table 6.5**) as well as *CCNE2* in the G1/S Checkpoint pathway which control the cell cycle. Additionally, *HDAC3* which is inhibited by butyrate was upregulated. Histone deacetylase 3 (HDAC3) directly interacts with and deacetylates cyclin A in the G1/S Checkpoint pathway (**Table 6.6**). Given that deacetylated cyclin A promotes cell proliferation butyrate inhibition of HDAC3 deacetylation activity is predicted to reduce cell proliferation.

Several genes involved in the regulation of HMGB1 Signaling Pathway were downregulated by butyrate including *TLR4* (-2.744) an innate receptor to which HMGB1 released from cells has been reported to bind and the RELA subunit of NF-κB (-1.531). (**Table 6.5**). However, expression of SERPINE1 a protein regulated by nuclear HMGB1 was increased more than 16-fold. Like the histones, HMGB1 is an important chromatin protein. In the nucleus HMGB1 interacts with nucleosomes, transcription factors, and histones, thereby organising DNA and regulating transcription[158, 159]. The presence of HMGB1 in the nucleus depends on post-translational acetylation[159]. It is therefore possible that butyrate inhibits deacetylation of HMGB1 possibly through HDAC3, increasing the concentration of HMGB1 in the nucleus and upregulating *SERPINE1*.

Table 6.2. Regulation of sirtuin signalling pathway (acetate vs. control)

Symbol	Entrez Gene Name	Type(s)	Expr Fold Change
ATG3	autophagy related 3	enzyme	1.122
ATG12	autophagy related 12	other	1.119
BAX	BCL2 associated X, apoptosis regulator	transporter	1.133
EPAS1	endothelial PAS domain protein 1	transcription regulator	1.263
GABARAPL1	GABA type A receptor associated protein like 1	other	1.259
H1F0	H1 histone family member 0	other	1.24
HIF1A	hypoxia inducible factor 1 subunit alpha	transcription regulator	1.164
KAT2A	lysine acetyltransferase 2A	enzyme	-1.19
MT-ND1	NADH dehydrogenase, subunit 1 (complex I)	enzyme	-1.232
MT-ND2	MTND2	enzyme	-1.201
MYC	MYC proto-oncogene, bHLH transcription factor	transcription regulator	-1.192
NAMPT	nicotinamide phosphoribosyltransferase	cytokine	1.412
NDUFB7	NADH:ubiquinone oxidoreductase subunit B7	enzyme	-1.124
NDUFS4	NADH:ubiquinone oxidoreductase subunit S4	enzyme	1.28
NEDD4	neural precursor cell expressed, developmentally down-regulated 4, E3 ubiquitin protein ligase	enzyme	1.27
NQO1	NAD(P)H quinone dehydrogenase 1	enzyme	1.318
PCK1	phosphoenolpyruvate carboxykinase 1	kinase	1.534
PFKFB3	6-phosphofructo-2-kinasefructose-2,6-biphosphatase 3	kinase	1.378
PPARG	peroxisome proliferator activated receptor gamma	ligand-dependent nuclear recepto	1.185
SIRT6	sirtuin 6	enzyme	1.226
TIMM10	translocase of inner mitochondrial membrane 10	transporter	-1.145

Table 6.3. Regulation of signalling by Rho Family GTPases (acetate vs. control)

Symbol	Entrez Gene Name	Type(s)	Expr Fold Change
ACTA1	actin alpha 1, skeletal muscle	other	3.855
ACTC1	actin alpha cardiac muscle 1	enzyme	19.68
ARHGEF4	Rho guanine nucleotide exchange factor 4	other	1.506
CDC42EP1	CDC42 effector protein 1	other	-1.196
CDC42EP5	CDC42 effector protein 5	other	-2.151
CDH17	cadherin 17	transporter	1.296
GNAI1	G protein subunit alpha i1	enzyme	1.122
GNG7	G protein subunit gamma 7	enzyme	1.433
LIMK2	LIM domain kinase 2	kinase	-1.133
MAPK10	mitogen-activated protein kinase 10	kinase	-3.067
MSN	moesin	other	1.147
NEDD4	neural precursor cell expressed, developmentally down-regulated 4, E3 ubiquitin protein ligase	enzyme	1.27
PKN1	protein kinase N1	kinase	1.118
RHOQ	ras homolog family member Q	enzyme	1.21
RHOV	ras homolog family member V	enzyme	1.202
ROCK2	Rho associated coiled-coil containing protein kinase 2	kinase	1.145
SEPT10	septin 10	transcription regulator	1.131
VIM	vimentin	other	-1.306

Table 6.4. Regulation of HMGB1 Signalling pathway (butyrate vs. control)

Symbol	Entrez Gene Name	Type(s)	Expr Fold Change
CD70	CD70 molecule	cytokine	-2.279
CLCF1	cardiotrophin like cytokine factor 1	cytokine	-2.372
CSF2	colony stimulating factor 2	cytokine	-4.834
ICAM1	intercellular adhesion molecule 1	transmembrane receptor	-2.054
IFNGR1	interferon gamma receptor 1	transmembrane receptor	1.549
IL1R1	interleukin 1 receptor type 1	transmembrane receptor	-1.928
MAP2K7	mitogen-activated protein kinase kinase 7	kinase	-2.703
PIK3C2A	phosphatidylinositol-4-phosphate 3-kinase catalytic subunit type 2 alpha	kinase	2.078
RELA	RELA proto-oncogene, NF-kB subunit	transcription regulator	-1.531
RHOD	ras homolog family member D	enzyme	2.021
RHOV	ras homolog family member V	enzyme	1.556
SERPINE1	serpin family E member 1	other	16.558
TLR4	toll like receptor 4	transmembrane receptor	-2.744
TNFSF9	TNF superfamily member 9	cytokine	-1.738

Table 6.5. Regulation of Cell Cycle: G2/M DNA Damage Checkpoint pathway (butyrate vs. control)

Symbol	Entrez Gene Name	Type(s)	Expr Fold Change
ABL1	ABL proto-oncogene 1, non-receptor tyrosine kinase	kinase	-1.595
CCNB2	cyclin B2	other	-1.586
CKS1B	CDC28 protein kinase regulatory subunit 1B	kinase	1.852
PLK1	polo like kinase 1	kinase	-2.035
PTPMT1	protein tyrosine phosphatase, mitochondrial 1	phosphatase	-1.675
YWHAG	tyrosine 3-monooxygenasetryptophan 5-monooxygenase activation protein gamma	other	2.531

Table 6.6. Regulation of Cell Cycle: G1/S Checkpoint pathway (butyrate vs. control)

Symbol	Entrez Gene Name	Type(s)	Expr Fold Change
ABL1	ABL proto-oncogene 1, non-receptor tyrosine kinase	kinase	-1.595
CCND1	cyclin D1	transcription regulator	-2.265
CCNE2	cyclin E2	other	-3.382
CDKN2D	cyclin dependent kinase inhibitor 2D	transcription regulator	2.533
E2F8	E2F transcription factor 8	transcription regulator	-2.433
HDAC3	histone deacetylase 3	transcription regulator	1.644
MYC	MYC proto-oncogene, bHLH transcription factor	transcription regulator	-7.166

Expression2Kinases (X2K) was used to identify upstream regulators likely responsible for observed patterns in genome-wide gene expression induced by acetate and butyrate. The inferred networks of transcription factors, proteins and kinases predicted to regulate the expression of the inputted gene lists are indicated in **Figure 6.5**.

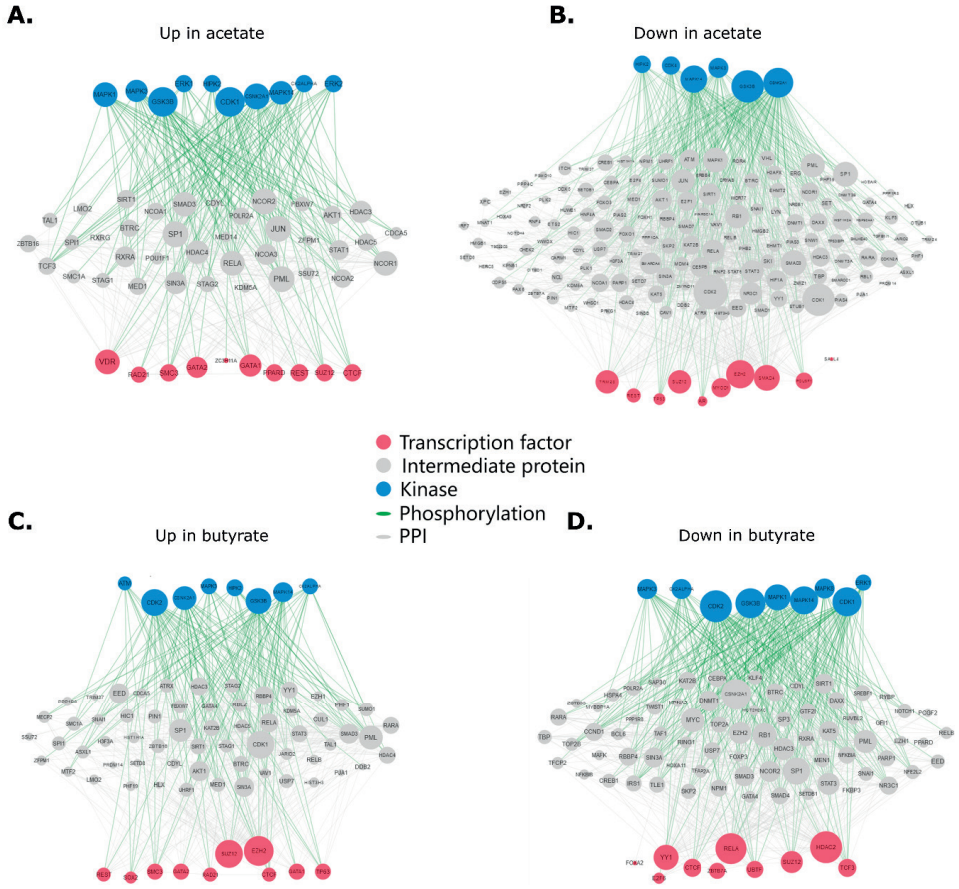

Figure 6.5 (A-D). X2K network analysis based on differentially expressed gene lists. Genes with a minimal fold change of log2 (1.5) and p-value < 0.05 were analysed for transcription factor (TFEA) and kinase (KEA) enrichment using X2K. Shown are interaction between transcription factors, intermediate proteins and kinases when organoids were stimulated with acetate or butyrate.

The top 10 predicted transcription factors and kinases (log2 cut off 1.5 and p-value < 0.05) that were up- or downregulated as a result of acetate and butyrate exposure are shown in Table 6.9. Implicated in the transcriptomic response to butyrate were transcription factors GATA1 and RELA which are known substrates for HDAC3. Some of the other transcription factors listed in Table 6.9 may be unidentified substrates for post-translational modification enzymes identified in the acetate or butyrate induced transcriptome (such as *KAT2A*, *SIRT6* or *HDAC3*).

Table 6.7. Transcription factor and kinase enrichment analysis based on differentially expressed gene lists. Genes with a minimal fold change of log2 (1.5) and p-value < 0.05 were analyzed for transcription factor (TFEA) and kinase (KEA) enrichment using X2K. Shown are the top 10 regulated factors when organoids were stimulated with acetate or butyrate. Red colour indicates p-value > 0.05.

Acetate (2.5 mM)			
Down in acetate		**Down in acetate**	
TFEA	***p-value***	***KEA***	***p-value***
REST	6.68E-09	CDK1	1.28E-23
SUZ12	1.11E-08	CSNK2A1	1.79E-21
REST	2.23E-08	CDK2	1.43E-18
TP53	0.01585	MAPK14	2.34E-18
SMAD4	0.01754	CDK4	6.22E-17
EZH2	0.02395	GSK3B	7.88E-17
AR	0.06142	MAPK1	2.55E-16
EZH2	0.06994	HIPK2	8.00E-15
TRIM28	0.07271	ATM	2.03E-14
SALL4	0.08036	MAPK3	5.57E-13

Butyrate (1 mM)			
Down in Butyrate		**Down in Butyrate**	
TFEA	***p-value***	***KEA***	***p-value***
UBTF	0.000122	MAPK1	6.01E-19
SUZ12	0.000174	MAPK14	4.36E-16
ZBTB7A	0.000189	CSNK2A1	1.04E-14
RELA	0.000895	CK2ALPHA	1.24E-14
CTCF	0.00516	CDK1	4.73E-14
TCF3	0.01002	CDK2	5.24E-14
FOXA2	0.01791	MAPK3	1.47E-13
YY1	0.02933	GSK3B	5.31E-13
HDAC2	0.03932	MAPK8	8.49E-13
E2F6	0.05342	ERK1	7.44E-10

Up in acetate		**Up in acetate**	
TFEA	***p-value***	***KEA***	***p-value***
SMC3	0.02308	MAPK3	1.15E-11
RAD21	0.02891	CDK1	2.19E-10
GATA1	0.03991	MAPK1	9.87E-09
VDR	0.07167	ERK2	2.17E-08
CTCF	0.08494	ERK1	3.41E-08
ZC3H11A	0.1182	CSNK2A1	4.28E-08
REST	0.1206	CK2ALPHA	1.07E-07
GATA2	0.1692	GSK3B	1.43E-07
SUZ12	0.2168	MAPK14	6.51E-07
PPARD	0.2428	HIPK2	1.42E-06

Up in butyrate		**Up in butyrate**	
TFEA	***p-value***	***KEA***	***p-value***
SUZ12	5.80E-14	HIPK2	1.08E-09
REST	1.91E-08	CDK1	2.36E-09
REST	1.13E-06	CK2ALPHA	4.77E-09
EZH2	9.88E-05	CSNK2A1	5.66E-09
SUZ12	0.00033	GSK3B	1.00E-07
RAD21	0.001882	MAPK3	7.34E-07
SMC3	0.002604	CDK2	1.3E-06
EZH2	0.003035	MAPK14	3.87E-06
CTCF	0.00419	AKT1	6.39E-06
GATA1	0.007389	ATM	2.12E-05

Epigenetic Effect of SCFAs in Ileum Organoids

As butyrate is a known inhibitor of Class I histone deacetylases (including histone 3 deacetylase), and the IPA analysis suggested acetate exposure may have epigenetic effects via acetylation of at least two histones, we measured total histone 3 acetylation in organoids 5 hours after SCFA incubation. The percentage of total histone H3 acetylation increased in organoids exposed to butyrate and acetate compared to control **(Figure 6.6)**. Although we

observed a tendency for higher histone H3 acetylation in SCFA-treated organoids, these were not statistically different from control ($p > 0.05$) due to high variation among the treatment samples **(Figure 6.6)**. This is most likely due to the variation we observed in the number of organoids per well.

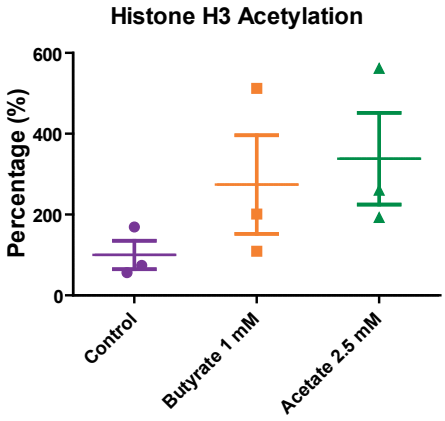

Figure 6.6. Percentage of histone H3 acetylation measured from ileum organoids as a result of 5 hours acetate (2.5 mM) and butyrate (1 mM) exposure. Results are shown as mean ± SEM, n = 3.

CONCLUDING REMARKS

The top canonical pathway predicted to be upregulated by acetate was the Sirtuin Signalling Pathway which contains a group of proteins regulating a wide range of cellular processes such as transcription, apoptosis and inflammation, mainly through deacetylase activity[160]. Three of the regulated genes in this pathway are known to induce epigenetic effects, i.e. *H1F0*, *SIRT6* and *KAT2A*. The Sirtuin pathway is also known to suppress histone deacetylation of pro-inflammatory cytokines and transcription factors which lead to suppression of inflammation[161]. This underlying mechanism may explain the anti-inflammatory effect of acetate on immune cells (**Chapter 4 & 5**). Acetate exposure increased histone 3 acetylation in organoids, although this was not significant due to the high variability, which we hypothesised to be due to variation in the number of organoids in replicate wells. The second top canonical pathway regulated by acetate was the Rho Family GTPases signalling pathway, this pathway has been shown to regulate many aspects of intracellular actin dynamics including organelle development, cytoskeletal dynamics, cell movement, and other common cellular functions. The cellular effects arising from regulation of this pathway are still to be elucidated but might involve proliferation and epithelial remodelling.

Butyrate, a known HDAC3 inhibitor had a much stronger effect on the transcriptome than acetate, presumably through epigenetic mechanisms affecting chromatin as well as acetylation of protein substrates for HDAC3. Consistent with this hypothesis we observed regulation of GATA1 and RELA transcription factors which are known substrates for HDAC3. Our results with butyrate are difficult to compare to a previous study by Lukovac et al. (2014) as they used 5 fold higher concentrations of butyrate[135]. Besides, our preliminary data suggest that butyrate may have some toxicity at 5 mM.

The finding that acetate significantly alters gene expression in intestinal organoids has major implications for understanding the impact of this bacterial metabolite on intestinal function *in vivo* and warrants further study. In future experiments we aim to investigate transcriptional and functional effects of longer periods of exposure to acetate on both the colon and ileum. Polarised monolayers of organoids cells[149] will also be used to reduce variability between replicates for biochemical and cellular assays.

ACKNOWLEDGEMENT

The authors would like to thank Nico Taverne for providing porcine 3D ileum organoids for the transcriptomic experiment.

Supplementary Figure S6.1. IPA analysis. Regulation of canonical pathways induced by acetate.

Supplementary Table S6.1: Unidentified identifiers for differentially expressed genes, after conversion using G:Profiler ($p < 0.05$, log2 fold change > 1.5) when treated with acetate (first two tables), or butyrate (last two tables).

Acetate Down-regulated:									
Unidentified gene identifiers	**Chromo-some**	**Region**	**Max group mean**	**Log_2 fold change**	**Fold change**	**P-value**	**FDR p-value**	**Bonfer-roni**	**description**
ENSSSCG00000001455	7	complement (78856611..78857570)	0.087626	4.699147	25.97672	0.043819	0.76843	1	MHC class II histocompatibility antigen SLA-DRB1 [Source:NCBI gene;Acc:100153386]
ENSSSCG00000002608	6	49895083..49931417	0.017089	1.862174	3.63555	0.023372	0.634052	1	olfactory receptor 11H12-like [Source:NCBI gene;Acc:100523076]
ENSSSCG00000003045	1	complement (223839780..224125540)	0.020633	3.291713	9.792744	0.019553	0.605902	1	ATPase Na+/K+ transporting subunit alpha 3 [Source:NCBI gene;Acc:100329126]
ENSSSCG00000005257	3	complement (41482260..41487800)	0.073242	3.29759	9.832715	0.014336	0.58157	1	transient receptor potential cation channel subfamily M member 3 [Source:NCBI gene;Acc:100157158]
ENSSSCG00000007978	3	complement (63205017..63486666)	0.033534	3.297161	9.829796	0.01457	0.58157	1	hemoglobin subunit alpha [Source:NCBI gene;Acc:110259958]
ENSSSCG00000008250	X	complement (103325989..103327383)	0.073483	4.978641	31.52972	0.033238	0.705939	1	catenin alpha 2 [Source:NCBI gene;Acc:100525337]
ENSSSCG00000012645	2	125663425..125719312	0.056149	2.129775	4.376491	0.019106	0.601339	1	DDB1- and CUL4-associated factor 12-like protein 2 [Source:NCBI gene;Acc:100521308]
ENSSSCG00000014233	15	44066193..44407632	0.020337	3.375226	10.37634	0.000991	0.209093	1	zinc finger protein 474 [Source:NCBI gene;Acc:100525452]

Continue

Supplementary Table S6.1: Unidentified identifiers for differentially expressed genes, after conversion using G:Profiler ($p < 0.05$, log2 fold change > 1.5) when treated with acetate (first two tables), or butyrate (last two tables).

Acetate Down-regulated:									
Unidentified gene identifiers	**Chromo-some**	**Region**	**Max group mean**	**Log_2 fold change**	**Fold change**	**P-value**	**FDR p-value**	**Bonfer-roni**	**description**
ENSSSCG00000026701	2	142505136..142527509	0.017363	2.817662	7.050189	0.012764	0.563445	1	phosphoethanolamine/ phosphocholine phosphatase [Source:NCBI gene;Acc:100621753]
ENSSSCG00000029442	X	74463059..74968349	0.015905	5.414098	42.63889	0.020078	0.611464	1	protocadherin alpha-7 [Source:NCBI gene;Acc:102160218]
ENSSSCG00000029771	7	complement (20849712..20850023)	0.278108	2.91826	7.559337	0.046899	0.784094	1	protocadherin 11 X-linked [Source:NCBI gene;Acc:414736]
ENSSSCG00000032640	1	complement (261228701..261256850)	7.210892	1.801106	3.484872	7.52E-09	6.07E-05	0.000182	histone H4 [Source:NCBI gene;Acc:110261675]
ENSSSCG00000034749	Y	complement (4680259..4704188)	0.809013	8.173292	288.6728	0.001712	0.256098	1	None
ENSSSCG00000036341	14	48943274..49010871	0.014467	5.100439	34.30718	0.029502	0.678111	1	G protein-coupled receptor 143 [Source:NCBI gene;Acc:100624736]
ENSSSCG00000037214	Y	4758466..4783794	0.385653	8.348846	326.0267	0.000463	0.135131	1	None
ENSSSCG00000037429	5	40454911..40455240	0.543074	5.748079	53.74576	0.013422	0.568602	1	shroom family member 2 [Source:NCBI gene;Acc:100522965]
ENSSSCG00000038998	9	complement (113438776..113439696)	0.102813	4.845724	28.75466	0.038452	0.746439	1	None

Continue

Supplementary Table S6.1: Unidentified identifiers for differentially expressed genes, after conversion using G:Profiler ($p < 0.05$, log2 fold change > 1.5) when treated with acetate (first two tables), or butyrate (last two tables).

Acetate Down-regulated:									
Unidentified gene identifiers	**Chromo-some**	**Region**	**Max group mean**	**Log_2 fold change**	**Fold change**	**P-value**	**FDR p-value**	**Bonfer-roni**	**description**
ENSSSCG00000039428	9	complement (10541283..10542795)	0.126706	5.777227	54.84266	0.022205	0.628374	1	olfactory receptor 2A1/2A42-like [Source:NCBI gene;Acc:100525599]
ENSSSCG00000039803	6	84257809..84258372	0.241407	2.800299	6.965846	0.032305	0.698315	1	None
ENSSSCG00000040871	6	complement (47986147..47997228)	0.023288	3.296744	9.826951	0.013909	0.575445	1	None
ENSSSCG00000001455	7	complement (24868656..24914037)	0.032137	4.845676	28.75371	0.037054	0.734167	1	MHC class II histocompatibility antigen SLA-DRB1 [Source:NCBI gene;Acc:100153386]
Acetate Up-regulated:									
Unidentified gene identifiers	**Chromo-some**	**Region**	**Max group mean**	**Log_2 fold change**	**Fold change**	**P-value**	**FDR p-value**	**Bon-fer-roni**	**description**
ENSSSCG00000007642	3	7856701..7876040	0.038981	-1.99864	-3.99622	0.015348	0.588801	1	alpha-2-glycoprotein 1, zinc-binding [Source:NCBI gene;Acc:100519648]
ENSSSCG00000031997	8	51576485..51579375	0.093432	-1.64501	-3.12751	0.030982	0.693806	1	None
ENSSSCG00000033190	18	complement (42062327..42076551)	0.118997	-2.28557	-4.87557	0.005998	0.442082	1	aquaporin 1 (Colton blood group) [Source:NCBI gene;Acc:407773]

Continue

ENSSSCG00000038035	6	81509567..81519072	0.080799	-5.08129	-33.8549	0.041018	0.757013	1	elongation factor 1-alpha, somatic form-like [Source:NCBI gene;Acc:100620900]
ENSSSCG00000039584	13	112751265..112753925	0.498275	-1.83928	-3.57832	0.04004	0.751363	1	None
Butyrate down-regulated:									
Unidentified gene identifiers	**Chromo-some**	**Region**	**Max group mean**	**Log_2 fold change**	**Fold change**	**P-value**	**FDR p-value**	**Bonfer-roni**	**description**
ENSSSCG00000001441	7	24274149..24286960	10.10294	2.259787	4.789207	0	0	0	butyrophilin-like protein 1 [Source:NCBI gene;Acc:100512174]
ENSSSCG00000002348	7	96984542..96990397	3.133309	1.600909	3.033344	0	0	0	acyl-CoA thioesterase 6 [Source:NCBI gene;Acc:100152868]
ENSSSCG00000002877	6	44243314..44357540	2.546945	2.171006	4.503372	0	0	0	zinc finger protein 181 [Source:NCBI gene;Acc:100513473]
ENSSSCG00000002900	6	45184684..45195058	1.893706	1.57515	2.979664	2.66E-15	2.47E-14	6.46E-11	proline and serine rich 3 [Source:NCBI gene;Acc:106504209]
ENSSSCG00000003243	6	complement (58137569..58152660)	0.671589	1.567878	2.964683	2.18E-10	1.45E-09	5.29E-06	zinc finger protein 432 [Source:NCBI gene;Acc:100624217]
ENSSSCG00000003839	6	155800840..155894915	6.409979	2.766972	6.806777	0	0	0	phospholipid phosphatase 3 [Source:NCBI gene;Acc:100512419]
ENSSSCG00000004246	1	43171887..43198297	1.930329	1.504333	2.836936	2.62E-11	1.88E-10	6.36E-07	None

Continue

Supplementary Table S6.1: Unidentified identifiers for differentially expressed genes, after conversion using G:Profiler ($p < 0.05$, log2 fold change > 1.5) when treated with acetate (first two tables), or butyrate (last two tables).

Butyrate down-regulated:									
Unidentified gene identifiers	**Chromo-some**	**Region**	**Max group mean**	**Log_2 fold change**	**Fold change**	**P-value**	**FDR p-value**	**Bonfer-roni**	**description**
ENSSSCG00000005398	1	complement (243035154..243039581)	2.955452	2.007342	4.020407	0	0	0	acyl-coenzyme A amino acid N-acyltransferase 2-like [Source:NCBI gene;Acc:110255172]
ENSSSCG00000007454	17	complement (49258553..49337793)	20.84095	1.732559	3.323167	0	0	0	zinc finger MYND-type containing 8 [Source:NCBI gene;Acc:100155989]
ENSSSCG00000007964	3	38934599..38951526	0.045851	3.337304	10.10715	0.000153	0.000586	1	MEFV, pyrin innate immunity regulator [Source:NCBI gene;Acc:100517333]
ENSSSCG00000008722	8	complement (2842123..3005466)	0.915487	1.944108	3.847999	0	0	0	SH3 domain and tetratricopeptide repeats 1 [Source:NCBI gene;Acc:100737944]
ENSSSCG00000008954	8	70141611..70149557	47.37662	3.997348	15.97062	0	0	0	None
ENSSSCG00000008965	8	complement (70645057..70697907)	0.402263	1.840185	3.580559	2.57E-11	1.84E-10	6.23E-07	betacellulin [Source:NCBI gene;Acc:100505411]
ENSSSCG00000008981	8	71940500..71988112	1.613645	2.627846	6.181024	0	0	0	starch binding domain 1 [Source:NCBI gene;Acc:100522745]
ENSSSCG00000009627	14	6853069..6857835	0.529099	2.225142	4.67557	2.18E-09	1.34E-08	5.29E-05	None
ENSSSCG00000010839	10	complement (11797572..11835322)	0.274257	1.953918	3.874252	0.000356	0.001301	1	None

Continue

Butyrate down-regulated:									
Unidentified gene identifiers	**Chromo-some**	**Region**	**Max group mean**	**Log_2 fold change**	**Fold change**	**P-value**	**FDR p-value**	**Bonfer-roni**	**description**
ENSSSCG00000011531	13	60915098..60925744	2.513689	1.803202	3.48994	0	0	0	histone-lysine N-methyltransferase SETMAR [Source:NCBI gene;Acc:100514009]
ENSSSCG00000012392	X	57374316..57374891	0.584692	1.584919	2.999909	0.00513	0.015833	1	None
ENSSSCG00000012812	X	125452699..125461489	0.454594	1.714427	3.281664	0.004818	0.014935	1	None
ENSSSCG00000014672	9	complement (4174294..4188413)	0.729559	1.818471	3.527071	1.38E-12	1.09E-11	3.35E-08	tripartite motif-containing protein 34 [Source:NCBI gene;Acc:100738479]
ENSSSCG00000016091	15	complement (104071283..104099195)	1.8465	1.751579	3.367269	0	0	0	potassium channel tetramerization domain containing 18 [Source:NCBI gene;Acc:100523334]
ENSSSCG00000020988	6	53718935..53726017	4.979299	2.012543	4.034927	0	0	0	zinc finger protein 114 [Source:NCBI gene;Acc:106510560]
ENSSSCG00000021322	X	20221414..20275192	5.041294	2.699198	6.494409	0	0	0	zinc finger protein X-linked [Source:NCBI gene;Acc:397294]
ENSSSCG00000021414	2	142875088..142877496	0.093584	4.183158	18.16586	0.001256	0.004285	1	protocadherin beta-17-like [Source:NCBI gene;Acc:100739498]
ENSSSCG00000021656	13	complement (135864539..136156061)	0.097835	1.511391	2.850848	0.001471	0.004966	1	None

Continue

Supplementary Table S6.1: Unidentified identifiers for differentially expressed genes, after conversion using G:Profiler ($p < 0.05$, log2 fold change > 1.5) when treated with acetate (first two tables), or butyrate (last two tables).

Butyrate down-regulated:									
Unidentified gene identifiers	**Chromo-some**	**Region**	**Max group mean**	**Log_2 fold change**	**Fold change**	**P-value**	**FDR p-value**	**Bonfer-roni**	**description**
ENSSSCG00000022083	5	84986748..85148983	0.071864	1.738414	3.336681	0.007931	0.023643	1	ankyrin repeat and sterile alpha motif domain containing 1B [Source:NCBI gene;Acc:100513089]
ENSSSCG00000022361	8	complement (118815752..118867551)	0.190734	1.922018	3.789529	0.006217	0.018878	1	B cell scaffold protein with ankyrin repeats 1 [Source:NCBI gene;Acc:100525061]
ENSSSCG00000022466	3	25239062..25245917	1.682419	1.738687	3.337314	5.75E-09	3.42E-08	0.000139	ERI1 exoribonuclease family member 2 [Source:NCBI gene;Acc:100526162]
ENSSSCG00000023403	10	24340150..24454427	1.894241	1.624724	3.083832	0	0	0	leucine rich repeat containing G protein-coupled receptor 6 [Source:NCBI gene;Acc:100511400]
ENSSSCG00000023596	14	complement (60998430..61030598)	0.24894	1.522822	2.873525	3.66E-08	2.04E-07	0.000888	zinc finger protein 33B [Source:NCBI gene;Acc:100738050]
ENSSSCG00000026960	1	115219883..115345923	0.973047	1.801084	3.484819	0	0	0	zinc finger protein 280D [Source:NCBI gene;Acc:100513772]
ENSSSCG00000027790	13	complement (99745467..99786519)	11.52014	1.591401	3.013419	0	0	0	NACHT, LRR and PYD domains-containing protein 1a-like [Source:NCBI gene;Acc:100514323]

Continue

Butyrate down-regulated:									
Unidentified gene identifiers	**Chromo-some**	**Region**	**Max group mean**	**Log_2 fold change**	**Fold change**	**P-value**	**FDR p-value**	**Bonfer-roni**	**description**
ENSSSCG00000028195	15	complement (32547059..32592851)	4.64195	1.654713	3.148605	0	0	0	glutamate rich 1 [Source:NCBI gene;Acc:100620858]
ENSSSCG00000028345	14	complement (60884782..60905183)	1.717285	2.337342	5.053708	0	0	0	zinc finger protein 33B [Source:NCBI gene;Acc:100627762]
ENSSSCG00000028635	3	complement (11841991..12026009)	4.124334	1.505013	2.838273	0	0	0	general transcription factor II-I repeat domain-containing protein 2 [Source:NCBI gene;Acc:100620992]
ENSSSCG00000030901	7	24323772..24334955	1.698269	2.229322	4.689135	1.11E-15	1.06E-14	2.69E-11	None
ENSSSCG00000031121	9	125300365..125337850	5.169511	1.843687	3.589262	0	0	0	tRNA splicing endonuclease subunit 15 [Source:NCBI gene;Acc:100516387]
ENSSSCG00000031589	14	complement (60794333..60861636)	0.121477	2.574617	5.957126	2.80E-06	1.30E-05	0.067911	zinc finger protein 37A [Source:NCBI gene;Acc:100152623]
ENSSSCG00000031644	1	complement (16272696..16275341)	0.281772	2.394624	5.258402	0.012145	0.035056	1	None
ENSSSCG00000031849	X	complement (58941164..58947059)	0.200587	2.234131	4.704793	0.000889	0.003095	1	None
ENSSSCG00000031979	9	complement (12442414..12451687)	30.20611	1.733256	3.324774	0	0	0	potassium channel tetramerization domain containing 14 [Source:NCBI gene;Acc:110255405]

Continue

Supplementary Table S6.1: Unidentified identifiers for differentially expressed genes, after conversion using G:Profiler ($p < 0.05$, log2 fold change > 1.5) when treated with acetate (first two tables), or butyrate (last two tables).

Butyrate down-regulated:									
Unidentified gene identifiers	**Chromo-some**	**Region**	**Max group mean**	**Log_2 fold change**	**Fold change**	**P-value**	**FDR p-value**	**Bonfer-roni**	**description**
ENSSSCG00000032190	8	131976014..131998159	0.123657	3.323573	10.01141	0.016175	0.045649	1	chromosome 8 C4orf36 homolog [Source:NCBI gene;Acc:100627417]
ENSSSCG00000032450	12	complement (44271412..44289645)	5.799669	1.798666	3.478985	0	0	0	LYR motif containing 9 [Source:NCBI gene;Acc:100623359]
ENSSSCG00000032594	6	complement (59239779..59254652)	1.923512	1.637583	3.111441	0	0	0	uncharacterized LOC110261048 [Source:NCBI gene;Acc:110261048]
ENSSSCG00000032969	6	58189335..58201899	0.073252	2.759967	6.773809	4.53E-05	0.000185	1	zinc finger protein 84-like [Source:NCBI gene;Acc:100517161]
ENSSSCG00000033366	3	68539848..68545430	0.899941	1.6344	3.104584	2.55E-15	2.38E-14	6.19E-11	polycomb group ring finger 1 [Source:NCBI gene;Acc:100514636]
ENSSSCG00000033434	11	complement (5317557..5333839)	0.211417	1.622565	3.07922	0.017354	0.048706	1	None
ENSSSCG00000033464	8	67304325..67305962	0.773683	1.811015	3.508891	1.33E-08	7.67E-08	0.000321	None
ENSSSCG00000034074	3	25246175..25247353	0.149594	3.057302	8.324146	0.005772	0.017654	1	None
ENSSSCG00000034540	6	complement (57089528..57129251)	0.222625	1.903916	3.742277	1.03E-10	7.02E-10	2.48E-06	protein ZNF738-like [Source:NCBI gene;Acc:102158906]

Continue

Butyrate down-regulated:									
Unidentified gene identifiers	**Chromo-some**	**Region**	**Max group mean**	**Log_2 fold change**	**Fold change**	**P-value**	**FDR p-value**	**Bonfer-roni**	**description**
ENSSSCG00000034555	5	62106284..62124604	0.035526	3.851751	14.43752	0.003833	0.012059	1	killer cell lectin-like receptor subfamily B member 1B allele B [Source:NCBI gene;Acc:100520491]
ENSSSCG00000034610	5	30188571..30332703	10.35819	1.922448	3.790658	0	0	0	high mobility group AT-hook 2 [Source:NCBI gene;Acc:100513206]
ENSSSCG00000035073	9	92843230..92925360	0.072339	1.677332	3.198358	0.005915	0.018046	1	multidrug resistance protein 1 [Source:NCBI gene;Acc:100522455]
ENSSSCG00000035649	2	complement (44315662..44366880)	1.284465	1.509634	2.847378	4.67E-12	3.54E-11	1.13E-07	calcitonin-related polypeptide beta [Source:NCBI gene;Acc:396563]
ENSSSCG00000035650	2	57245386..57271405	4.916321	2.580477	5.981373	0	0	0	tripartite motif containing 52 [Source:NCBI gene;Acc:100626428]
ENSSSCG00000036078	15	62264268..62416294	0.068189	2.378608	5.200347	0.001072	0.003698	1	None
ENSSSCG00000037214	14	48943274..49010871	0.014467	3.204037	9.215336	0.017755	0.049705	1	None
ENSSSCG00000037324	17	32594220..32597054	2.923211	1.751889	3.367992	0	0	0	None
ENSSSCG00000037571	6	62205215..62215077	0.290109	2.009528	4.026504	0.007039	0.021184	1	None
ENSSSCG00000038171	1	complement (242978615..243050442)	1.784049	2.34527	5.081554	0	0	0	acyl-coenzyme A amino acid N-acyltransferase 2 [Source:NCBI gene;Acc:100515185]
ENSSSCG00000038260	5	79281586..79288705	2.115734	2.101582	4.291798	0	0	0	None

Continue

Supplementary Table S6.1: Unidentified identifiers for differentially expressed genes, after conversion using G:Profiler ($p < 0.05$, log2 fold change > 1.5) when treated with acetate (first two tables), or butyrate (last two tables).

Butyrate down-regulated:									
Unidentified gene identifiers	**Chromo-some**	**Region**	**Max group mean**	**Log_2 fold change**	**Fold change**	**P-value**	**FDR p-value**	**Bonfer-roni**	**description**
ENSSSCG00000038998	5	40454911..40455240	0.543074	5.744827	53.62475	0.017735	0.049666	1	None
ENSSSCG00000039084	1	43258485..43265580	1.149191	1.81073	3.508199	1.59E-11	1.16E-10	3.86E-07	None
ENSSSCG00000039368	10	25738231..25789518	3.065736	1.587984	3.006289	0	0	0	solute carrier family 35 member D2 [Source:NCBI gene;Acc:100514312]
ENSSSCG00000039443	1	104157073..104170987	5.279409	2.535015	5.795831	0	0	0	dynactin-associated protein [Source:NCBI gene;Acc:106508962]
ENSSSCG00000039531	4	122648447..122792723	0.19121	1.576465	2.982382	1.95E-05	8.28E-05	0.471621	None
ENSSSCG00000039688	3	114503150..114508440	1.878528	1.881314	3.684104	0	0	0	None
ENSSSCG00000039695	3	111564931..111570490	0.808278	1.883438	3.689533	0	0	0	coiled-coil domain containing 121 [Source:NCBI gene;Acc:100520301]
ENSSSCG00000040032	5	99297125..99298088	0.610097	2.381957	5.212433	1.74E-05	7.45E-05	0.422134	None
ENSSSCG00000040169	15	133014490..133032001	0.165151	2.257485	4.781573	3.44E-07	1.75E-06	0.008329	None
ENSSSCG00000040187	2	complement (66650447..66711337)	3.162135	1.585142	3.000373	0	0	0	zinc finger protein 791-like [Source:NCBI gene;Acc:106508100]

Continue

Butyrate up-regulated:									
Unidentified gene identifiers	**Chromo-some**	**Region**	**Max group mean**	**Log_2 fold change**	**Fold change**	**P-value**	**FDR p-value**	**Bonfer-roni**	**description**
ENSSSCG00000000148	5	complement (11509336..11543032)	0.078966	-4.31043	-19.8413	7.93E-08	4.27E-07	0.00192	apolipoprotein L3-like [Source:NCBI gene;Acc:106510284]
ENSSSCG00000000483	5	complement (32644709..32673639)	9.033349	-1.61586	-3.06494	0	0	0	Mdm1 nuclear protein [Source:NCBI gene;Acc:100625194]
ENSSSCG00000001859	7	55806636..55807790	17.71863	-2.17471	-4.51495	0	0	0	GDP-D-glucose phosphorylase 1 [Source:NCBI gene;Acc:100156697]
ENSSSCG00000001931	7	61033831..61078507	0.744604	-2.25341	-4.76808	1.13E-13	9.50E-13	2.74E-09	GRAM domain containing 2A [Source:NCBI gene;Acc:100158151]
ENSSSCG00000002140	7	78470339..78480705	0.048015	-1.71585	-3.2849	0.00401	0.012581	1	kelch like family member 33 [Source:NCBI gene;Acc:100154698]
ENSSSCG00000003045	6	49895083..49931417	0.052636	-1.59844	-3.02816	0.001342	0.004561	1	ATPase Na+/K+ transporting subunit alpha 3 [Source:NCBI gene;Acc:100329126]
ENSSSCG00000004081	1	13715672..14042954	0.050566	-1.62093	-3.07573	0.012872	0.037031	1	None
ENSSSCG00000004572	1	109825438..109827175	0.463051	-2.74718	-6.71405	1.76E-06	8.34E-06	0.042553	C2 calcium dependent domain containing 4B [Source:NCBI gene;Acc:100738739]

Continue

Supplementary Table S6.1: Unidentified identifiers for differentially expressed genes, after conversion using G:Profiler ($p < 0.05$, log2 fold change > 1.5) when treated with acetate (first two tables), or butyrate (last two tables).

Butyrate up-regulated:									
Unidentified gene identifiers	**Chromo-some**	**Region**	**Max group mean**	**Log_2 fold change**	**Fold change**	**P-value**	**FDR p-value**	**Bonfer-roni**	**description**
ENSSSCG00000004598	1	complement (114287627..114386473)	10.51405	-3.13879	-8.80785	0	0	0	myocardial zonula adherens protein [Source:NCBI gene;Acc:100154487]
ENSSSCG00000005738	1	complement (272776846..272824184)	5.590601	-1.5392	-2.90633	0	0	0	ral guanine nucleotide dissociation stimulator [Source:NCBI gene;Acc:100513970]
ENSSSCG00000006719	4	complement (101563728..101573906)	0.21562	-1.89681	-3.7239	1.05E-05	4.60E-05	0.25402	hydroxy-delta-5-steroid dehydrogenase, 3 beta- and steroid delta-isomerase 1 [Source:NCBI gene;Acc:445539]
ENSSSCG00000007665	3	8494530..8497318	0.344692	-1.92525	-3.79804	3.41E-06	1.57E-05	0.082751	insulin receptor substrate 1-like [Source:NCBI gene;Acc:100515824]
ENSSSCG00000010064	14	complement (49801161..49807602)	0.278076	-1.60527	-3.04252	0.003885	0.012214	1	glutathione S-transferase theta-1 [Source:NCBI gene;Acc:100153094]
ENSSSCG00000010609	14	complement (115133419..115172417)	0.777489	-1.90235	-3.73822	2.22E-06	1.04E-05	0.053827	None
ENSSSCG00000011291	13	complement (26253910..26265856)	0.102737	-3.21809	-9.30557	0.002215	0.007271	1	None

Continue

Butyrate up-regulated:									
Unidentified gene identifiers	**Chromo-some**	**Region**	**Max group mean**	**Log_2 fold change**	**Fold change**	**P-value**	**FDR p-value**	**Bonfer-roni**	**description**
ENSSSCG00000012832	X	complement (487572..513928)	0.057418	-2.45544	-5.48481	2.23E-05	9.42E-05	0.540889	matrix-remodeling-associated protein 5 [Source:NCBI gene;Acc:100519997]
ENSSSCG00000014079	2	complement (84142287..84219767)	0.043474	-2.1566	-4.45862	0.006845	0.020646	1	None
ENSSSCG00000014993	9	33917370..34033888	0.492114	-1.52881	-2.88548	0.000204	0.000767	1	None
ENSSSCG00000016224	15	124565318..124566979	0.249336	-1.96887	-3.9146	0.000483	0.001738	1	None
ENSSSCG00000016401	15	complement (139610625..139665202)	0.48637	-2.59058	-6.02339	0	0	0	kinesin family member 1A [Source:NCBI gene;Acc:100517246]
ENSSSCG00000020838	5	17585590..17591134	3.792191	-3.99826	-15.9807	0	0	0	keratin, type II cuticular Hb6-like [Source:NCBI gene;Acc:100621639]
ENSSSCG00000023127	6	12421018..12426270	0.253263	-3.97688	-15.7456	0.005931	0.018091	1	chymotrypsinogen B2 [Source:NCBI gene;Acc:100621642]
ENSSSCG00000023156	3	68618571..68624344	1.103944	-2.87495	-7.3358	0	0	0	chromosome 3 C2orf81 homolog [Source:NCBI gene;Acc:100513788]
ENSSSCG00000023812	3	complement (60064302..60114275)	1.120152	-1.63507	-3.10602	2.08E-08	1.18E-07	0.000504	None
ENSSSCG00000024281	6	47613763..47614785	2.453724	-1.52515	-2.87816	0.001877	0.006225	1	galectin-7-like [Source:NCBI gene;Acc:110260983]

Continue

Supplementary Table S6.1: Unidentified identifiers for differentially expressed genes, after conversion using G:Profiler ($p < 0.05$, log2 fold change > 1.5) when treated with acetate (first two tables), or butyrate (last two tables).

Butyrate up-regulated:									
Unidentified gene identifiers	**Chromo-some**	**Region**	**Max group mean**	**Log_2 fold change**	**Fold change**	**P-value**	**FDR p-value**	**Bonfer-roni**	**description**
ENSSSCG00000024500	13	complement (207195537..207204827)	8.71256	-1.52216	-2.87221	0	0	0	cilia and flagella associated protein 410 [Source:NCBI gene;Acc:100621858]
ENSSSCG00000024588	2	complement (75538359..75542331)	1.503294	-2.50217	-5.66538	0	0	0	TLE family member 6, subcortical maternal complex member [Source:NCBI gene;Acc:100623564]
ENSSSCG00000025655	1	239209387..239251317	0.089355	-2.60818	-6.09734	0.000199	0.000751	1	None
ENSSSCG00000026512	2	complement (44042923..44049006)	1.442448	-2.1508	-4.44075	4.00E-15	3.67E-14	9.69E-11	calcitonin-related polypeptide beta [Source:NCBI gene;Acc:100124407]
ENSSSCG00000026701	12	complement (25441225..25449239)	0.30059	-2.2688	-4.81921	4.24E-07	2.13E-06	0.01027	phosphoethanolamine/ phosphocholine phosphatase [Source:NCBI gene;Acc:100621753]
ENSSSCG00000027025	13	complement (122391783..122392670)	0.278075	-1.68221	-3.20919	0.011322	0.03284	1	transmembrane epididymal protein 1A-like [Source:NCBI gene;Acc:102166240]
ENSSSCG00000027232	1	complement (137199072..137297207)	0.036581	-6.07089	-67.2234	0.014205	0.040575	1	family with sequence similarity 169 member B [Source:NCBI gene;Acc:100623531]

Continue

Butyrate up-regulated:									
Unidentified gene identifiers	**Chromo-some**	**Region**	**Max group mean**	**Log_2 fold change**	**Fold change**	**P-value**	**FDR p-value**	**Bonfer-roni**	**description**
ENSSSCG00000027890	3	complement (9821272..9847024)	4.425769	-2.31755	-4.98487	0	0	0	RAS p21 protein activator 4B [Source:NCBI gene;Acc:100624152]
ENSSSCG00000028062	X	complement (83597179..83599213)	0.176445	-1.72002	-3.2944	0.01714	0.048131	1	transcription elongation factor A protein-like 3 [Source:NCBI gene;Acc:100621480]
ENSSSCG00000029321	4	complement (86166016..86170278)	0.692635	-1.60705	-3.04627	0.000246	0.000918	1	None
ENSSSCG00000031706	2	complement (47045931..47120943)	5.448767	-2.48678	-5.60527	0	0	0	None
ENSSSCG00000032309	18	54431140..54470801	0.26549	-1.99772	-3.99369	0.000311	0.001147	1	None
ENSSSCG00000032949	1	complement (108730293..108763353)	2.806953	-2.59111	-6.02562	0	0	0	aph-1 homolog B, gamma-secretase subunit [Source:NCBI gene;Acc:100624829]
ENSSSCG00000033090	2	complement (75547473..75550616)	0.737417	-3.05569	-8.31486	7.00E-10	4.48E-09	1.70E-05	None
ENSSSCG00000033235	5	complement (17571162..17579963)	1.695502	-3.30351	-9.87316	0	0	0	keratin, type II microfibrillar, component 7C-like [Source:NCBI gene;Acc:100621844]
ENSSSCG00000033787	14	51624286..51644457	2.269769	-2.54226	-5.82503	0	0	0	proline dehydrogenase 1, mitochondrial [Source:NCBI gene;Acc:110256626]

Continue

Supplementary Table S6.1: Unidentified identifiers for differentially expressed genes, after conversion using G:Profiler ($p < 0.05$, log2 fold change > 1.5) when treated with acetate (first two tables), or butyrate (last two tables).

Butyrate up-regulated:									
Unidentified gene identifiers	**Chromo-some**	**Region**	**Max group mean**	**Log_2 fold change**	**Fold change**	**P-value**	**FDR p-value**	**Bonfer-roni**	**description**
ENSSSCG00000033864	15	complement (139646918..139674853)	0.086949	-2.95163	-7.73623	0.002008	0.006638	1	None
ENSSSCG00000033937	9	33721060..33770390	0.28009	-2.33926	-5.06044	1.84E-08	1.05E-07	0.000446	None
ENSSSCG00000034069	1	complement (147939952..147963552)	0.134243	-3.50927	-11.3866	0.001112	0.003825	1	None
ENSSSCG00000034702	17	54557574..54559861	0.076348	-2.49974	-5.65582	0.006387	0.019357	1	None
ENSSSCG00000034739	9	complement (109740516..109809999)	0.930081	-2.70246	-6.50911	0	0	0	None
ENSSSCG00000035224	12	25426079..25444517	0.227096	-2.71166	-6.55074	1.57E-09	9.73E-09	3.79E-05	ABI gene family member 3 [Source:NCBI gene;Acc:100621521]
ENSSSCG00000035256	3	17978746..17985101	1.006683	-3.11521	-8.66508	0	0	0	sialophorin [Source:NCBI gene;Acc:100623653]
ENSSSCG00000035577	5	9361818..9417874	0.122788	-2.57612	-5.96332	0.000322	0.001185	1	None
ENSSSCG00000035617	9	complement (119858969..119896385)	2.357047	-1.50066	-2.82973	0	0	0	quinone oxidoreductase-like protein 2 [Source:NCBI gene;Acc:106505010]
ENSSSCG00000036305	6	65255823..65259126	5.982891	-2.45618	-5.48762	0	0	0	small integral membrane protein 1 (Vel blood group) [Source:NCBI gene;Acc:100625759]

Continue

Butyrate up-regulated:									
Unidentified gene identifiers	**Chromo-some**	**Region**	**Max group mean**	**Log_2 fold change**	**Fold change**	**P-value**	**FDR p-value**	**Bonfer-roni**	**description**
ENSSSCG00000036748	3	complement (46071315..46081668)	0.555556	-1.62857	-3.09206	1.23E-05	5.37E-05	0.2989	zinc finger protein 2 [Source:NCBI gene;Acc:100521785]
ENSSSCG00000036884	4	93651708..93676153	0.055236	-3.23232	-9.39775	9.01E-06	3.99E-05	0.218304	None
ENSSSCG00000036948	10	23628938..23663545	0.031994	-2.01628	-4.0454	0.002173	0.00715	1	immunoglobulin-like and fibronectin type III domain containing 1 [Source:NCBI gene;Acc:102167611]
ENSSSCG00000037391	18	55943496..55955067	0.91873	-1.50784	-2.84383	1.52E-11	1.11E-10	3.68E-07	zinc finger protein 775 [Source:NCBI gene;Acc:110257534]
ENSSSCG00000037466	6	55781905..55824239	0.076417	-2.19607	-4.58228	0.011031	0.032041	1	sialic acid-binding Ig-like lectin 5 [Source:NCBI gene;Acc:100515551]
ENSSSCG00000037566	6	complement (88704599..88712853)	1.655641	-2.28145	-4.86168	0	0	0	myotubularin-related protein 9 [Source:NCBI gene;Acc:106510645]
ENSSSCG00000037796	9	130915700..130919520	0.17613	-2.36287	-5.14394	1.88E-05	8.02E-05	0.45623	None
ENSSSCG00000037879	6	complement (47588661..47591122)	11.87566	-1.76334	-3.39483	1.27E-10	8.66E-10	3.09E-06	galectin 7 [Source:NCBI gene;Acc:100217394]
ENSSSCG00000037941	5	complement (41172539..41424734)	0.037533	-2.56272	-5.90822	0.009832	0.028837	1	None
ENSSSCG00000038009	6	62528293..62548163	0.038016	-2.83117	-7.11649	0.001926	0.00638	1	zinc finger protein 850-like [Source:NCBI gene;Acc:100737912]

Continue

Supplementary Table S6.1: Unidentified identifiers for differentially expressed genes, after conversion using G:Profiler ($p < 0.05$, log2 fold change > 1.5) when treated with acetate (first two tables), or butyrate (last two tables).

Butyrate up-regulated:									
Unidentified gene identifiers	**Chromo-some**	**Region**	**Max group mean**	**Log_2 fold change**	**Fold change**	**P-value**	**FDR p-value**	**Bonfer-roni**	**description**
ENSSSCG00000038036	1	complement (261896308..261945723)	0.064743	-3.73058	-13.2744	2.69E-05	0.000113	0.653046	None
ENSSSCG00000038112	2	complement (7028909..7033883)	0.163503	-4.34168	-20.2757	5.03E-07	2.51E-06	0.012191	speedy/RINGO cell cycle regulator family member C [Source:NCBI gene;Acc:100518768]
ENSSSCG00000038331	2	59545870..59557993	0.105821	-1.85996	-3.62997	0.001173	0.004019	1	IQ motif containing N [Source:NCBI gene;Acc:110259318]
ENSSSCG00000038606	1	103906316..103921908	0.429038	-3.43464	-10.8126	8.15E-13	6.53E-12	1.97E-08	uncharacterized LOC102160380 [Source:NCBI gene;Acc:102160380]
ENSSSCG00000038684	3	complement (59957461..59991512)	0.168026	-2.52093	-5.73951	0.000896	0.003121	1	None
ENSSSCG00000039926	Y	complement (6512528..6524995)	0.051039	-2.81884	-7.05595	0.000939	0.003262	1	matrix-remodeling-associated protein 5-like [Source:NCBI gene;Acc:110257935]
ENSSSCG00000040260	3	complement (7581544..7623302)	1.106706	-1.78548	-3.44733	0	0	0	transmembrane protein 238-like [Source:NCBI gene;Acc:110259862]
ENSSSCG00000040412	3	complement (28815796..28816799)	0.17301	-2.94198	-7.68464	0.010749	0.031288	1	None

Continue

Butyrate up-regulated:									
Unidentified gene identifiers	**Chromo-some**	**Region**	**Max group mean**	**Log_2 fold change**	**Fold change**	**P-value**	**FDR p-value**	**Bonfer-roni**	**description**
ENSSSCG00000040467	15	48784307..48835517	0.132044	-1.68154	-3.20769	0.000172	0.000655	1	None
ENSSSCG00000040753	17	complement (47884368..47888879)	0.145138	-6.67593	-102.248	0.007085	0.021304	1	WAP four-disulfide core domain 10A-like [Source:NCBI gene;Acc:100302697]
ENSSSCG00000040837	10	complement (68578573..68621321)	2.789626	-2.35021	-5.09898	0	0	0	None
ENSSSCG00000040885	7	complement (23822741..23825399)	1.248746	-2.10547	-4.30339	3.89E-15	3.57E-14	9.42E-11	sperm acrosome membrane-associated protein 4-like [Source:NCBI gene;Acc:110261493]
ENSSSCG00000040909	6	167973089..167974427	0.203166	-6.33325	-80.6303	0.014357	0.040963	1	None
ENSSSCG00000040925	6	4660531..4668003	0.282976	-3.0928	-8.53152	8.47E-12	6.30E-11	2.05E-07	None

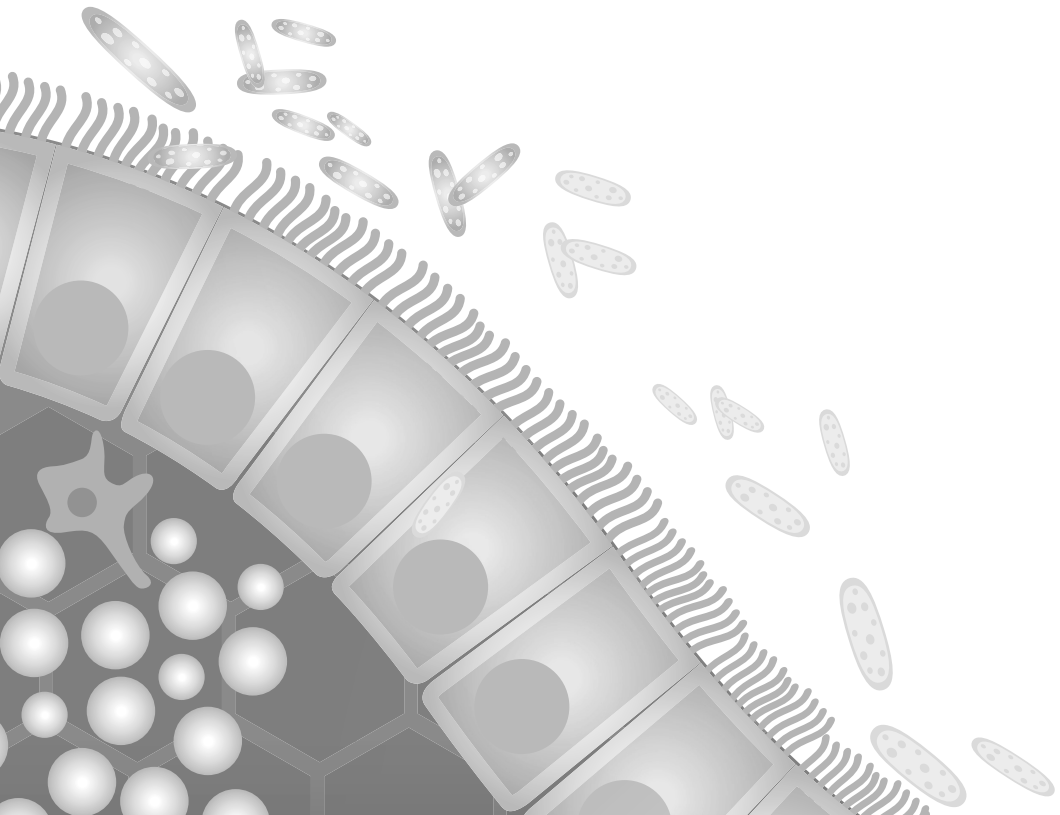

Chapter 7

Administration of novel *Faecalibacterium prausnitzii* strains leads to attenuation of clinical symptoms and shifts microbial composition in DSS-induced colitis

Nuning Winaris[1,2], Ellen Kranenbarg1, Editha Renesteen[1], Simen Fredriksen[1], Eleni Tsompanidou[3,6], Hermi J.M. Harmsen[3], Paul O. Sheridan[4], Alan W. Walker[4], Sylvia H. Duncan[4], Gemma Henderson[5], Wendy Ossieur[5], Jerry M. Wells[1]

[1] Host-Microbe Interactomics Group, Department of Animal Science, Wageningen University & Research, Wageningen, Netherlands

[2] Master Program in Biomedical Sciences, Faculty of Medicine, Universitas Brawijaya, Malang, Indonesia

[3] Department of Medical Microbiology, University of Groningen, University Medical Center Groningen, Groningen, Netherland

[4] Gut Health Group, Rowett Institute, University of Aberdeen, Foresterhill, Aberdeen, Scotland, UK

[5] Human Health Innovation, Chr. Hansen, Hørsholm, Denmark

[6] Winclove Probiotics, Amsterdam, Netherland

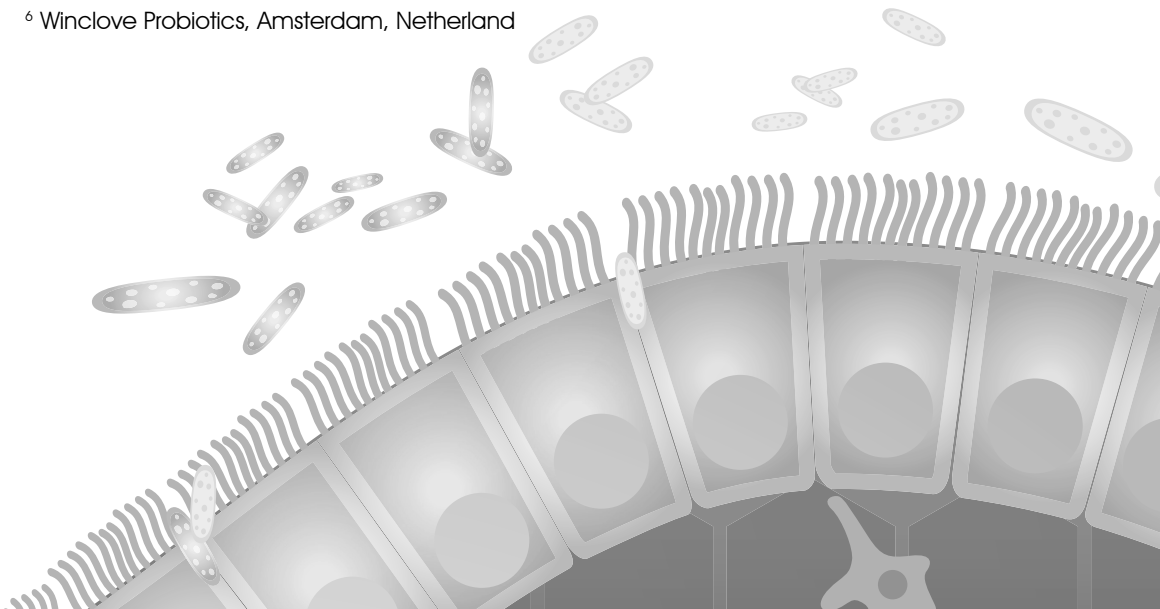

Abstract

Faecalibacterium prausnitzii has been reported as a promising probiotic for the treatment and prevention of inflammatory bowel disease. In a previous *in vitro* study we identified *F. prausnitzii* strains with different immune profiles, namely immuno-stimulatory, immunomodulatory and 'silent' or inhibitory profiles. Here we investigated selected *F. prausnitzii* strains with different immune profiles for their capacity to attenuate DSS-induced colitis in mouse model. We observed the best attenuation of the clinical symptoms after administration of *F. prausnitzii* with a 'silent' immune profile, which confirm our hypothesis that the bacterial strains that induced an 'silent' profile can attenuate colonic inflammation,. We identified specific members of the microbiota associated with DSS-induced colitis and showed that administration of specific *F. prausnitzii* strains accelerated the recovery of the microbiota after cessation of DSS-induced colitis.

Keywords: *Faecalibacterium prausnitzii*, colitis model, IBD treatment

INTRODUCTION

The human intestinal microbiota can modulate our immune system and metabolism, and can influence the development and physiology of our gastrointestinal tract[162]. Considerable progress has been made in identifying, isolating and culturing members of the gut microbiota, but we are only beginning to understand the complex interplay between the microbiome, host genetics and environmental influences, such as diet. It is now clear that the microbial community has a beneficial role in normal homeostasis and that this beneficial relationship with the host microbiota is lost under inflammatory conditions leading to the emergence of opportunist pathobionts that can contribute to the pathophysiology of different diseases.

The involvement of microbiota-host interactions in many aspects of human biology in health and disease opens up many possibilities for deliberately modulating these metabolic and immune interactions to prevent or to treat disease. Over the past few years several species or groups of bacteria have been identified that appear to have clear effects on human physiology. Intestinal disruption which leads to depletion of these beneficial bacteria, may lead to drastic changes in the microbiota, known as dysbiosis. Various studies indicated that dysbiosis was associated with chronic inflammatory diseases[1]. One well-known disease that is associated with dysbiosis is inflammatory bowel disease (IBD), a chronic inflammation syndrome which consist of two major diseases, Crohn's disease (CD) and ulcerative colitis (UC). Intestinal microbiota composition analysis from IBD patients is characterized by a notable depletion of health-associated bacteria such as *Firmicutes* and *Bacteroidetes*, and increased abundance of *Proteobacteria,* which includes pathobiont adherent-invasive *Escherichia coli* (AIEC)[12, 13, 163, 164].

A few specific colonic bacteria have been shown to have anti-inflammatory effects on immune cells and have protective effects in mouse models of IBD[22, 45, 165]. One example is *Faecalibacterium prausnitzii* , one of the 18 species conserved in the intestinal microbiota of healthy humans. *F. prausnitzii* is a Gram positive and extremely oxygen sensitive (EOS) bacterium, well-known as a butyrate producer which likely explains its immunomodulatory capacity to maintain an anti-inflammatory status in the gut. Relative abundance of *F. prausnitzii* can be used as an indicator of gut health since it is known that lower abundancy of this species is strongly associated with both types of IBD, CD[20, 100] and UC[166, 167].

In IBD, Th1 cells accumulate in the intestinal tract of individuals with CD and are directly associated with disease. Oral administration of *F. prausnitzii* strain A2-165 or its supernatant protects against 2,4,6-trinitrobenzene sulfonic acid (TNBS)-induced colitis in mice, a Th1-driven model of human IBD[22, 45]. Furthermore, this *F. prausnitzii* strain A2-165 is also known to have a high capacity to induce anti-inflammatory interleukin-10 (IL-10) in human and murine dendritic cells (DCs) *in vitro*, as well as to modulate T cell responses

in vivo, underlying its mechanism of attenuating inflammatory symptoms in TNBS/DNBS-induced colitis mice[21]. Similar findings were also shown by Qiu *et al*., (2013), where oral administration of *F. prausnitzii* strain A2-162 (ATCC 27766) gave a protective effect in a TNBS-induced rat colitis model[168]. Serum cytokine analysis of these rats showed elevated levels of anti-inflammatory cytokines IL-10 and transforming growth factor-beta 1 (TGF-β1), as well as induced forkhead box P3 (Foxp3) and regulatory T cell (Treg) regulation[168].

Another study by Rossi *et al*., (2015) showed that intra-rectal administration of *F. prausnitzii* strain HTF-F and its extracellular polymeric matrix (EPS) lead to attenuation of clinical parameters in dextran sulfate sodium (DSS)-induced colitis model, an acute model of colitis[23]. Additionally, colonization of young conventionally reared mice with a cocktail of 17 spore-forming strains of commensal *Clostridium* spp. was shown to induce butyrate-mediated accumulation of regulatory T cells (cTregs) in the colon and decrease severity of inflammation in various disease models[26]. These findings suggest that not only the bacteria themselves but also their products and metabolites play a role in the maintenance of homeostasis and can have beneficial effects. Moreover, these studies support the concept of using microbial symbionts or their products for novel prophylactic or therapeutic applications in humans.

In this study we focused on a collection of novel *F. prausnitzii* strains isolated from healthy donors, with the aim to compare the protective capacity of different *F. prausnitzii* strains *in vitro* and investigate their protective mechanisms against DSS-induced colitis *in vivo*. Cytokine profiles of human peripheral blood mononuclear cells (PBMCs) were investigated to screen for immunomodulatory properties of these *F. prausnitzii* strains *in vitro.* Furthermore, selected strains were tested in a mouse DSS-induced colitis model. Disease parameters including body weight loss, colon length, disease activity index (DAI), microscopic evaluation of colon damage, as well as 16S rRNA gene analysis for microbiota composition were performed to assess severity of DSS-induced colitis symptoms in control and treatment groups. We show that certain strains of *F. prausnitzii* attenuate the clinical symptoms of DSS colitis in this mouse model which suggest that these strains might be interesting candidates for future IBD treatments.

MATERIALS AND METHODS

Animals

Four-week old female BALB/c mice were used for this DSS-induced colitis study. The mice were acclimatized for 12 days to stabilize their microbiota composition. After acclimatization the mice were weighed and randomized into 7 experimental groups. Standardized diet (Teklad 2918, Envigo) and drinking water were provided *ad libitum*. The animal experiment

was approved by the Ethical Committee of Wageningen University & Research (experimental number 2017.W-0013.006).

Bacterial preparation and administration

F. prausnitzii strains HTF-05B, HTF-111, HTF-217 and HTF-221 were provided by Chr. Hansen. Briefly, bacteria were grown in semi-optimized production medium and cultures were pelleted by centrifugation and diluted in its vehicle, a PBS cysteine buffer with 15% glycerol solution. This bacterial solution was aliquoted and cryopreserved at - 80°C.

Bacteria were administered orally for a total 17 days; 5 days prior to DSS, 7 days during DSS and 5 days during the recovery period when DSS was no longer administered (see **Figure 7.1**). Syringes containing anaerobic bacterial solution were transferred to the animal facility using an anaerobic box. Each mouse in the treatment groups received 100 µl bacterial solution (containing approximately 10^9 bacteria/ml) of a specific *F.prausnitzii* strain, whereas control groups were given 100 µl of the vehicle.

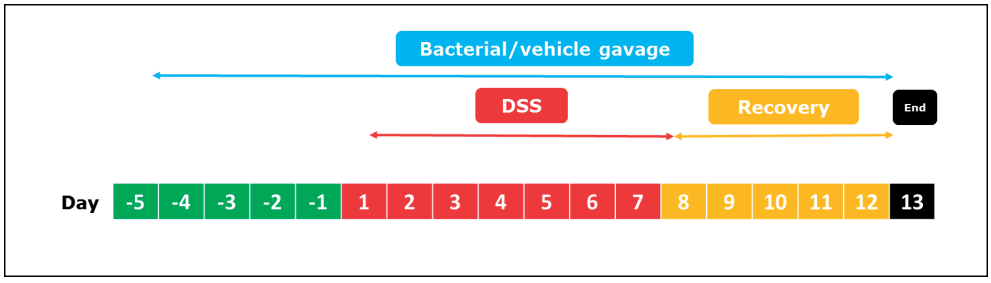

Figure 7.1. Experimental setup for DSS-induced colitis model. Mice were orally administered the *F. prausnitzii* strains or vehicle throughout whole experiment (indicated by blue colour). The DSS was administered along with the bacterial gavage for 7 days (red), followed by recovery without DSS treatment, but with bacterial gavages for 5 days (yellow). All mice were sacrificed on day 18 to collect biological samples.

Dextran sulphate sodium (DSS)-induced colitis

Drinking water containing 3.5% DSS (Sigma-Aldrich) was given for a total of 7 days to assigned groups and was refreshed every 3 days during DSS period. After days 7 it was replaced by normal drinking water. The non-DSS group received normal drinking water throughout experimental period. The experimental design for this study is shown in **Figure 7.1**.

Collection of Biological samples

Body weight of mice was measured daily and faces were scored and collected daily prior to bacterial administration, as well as during DSS and recovery periods. All samples were stored at -80°C. After the recovery period, mice were sacrificed to collect blood (serum), measure

the colon length and weigh the spleen. Additionally, samples were taken to histologically assess colon damage and to quantify faecal lipocalin-2 and colonic MPO levels, as well as to investigate gene expression.

Disease Activity Index (DAI)

Body weight loss, stool consistency and the presence of blood in stool were scored daily during the DSS and recovery period to determine disease activity index (DAI). The DAI scores were determined as previously described by Cooper et al. (1993)[169].

Histological evaluation of colon damage

Colon tissue from animals in all groups was collected for histological analysis using the swiss-roll technique[170]. Subsequently, swiss rolls were fixed in 4% paraformaldehyde (PFA), embedded in paraffin, sectioned at 5 µm, and stained with haematoxylin and eosin (H&E) for light microscopic assessment. Evaluation of colon damage was examined using an Olympus BX 40 microscope equipped with an Olympus Camedia DP 70 digital camera, and the images were analysed using Olympus DP-Soft.

Quantification of Lipocalin-2/NGAL by ELISA

Faecal samples were dissolved in PBS and homogenized using FastPrep-24 5G™ High-Speed Homogenizer for 40 seconds at a 6.0 m/sec. and then centrifuged at 13,000 rpm for 1 minute at room temperature. Finally, the supernatant was collected for measurement of lipocalin-2 using a Mouse Lipocalin-2/NGAL ELISA kit (R&D Systems) according to manufacturer's instructions.

Bicinchoninic acid (BCA) protein assay and Myeloperoxidase (MPO) assay

Frozen colon tissue was put in a gentleMACS M tube (Mylteni Biotec) containing 300 µl freshly prepared protein extraction buffer (0.2 M Sucrose and 20 mM Tris, pH 7.4 + protein inhibitor tablet (0463132001 Roche). The tissue was homogenized by using a gentleMACS Dissociator (MACS Miltenyi Biotec) using the Protein_01 program. Homogenized tissue was centrifuged at 4,000 x g for 5 minutes at 4°C and supernatant was collected for BCA and MPO assays.

To measure total protein content a BCA protein assay (Thermo Scientific Pierce Biotechnology) was performed according to manufacturer's protocol. To investigate the local inflammation status in ileum, the MPO protein concentration was determined using a Myeloperoxidase (MPO) ELISA kit (Hycult Biotechnology) according to manufacturer's instructions. The results of the MPO ELISA were expressed relative to the total amount of protein.

Cytokine measurements in serum

The concentrations of various cytokines, including interleukin-10 (IL-10), interleukin-12p70 (IL-12p70), interleukin-1 beta (IL-1β), tumour necrosis factor-alpha (TNF-α), and interferon-

gamma (IFN-γ) in serum samples were measured by magnetic bead-based multiplex immunoassay using the Bio-Plex Pro™ Assay (Bio-Rad) according to the manufacturer's instructions. Samples were analysed using a MAGPIX® System (Luminex), with Bioplex Manager Pro software.

Colonic RNA extraction and cDNA synthesis

RNA isolation from colon tissue was performed using a RNAeasy isolation kit (Qiagen according to manufacturer's instructions). Quality and quantity of RNA were determined by measuring the absorbance at 260 and 280 nm using a Denovix DS-11 Spectrophotometer (GC Biotech). Subsequently, cDNA synthesis was performed, using qScript cDNA synthesis kit (Quantabio). Briefly, 4 µl qScript reaction mix (5x) was mixed with 1 µl qScript Reverse Transcriptase, and 1 µg of total RNA (concentration) and RNase free water was added to a total volume 20 µl for plus RT. As a control for genomic DNA contamination we used the same procedure in which the qScript Reverse Transcriptase was replaced by RNase free water. The cDNA synthesis reaction was performed in a BIORAD PCR machine at 22°C for 5 minutes, followed by 42°C for 30 minutes, and 85°C inactivation for 5 minutes. Samples were then cooled to 4°C and stored at -20 °C prior to qPCR analysis.

Quantitative real-time polymerase chain reaction (RT-PCR)

Real-time PCR (RT-PCR) reactions were performed in a Rotorgene 2000 real-time cycler (Qiagen) using GoTaq master mix (Promega), according to the manufacturer's instructions, in a final volume of 25 µl (12.5 µl GoTaq qPCR master mix, 1.75 µl primer mix (5 µM each), 5.75 µl RNAse free water and 5 µl cDNA template (1:20 dilution)). The qPCR conditions were as follows: initial denaturation at 95°C for 2 minutes, followed by 40 cycles at 95°C for 15 seconds and 60°C for 60 seconds. Housekeeping gene hypoxanthine-guanine phosphoribosyltransferase (*HGPRT*) was used to measure the relative expression of *Mucin-2* (*Muc-2*), *Trefoil factor-3* (*Tff-3*). Comparative quantitation analysis and Pfaffl method were used to calculate relative gene expression in this study[171].

16S rRNA gene Analysis for Microbiota Composition

Faecal samples were collected at different time points **(Figure 1)**; Day -5 (before start of gavages), Day 1 (starting point of DSS period), Day 7 (the end of DSS period), Day 10 (in the middle of recovery period), Day 13 (day of sacrifice). DNA was extracted from faeces samples using a PowerFecal DNA Isolation Kit (Mo Bio, QIAGEN) according to manufacturer's protocol, with some modifications. DNA quality and quantity were checked by measuring the absorbance at 260 and 280 nm using a Denovix DS-11 Spectrophotometer (GC Biotech) and a Qubit dsDNA BR Assay (ThermoFisher). The 16S rRNA gene V3-V4 region was amplified with primers 341F (CCTAYGGGRBGCASCAG) and 806R (GGACTACNNGGGTATCTAAT) and sequenced on an Illumina HiSeq machine with rapid-run mode 250 bp paired end sequencing. The primers were removed with cutadapt 2.3 [172] using default settings before being

processed in DADA2[173] following the v1.4 workflow for paired end big data. Taxonomy was assigned with SILVA database v132[174]. Amplicon sequence variants (ASVs) with taxonomic assignment as eukaryotic or chloroplast were discarded, and read counts were rarefied the minimum library size (44726 reads). Alpha and beta diversity were calculated with R packages Phyloseq [175] and vegan[176], and the adonis function in vegan was used to perform PERMANOVA. ASVs with different abundance between groups were detected using the R randomForest package[177].

Statistical analysis

Statistical analysis was performed by using GraphPad Prism® software (version 5, GraphPad Software). Results of significant differences among the experimental groups as analysed by student t-test were depicted as (*p<0.05, **p<0.01, ***p<0.001). Some clinical parameters such as body weight and DAI were statistically analysed using non-parametric test one-way ANOVA to show significant difference among the groups at each time point.

RESULTS

Novel *F. prausnitzii* strains attenuate disease parameters in DSS-induced colitis

Four selected *F. prausnitzii* strains as well as the previously reported beneficial strain (A2-165) were administered orally by daily gavage to the treatment groups for 17 days. The bacterial gavage was given 5 days prior to DSS period, 7 days during DSS period itself, followed by 5 days of recovery period. Body weight and stool consistency were measured throughout the study and used to determine the disease activity index (DAI) during DSS and recovery periods. In addition to DAI, faecal samples were also collected at intervals to measure the inflammation marker (Lipocalin-2) and effect of treatments on microbiota. At the end of the study mice were sacrificed and other clinical parameters including colon length and spleen weight were measured. Colon tissue and blood samples were also collected for analysis of inflammation markers.

As expected, administration of DSS (from day 1 to day 7 in **Figure 7.2A)** led to a significant reduction in body weight starting about 6 days after the onset of DSS administration whereas the body weight of the vehicle only control group (no DSS) gradually increased over the same period (**Figure 7.2A**). After cessation of DSS on day 8, the body weight continued to decrease for 2 or 3 days (depending on intervention) but then increased to a value similar to that of the vehicle control (**Figure 7.2A**). Oral administration of *F. prausnitzii* strain HTF-217 significantly reduced the weight loss on Day 8 and significantly increased body weight during the recovery period (Day 10 and Day 11 **Figure 7.2A**). Two other strains A2-165 and HTF-111 also significantly increased body weight on Day 10 compared to the mice administered DSS and vehicle control.

All strains of *F. prausnitzii* significantly reduced the combined disease activity index (DAI) compared to the vehicle control from Day 6 of DSS administration to Day 11 in the recovery period, however it was evident that some strains attenuated colitis more than others (HTF217> HTF111> HTF-221, A2-165 and HTF-05B) (**Figure 7.2B**). Furthermore, administration of *F. prausnitzii* strains also attenuated the shortening of the colon, a commonly reported characteristic of DSS-induced colitis in mice. However, this was only significant for strains A2-165, HTF-111, and HTF-05B (**Figure 7.2C**). For strain HTF-111 the colon length (average 8.7 cm) was similar to the vehicle control group (average 8.9 cm).

We observed that DSS-induced colitis caused an enlargement of the spleen and that all *F. prausnitziii* treated mice had smaller spleens than the DSS control group. However, this was only significant for two strains due to high variability (**Figure 7.2D**).
Histopathological changes were assessed in 'swiss roll' sections of mouse colons at the end of the experiment. Pathological features were observed in areas of the colon of the DSS treated group but not the control group (no DSS) or the groups administered strains HTF-111 and HTF-217. The mice that received HFT-05B, A2-165 and HTF-221 showed mild signs of intestinal damage compared to the control (**Figure 7.2E**).

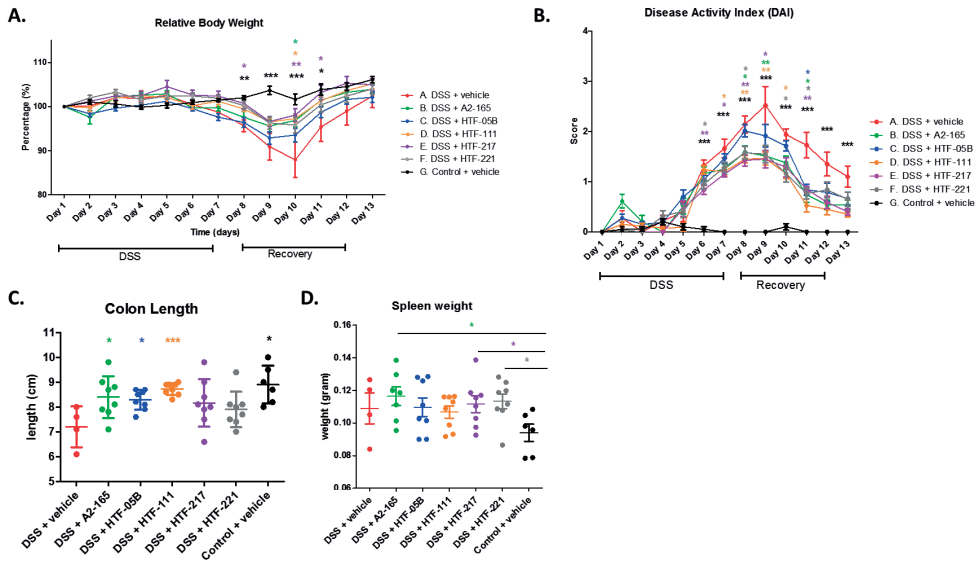

Figure 7.2 (A-E). Disease parameters measured in DSS-induced colitis model. **(A)** average relative body weights; **(B)** disease activity index (DAI); **(C)** colon lengths; **(D)** spleen weights **(E)** H&E-stained image of swiss roll section made from the distal to proximal end of mice colon (objective 10x). Error bars represent SEM, n = 4 (DSS treated group); 6 – 8 (all other groups), with *p<0.05, **p<0.01, ***p<0.001.

Continue on page 150

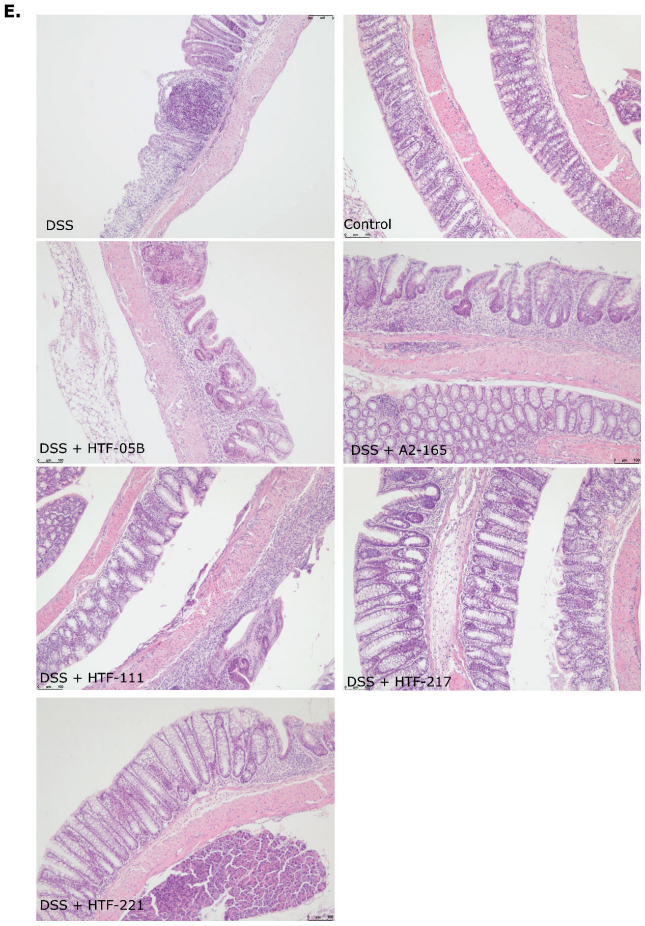

Figure 7.2 (A-E). Disease parameters measured in DSS-induced colitis model. **(A)** average relative body weights; (**B)** disease activity index (DAI); **(C)** colon lengths; **(D)** spleen weights **(E)** H&E-stained image of swiss roll section made from the distal to proximal end of mice colon (objective 10x). Error bars represent SEM, n = 4 (DSS treated group); 6 – 8 (all other groups), with *p<0.05, **p<0.01, ***p<0.001.

To further assess the protective capacity of *F. prausnitzii* strains against DSS-induced colitis we measured lipocalin in the faeces, collected daily throughout the experiment, as well as myeloperoxidase in colon tissue and serum concentrations of inflammatory cytokines at the end of the experiment. On the last day of DSS treatment (Day 7) and during the recovery period, the amounts of faecal lipocalin increased 10 to 20-fold in DSS treated groups compared to the vehicle control (**Figure 7.3**). The administration of strains HTF-111 and HTF-221 led to a significant decrease of Lipocalin-2 protein concentration on Day 9 (during recovery period) (**Figure 7.3**).

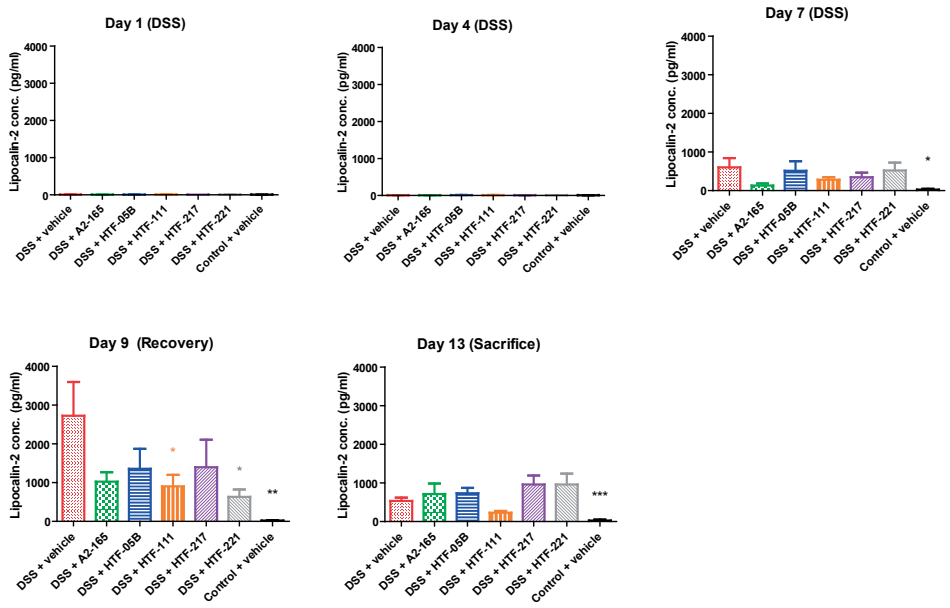

Figure 7.3. (A-E) Inflammation marker Lipocalin-2 concentration (per mg feaces) measured from faecal samples collected at different days during DSS and recovery periods. Error bars represent SEM, n = 4 (DSS treated group); 6 – 8 (all other groups), with *p<0.05, **p<0.01, ***p<0.001.

To investigate the systemic inflammatory status of the mice, concentrations of pro- (IL-12p70, IL-1β, TNF-α and IFN-γ) and anti-inflammatory (IL-10) cytokines, were measured in serum. There were no significant differences observed between the DSS and treatment groups for all cytokines measured (**Supplementary figure 7.S1**).

To investigate possible protective effects of *F. prausnitzii* on intestinal barrier functions in the DSS colitis model, we measured relative expression of *Muc-2*, the secreted mucin and *Tff-3* which is important for wound healing in the colon, by RT-qPCR. Using RNA obtained from colonic tissue, we showed that the relative expression of *Muc-2* significantly decreased 4 to 6-fold compared to the DSS vehicle group for three of the five *F. prausnitzii* strains (A2-165, HTF-217, HTF-221). Unfortunately, no significant effect was observed for *Tff-3* expression level among the groups (**Figure 7.4**).

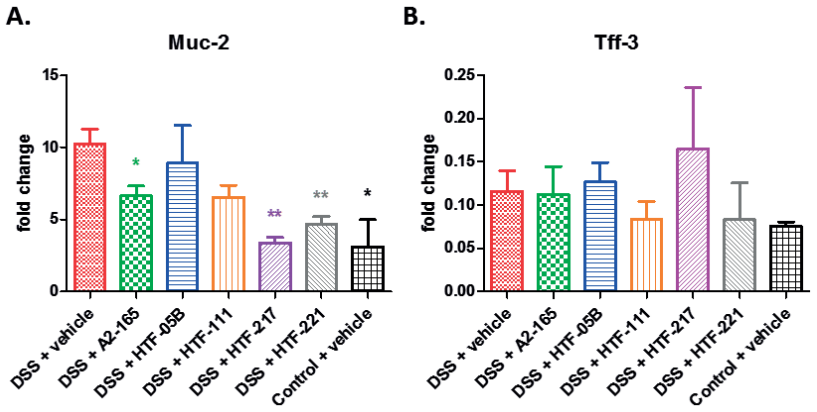

Figure 7.4 (A-B). Gene expression level measured in colonic samples. Fold changes of (A) *Muc-2* and (B) *Tff-3* gene expression relative to housekeeping gene *HPGRT*. Error bars represent SEM, n = 4 (DSS treated group); 6 – 8 (all other groups), with *p<0.05, **p<0.01, ***p<0.001.

While all *F. prausnitzii* strains had an attenuating effect on some of the disease parameters associated with DSS-colitis there were marked differences in efficacy (**Table 7.1**). In terms of the number of disease parameters significantly attenuated, strain HTF-111 appeared to be the most effective intervention. Second was strain HTF-217 which significantly reduced the DAI for 5 days and body weight loss for 3 days consecutively (**Figure 7.2**), followed by HTF-221 and then A2-165. Strain HTF-05B was the least effective intervention.

Table 7.1. Protective effect of various *F. prausnitzii* strains measured from disease parameters of DSS-induced colitis model

Disease parameters	Strains				
	A2-165	HTF-05B	HTF-111	HTF-217	HTF-221
Body weight*	•		•	•••	
DAI*	•••	•	••••	•••••	••••
Colon length	•	•	•		
Less histological damage			•	•	
Lipocalin-2			•		•

Asterisk symbol (*) indicates parameter was significantly changed for multiple days.

Administration of novel *F. prausnitzii* strains lead to distinct shift in microbiota composition in DSS-induced colitis model

Bacterial DNA was extracted from mouse faecal samples, collected at different time points throughout the study, for sequencing of 16S rRNA gene amplicons to characterize the microbiota. In the 5 days before DSS administration there were no major changes in the microbiota composition. Before DSS treatment the top nine most abundant bacterial genera

included *Lactobacillus, Roseburia*, *Lachnoclostridium, Bacteroides, Alistipes, Alloprevotella*. *Faecalibacterium* and its sole known species *F. prausnitzii* were present in relatively low abundance as previously reported[178].

After 6 days of DSS administration there were major alterations in the gut microbiota composition. In all the groups administered DSS the relative abundance of *Alistipes* was considerably decreased at the end of this period. There were also smaller increases of *Odoribacter*, a Gram-negative genus that includes opportunistic pathogens. The relative abundance of *Roseburia*, *Alloprevotella*, and *Rikenellaceae* decreased notably in this period. In group G, which was administered the vehicle but no DSS in this period, *Roseburia, Alistipes*, and *Rikenellaceae* were not decreased (**A-F**, **Figure 7.5**). However, the relative abundance of *Bacteroides* was notably increased. At the end of the recovery period the relative abundance of *Rikenellaceae*, *Alistipes*, and *Alloprevotella* were increased in all groups administered DSS, while the relative abundance of *Bacterioides* decreased. In group G (no DSS) the abundance was similar to that at the beginning of the experiment (**Figure 7.5**).

We compared alpha diversity between the groups at different time points using Shannon's diversity index (**Figure 7.6**) and pairwise Wilcoxon rank sum tests. Alpha diversity was highly variable between groups and time points. At the beginning of the experiment, group G (control) had a significantly higher alpha diversity compared to group A (p = 0.02), D (p = 0.002) and E (p = 0.04). On day 7, the alpha diversity dropped dramatically for the groups that received DSS. On day 10 the mice treated with HTF-111 (group D) reached the lowest alpha diversity. The diversity of the treatment groups increased again on day 13, though not fully reaching the values observed at the beginning of the experiment (**Figure 7.6**).

To visualize the shift in microbiota composition throughout the study a principal coordinates analysis (PCoA) plot of Bray-Curtis dissimilarity was created (**Figure 7.7**), showing that the samples cluster somewhat by timepoints and groups. PERMANOVA found this clustering to be significant ($p < 0.0001$) for both group ($R^2 = 0.04$) and timepoint ($R^2 = 0.35$). The groups were relatively clustered before bacterial administration, while they became more dispersed at the later time points. The variation on axis 1 slightly increased among the groups after 5 days of bacterial administration, except for the DSS group. At the end of the DSS period, the microbiota of all groups was dissimilar to that at the start of DSS treatment but this was substantially less for the control group which received vehicle only. During the recovery period (i.e. no DSS) the microbiota became more similar to that observed prior to the DSS treatment, with the control group (vehicle only) being most similar. Highest variation in the microbiota within each group was observed in the middle of recovery period (Day 10) (**Figure 7.7**).

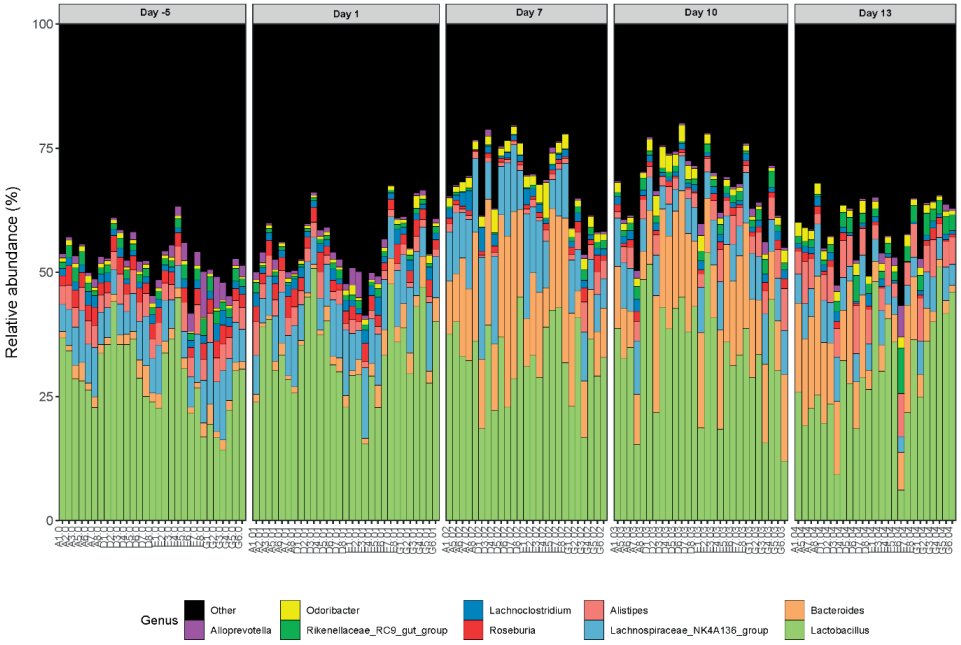

Figure 7.5. Distribution of genera among observed groups at different time points. Relative abundance of each genus represented in different colours. Groups observed for this microbiota composition analysis; DSS only (group A), DSS + HTF-111 (Group D), DSS + HTF-217 (Group E) and untreated control (Group G).

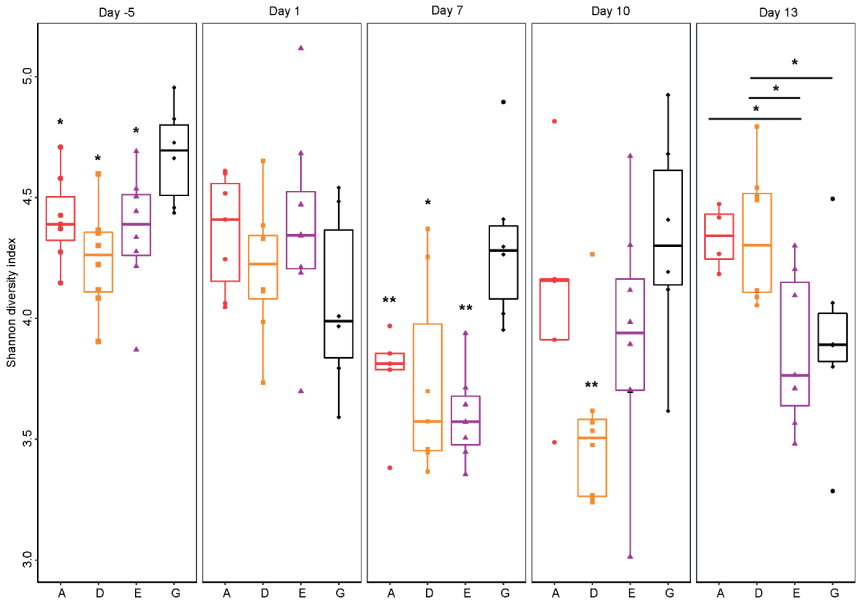

Figure 7.6. Shannon Alpha diversity comparisons between the groups at different time points. Groups observed for this analysis; DSS only (A), DSS + HTF-111 (D), DSS + HTF-217 (E) and untreated control (G). n = 4 (DSS treated group); 6 – 8 (all other groups), with *p<0.05, **p<0.01, ***p<0.001.

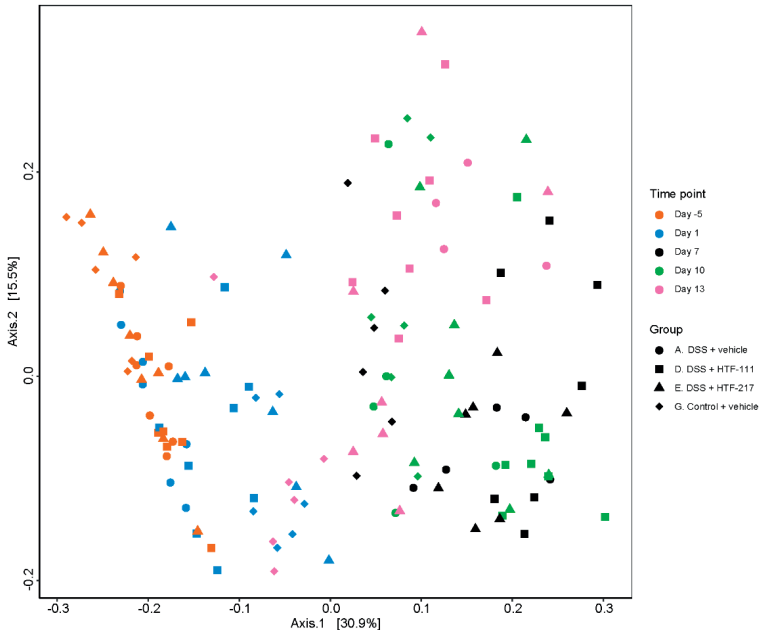

Figure 7.7. Principal coordinates analysis (PCoA) plot of Bray-Curtis distance for microbiota composition. Different colours represent different time points of sample collection, while different shapes represent different treatment groups. Axis.1 explained 30.9% of variation (PC1), and Axis.2 explained 15.5% of variation (PC2).

DISCUSSION

Four novel *F. prausnitzii* strains, (**Chapter 3**), and strain A2-165 which was previously reported to attenuate disease in mouse models of colitis[21, 22] were tested in the mouse DSS-colitis model. The other novel strains used in this *in vivo* study were selected based on their different immunomodulatory properties using *in vitro* immune assays (**Chapter 3**).

All *F. prausnitzii* strains attenuated the colitis disease activity index (DAI). Strains HTF-111 and HTF-221 also decreased the gut inflammatory marker lipocalin 2 and three strains reduced shortening of the colon, a characteristic of colitis. The lack of effect of strain HTF-05B on the DAI might be related to its capacity to induce strong cytokine responses in PBMCs (**Chapter 3**). Previous studies on attenuation of colitis by *F. prausnitzii,* selected strains such as A2-165, based on their capacity to induce high amount of IL-10 and little IL-12, with the hypothesis that IL-10 signalling in immune cells and tissue would suppress inflammation and promote Treg induction by dendritic cells[21, 22]. However, *in vitro* we found that A2-165 induced high amounts of the inflammatory cytokine TNF-α as well as IL-10 (**Chapter 3**). In contrast, the three best performing strains in our study (HTF-111, HTF-221 and HTF-217) elicited

relatively low levels of all cytokines (**Chapter 3**). Moreover, addition of these strains with another inflammatory stimulus (i.e. heat-inactivated bacteria/HIB) significantly attenuated the cytokine response compared to the HIB stimulus alone (**Chapter 3**). The attenuating effect of these strains suggests that the anti-inflammatory mechanism observed *in vitro* may also occur *in vivo*, reducing the inflammatory colon tissue damage caused by DSS-induced loss of the physical mucus barrier.

We found the most crucial protective effects of our strains toward the end of DSS treatment and during the recovery period (**Figure 7.2**). As can be seen from the inflammation marker lipocalin, the onset of intestinal inflammation is rapid, with levels increasing over 100-fold, but once DSS is removed from the drinking water, the local inflammation rapidly resolves (**Figure 7.3**).

To investigate the recovery of the epithelial barrier function, we measured expression of *Tff-3*, which promotes mucosal repair[179] and *Muc-2* gene expression, which plays an important role in maintaining epithelial barrier function in the gut. *Muc*-2 gene expression known to be upregulated in inflammation state[180-183], whereas *Tff-3* expression is reported to be lowered in IBD cases and loss of *Tff3* in mice has been shown to increase susceptibility to colitis by impairing tissue repair[184].

At the end of the recovery period RNA expression of *Muc-2* was lowest in the colon tissue of mice treated with strains HTF-111 and HTF-221 and the control whereas the DSS treated mice had the highest levels of *Muc-2* expression. This could be due to the fact that that the repair process of epithelial barrier was accelerated by strains HTF-111 and HTF-221 and inflammatory cytokines which increase *Muc-2* transcription were reduced compared to the DSS group and other interventions.

As for the other disease parameters, histology of the colon revealed only limited pathology after five days of recovery, although we observed signs of damage on epithelial surface in the animals treated with DSS alone. Only mild signs of pathology were observed in treatment groups HTF-05B, HTF-221 and A2-165, but mice treated with HTF-111 and HTF-217 were comparable to the control group without DSS.

As reported previously, DSS-induced colitis induced major alterations in microbiota composition[185]. In humans epithelial damage caused by inflammatory responses has been found to increase permeability of the gut and production of reactive oxygen species which kills EOS commensal bacteria and leads to expansion of *Proteobacteria* phylum[12, 186]. In previous DSS-induced colitis studies, the two bacterial families *Enterobacteriaceae*[187] and *Bacteroidaceae*[187-189], which include known pathobionts such as enterotoxigenic *Bacteroides fragilis* (ETBF)[190] and adherent invasive *E. coli* (AIEC)[163, 164] were reported

to be present in high abundance. In our study we indeed observed a substantial increase in *Bacterioides* at the end of DSS and during the recovery period, when the inflammation was most pronounced. However, *Enterobacteriaceae* was only present in low abundance (0.18%) in this study. After the recovery period, the relative abundance of *Rikenellaceae,* which is associated with a healthy gut condition, slowly increased and the abundance of *Bacteriodes* decreased, particularly in the groups treated with strains HTF-111 and HTF-217. This indicated that the microbiota composition was reverting to a more health-associated composition in the groups where *F. prausnitzii* significantly attenuated the colitis. Furthermore, only minor alterations in the microbiota composition were observed in the groups administered HTF-111 and HTF-217, the *F. prausnitzii* strains that showed the best protection capacities in our DSS-induced colitis study. The daily handling and gavage also led to microbiota changes in the control group, but that this change was smaller than that of the other groups.

IBD is often characterized by microbial dysbiosis in the gut[12, 13]. However, it remains unclear whether the alteration of the microbiota composition serves as a cause or an effect in the development of human IBD[191]. This study allowed us to monitor dynamic changes in microbiota composition that happened during colitis development. Furthermore, we were able to identify specific bacteria that were associated with inflammation status in this DSS-induced colitis study. From this study we conclude that the intervention of certain *F. prausnitzii* strains may help to restore the balance in faecal microbiota composition which was induced by the colitis.

ACKNOWLEDGEMENT

The authors would like to thank Anja Taverne-Thiele, for technical support in the histology sample preparation, microscopical observations and help during animal experiment preparation.

Supplementary Figures

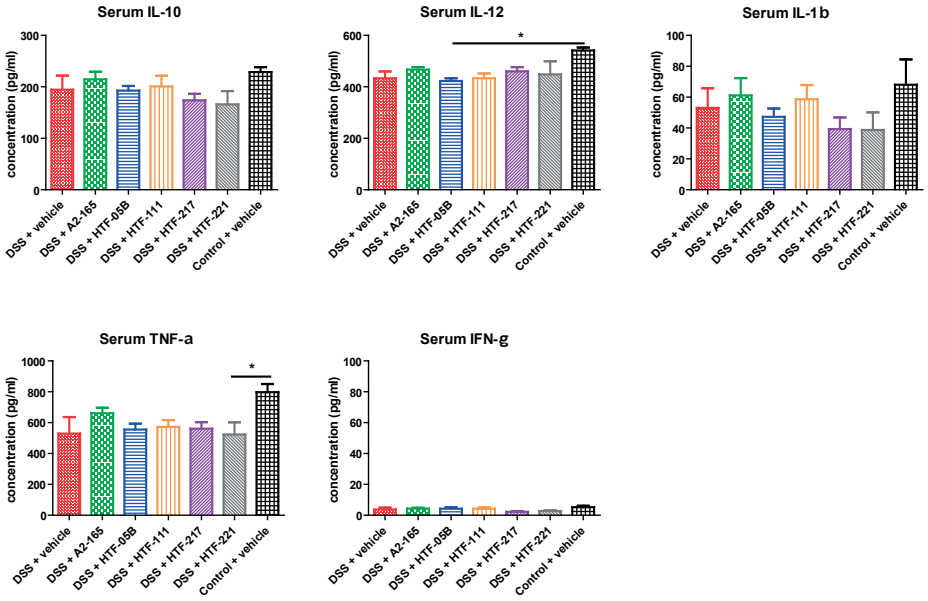

Figure 7.S1 (A-E). Cytokine concentrations measured in blood serum. No significant differences of cytokines level IL-10, IL-12, IL-1β, IFN-γ and TNF-α measured from blood serum except for control group. Error bars represent SEM, n = 4 (DSS treated group); 6 – 8 (all other groups), with *p<0.05, **p<0.01, ***p<0.001.

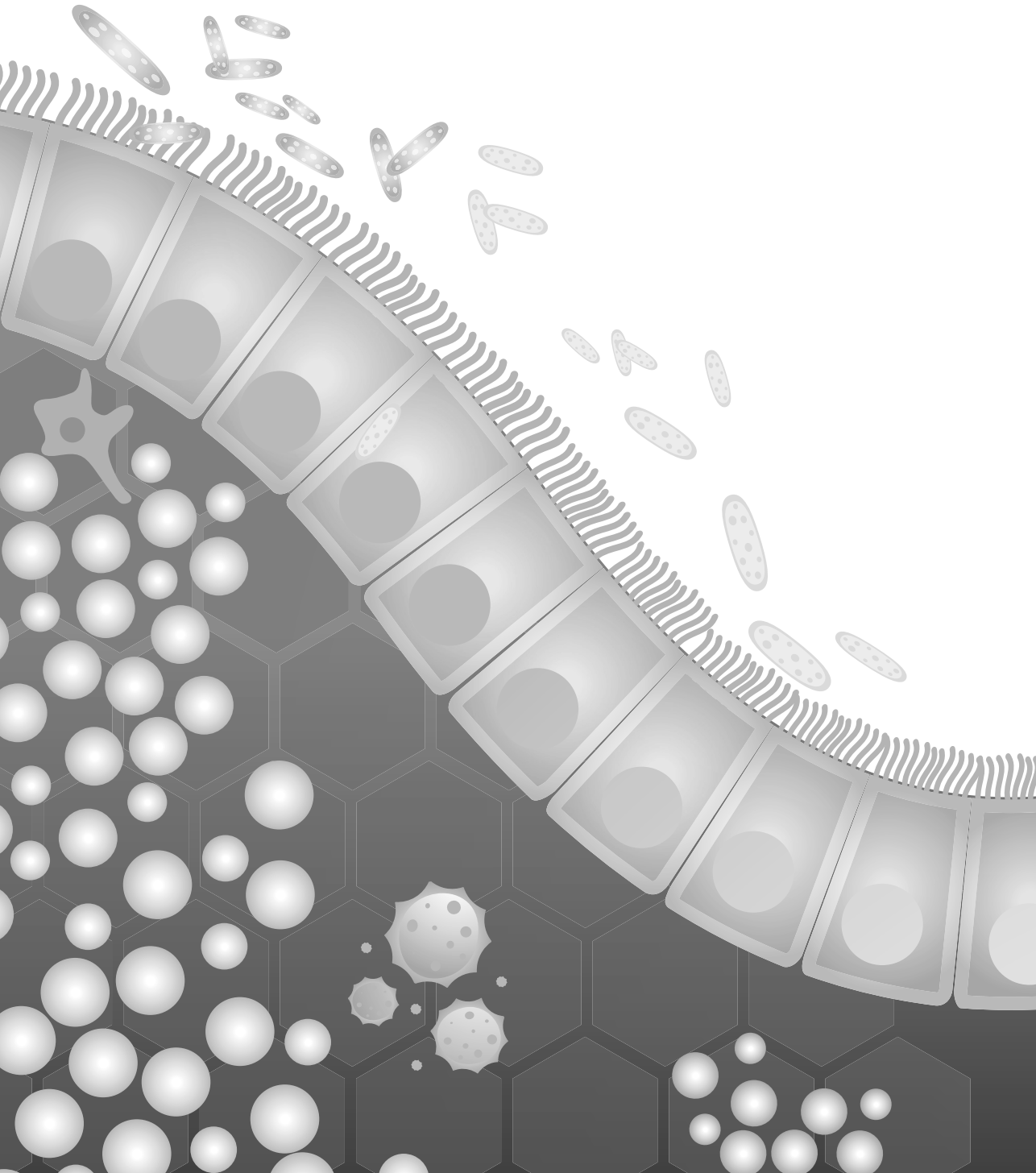

Chapter 8

General Discussion

Nuning Winaris

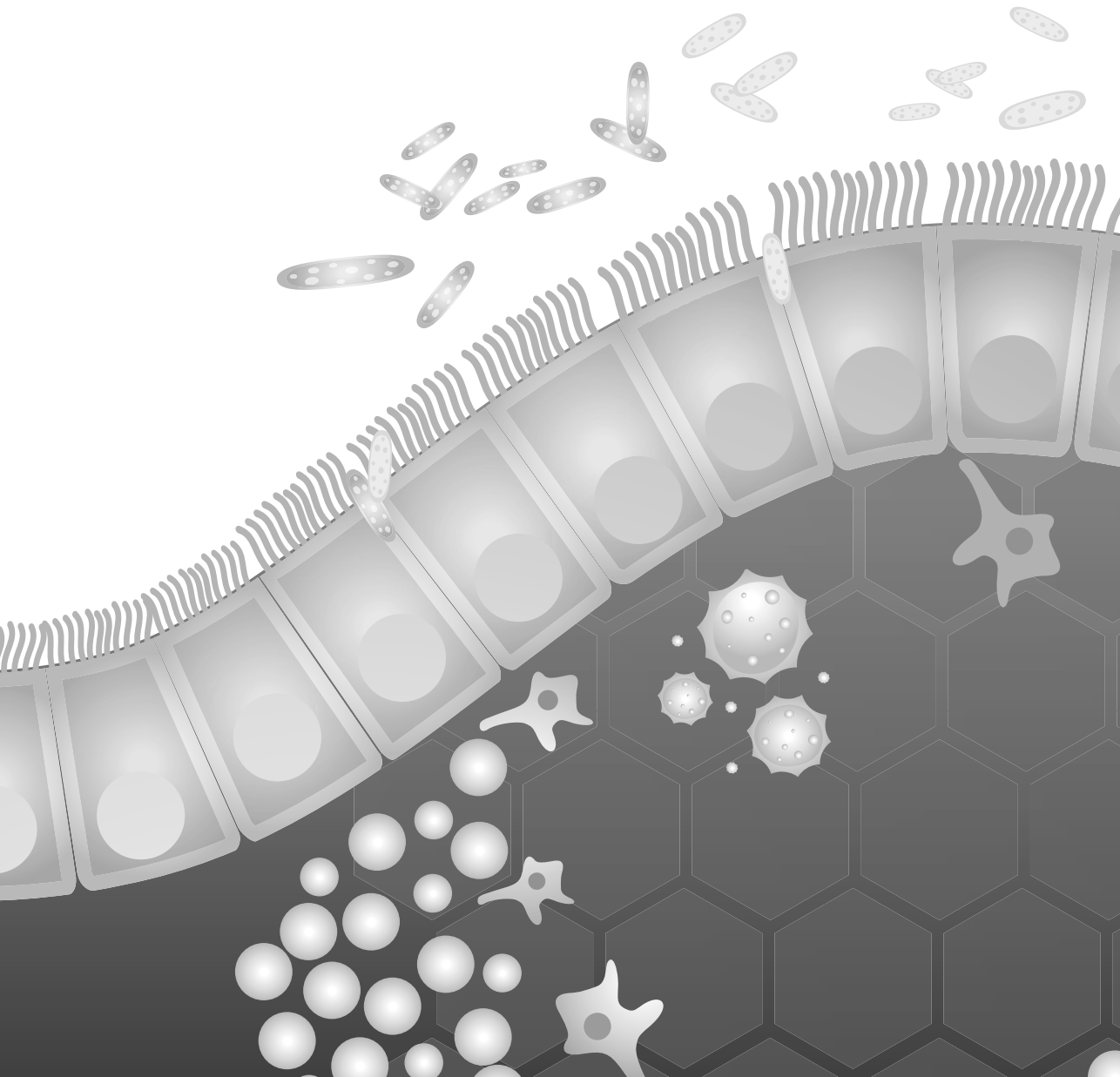

Over the past decade, research on host-microbe interactions has shifted from studies on the effect of bacteria on (gastro-intestinal) pathology towards the capacity of the microbiota to modulate the immune system of humans and mammals. A current trend is aim to exploit the gut microbiome and its metabolites as new therapies or preventions for chronic diseases in humans, which have increased significantly in high-income countries over the past 50 years. This includes inflammatory bowel disease (IBD), Type 1 diabetes, allergic diseases, and autoimmune diseases. IBD is defined by chronic inflammation that can either affect the whole intestinal track as observed in Crohn's disease (CD) or be concentrated in large intestine as in ulcerative colitis (UC). Many factors have been attributed to the development of this disease, including genetic predisposition, environmental factors, gut microbiota and host immune response[7]. IBD is one of many diseases that are associated with a dramatic change in microbiota composition, also commonly referred to as dysbiosis[7]. As the changed composition of the microbiota appears to contribute to the pathophysiology of this disease[12, 13, 163, 164], the current paradigm is centred around identification and administration of specific bacteria and/or bacterial metabolites that would restore the microbial balance and thereby modulate the immune response to prevent inflammation.

In this thesis we investigated the immunomodulatory effects of colonic anaerobic bacteria and their metabolites, particularly short-chain fatty acids (SCFA), in order to select therapeutic candidate strains for intestinal prevention and treatment of IBD or other inflammatory gut diseases. We screened more than one hundred colonic anaerobic strains isolated from healthy human donors in various *in vitro* immune assays to investigate their capacity to modulate the immune response. Despite the interesting results obtained from the strain collection in **Chapter 2**, there was only sufficient time for *in vivo* colitis experiments with a selection of the novel strains of *F. prausnitzii* described in **Chapter 3**. *F. prausnitzii* is a strict anaerobe, previously reported to induce high anti-inflammatory cytokine secretion *in vitro* as well as confer protection against chemically induced colitis in *vivo*[21-23, 45]. In order to investigate the correlation between the results of the *in vitro* immune assays and their protective capacity *in vivo*, we conducted DSS induced colitis studies in mice. Furthermore, we investigated the immunomodulatory capacity of bacterial metabolites, specifically the SCFA acetate and butyrate. To test the effect of the SCFA we used different types of (immune) cells as well as an organoid model of the intestinal epithelium. To gain more insights into the molecular mechanisms of both acetate and butyrate in regulating immune response and intestinal function we performed transcriptomic studies on $CD14^+$ monocytes and porcine 3D ileum organoids.

Colonic anaerobic bacteria as novel prophylactic or therapeutic candidate

Screening of more than 100 colonic anaerobic bacterial strains in various immune assays revealed several categories of immune profiles. Even strains and genome-based phylogenetic groups of strains from the same species can exhibit markedly different immune profiles

showing that these properties tend to be highly strain specific **(Chapter 3)**. Some immune profiles were typical for a species (e.g. high IL-10 responses in PBMC assays), but there were often some strains which were the exception. Other strain properties investigated by our collaborators included presence of antibiotic resistance genes, aerotolerance and metabolism of different carbon sources. There was no correlation between the immune profile, and these other strain characteristics (unpublished data).

Immune profiles of colonic anaerobic bacteria were mainly based on their capacity to induce cytokine secretion in human PBMC cultures, with or without an additional immune stimulus of heat-inactivated bacteria (HIB). One limitation of PBMC as a model is that they are a mixture of lymphocytes (B and T cells) and myeloid cells (mainly monocytes) rather than dendritic cells (DC) and macrophages which are found in the dome of the Peyer's patches and intestinal lamina propria [192]. Furthermore, specific sub-sets of conditioned DC and macrophages are associated with the intestinal mucosa, which are difficult to generate *in vivo* or isolate from gut tissue in sufficient numbers for assays. For these reasons PBMC have been frequently used as a model for screening immunomodulatory activity, in vaccine development[193], cytotoxicity assays[194], and autoimmune disorders[195]. Foligne et al., (2007) and Meijerink et al. (2010a and 2010b) also suggested that PBMC are a powerful tool to screen the immunomodulatory properties of Lactobacillus strains[39, 196, 197], although a larger range of IL-10 secretion was obtained from experiments using a pure DC population[196].

In this study we did not only focus on the IL-10/IL-12 ratio, as is usually done, to predict protective capacity of our bacterial strains. Rather we incorporated several pro-inflammatory cytokines (IL-1β, TNF-α and IFN-γ) besides IL-10 and IL-12. For example, in the case of *F. prausnitzii*, stimulated PBMC secrete only low amounts of IL-12. Therefore, the IL-10/IL-12 ratio will mainly reflect the IL-10 secretion. We therefore measured a panel of secreted cytokines including an IL-10/ TNF-α ratio will therefore be more informative than an IL-10/ IL-12 ratio about the immune status. Additionally, we tested the capacity of our strains to suppress an ongoing inflammatory response by including a heat inactivated bacteria (HIB) stimulus which strongly induced both pro-and anti-inflammatory cytokine secretion in PBMCs. Our hypothesis was that bacteria inducing the highest IL-10/IL-12 ratio in PBMCs might have the strongest anti-inflammatory effect in HIB stimulated PBMCs. Examples of this were indeed observed but interestingly, we also identified bacterial strain that behaved differently to that predicted from the IL-10/IL-12 ratio.

Furthermore, nitric oxide (NO) was also measured after incubation of the strains with murine macrophage RAW 264.7 cells as an indicator of macrophage activation. Overall, the NO response as a result from stimulation with bacterial pellet was lower than the LPS (1 µg/ml) stimulation, even though there were some strains that induced high NO (more than 90%

compared relative to LPS), such as *D. longicatena* strain HTF-113 and *P. copri* strain HTF-155. Production of NO endows macrophages with cytostatic or cytotoxic activity against viruses, bacteria, fungi, protozoa, helminths, and tumour cells. However, sustained production of NO can cause collateral damage to the host. As uncontrolled inflammation and oxidative stress have been proposed as a mechanism underlying the pathophysiology of IBD[55-57], we also tested the capacity of the strains to induce NO in macrophages.

Based on our immune screening, we observed that human colonic anaerobic bacteria have various types of immune profiles. These profiles were categorized in three different groups; the immunostimulatory, immunomodulatory and immuno-inhibitory or 'silent' profile (**Chapter 2 & 3**). The silent' immune profile was considered the most interesting profile of the three, because these strains induced relatively low amounts of cytokine secretion, but increased anti-inflammatory and decreased pro-inflammatory cytokines induced by a HIB stimulus. Bacteria grouped in this 'silent' immune profile also induced low amounts of NO.

Bacteria with the 'silent' profile also performed best in our *in vivo* colitis model. For example, *F. prausnitzii* HTF-111 and HTF-217, were shown to confer the best protection against the clinical parameters measured in DSS-induced colitis (**Chapter 7**). For example, these strains attenuated diarrhoea and reduced the amount of blood in the stool, as reflected in the disease activity index (DAI). Moreover, mice treated with these strains did not have a shortening of their colon and showed reduction of the inflammation marker lipocalin-2 protein in faeces. Foligne et al. (2007) suggested that a correlation between the capacity of a certain probiotic strain to induce a high IL-10/IL-12 ratio measured in an *in vitro* PBMCs assay and the protective capacity of this strain in a mouse colitis model[39]. However, strains HTF-111 and HTF-217, which had the best protective effect *in vivo* induced a low ratio of IL-10/IL-12. This highlights the added value of our screening method, which incorporates measurement of several cytokines, and importantly, the immunomodulatory effect on a strong inflammatory stimulus with HIB. Strains HTF-111 and HTF-217 administrations in DSS-induce colitis model also lead to a change in microbiota composition, particularly at the end of the DSS administration and during recovery period (**Chapter 7**). A substantial increase in *Bacterioides* was observed at the end of DSS and during the recovery period, when the inflammation was most pronounced. However, *Enterobacteriaceae*, which are reported increase in IBD were only detected in low abundance (0.18%) in our study. After the recovery period, the relative abundance of *Rikenellaceae,* which is associated with a healthy gut condition, slowly increased and the abundance of *Bacteriodes* decreased, particularly in the groups administered strains HTF-111 and HTF-217. This indicated that the microbiota composition was reverting to a more health-associated composition in the groups where *F. prausnitzii* significantly attenuated the colitis. Furthermore, only minor alterations in the microbiota composition were observed in the groups administered with HTF-111 and HTF-217, the *F. prausnitzii* strains that showed the best protection in DSS-induced colitis. In contrast, HTF-05B a strain with an 'immunostimulatory'

profile, that strongly induced both, pro- and anti-inflammatory cytokines, as well as induced high amount of NO performed poorly in our DSS-induced colitis study, having little effect on the inflammation induced by DSS. The previously reported 'control' *F. prausnitzii* strain A2-165, which had an 'immunomodulatory' profile, did not attenuate colitis to the same extent as the strains with a 'silent' immune profile. *F. prausnitzii* strain A2-165 previously showed protective effect against TNBS-induced colitis[21, 22]. This finding highlights the beneficial effect on using bacteria that belong to 'silent' profile as therapeutic candidates for IBD treatment.

Furthermore, we also found some other interesting immune phenotypes in our screening, including the ability of certain strains to shield their surface ligands or microbe- or pathogen-associated molecular patterns (MAMPs or PAMPs). Some colonic anaerobic bacteria, such as *D. longicatena* strain HTF-28 has the ability to avoid toll-like receptor (TLR) recognition, most likely by producing extracellular polymeric substances/matrix (EPS/EPM). Thus, they do not trigger TLR signalling pathways or activate transcription factor NF-κB which would normally lead to cytokine secretion (**Chapter 2**). Interestingly, strain HTF-28 was able to induce moderate amounts of cytokines, which could possibly be explained by activation of other MAMPs or PAMPs receptors such as C-type lectins[94] or intracellular nucleotide-binding oligomerization domain-like (NOD) receptors[93] and TLR9 after phagocytosis[198]. Another example of a strain with a low capacity to induce cytokines secretion and NF-κB activation was *I. bartlettii* strain HTF-135, which also produces and EPS-like structure that may shield MAMP recognition by host PRRs. We therefore conclude that the various types of EPSs produced by colonic anaerobic bacteria, can influence their immunomodulatory properties.

Bacterial metabolite short-chain fatty acids (SCFA) contribute to intestinal homeostasis

During our PBMC immune screening, we found that bacterial culture supernatant also had a strong anti-inflammatory effect on modulating cytokines secreted by PBMC. Many colonic bacterial strains are capable of producing SCFA such as butyrate, propionate, acetate and/or formate in different amounts. The bacterial growth medium used to culture our bacterial strains also included a combination of SCFAs (butyrate among others). Therefore, it was not possible to determine whether the immune response to culture supernatant was influenced by SCFA or other anti-inflammatory factors produced during bacterial growth without measuring the SCFA produced and setting up a specific control for every culture. We therefore chose not to pursue the screening of culture supernatants in PBMC assays. However, having observed that the SCFA in medium attenuated cytokine secretion in HIB-stimulated PBMCs we chose to study this mechanism in more detail.

Depending on the type of fibre consumed, the concentration of SCFA in the proximal colon ranges from 70 -140 mM, and from 20-70 mM in the distal colon[58, 59]. Acetate

concentrations in the plasma and serum are around 50-100 µmol/L, whereas these are only 0.5 - 10 µmol/L for butyrate and propionate[59, 60]. The concentrations are anticipated to be much higher in the lamina propria and portal vein. In a preliminary study we tested SCFA concentrations ranging from 0.5 – 5 mM, and found that 5mM of butyrate affected cell viability. To prevent deleterious effects on cell function we decided to use 1mM butyrate and 2.5 mM acetate in our study. These concentrations were also comparable with the concentrations used in other studies[73, 117, 199].

In our *in vitro* study, increasing concentrations of butyrate and acetate (up to 5 mM) did not induce cytokine secretion in immune cell cultures (PBMC, $CD14^+$ monocyte and monocyte-derived dendritic cells/MDDC). However, cytokine secretion in these immune cells was triggered by stimulation with HIB alone. Butyrate, which is known as an anti-inflammatory molecule[58, 64, 136], was able to significantly decrease secretion of HIB induced pro-inflammatory cytokines. Surprisingly, in our study we showed that butyrate strongly decreased the secretion of the anti-inflammatory cytokine IL-10. Moreover, butyrate reduced the viability of immune cells in a dose dependent manner, which could be detrimental to the host (**Chapter 4**). We concluded that the effect of butyrate on cell viability is not pH dependent, as the concentration we used in this study (1 mM) did not change the pH significantly. Moreover, in a separate experiment we showed that much larger pH changes were required to affect viability. Acetate at concentrations up to 5 mM, had a stronger effect on the pH than butyrate, but did not affect cell viability. We therefore concluded that butyrate reduces cell viability at concentrations which are well tolerated for acetate. Additionally, we found that 1mM butyrate slowed the growth of intestinal organoids, whereas 2.5 mM of acetate did not have any effects (**Chapter 6**). The deleterious effects of butyrate on growth and viability of cells have been reported before by Kaiko et al. (2016), where they showed that butyrate inhibited stem cell proliferation and delayed wound healing[73].

As mentioned above, butyrate strongly decreases induced pro-inflammatory cytokine secretion, as described in other studies[125, 199, 200]. However, to our knowledge, only few studies reported that butyrate also strongly inhibits the secretion of the anti-inflammatory cytokine IL-10[125, 200]. This omission hampers proper interpretation of the biological effect of butyrate, as the combined effect on pro-and anti-inflammatory cytokines might be skewed. In contrast to butyrate, we found that acetate did not reduce IL-10 secretion in HIB stimulated PBMCs and sometimes even increased the concentration. Combined with the attenuation of the HIB induced secretion of pro-inflammatory cytokines, this might make acetate a better anti-inflammatory agent. Acetate not only inhibits the secretion of pro-inflammatory cytokines, but induces secretion of the anti-inflammatory IL-10.

Despite other reports that SCFAs modulate immune responses via GPCR signalling[115, 201], we found that the effect of butyrate on the (HIB induced) cytokine secretion was independent

from G protein-coupled receptors (GPCR). In our study, the inhibitors (PTX and U73122) used to block these receptors expressed in MDDC did not significantly attenuate the effect of butyrate on cytokine secretion (**Chapter 4**). The reasons for this are unclear but it may be due to different concentration SCFA, and time of incubation.

Previously Lin et al, (2015) reported that SCFAs induced TLR-mediated NF-κB activation through inhibition of HDAC. In this study butyrate and propionate as well as TSA, an inhibitor of HDAC, enhanced TLR-mediated NF-κB activation induced by specific ligands in HEK293 and HeLa 57A that expressed TLR receptors[117]. When similar assays were repeated with TLR1/2, TLR2 and TLR2/6 reporter cell lines we observed that acetate and butyrate decreased NF-κB activation due to the specific TLR ligands or TNF-α control. Moreover, we found that TSA, which like butyrate inhibits class 1 histone deacetylase HDAC3, also suppressed NF-κB activation in TLR2 reporter cells. A plausible explanation for this was uncovered in **Chapter 5** where we found that TLR2 was specifically down-regulated by butyrate exposure. This would not affect the response to LPS as described by Lin et al., (2015) but it might reduce immune activation and cytokine production to the heat-inactivated Gram-positive bacteria used in our study. Although our results with the TLR1/2 reporter differ from those of Lin et al., we found similar results with the TLR4 and TLR5 reporter cell lines, where both TSA and butyrate increased TNF-α or specific ligand induced NF-κB signalling.

The similar results obtained with TSA and butyrate suggest that inhibition of histone deacetylase 3 underlies the anti-inflammatory mechanism. Suppression of HDAC3 by butyrate is known to increase histone acetylation of the RELA subunit of NF-κB which is one of the substrates of HDAC3. Activity of NF-κB is known to be regulated by post-translational modification of the protein subunits thus providing an explanation for the effects of butyrate on NF-κB activation. Interestingly, whereas TSA and butyrate increased NF-κB activation in TLR4 and TLR5 reporter cells stimulated with a specific agonist or TNF-α, the was no effect of acetate. This suggests a different mechanism of immunomodulation for acetate than butyrate.

To further investigate the possible mechanisms by which acetate and butyrate might affect the immune system, we looked at transcriptome data of $CD14^+$ monocytes in a healthy and in an inflamed state (simulated by HIB). As expected from the previous results showing clear regulatory effects of SCFA, we again found that both acetate and butyrate have a distinctive transcriptomic signature in mediating the anti-inflammatory status in the gut. Butyrate evoked a larger number of differentially expressed genes compared to acetate. More importantly, butyrate also activated a higher number of canonical pathways, particularly cellular stress-, disease- and inflammatory response-related pathways. This suggests that the viability of host cells might be reduced by butyrate treatment, which might be reflected by the decrease in viability we found in cells treated with butyrate alone for 24 hours. However, when we

added a stimulus (HIB) there is no effect of butyrate in cell viability. In contrast to butyrate, acetate did not affect viability even after 24 hours and we indeed found that acetate mainly induced canonical pathways which were related to cellular metabolism process. Only when acetate was combined with HIB (to simulate inflammation), acetate appeared to decrease the inflammatory response and maintained an anti-inflammatory status via immune response related pathways such as the interferon and TLR signalling pathways, which are responsible for the modulation of cytokine responses (**Chapter 5**). Hence, we conclude that acetate may a better therapeutic candidate to control inflammation, as it does not appear to affect gene transcription in a healthy situation, but has a significant effect on attenuating inflammatory responses.

Furthermore, we used porcine 3D ileal organoids to study transcriptomic effect of acetate and butyrate in epithelial tissue (**Chapter 6**). The top canonical pathway regulated by butyrate in intestinal organoid was HMGB1 Signalling Pathway. Several genes involved in this pathway were downregulated by butyrate, including *TLR4*, an innate receptor to which HMGB1 released from cells has been reported to bind and the RELA subunit of NF-κB. However, expression of SERPINE1 a protein regulated by nuclear HMGB1 was increased more than 16-fold. Like the histones, HMGB1 is an important chromatin protein. In the nucleus HMGB1 interacts with nucleosomes, transcription factors, and histones, thereby organising DNA and regulating transcription[158, 159]. The presence of HMGB1 in the nucleus depends on post-translational acetylation[159]. It is therefore possible that butyrate inhibits deacetylation of HMGB1 possibly through HDAC3, increasing the concentration of HMGB1 in the nucleus and upregulating *SERPINE1*.

Butyrate was also predicted to regulate cell cycle-related pathways e.g. by down regulating cyclin genes *CCNB2* in the G2/M DNA Damage Checkpoint pathway and *CCND1* and *CCNE2* in the G1/S Checkpoint pathway, which known to control the cell cycle. Additionally, *HDAC3* which is inhibited by butyrate was upregulated. Histone deacetylase 3 (HDAC3) directly interacts with and deacetylates cyclin A in the G1/S Checkpoint pathway. Given that deacetylated cyclin A promotes cell proliferation butyrate inhibition of HDAC3 deacetylation activity is predicted to reduce cell proliferation, which has been demonstrated previously in Kaiko et al (2016) study[73].

On the other hand, we found that acetate was predicted to upregulate the Sirtuin Signalling Pathway in epithelial tissue of 3D ileal organoids by regulating genes that are known to induce epigenetic effects, i.e. *H1F0*, *SIRT6* and *KAT2A*. Sirtuin, which contains a group of proteins, regulating a wide range of cellular processes such as transcription, apoptosis and inflammation, mainly through deacetylase activity[160]. The Sirtuin pathway is also known to suppression of histone deacetylation of pro-inflammatory cytokines and transcription factors which lead to suppression of inflammation[161]. Additionally, we also observed an increased

percentage of histone 3 acetylation measured from acetate-treated organoids, although this was not significant due to the high variability, which we hypothesised to be due to variation in the number of organoids in replicate wells. Thus, we cannot conclude that acetate increase histone 3 acetylation in epithelial porcine 3D ileum organoid.

However, the finding that acetate significantly alters gene expression in intestinal organoids, which has not been well explained before in Lukovac et al (2014) study[135], and it has major implications for understanding the impact of this bacterial metabolite on intestinal function *in vivo* and warrants further study. In future experiments we aim to investigate transcriptional and functional effects of longer periods of exposure to acetate on both the colon and ileum. Polarised monolayers of organoids cells[149] will also be used to reduce variability between replicates for biochemical and cellular assays

CONCLUDING REMARKS AND FUTURE PERSPECTIVES

The gut microbiome is a fascinating potential source of next-generation probiotics or therapeutic candidates for chronic inflammation diseases such as IBD. Among the 100 anaerobic colonic bacteria screened we found several potential therapeutic candidates. Interestingly, the best therapeutic candidate in our study belonged to the group of gut bacteria that have a 'silent' immune profile. The bacteria belonging to this immune profile show a low capacity to induce cytokine secretion in PBMC, and induce low amounts of NO secretion in murine macrophages. However, when PBMC were stimulated with HIB to mimic an inflammation, these 'silent' strains of bacteria attenuated pro-inflammatory cytokine secretion while maintaining or even increasing secretion of the anti-inflammatory cytokine IL-10. We hypothesize that this 'silent' profile would be beneficial in the gut of IBD patients as would attenuate inflammation during the 'flare-up' in colitis patients.

Bacterial metabolite-based therapeutics have also been proposed as a promising alternative for the treatment of various human diseases, such as IBD[202]. Bacterial metabolites such as SCFA, play an important role in maintaining an anti-inflammatory tone in the intestinal mucosa. Moreover, there appears to be a significant role of SCFA other than butyrate in mediating anti-inflammatory effects. A disadvantage of butyrate is that it suppressed production of the anti-inflammatory cytokine IL-10 induced by bacterial stimulus (HIB) in our studies. However, it also strongly suppressed pro-inflammatory cytokines and may therefore be still an effective anti-inflammatory therapy. Butyrate also affected cell viability, suggesting that high concentrations of butyrate (≥1 mM) could be toxic for the immune and epithelial cells. This was also reflected by our transcriptomic analysis, which showed that many cellular stress-, and disease response-related pathways were activated after stimulation with butyrate. Acetate on the other hand was found to be a more favourable therapeutic candidate for IBD treatment, as it did not affect cell viability. More importantly, while acetate was able to decrease the secretion of pro-inflammatory cytokines, it also maintained, or in some donors even increased, IL-10 secretion induced by HIB. This modulation effect was only observed when an inflammatory stimulus was added, which was also in line with the transcriptomic analysis. Overall, acetate might generate a more pronounced anti-inflammatory response, based on the ratio of pro-and anti-inflammatory cytokines, and it might not have any effects during remission in IBD patients.

Future studies with combinations of different strains or genera of symbiont bacteria should be included to investigate the persistence of the administered bacteria in germ-free mice, to ensure that the administered bacteria will stay for a prolonged period in the gut. Moreover, the protective capacity of such bacterial consortia against chemically-induced colitis model should be tested, to determine whether a cocktail of several bacteria might be more effective than single strains. Additionally, administration of acetate, via either the drinking water or the

food should be tested in colitis models to confirm the anti-inflammatory properties found *in vitro*. In the future, clinical trials should be conducted in order to assess the efficacy and safety of single strains, microbial consortia or SCFA administration for therapeutic application in IBD patients.

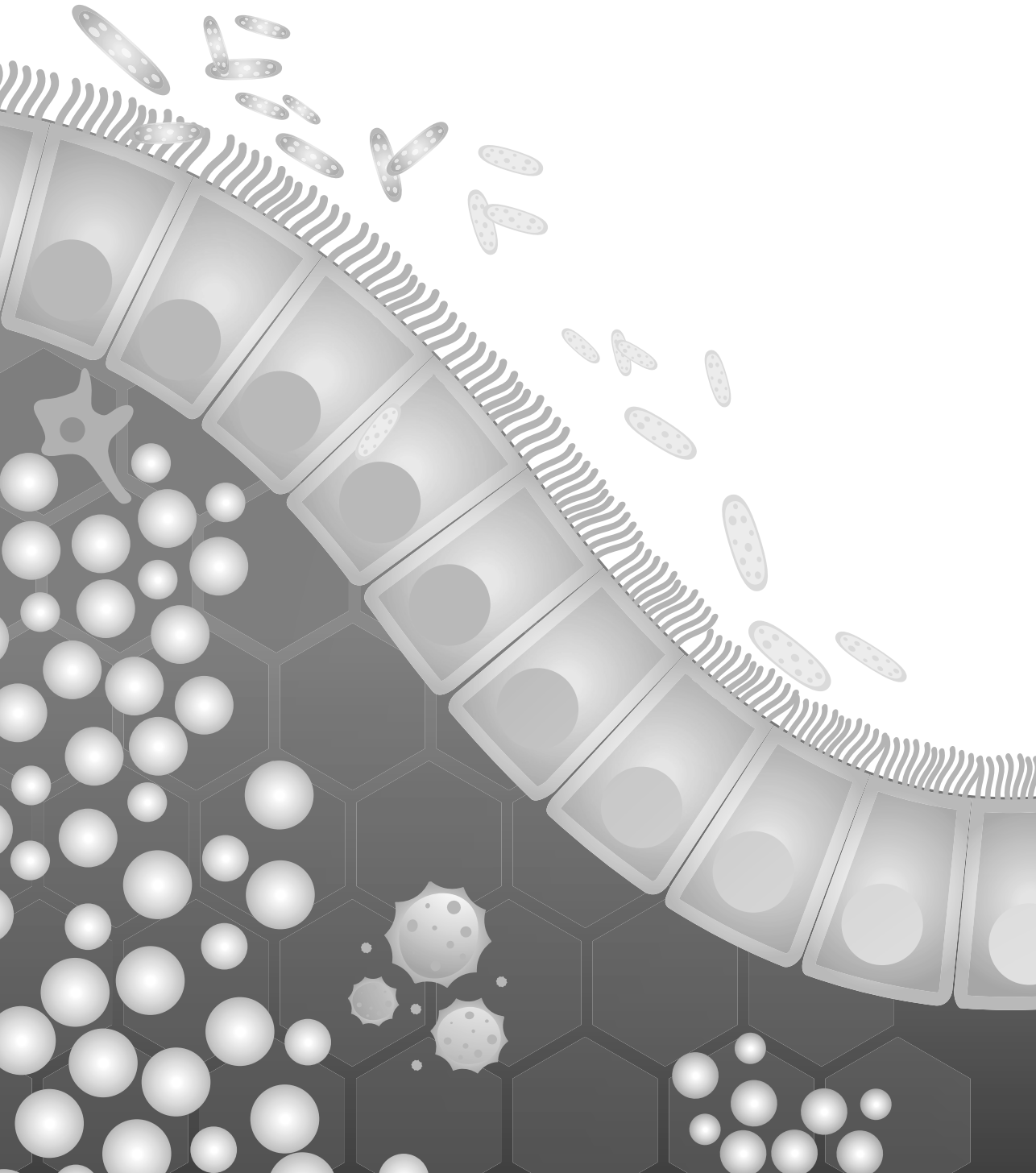

References

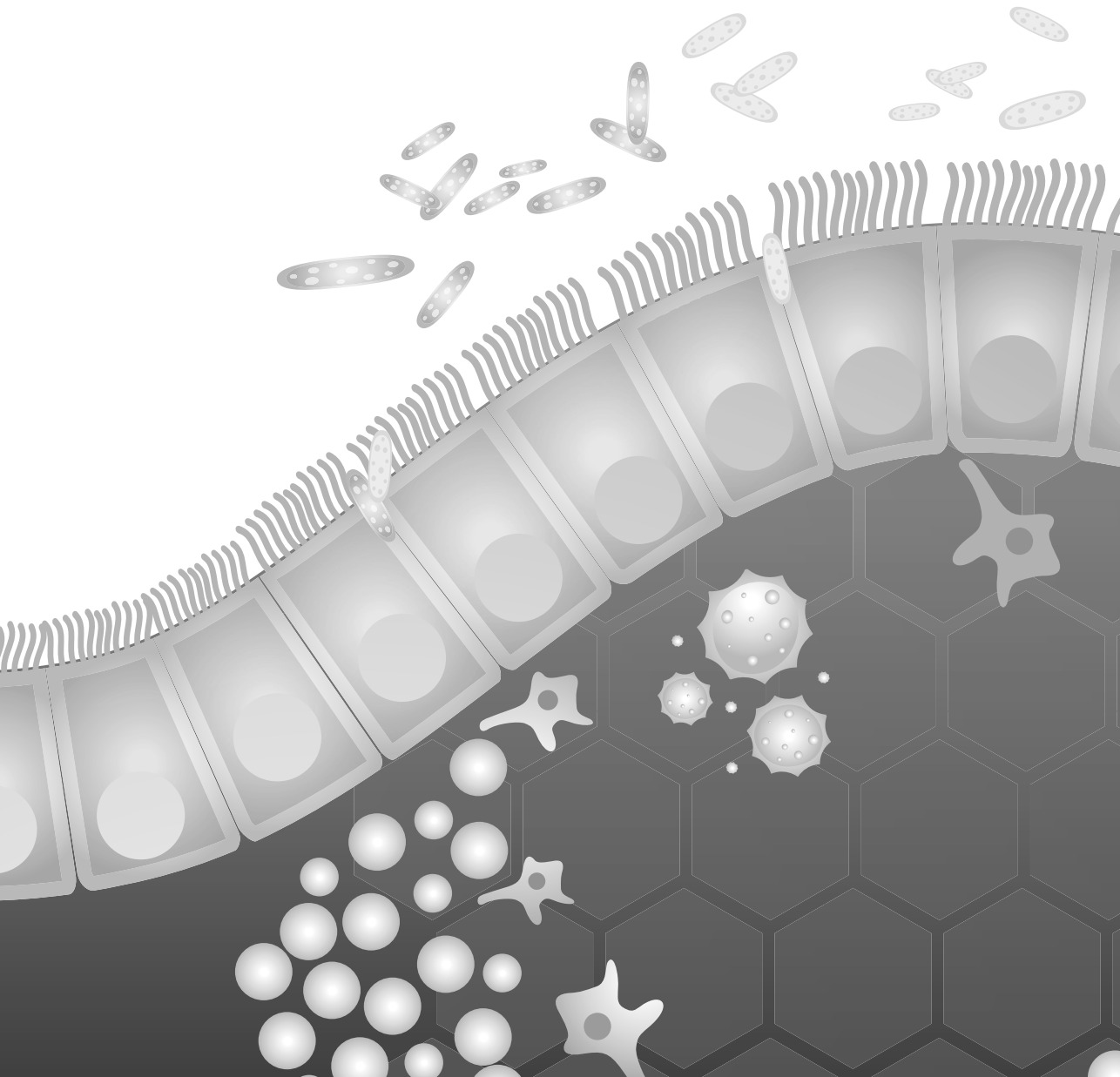

REFERENCES

1. Nagpal, R., H. Yadav, and F. Marotta, *Gut microbiota: the next-gen frontier in preventive and therapeutic medicine?* Frontiers in medicine, 2014. **1**: p. 15-15.
2. Kaplan, G.G., *The global burden of IBD: from 2015 to 2025.* Nature Reviews Gastroenterology &Amp; Hepatology, 2015. **12**: p. 720.
3. Kaplan, G.G. and S.C. Ng, *Understanding and Preventing the Global Increase of Inflammatory Bowel Disease.* Gastroenterology, 2017. **152**(2): p. 313-321.e2.
4. Manichanh, C., et al., *The gut microbiota in IBD.* Nature Reviews Gastroenterology & Hepatology, 2012. **9**(10): p. 599-608.
5. Coward, S., et al., *Funding a Smoking Cessation Program for Crohn's Disease: An Economic Evaluation.* American Journal of Gastroenterology, 2015. **110**(3).
6. Molodecky, N.A., et al., *Increasing Incidence and Prevalence of the Inflammatory Bowel Diseases With Time, Based on Systematic Review.* Gastroenterology, 2012. **142**(1): p. 46-54.e42.
7. Ana Brajdić, B.M.-S., *Insights to the Ethiopathogenesis of the Inflammatory Bowel Disease*, I. Szabo, Editor. 2012.
8. Halfvarson, J., et al., *Inflammatory bowel disease in a Swedish twin cohort: a long-term follow-up of concordance and clinical characteristics.* Gastroenterology, 2003. **124**(7): p. 1767-1773.
9. M. Orholm, V.B.T.I.A.S.L.P.R.K.O.K., *Concordance of Inflammatory Bowel Disease among Danish Twins: Results of a Nationwide Study.* Scandinavian Journal of Gastroenterology, 2000. **35**(10): p. 1075-1081.
10. Spehlmann, M.E., et al., *Epidemiology of inflammatory bowel disease in a German twin cohort: results of a nationwide study.* Inflamm Bowel Dis, 2008. **14**(7): p. 968-76.
11. Thompson, N.P., et al., *Genetics versus environment in inflammatory bowel disease: results of a British twin study.* BMJ (Clinical research ed.), 1996. **312**(7023): p. 95-96.
12. Sartor, R.B. and S.K. Mazmanian, *Intestinal Microbes in Inflammatory Bowel Diseases.* Am J Gastroenterol Suppl, 2012. **1**(1): p. 15-21.
13. Frank, D.N., et al., *Molecular-phylogenetic characterization of microbial community imbalances in human inflammatory bowel diseases.* Proceedings of the National Academy of Sciences of the United States of America, 2007. **104**(34): p. 13780-13785.
14. Chapat, L., et al., *Lactobacillus casei reduces CD8+ T cell-mediated skin inflammation.* European Journal of Immunology, 2004. **34**(9): p. 2520-2528.
15. Dongarra, M.L., et al., *Mucosal immunology and probiotics.* Curr Allergy Asthma Rep, 2013. **13**(1): p. 19-26.
16. Maassen, C.B.M., et al., *Strain-dependent induction of cytokine profiles in the gut by orally administered Lactobacillus strains.* Vaccine, 2000. **18**(23): p. 2613-2623.
17. McCarthy, J., et al., *Double blind, placebo controlled trial of two probiotic strains in interleukin 10 knockout mice and mechanistic link with cytokine balance.* Gut, 2003. **52**(7): p. 975-980.
18. Sánchez, B., et al., *Probiotics, gut microbiota, and their influence on host health and disease.* Molecular Nutrition & Food Research, 2017. **61**(1): p. 1600240.

19. Scott, K.P., et al., *Manipulating the gut microbiota to maintain health and treat disease.* Microbial ecology in health and disease, 2015. **26**: p. 25877-25877.
20. Miquel, S., et al., *Faecalibacterium prausnitzii and human intestinal health.* Current Opinion in Microbiology, 2013. **16**(3): p. 255-261.
21. Rossi, O., et al., *Faecalibacterium prausnitzii A2-165 has a high capacity to induce IL-10 in human and murine dendritic cells and modulates T cell responses.* Scientific Reports, 2016. **6**: p. 18507.
22. Sokol, H., et al., *Faecalibacterium prausnitzii is an anti-inflammatory commensal bacterium identified by gut microbiota analysis of Crohn disease patients.* Proceedings of the National Academy of Sciences of the United States of America, 2008. **105**(43): p. 16731-16736.
23. Rossi, O., et al., *Faecalibacterium prausnitzii Strain HTF-F and Its Extracellular Polymeric Matrix Attenuate Clinical Parameters in DSS-Induced Colitis.* PLOS ONE, 2015. **10**(4): p. e0123013.
24. Mazmanian, S.K., J.L. Round, and D.L. Kasper, *A microbial symbiosis factor prevents intestinal inflammatory disease.* Nature, 2008. **453**(7195): p. 620-625.
25. Round, J.L., et al., *The Toll-like receptor 2 pathway establishes colonization by a commensal of the human microbiota.* Science (New York, N.Y.), 2011. **332**(6032): p. 974-977.
26. Atarashi, K., et al., *Induction of colonic regulatory T cells by indigenous Clostridium species.* Science (New York, N.Y.), 2011. **331**(6015): p. 337-341.
27. Brijs, K., et al., *Osteonecrosis of the jaw in patients with inflammatory bowel disease treated with tumour necrosis factor alpha inhibitors.* International Journal of Oral and Maxillofacial Surgery.
28. Smith, M.K., et al., *Crohn's-like disease in a patient exposed to anti-Interleukin-17 blockade (Ixekizumab) for the treatment of chronic plaque psoriasis: a case report.* BMC Gastroenterology, 2019. **19**(1): p. 162.
29. Schoenefuss, F. and P. Hoffmann, *Serum gamma-globulin and albumin concentrations predict secondary loss of response to anti-TNFalpha in inflammatory bowel disease patients.* Eur J Gastroenterol Hepatol, 2019.
30. Khoruts, A., et al., *Changes in the composition of the human fecal microbiome after bacteriotherapy for recurrent Clostridium difficile-associated diarrhea.* J Clin Gastroenterol, 2010. **44**(5): p. 354-60.
31. Turnbaugh, P.J., et al., *An obesity-associated gut microbiome with increased capacity for energy harvest.* Nature, 2006. **444**(7122): p. 1027-1031.
32. Vijay-Kumar, M., et al., *Metabolic syndrome and altered gut microbiota in mice lacking Toll-like receptor 5.* Science (New York, N.Y.), 2010. **328**(5975): p. 228-231.
33. Wen, L., et al., *Innate immunity and intestinal microbiota in the development of Type 1 diabetes.* Nature, 2008. **455**(7216): p. 1109-1113.
34. Costello, S.P., et al., *Effect of Fecal Microbiota Transplantation on 8-Week Remission in Patients With Ulcerative Colitis: A Randomized Clinical Trial.* JAMA, 2019. **321**(2): p. 156-164.
35. Moayyedi, P., et al., *Fecal Microbiota Transplantation Induces Remission in Patients With Active Ulcerative Colitis in a Randomized Controlled Trial.* Gastroenterology, 2015. **149**(1): p. 102-109.e6.
36. Paramsothy, S., et al., *Multidonor intensive faecal microbiota transplantation for active ulcerative colitis: a randomised placebo-controlled trial.* The Lancet, 2017. **389**(10075): p. 1218-1228.

37. Rossen, N.G., et al., *Findings From a Randomized Controlled Trial of Fecal Transplantation for Patients With Ulcerative Colitis.* Gastroenterology, 2015. **149**(1): p. 110-118.e4.
38. Kwon, H.-K., et al., *Generation of regulatory dendritic cells and CD4+Foxp3+ T cells by probiotics administration suppresses immune disorders.* Proceedings of the National Academy of Sciences of the United States of America, 2010. **107**(5): p. 2159-2164.
39. Foligne, B., et al., *Correlation between in vitro and in vivo immunomodulatory properties of lactic acid bacteria.* World journal of gastroenterology, 2007. **13**(2): p. 236-243.
40. Hill, C., et al., *The International Scientific Association for Probiotics and Prebiotics consensus statement on the scope and appropriate use of the term probiotic.* Nature Reviews Gastroenterology &Amp; Hepatology, 2014. **11**: p. 506.
41. O'Toole, P.W., J.R. Marchesi, and C. Hill, *Next-generation probiotics: the spectrum from probiotics to live biotherapeutics.* Nature Microbiology, 2017. **2**(5): p. 17057.
42. Rodríguez, J.M., et al., *The composition of the gut microbiota throughout life, with an emphasis on early life.* Microbial ecology in health and disease, 2015. **26**: p. 26050-26050.
43. Hart, A.L., A.J. Stagg, and M.A. Kamm, *Use of probiotics in the treatment of inflammatory bowel disease.* J Clin Gastroenterol, 2003. **36**(2): p. 111-9.
44. Atarashi, K., et al., *Treg induction by a rationally selected mixture of Clostridia strains from the human microbiota.* Nature, 2013. **500**: p. 232.
45. Martín, R., et al., *Functional Characterization of Novel Faecalibacterium prausnitzii Strains Isolated from Healthy Volunteers: A Step Forward in the Use of F. prausnitzii as a Next-Generation Probiotic.* Frontiers in microbiology, 2017. **8**: p. 1226-1226.
46. Akira, S. and K. Takeda, *Toll-like receptor signalling.* Nature Reviews Immunology, 2004. **4**(7): p. 499-511.
47. Schwandner, R., et al., *Peptidoglycan- and Lipoteichoic Acid-induced Cell Activation Is Mediated by Toll-like Receptor 2.* Journal of Biological Chemistry, 1999. **274**(25): p. 17406-17409.
48. Takeuchi, O., et al., *Differential Roles of TLR2 and TLR4 in Recognition of Gram-Negative and Gram-Positive Bacterial Cell Wall Components.* Immunity, 1999. **11**(4): p. 443-451.
49. Triantafilou, M., et al., *Membrane Sorting of Toll-like Receptor (TLR)-2/6 and TLR2/1 Heterodimers at the Cell Surface Determines Heterotypic Associations with CD36 and Intracellular Targeting.* Journal of Biological Chemistry, 2006. **281**(41): p. 31002-31011.
50. Schröder, N.W.J., et al., *Lipopolysaccharide Binding Protein Binds to Triacylated and Diacylated Lipopeptides and Mediates Innate Immune Responses.* The Journal of Immunology, 2004. **173**(4): p. 2683.
51. Kawai, T. and S. Akira, *Signaling to NF-κB by Toll-like receptors.* Trends in Molecular Medicine, 2007. **13**(11): p. 460-469.
52. Rogler, G. and T. Andus, *Cytokines in inflammatory bowel disease.* World J Surg, 1998. **22**(4): p. 382-9.
53. Singh, U.P., et al., *Chemokine and cytokine levels in inflammatory bowel disease patients.* Cytokine, 2016. **77**: p. 44-9.

54. Raab, Y., et al., *Neutrophil mucosal involvement is accompanied by enhanced local production of interleukin-8 in ulcerative colitis.* Gut, 1993. **34**(9): p. 1203-6.
55. Cross, R.K. and K.T. Wilson, *Nitric oxide in inflammatory bowel disease.* Inflamm Bowel Dis, 2003. **9**(3): p. 179-89.
56. Kolios, G., V. Valatas, and S.G. Ward, *Nitric oxide in inflammatory bowel disease: a universal messenger in an unsolved puzzle.* Immunology, 2004. **113**(4): p. 427-437.
57. Soufli, I., et al., *Overview of cytokines and nitric oxide involvement in immuno-pathogenesis of inflammatory bowel diseases.* World journal of gastrointestinal pharmacology and therapeutics, 2016. **7**(3): p. 353-360.
58. Corrêa-Oliveira, R., et al., *Regulation of immune cell function by short-chain fatty acids.* Clinical & translational immunology, 2016. **5**(4): p. e73-e73.
59. Thorburn, A.N., et al., *Evidence that asthma is a developmental origin disease influenced by maternal diet and bacterial metabolites.* Nature Communications, 2015. **6**(1): p. 7320.
60. Deroover, L., et al., *Wheat Bran Does Not Affect Postprandial Plasma Short-Chain Fatty Acids from (13)C-inulin Fermentation in Healthy Subjects.* Nutrients, 2017. **9**(1): p. 83.
61. den Besten, G., et al., *The role of short-chain fatty acids in the interplay between diet, gut microbiota, and host energy metabolism.* Journal of lipid research, 2013. **54**(9): p. 2325-2340.
62. Pomare, E.W., W.J. Branch, and J.H. Cummings, *Carbohydrate fermentation in the human colon and its relation to acetate concentrations in venous blood.* The Journal of clinical investigation, 1985. **75**(5): p. 1448-1454.
63. Bilotta, A.J. and Y. Cong, *Gut microbiota metabolite regulation of host defenses at mucosal surfaces: implication in precision medicine.* Precision clinical medicine, 2019. **2**(2): p. 110-119.
64. Donohoe, D.R., et al., *The Warburg effect dictates the mechanism of butyrate-mediated histone acetylation and cell proliferation.* Molecular cell, 2012. **48**(4): p. 612-626.
65. Kelly, C.J., et al., *Crosstalk between Microbiota-Derived Short-Chain Fatty Acids and Intestinal Epithelial HIF Augments Tissue Barrier Function.* Cell host & microbe, 2015. **17**(5): p. 662-671.
66. Vinolo, M.A., S.M. Hirabara, and R. Curi, *G-protein-coupled receptors as fat sensors.* Curr Opin Clin Nutr Metab Care, 2012. **15**(2): p. 112-6.
67. Vinolo, M.A.R., et al., *Regulation of inflammation by short chain fatty acids.* Nutrients, 2011. **3**(10): p. 858-876.
68. Smith, P.M., et al., *The microbial metabolites, short-chain fatty acids, regulate colonic Treg cell homeostasis.* Science (New York, N.Y.), 2013. **341**(6145): p. 569-573.
69. Sun, L. and R.D. Ye, *Role of G protein-coupled receptors in inflammation.* Acta pharmacologica Sinica, 2012. **33**(3): p. 342-350.
70. Maslowski, K.M., et al., *Regulation of inflammatory responses by gut microbiota and chemoattractant receptor GPR43.* Nature, 2009. **461**(7268): p. 1282-1286.
71. Pluznick, J., *A novel SCFA receptor, the microbiota, and blood pressure regulation.* Gut microbes, 2014. **5**(2): p. 202-207.

72. Thangaraju, M., et al., *GPR109A Is a G-protein–Coupled Receptor for the Bacterial Fermentation Product Butyrate and Functions as a Tumor Suppressor in Colon.* Cancer Research, 2009. **69**(7): p. 2826.
73. Kaiko, G.E., et al., *The Colonic Crypt Protects Stem Cells from Microbiota-Derived Metabolites.* Cell, 2016. **165**(7): p. 1708-1720.
74. Hague, A., et al., *Sodium butyrate induces apoptosis in human colonic tumour cell lines in a p53-independent pathway: Implications for the possible role of dietary fibre in the prevention of large-bowel cancer.* International Journal of Cancer, 1993. **55**(3): p. 498-505.
75. Ishiguro, K., et al., *Suppressive action of acetate on interleukin-8 production via tubulin-α acetylation.* Immunology & Cell Biology, 2014. **92**(7): p. 624-630.
76. Ishiguro, K., et al., *Acetate inhibits NFAT activation in T cells via importin β1 interference.* European Journal of Immunology, 2007. **37**(8): p. 2309-2316.
77. Round, J.L. and S.K. Mazmanian, *The gut microbiota shapes intestinal immune responses during health and disease.* Nat Rev Immunol, 2009. **9**(5): p. 313-23.
78. Sekirov, I., et al., *Gut microbiota in health and disease.* Physiol Rev, 2010. **90**(3): p. 859-904.
79. Fanning, S., et al., *Bifidobacterial surface-exopolysaccharide facilitates commensal-host interaction through immune modulation and pathogen protection.* Proceedings of the National Academy of Sciences, 2012. **109**(6): p. 2108.
80. Hidalgo-Cantabrana, C., et al., *Genomic Overview and Biological Functions of Exopolysaccharide Biosynthesis in Bifidobacterium spp.* Applied and Environmental Microbiology, 2014. **80**(1): p. 9.
81. Murofushi, Y., et al., *The toll-like receptor family protein RP105/MD1 complex is involved in the immunoregulatory effect of exopolysaccharides from Lactobacillus plantarum N14.* Molecular Immunology, 2015. **64**(1): p. 63-75.
82. Al-Hassi, H.O., et al., *Altered human gut dendritic cell properties in ulcerative colitis are reversed by Lactobacillus plantarum extracellular encrypted peptide STp.* Mol Nutr Food Res, 2014. **58**(5): p. 1132-43.
83. Bernardo, D., et al., *Microbiota/host crosstalk biomarkers: regulatory response of human intestinal dendritic cells exposed to Lactobacillus extracellular encrypted peptide.* PLoS One, 2012. **7**(5): p. e36262.
84. Martin, R., et al., *The commensal bacterium Faecalibacterium prausnitzii is protective in DNBS-induced chronic moderate and severe colitis models.* Inflamm Bowel Dis, 2014. **20**(3): p. 417-30.
85. Zhu, H., et al., *Oxidative stress and redox signaling mechanisms of alcoholic liver disease: updated experimental and clinical evidence.* J Dig Dis, 2012. **13**(3): p. 133-42.
86. Shetty, S.A., et al., *Reclassification of Eubacterium hallii as Anaerobutyricum hallii gen. nov., comb. nov., and description of Anaerobutyricum soehngenii sp. nov., a butyrate and propionate-producing bacterium from infant faeces.* International Journal of Systematic and Evolutionary Microbiology, 2018. **68**(12): p. 3741-3746.

87. Poltorak, A., et al., *Defective LPS signaling in C3H/HeJ and C57BL/10ScCr mice: mutations in Tlr4 gene.* Science, 1998. **282**(5396): p. 2085-8.
88. Shah, H.N. and M.D. Collins, *Reclassification of Bacteroides multiacidus (mitsuoka, terada, watanabe and uchida) in a new genus Mitsuokella, as Mitsuokella multiacidus comb. nov.* Zentralblatt für Bakteriologie Mikrobiologie und Hygiene: I. Abt. Originale C: Allgemeine, angewandte und ökologische Mikrobiologie, 1982. **3**(4): p. 491-494.
89. Neville, B.A., et al., *Pro-inflammatory flagellin proteins of prevalent motile commensal bacteria are variably abundant in the intestinal microbiome of elderly humans.* PloS one, 2013. **8**(7): p. e68919-e68919.
90. Hayashi, F., et al., *The innate immune response to bacterial flagellin is mediated by Toll-like receptor 5.* Nature, 2001. **410**(6832): p. 1099-103.
91. Patterson, A.M., et al., *Human Gut Symbiont Roseburia hominis Promotes and Regulates Innate Immunity.* Front Immunol, 2017. **8**: p. 1166.
92. Tamanai-Shacoori, Z., et al., *Roseburia spp.: a marker of health?* Future Microbiol, 2017. **12**: p. 157-170.
93. Kim, Y.K., J.S. Shin, and M.H. Nahm, *NOD-Like Receptors in Infection, Immunity, and Diseases.* Yonsei medical journal, 2016. **57**(1): p. 5-14.
94. Hoving, J.C., G.J. Wilson, and G.D. Brown, *Signalling C-type lectin receptors, microbial recognition and immunity.* Cellular microbiology, 2014. **16**(2): p. 185-194.
95. Kingeter, L.M. and X. Lin, *C-type lectin receptor-induced NF-kappaB activation in innate immune and inflammatory responses.* Cell Mol Immunol, 2012. **9**(2): p. 105-12.
96. Vatanen, T., et al., *Variation in Microbiome LPS Immunogenicity Contributes to Autoimmunity in Humans.* Cell, 2016. **165**(4): p. 842-53.
97. Davis, K.M. and J.N. Weiser, *Modifications to the Peptidoglycan Backbone Help Bacteria To Establish Infection.* Infection and Immunity, 2011. **79**(2): p. 562.
98. Wolfert, M.A., A. Roychowdhury, and G.-J. Boons, *Modification of the structure of peptidoglycan is a strategy to avoid detection by nucleotide-binding oligomerization domain protein 1.* Infection and immunity, 2007. **75**(2): p. 706-713.
99. Lopez-Siles, M., et al., *Faecalibacterium prausnitzii: from microbiology to diagnostics and prognostics.* The ISME journal, 2017. **11**(4): p. 841-852.
100. Quévrain, E., et al., *Identification of an anti-inflammatory protein from Faecalibacterium prausnitzii, a commensal bacterium deficient in Crohn's disease.* Gut, 2016. **65**(3): p. 415-425.
101. Khan, M.T., et al., *The gut anaerobe Faecalibacterium prausnitzii uses an extracellular electron shuttle to grow at oxic-anoxic interphases.* The ISME journal, 2012. **6**(8): p. 1578-1585.
102. Műzes, G., et al., *Changes of the cytokine profile in inflammatory bowel diseases.* World journal of gastroenterology, 2012. **18**(41): p. 5848-5861.
103. Ma, X., et al., *The interleukin 12 p40 gene promoter is primed by interferon gamma in monocytic cells.* J Exp Med, 1996. **183**(1): p. 147-57.

104. Cunha, F.Q., S. Mohcada, and F.Y. Liew, *Interleukin-10 (IL-10) inhibits the induction of nitric oxide synthase by interferon-γ in murine macrophages.* Biochemical and Biophysical Research Communications, 1992. **182**(3): p. 1155-1159.
105. den Besten, G., et al., *The role of short-chain fatty acids in the interplay between diet, gut microbiota, and host energy metabolism.* J Lipid Res, 2013. **54**(9): p. 2325-40.
106. Pluznick, J., *A novel SCFA receptor, the microbiota, and blood pressure regulation.* Gut Microbes, 2014. **5**(2): p. 202-7.
107. Marino, E., et al., *Gut microbial metabolites limit the frequency of autoimmune T cells and protect against type 1 diabetes.* Nat Immunol, 2017. **18**(5): p. 552-562.
108. Zhang, M., et al., *Faecalibacterium prausnitzii Inhibits Interleukin-17 to Ameliorate Colorectal Colitis in Rats.* PLOS ONE, 2014. **9**(10): p. e109146.
109. Mittal, S.K. and P.A. Roche, *Suppression of antigen presentation by IL-10.* Current opinion in immunology, 2015. **34**: p. 22-27.
110. Kuhn, R., et al., *Interleukin-10-deficient mice develop chronic enterocolitis.* Cell, 1993. **75**(2): p. 263-74.
111. Moore, K.W., et al., *Interleukin-10 and the interleukin-10 receptor.* Annu Rev Immunol, 2001. **19**: p. 683-765.
112. O'Garra, A., et al., *IL-10-producing and naturally occurring CD4+ Tregs: limiting collateral damage.* The Journal of clinical investigation, 2004. **114**(10): p. 1372-1378.
113. Trinchieri, G., *Regulatory role of T cells producing both interferon gamma and interleukin 10 in persistent infection.* The Journal of experimental medicine, 2001. **194**(10): p. F53-F57.
114. Shouval, D.S., et al., *Interleukin 10 receptor signaling: master regulator of intestinal mucosal homeostasis in mice and humans.* Advances in immunology, 2014. **122**: p. 177-210.
115. Singh, N., et al., *Activation of Gpr109a, Receptor for Niacin and the Commensal Metabolite Butyrate, Suppresses Colonic Inflammation and Carcinogenesis.* Immunity, 2014. **40**(1): p. 128-139.
116. Chang, P.V., et al., *The microbial metabolite butyrate regulates intestinal macrophage function via histone deacetylase inhibition.* Proceedings of the National Academy of Sciences of the United States of America, 2014. **111**(6): p. 2247-2252.
117. Lin, M.Y., et al., *Redirection of Epithelial Immune Responses by Short-Chain Fatty Acids through Inhibition of Histone Deacetylases.* Frontiers in immunology, 2015. **6**: p. 554-554.
118. Brestoff, J.R. and D. Artis, *Commensal bacteria at the interface of host metabolism and the immune system.* Nat Immunol, 2013. **14**(7): p. 676-84.
119. Kamada, N., et al., *Control of pathogens and pathobionts by the gut microbiota.* Nature immunology, 2013. **14**(7): p. 685-690.
120. Sommer, F. and F. Backhed, *The gut microbiota--masters of host development and physiology.* Nat Rev Microbiol, 2013. **11**(4): p. 227-38.
121. Ferreira, C.M., et al., *The central role of the gut microbiota in chronic inflammatory diseases.* J Immunol Res, 2014. **2014**: p. 689492.

122. Martin-Gallausiaux, C., et al., *Butyrate produced by gut commensal bacteria activates TGF-beta1 expression through the transcription factor SP1 in human intestinal epithelial cells.* Scientific Reports, 2018. **8**(1): p. 9742.
123. Hosseini, E., et al., *Propionate as a health-promoting microbial metabolite in the human gut.* Nutr Rev, 2011. **69**(5): p. 245-58.
124. Marzocco, S., et al., *Supplementation of Short-Chain Fatty Acid, Sodium Propionate, in Patients on Maintenance Hemodialysis: Beneficial Effects on Inflammatory Parameters and Gut-Derived Uremic Toxins, A Pilot Study (PLAN Study).* J Clin Med, 2018. **7**(10).
125. Cox, M.A., et al., *Short-chain fatty acids act as antiinflammatory mediators by regulating prostaglandin E(2) and cytokines.* World journal of gastroenterology, 2009. **15**(44): p. 5549-5557.
126. Inatomi, O., et al., *Butyrate blocks interferon-γ-inducible protein-10 release in human intestinal subepithelial myofibroblasts.* Journal of Gastroenterology, 2005. **40**(5): p. 483-489.
127. Mirmonsef, P., et al., *A comparison of lower genital tract glycogen and lactic acid levels in women and macaques: implications for HIV and SIV susceptibility.* AIDS research and human retroviruses, 2012. **28**(1): p. 76-81.
128. Furusawa, Y., et al., *Commensal microbe-derived butyrate induces the differentiation of colonic regulatory T cells.* Nature, 2013. **504**: p. 446.
129. Chen, G., et al., *Sodium Butyrate Inhibits Inflammation and Maintains Epithelium Barrier Integrity in a TNBS-induced Inflammatory Bowel Disease Mice Model.* EBioMedicine, 2018. **30**: p. 317-325.
130. Nastasi, C., et al., *The effect of short-chain fatty acids on human monocyte-derived dendritic cells.* Scientific reports, 2015. **5**: p. 16148-16148.
131. Hu, X., et al., *IFN-γ Suppresses IL-10 Production and Synergizes with TLR2 by Regulating GSK3 and CREB/AP-1 Proteins.* Immunity, 2006. **24**(5): p. 563-574.
132. Verma, A., et al., *Triterpenoids principle of Wedelia calendulacea attenuated diethynitrosamine-induced hepatocellular carcinoma via down-regulating oxidative stress, inflammation and pathology via NF-kB pathway.* Inflammopharmacology, 2018. **26**(1): p. 133-146.
133. Gilmore, T.D., *Introduction to NF-κB: players, pathways, perspectives.* Oncogene, 2006. **25**(51): p. 6680-6684.
134. Kawasaki, T. and T. Kawai, *Toll-like receptor signaling pathways.* Frontiers in immunology, 2014. **5**: p. 461-461.
135. Lukovac, S., et al., *Differential modulation by Akkermansia muciniphila and Faecalibacterium prausnitzii of host peripheral lipid metabolism and histone acetylation in mouse gut organoids.* mBio, 2014. **5**(4): p. e01438-14.
136. Parada Venegas, D., et al., *Short Chain Fatty Acids (SCFAs)-Mediated Gut Epithelial and Immune Regulation and Its Relevance for Inflammatory Bowel Diseases.* Frontiers in Immunology, 2019. **10**: p. 277.
137. Cummings, J.H., et al., *Short chain fatty acids in human large intestine, portal, hepatic and venous blood.* Gut, 1987. **28**(10): p. 1221-1227.
138. Clausen, M.R. and P.B. Mortensen, *Kinetic studies on colonocyte metabolism of short chain fatty acids and glucose in ulcerative colitis.* Gut, 1995. **37**(5): p. 684-689.

139. Ritzhaupt, A., et al., *Identification and characterization of a monocarboxylate transporter (MCT1) in pig and human colon: its potential to transport l-lactate as well as butyrate.* The Journal of Physiology, 1998. **513**(3): p. 719-732.
140. Bloemen, J.G., et al., *Short chain fatty acids exchange across the gut and liver in humans measured at surgery.* Clinical Nutrition, 2009. **28**(6): p. 657-661.
141. Kim, M.H., et al., *Short-Chain Fatty Acids Activate GPR41 and GPR43 on Intestinal Epithelial Cells to Promote Inflammatory Responses in Mice.* Gastroenterology, 2013. **145**(2): p. 396-406.e10.
142. Asarat, M., et al., *Short-Chain Fatty Acids Regulate Secretion of IL-8 from Human Intestinal Epithelial Cell Lines in vitro.* Immunological Investigations, 2015. **44**(7): p. 678-693.
143. Goverse, G., et al., *Diet-Derived Short Chain Fatty Acids Stimulate Intestinal Epithelial Cells To Induce Mucosal Tolerogenic Dendritic Cells.* The Journal of Immunology, 2017. **198**(5): p. 2172.
144. Miao, W., et al., *Sodium Butyrate Promotes Reassembly of Tight Junctions in Caco-2 Monolayers Involving Inhibition of MLCK/MLC2 Pathway and Phosphorylation of PKCβ2.* International journal of molecular sciences, 2016. **17**(10): p. 1696.
145. Peng, L., et al., *Butyrate enhances the intestinal barrier by facilitating tight junction assembly via activation of AMP-activated protein kinase in Caco-2 cell monolayers.* The Journal of nutrition, 2009. **139**(9): p. 1619-1625.
146. Valenzano, M.C., et al., *Remodeling of Tight Junctions and Enhancement of Barrier Integrity of the CACO-2 Intestinal Epithelial Cell Layer by Micronutrients.* PloS one, 2015. **10**(7): p. e0133926-e0133926.
147. Zheng, L., et al., *Microbial-Derived Butyrate Promotes Epithelial Barrier Function through IL-10 Receptor-Dependent Repression of Claudin-2.* Journal of immunology (Baltimore, Md. : 1950), 2017. **199**(8): p. 2976-2984.
148. Sato, T., et al., *Long-term Expansion of Epithelial Organoids From Human Colon, Adenoma, Adenocarcinoma, and Barrett's Epithelium.* Gastroenterology, 2011. **141**(5): p. 1762-1772.
149. van der Hee, B., et al., *Optimized procedures for generating an enhanced, near physiological 2D culture system from porcine intestinal organoids.* Stem Cell Research, 2018. **28**: p. 165-171.
150. Andrews, S. *FastQC: A quality control tool for high throughput sequence data*. 2017; v0.11.5:[Available from: http://www.bioinformatics.babraham.ac.uk/projects/fastqc/.
151. Zerbino, D.R., et al., *Ensembl 2018.* Nucleic Acids Research, 2017. **46**(D1): p. D754-D761.
152. van der Hee, B., et al., *Congruence of location-specific transcriptional programs in intestinal organoids during long-term culture.* bioRxiv, 2019: p. 600940.
153. Reimand, J., et al., *g:Profiler-a web server for functional interpretation of gene lists (2016 update).* Nucleic acids research, 2016. **44**(W1): p. W83-W89.
154. Sorci, G., et al., *RAGE in tissue homeostasis, repair and regeneration.* Biochimica et Biophysica Acta (BBA) - Molecular Cell Research, 2013. **1833**(1): p. 101-109.
155. Chikhirzhina, E., T. Starkova, and A. Polyanichko, *The Role of Linker Histones in Chromatin Structural Organization. 1. H1 Family Histones.* Biophysics, 2018. **63**(6): p. 858-865.
156. Vitiello, M., et al., *Multiple pathways of SIRT6 at the crossroads in the control of longevity, cancer, and cardiovascular diseases.* Ageing Research Reviews, 2017. **35**: p. 301-311.

157. Giaimo, B.D., et al., *The histone variant H2A.Z in gene regulation.* Epigenetics & Chromatin, 2019. **12**(1): p. 37.
158. Bianchi, M.E. and A. Agresti, *HMG proteins: dynamic players in gene regulation and differentiation.* Current Opinion in Genetics & Development, 2005. **15**(5): p. 496-506.
159. Klune, J.R., et al., *HMGB1: endogenous danger signaling.* Molecular medicine (Cambridge, Mass.), 2008. **14**(7-8): p. 476-484.
160. Preyat, N. and O. Leo, *Sirtuin deacylases: a molecular link between metabolism and immunity.* Journal of Leukocyte Biology, 2013. **93**(5): p. 669-680.
161. Mendes, K.L., D.d.F. Lelis, and S.H.S. Santos, *Nuclear sirtuins and inflammatory signaling pathways.* Cytokine & Growth Factor Reviews, 2017. **38**: p. 98-105.
162. Lazar, V., et al., *Aspects of Gut Microbiota and Immune System Interactions in Infectious Diseases, Immunopathology, and Cancer.* Frontiers in immunology, 2018. **9**: p. 1830-1830.
163. Rolhion, N. and A. Darfeuille-Michaud, *Adherent-invasive Escherichia coli in inflammatory bowel disease.* Inflamm Bowel Dis, 2007. **13**(10): p. 1277-83.
164. Seksik, P., *[Gut microbiota and IBD].* Gastroenterol Clin Biol, 2010. **34 Suppl 1**: p. S44-51.
165. Peran, L., et al., *Lactobacillus fermentum, a probiotic capable to release glutathione, prevents colonic inflammation in the TNBS model of rat colitis.* International Journal of Colorectal Disease, 2006. **21**(8): p. 737-746.
166. Sokol, H., et al., *Low counts of Faecalibacterium prausnitzii in colitis microbiota.* Inflamm Bowel Dis, 2009. **15**(8): p. 1183-9.
167. Machiels, K., et al., *A decrease of the butyrate-producing species Roseburia hominis and Faecalibacterium prausnitzii defines dysbiosis in patients with ulcerative colitis.* Gut, 2014. **63**(8): p. 1275-83.
168. Qiu, X., et al., *Faecalibacterium prausnitzii upregulates regulatory T cells and anti-inflammatory cytokines in treating TNBS-induced colitis.* J Crohns Colitis, 2013. **7**(11): p. e558-68.
169. Cooper, H.S., et al., *Clinicopathologic study of dextran sulfate sodium experimental murine colitis.* Lab Invest, 1993. **69**(2): p. 238-49.
170. Rossi, O., et al., *Faecalibacterium prausnitzii Strain HTF-F and Its Extracellular Polymeric Matrix Attenuate Clinical Parameters in DSS-Induced Colitis.* PLoS One, 2015. **10**(4): p. e0123013.
171. Pfaffl, M.W., *A new mathematical model for relative quantification in real-time RT-PCR.* Nucleic acids research, 2001. **29**(9): p. e45-e45.
172. Martin, M., *Cutadapt removes adapter sequences from high-throughput sequencing reads.* EMBnet.journal; Vol 17, No 1: Next Generation Sequencing Data Analysis, 2011.
173. Callahan, B.J., et al., *DADA2: High-resolution sample inference from Illumina amplicon data.* Nature methods, 2016. **13**(7): p. 581-583.
174. Quast, C., et al., *The SILVA ribosomal RNA gene database project: improved data processing and web-based tools.* Nucleic acids research, 2013. **41**(Database issue): p. D590-D596.
175. McMurdie, P.J. and S. Holmes, *phyloseq: An R Package for Reproducible Interactive Analysis and Graphics of Microbiome Census Data.* PLOS ONE, 2013. **8**(4): p. e61217.

176. Jari Oksanen, F.G.B., Michael Friendly, Roeland Kindt, Pierre Legendre, Dan McGlinn, Peter R. Minchin, R. B. O'Hara, Gavin L. Simpson, Peter Solymos, M. Henry H. Stevens, Eduard Szoecs, Helene Wagner, *Community Ecology Package: 'vegan'*. 2019.
177. Andy Liaw, M.W., *Classification and Regression by randomForest.* 2002.
178. Nguyen, T.L.A., et al., *How informative is the mouse for human gut microbiota research?* Disease models & mechanisms, 2015. **8**(1): p. 1-16.
179. Allaire, J.M., et al., *The Intestinal Epithelium: Central Coordinator of Mucosal Immunity.* Trends in Immunology, 2018. **39**(9): p. 677-696.
180. Tashiro, M., et al., *The N-terminal region of serum amyloid A3 protein activates NF-κB and up-regulates MUC2 mucin mRNA expression in mouse colonic epithelial cells.* PloS one, 2017. **12**(7): p. e0181796-e0181796.
181. Ahn, M.-H., et al., *Titanium dioxide particle-induced goblet cell hyperplasia: association with mast cells and IL-13.* Respiratory research, 2005. **6**(1): p. 34-34.
182. Ling, Y., et al., *The silence of MUC2 mRNA induced by promoter hypermethylation associated with HBV in Hepatocellular Carcinoma.* BMC Medical Genetics, 2013. **14**(1): p. 14.
183. Wu, J., et al., *Deoxycholic acid induces the overexpression of intestinal mucin, MUC2, via NF-kB signaling pathway in human esophageal adenocarcinoma cells.* BMC cancer, 2008. **8**: p. 333-333.
184. Mashimo, H., et al., *Impaired Defense of Intestinal Mucosa in Mice Lacking Intestinal Trefoil Factor.* Science, 1996. **274**(5285): p. 262.
185. Schwab, U., et al., *Effect of the amount and type of dietary fat on cardiometabolic risk factors and risk of developing type 2 diabetes, cardiovascular diseases, and cancer: a systematic review.* Food & nutrition research, 2014. **58**: p. 10.3402/fnr.v58.25145.
186. Sartor, C.D., et al., *Effects of strengthening, stretching and functional training on foot function in patients with diabetic neuropathy: results of a randomized controlled trial.* BMC Musculoskeletal Disorders, 2014. **15**(1): p. 137.
187. Osaka, T., et al., *Meta-Analysis of Fecal Microbiota and Metabolites in Experimental Colitic Mice during the Inflammatory and Healing Phases.* Nutrients, 2017. **9**(12): p. 1329.
188. Berry, D., et al., *Phylotype-level 16S rRNA analysis reveals new bacterial indicators of health state in acute murine colitis.* The ISME journal, 2012. **6**(11): p. 2091-2106.
189. Okayasu, I., et al., *A novel method in the induction of reliable experimental acute and chronic ulcerative colitis in mice.* Gastroenterology, 1990. **98**(3): p. 694-702.
190. Zamani, S., et al., *Detection of enterotoxigenic Bacteroides fragilis in patients with ulcerative colitis.* Gut pathogens, 2017. **9**: p. 53-53.
191. Börnigen, D., et al., *Functional profiling of the gut microbiome in disease-associated inflammation.* Genome Medicine, 2013. **5**(7): p. 65.
192. Stagg, A.J., *Intestinal Dendritic Cells in Health and Gut Inflammation.* Frontiers in immunology, 2018. **9**: p. 2883-2883.
193. Kumar, S., et al., *Ex vivo antigen-pulsed PBMCs generate potent and long lasting immunity to infection when administered as a vaccine.* Vaccine, 2017. **35**(7): p. 1080-1086.

194. Chan, L., K. McCulley, and P. Banerjee, *A high-throughput image cytometry-based screening method for the detection of IL2-induced peripheral blood mononuclear cell-mediated cytotoxicity.* The Journal of Immunology, 2016. **196**(1 Supplement): p. 143.11.
195. Bisping, G., et al., *Patients with inflammatory bowel disease (IBD) reveal increased induction capacity of intracellular interferon-gamma (IFN-gamma) in peripheral CD8+ lymphocytes co-cultured with intestinal epithelial cells.* Clinical and experimental immunology, 2001. **123**(1): p. 15-22.
196. Meijerink, M., et al., *Identification of genetic loci in Lactobacillus plantarum that modulate the immune response of dendritic cells using comparative genome hybridization.* PloS one, 2010. **5**(5): p. e10632-e10632.
197. Meijerink, M. and J.M. Wells, *Probiotic modulation of dendritic cells and T cell responses in the intestine.* Benef Microbes, 2010. **1**(4): p. 317-26.
198. Doyle, S.E., et al., *Toll-like receptors induce a phagocytic gene program through p38.* The Journal of experimental medicine, 2004. **199**(1): p. 81-90.
199. Liu, T., et al., *Short-Chain Fatty Acids Suppress Lipopolysaccharide-Induced Production of Nitric Oxide and Proinflammatory Cytokines Through Inhibition of NF-κB Pathway in RAW264.7 Cells.* Inflammation, 2012. **35**(5): p. 1676-1684.
200. Millard, A.L., et al., *Butyrate affects differentiation, maturation and function of human monocyte-derived dendritic cells and macrophages.* Clinical and experimental immunology, 2002. **130**(2): p. 245-255.
201. Macia, L., et al., *Metabolite-sensing receptors GPR43 and GPR109A facilitate dietary fibre-induced gut homeostasis through regulation of the inflammasome.* Nature Communications, 2015. **6**(1): p. 6734.
202. Suez, J. and E. Elinav, *The path towards microbiome-based metabolite treatment.* Nature Microbiology, 2017. **2**(6): p. 17075.

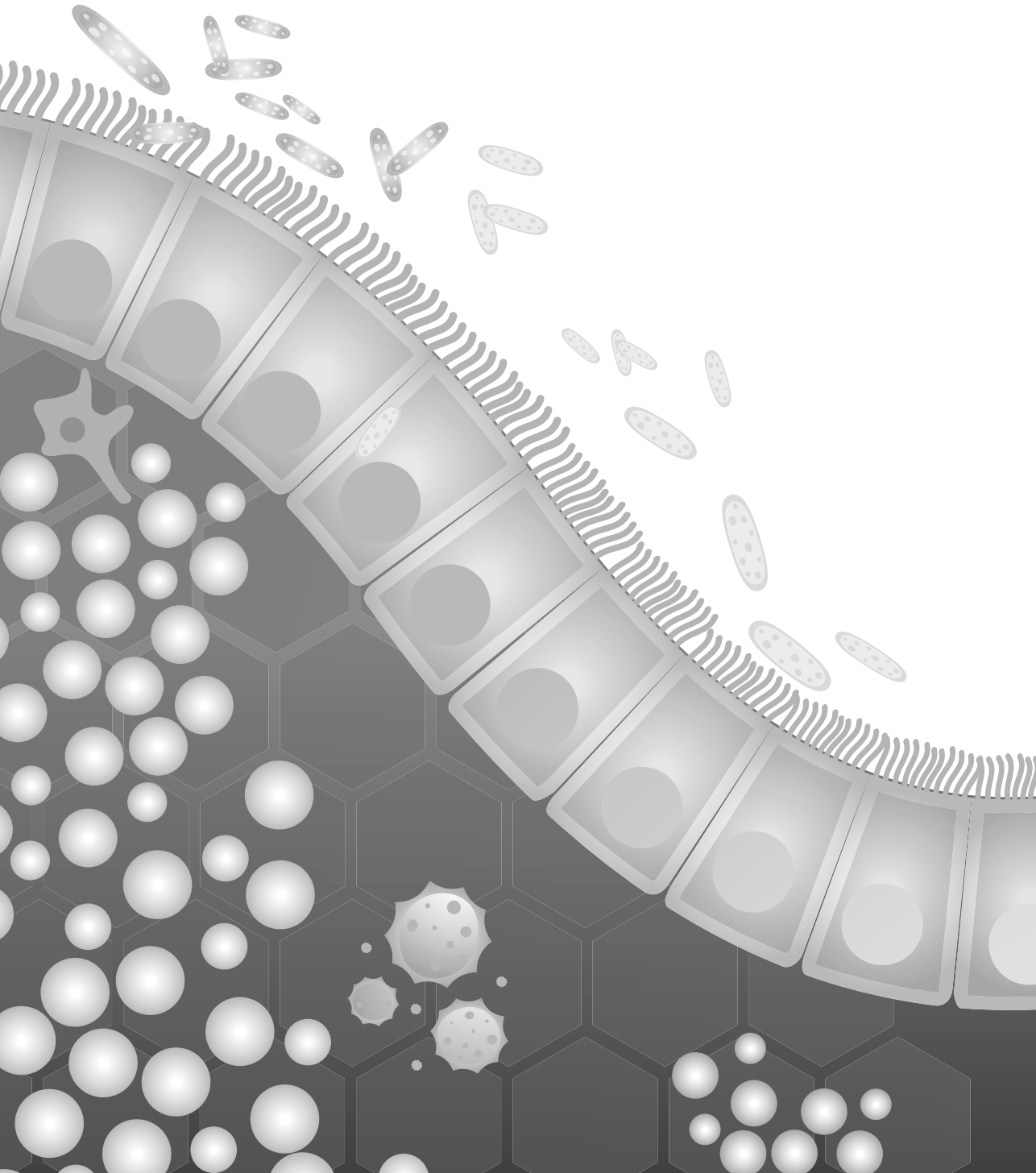

Summary

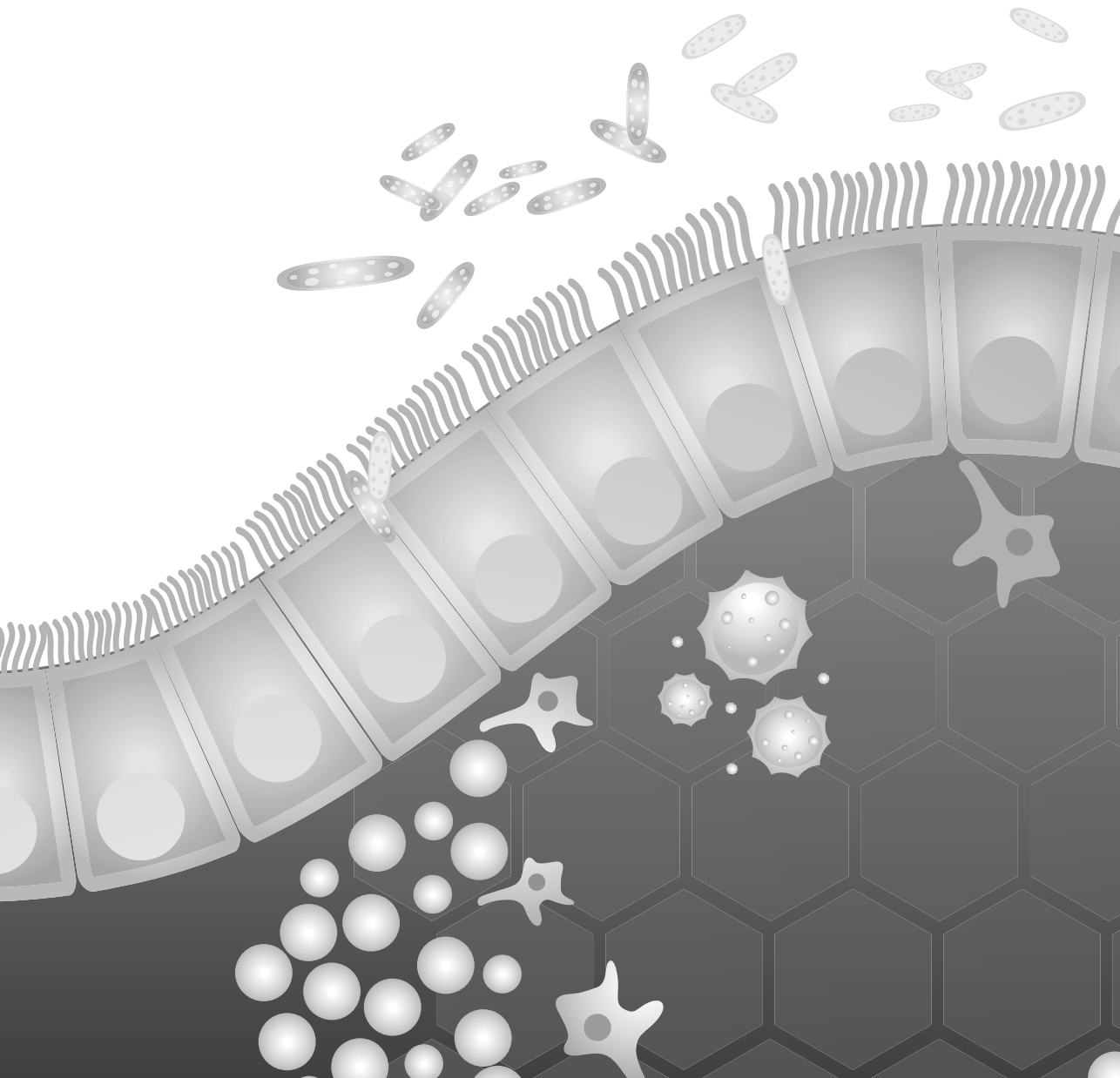

SUMMARY

The intestinal microbiota plays a crucial role in the homeostasis of the human gastrointestinal tract by maintaining an anti-inflammatory status. Microbial imbalance in the gut, which is often referred to as 'dysbiosis', is known to be one of the major contributors to many human diseases, including inflammatory bowel disease (IBD). IBD is characterized by a chronic inflammation, but the current available treatment with anti-inflammatory drugs is often not effective. Therefore, the overarching aim of this thesis was to try to find bacterial strains or bacterial metabolites that have an immunomodulatory (i.e. an anti-inflammatory) function and may therefore be used as a therapy or treatment of IBD. In collaboration with the Rowett Institute, University of Aberdeen in Scotland, UK and the Department of Medical Microbiology, at the University Medical Centre Groningen, The Netherlands, a large number of colonic anaerobic bacteria were isolated from healthy patients. In our lab, we cultured more than 100 of these different strains of bacteria under strictly anaerobic conditions. We observed their growth characteristics and investigated their immunomodulatory properties. A high ratio between secreted anti-and pro-inflammatory cytokines (IL-10/IL-12 ratio) has been reported to be an indicator of positive correlation between *in vitro* trials and the attenuation of clinical symptoms in *in vivo* mouse models of colitis. Our initial screening therefore started with stimulation of peripheral mononuclear blood lymphocytes (PBMCs) with standardized concentrations of the bacteria or their culture supernatant. We determined the cytokine secretion of these PBMC after bacterial stimulation and determined the IL-10/IL-12 ratio. Additionally we checked if the viability of the PBMC was not affected by the bacterial strains or their metabolites which were secreted in the supernatant. As IBD is characterized by periods of remission and occasional flare-ups (periods of higher inflammation), we investigated both healthy and disease situations. To achieve this, we added heat inactivated bacteria (HIB) to our PBMC culture. These HIB triggered a strong induction of both pro-and anti-inflammatory cytokines, which is reminiscent of actual inflammation. Co-stimulation with both HIB and our bacterial strains enabled us to investigate the effect of the bacterial strains 'during inflammation'. Additionally, we checked whether the bacterial strains were able to trigger NF-κB signalling via Toll like receptor (TLR) activation, which is one of the most known mechanisms to modulate immune response of the host. Finally, to assess oxidative stress, which is known to occur during flare-ups and damages the epithelial cells, we investigated whether the different bacterial strains were able to modulate nitric oxide (NO) secretion by a mouse macrophage (RAW 264.7) cell line. Again we were able to mimic an inflammatory situation by addition of bacterial lipopolysaccharides (LPS) to these cells and could thereby also investigate the effect of bacteria in an already inflamed gut.

In **Chapter 2** we summarize the characterisation of 68 different colonic anaerobic bacteria tested. Most importantly, we found that there is a large variation among the tested strains in their immunomodulatory properties. The variation in induction of cytokine and NO

secretion as well as in the ability to trigger NF-κB signalling between strains was significant. Interestingly, the bacterially induced immune profiles were highly strain dependent and not characteristic for a specific bacterial species. We must therefore conclude that generalizations cannot be made easily and any newly discovered strain needs to be individually investigated to determine its immunomodulatory properties. However, we could identify three different immune profiles, resulting from bacterial stimulation. The first 'immunostimulatory' profile was characterized by strongly inducing cytokine secretion in PBMCs. Most of these strains also elicited relatively high concentrations of NO secretion and strong NF-κB signalling after TLR activation. The second 'immunomodulatory' profile was characterized by induction of only moderate amounts of cytokine secretion. However, when an inflammatory status was mimicked (addition of HIB), these strains were able to attenuate the secretion of pro-inflammatory cytokines. The final 'immuno suppressive' or 'silent' profile was characterized by a low capacity to induce cytokine or NO secretion. More importantly, when HIB was added as an inflammatory stimulus, these strains attenuated the resulting pro-inflammatory cytokine response.

Several studies showed that there is a negative correlation between the relative abundance of *F. prausnitzii* and the disease severity of IBD, therefore a causal connection has been suggested. Indeed, several *in vivo* studies have shown that addition of certain strains of *F. prausnitzii* could attenuate clincal symptoms of colitis in mice. We therefore focused on another 28 bacterial strains that all belonged to the species of *F. prausnitzii* in **Chapter 3.** After thorough *in vitro* investigation we have to conclude that the immunomodulatory properties are really strain specific, as the tested properties of the strains (cytokine, NO secretion and NF-κB signaling via TLR activation) do not correlate with genomic phylogenetic clusters. Among the different strains tested, we found all three different immune profiles that were observed in Chapter 2. Moreover, the general assumption that all *F. prausnitzii* strains induce strong IL-10 secretion was found to not be universally true, as there were some 'silent' strains that hardly induced any IL-10 secretion. Interestingly, one of the strains that was the strongest activator of NF-κB signaling, hardly induced any cytokine secretion, which suggest some specific mechanism to prevent downstream effects. Indeed this strain manifested a 'silent' profile and as such was considered to be of interest for further *in vivo* trials.

During the *in vitro* screening procedures described above we observed that the culture supernatant of all strains tested was able to attenuate HIB induced cytokine secretion. Further investigations showed that the original growth medium (without any bacteria present), and especially the short chain fatty acids (SCFA) in the medium also triggered this attenuation effect. SCFA were reported to have immunomodulatory effects, but the studies were not all consistent. Most studies showed that butyrate induced IL-10 secretion by immune cells and thereby triggered regulatory T cell differentiation. In **Chapter 4** we compared the effects of acetate and butyrate on different immune cell mechanisms. We found that

butyrate decreased cell viability when administered at higher concentrations, whereas similar, or even higher concentrations of acetate did not affect cell viability. Interestingly, although both acetate and butyrate were able to attenuate HIB induced secretion of pro-inflammatory cytokines, only acetate was able to increase the anti-inflammatory cytokine IL-10. More importantly, butyrate actually decreased the secretion of the anti-inflammatory IL-10 *in vitro* in both PBMC as well as $CD14^+$ monocytes. This decreased IL-10 secretion could result in an overall more inflammatory response (lower IL-10/IL-12 ratio) compared to the response triggered by acetate. To investigate how butyrate and acetate elicited their effects, we tried to determine the mechanism by which they affected cytokine secretion. As G protein-coupled receptors (GPCR) are known to mediate the effect of SCFA, we blocked the expression of GPCR in monocyte-derived dendritic cells (MDDC) with specific inhibitors. The attenuating effects of SCFA on HIB induced cytokine secretion were still observed, suggesting that modulation of cytokine secretion used an GPCR-independent mechanism. Butyrate (and to a lesser extent acetate) are also known to affect histone acetylation and could thereby modulate gene transcription. We found that butyrate indeed increased histone acetylation, which may point to a mechanism used in modulation of cytokines secretion. Interestingly, NF-κB activation was also found to be differentially modulated by acetate compared to butyrate, although the underlying mechanism has not yet been elucidated.

As we found clear effects of both acetate and butyrate on cytokine secretion by PBMC and $CD14^+$ monocyte, we wondered if other biological pathways would be affected as well. We therefore stimulated $CD14^+$ monocytes with acetate and butyrate (with or without co-stimulation with HIB) and investigated the resulting transcription profile in **Chapter 5**. Our monocytes showed the same attenuation of pro-inflammatory cytokine secretion in HIB induced samples as was seen in the PBMC and $CD14^+$ monocyte. Acetate did not cause major effects in the number of regulated genes, but butyrate significantly affected the regulation of many different (immune) pathways and genes therein.

To compare the effects that SCFA might have on epithelial cells with the effects we found on immune cells, we investigated the effect of SCFA on an *ex vivo* 3D porcine ileum organoid model in **Chapter 6.** We exposed the organoid cells to acetate and butyrate and performed a transcriptomic analysis. Similar to the results of the transcriptomic analysis of $CD14^+$ monocyte, butyrate proved to elicit greater changes in gene expression compared to acetate and substantially affected apoptosis and cell-cycle related pathways. In contrast, acetate mainly affected cellular metabolism process- related pathways, suggesting a less damaging effect on gut epithelial function compared to butyrate.

To conclude our studies, we tested several bacterial strains that appeared promising in the *in vitro* trials, in an *in vivo* mouse DSS-induced colitis model in **Chapter 7**. We observed attenuation of the clinical symptoms after addition of these 'silent' strains, which confirm our

hypothesis that the bacterial strains that induced an 'silent' profile would be able to reduce colonic inflammation.

In the last chapter, **Chapter 8**, we summarize and discuss the combined results from this thesis in the context of other studies regarding host- microbe interactions, probiotics and the effects of SCFA. We explain how these findings contribute to a better understanding of the immunomodulatory properties of colonic anaerobic bacterial strains and their metabolites and provide suggestions for future research, and reflect on the overall aim of this thesis.

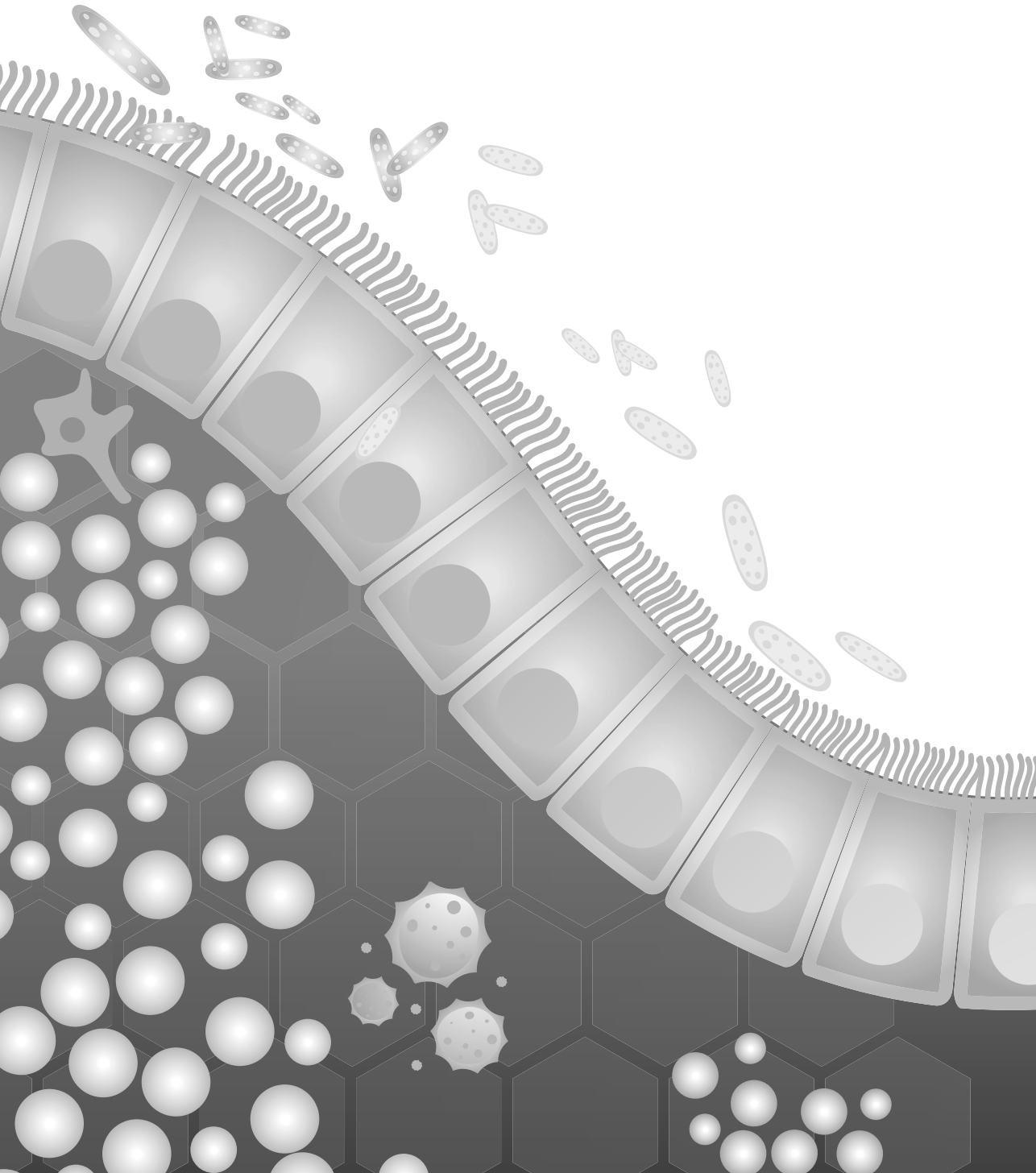

Appendices

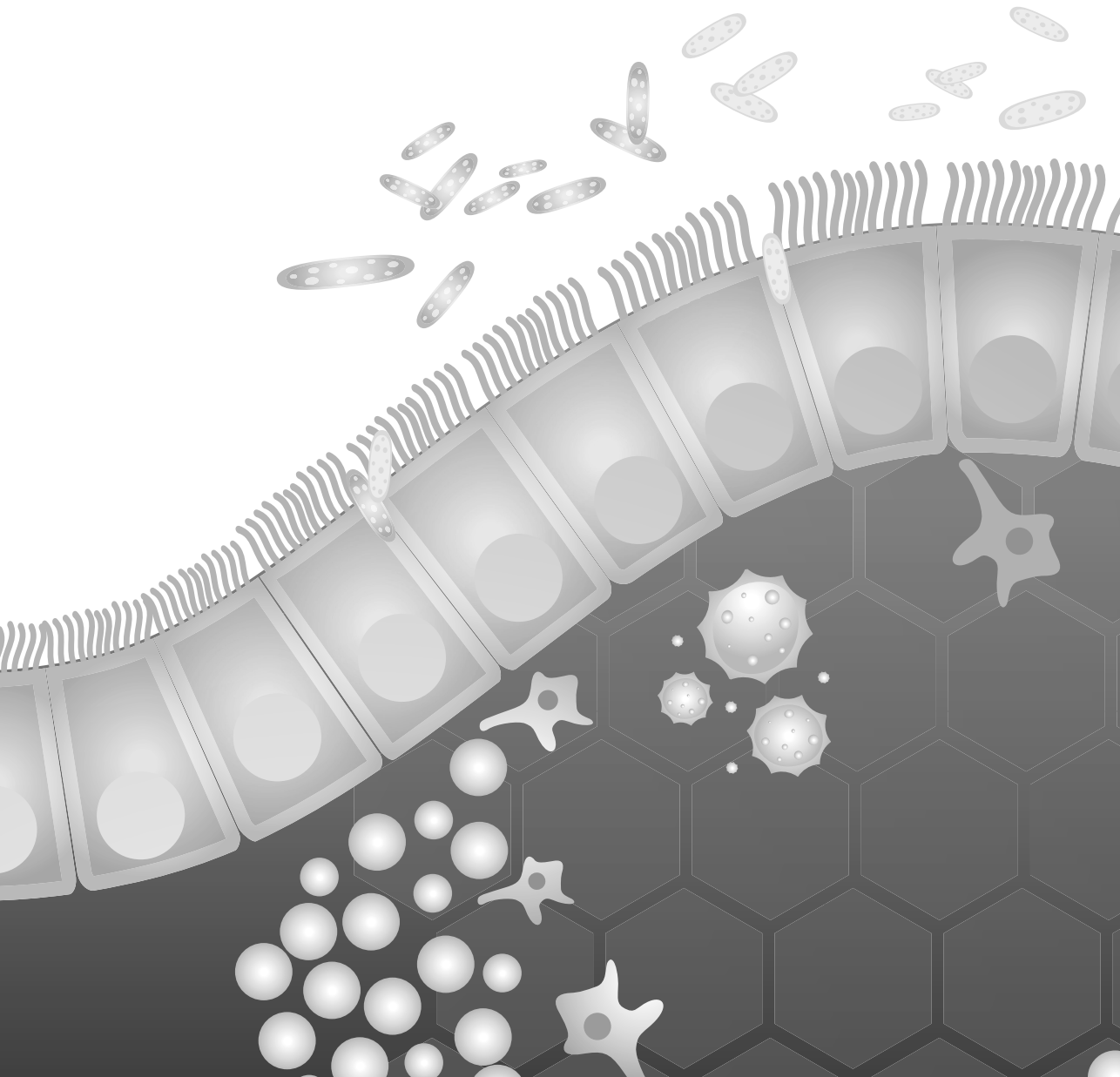

NEDERLANDSE SAMENVATTING

Darmbacteriën spelen een cruciale rol in het interne evenwicht (homeostase) van het menselijke verteringssysteem, doordat ze een continue ontstekingsremmende functie hebben. Een verstoorde samenstelling van de verschillende soorten darmbacteriën (dysbiosis), kan bijdragen aan allerlei ziektebeelden zoals de ziekte van Crohn en colitis (chronisch ontstoken darm). Beide ziektebeelden worden gekenmerkt door chronische ontsteking en worden daarom voornamelijk behandeld met ontstekingsremmers; maar deze behandelwijze is vaak niet effectief. Daarom was het doel van dit proefschrift om te onderzoeken of er bacteriesoorten waren, of stoffen die geproduceerd worden door bacteriën, die een ontstekingsremmende werking hebben en dus gebruikt kunnen worden als behandeling, of ter voorkoming van darmontstekingen.

In een samenwerkingsverband met het Rowett Instituut, van de University of Aberdeen in Scotland, Groot Brittannië en de afdeling Medische Microbiologie, van het Universitair Medisch Centrum Groningen, werden een groot aantal verschillende soorten darmbacteriën geïsoleerd uit gezonde mensen. In ons laboratorium van Host Microbe Interactions in Wageningen, kweekten we meer dan 100 van deze verschillende soorten darmbacteriën zonder blootstelling aan zuurstof (strikte anaerobe) condities, vergelijkbaar met de situatie in de menselijke darm . We observeerden de groei karakteristieken en onderzochten hun ontstekingsremmende eigenschappen.

Eerder onderzoek had aangetoond dat er een positief verband is tussen de verhouding van ontstekingsremmende en ontstekingsbevorderend signaalmoleculen (cytokines) in het bloed (IL-10/IL-12 ratio) en de vermindering van de klinische symptomen in levende muismodellen *(in vivo)*. Als de verhouding (IL-10/IL-12) hoger was, was er een aanzienlijk grotere kans dat de muizen zouden genezen van hun darmontsteking. Onze eerste selectie was daarom gericht op het meten van deze signaalmoleculen in het bloed. Hiervoor stimuleerden we witte bloedcellen (PBMC) van gezonde menselijke bloeddonoren met gestandaardiseerde hoeveelheden van de verschillende bacteriën, of met het medium waarin de bacteriën gegroeid waren. Dit medium zou eventuele gezondsheidsbevorderende stoffen die de bacteriën geproduceerd hadden kunnen bevatten. Verschillende signaalmoleculen die door de witte bloedcellen worden geproduceerd werden gemeten en we bepaalden de verhouding tussen de IL-10 en IL-12. Tegelijkertijd werd gekeken of de bacteriën, of hun uitscheidingsproducten (metabolieten) de levensvatbaarheid van de witte bloedcellen niet aantastte. Omdat darmontstekingen worden gekenmerkt door periodes zonder klachten die afgewisseld worden met periodes van aanzienlijke ontsteking, wilden we beide situaties onderzoeken. Daarom voegden we door hitte gedode bacteriën toe aan onze witte bloedcellen. Deze door hitte gedode bacteriën (heat inactivated bacteria, HIB) veroorzaakten uitscheiding van een groot aantal signaalmoleculen (zowel ontstekingsbevorderend als

ontstekingsremmend) door onze witte bloedcellen en was als zodanig goed vergelijkbaar met een echte ontstekingsreactie. Vervolgens werd bekeken of toevoeging van onze geïsoleerde darmbacteriën deze ontstekingsreactie kon beïnvloeden. Ook werd er bekeken of de verschillende darmbacteriën in staat waren om de NF-κB signalering te activeren, via Toll like receptors (TLR). Dit is een soort alarmfunctie die de cellen kunnen aanzetten als ze 'gevaarlijke bacteriën' herkennen en daarmee de belangrijkste methode om het aangeboren afweersysteem te activeren. Tenslotte hebben we gekeken naar oxidatieve stress. Dit is een proces, waarbij bepaalde witte bloedcellen stikstofoxide (NO) maken, dat giftig is voor ziekteverwekkers. Hoewel dit NO helpt bij de bestrijding van ziekteverwekkers, worden de eigen darmcellen ook beschadigd. Dit is een van de symptomen van darmontsteking. Wij wilden dus onderzoeken of de verschillende soorten darmbacteriën in staat zouden zijn om de productie NO te verminderen, of om zeker te weten dat ze deze niet zelf zouden veroorzaken. Dit alles hebben we onderzocht *in vitro*, waarbij we gebruikmaakten van witte bloedcellen (macrofagen) van muizen. Ook hier hebben we naast een 'gezonde situatie' een ontstekingsreactie nagebootst, in dit geval door gebruik te maken van een stof uit de celwand van Gram negatieve bacteriën (LPS).

In **hoofdstuk 2** laten we de resultaten zien van de eigenschappen van 68 verschillende -strikt aerobe- darmbacteriën , met betrekking tot de productie van signaalmoleculen die ze veroorzaakten, de activatie van alarmfunctie (NF-κB via TLR) en de productie van NO. De meest belangrijke conclusie die we konden trekken is dat de variatie die we zagen in ieder van die eigenschappen erg verschilde tussen de geteste darmbacteriën. De verhouding tussen de verschillende geproduceerde signaalmoleculen (immuun profielen) verschilde bovendien ook enorm tussen bacteriestammen (strains) binnen een bepaalde bacteriesoort. We moeten daarom vaststellen dat algemene aannames met betrekking tot bepaalde bacterie soorten niet kunnen worden gemaakt aangezien de onderlinge stammen alsnog flink kunnen verschillen. Het blijft daarom noodzakelijk om elke bacteriestam afzonderlijk te onderzoeken op mogelijke ontstekingsremmende functies. Wel konden we drie algemene immuunprofielen onderscheiden in de witte bloedcellen als een gevolg van blootstelling aan de verschillende geteste bacteriesoorten. De eerste hiervan was 'immuunstimulerend' en werd gekenmerkt door sterke uitscheiding van signaalmoleculen door witte bloedcellen. De meeste van de bacteriestammen die dit profiel veroorzaakten, hadden ook hoge NO waardes en activeerden de alarmfunctie (NF-κB via TLR) sterk. Het 'immuunmodulerend' tweede profiel werd gekenmerkt doordat slechts gemiddelde hoeveelheden signaalmoleculen door de witte bloedcellen geproduceerd werden. Echter, zodra een ontsteking werd nagebootst, door blootstelling aan door hitte gedode bacteriën, dan waren deze darmbacterie stammen in staat om deze ontsteking te remmen door de hoeveelheid ontstekingssignaalmoleculen die door de witte bloedcellen werd uitgescheiden te verminderen. Het laatste profiel was het immunosuppressieve, of 'stille' profiel en kenmerkte zich doordat het slechts heel weinig signaalmoleculen tot gevolg had en ook de productie van NO zeer laag bleef. Maar de meest

belangrijke vondst was, dat de darmbacteriën die dit profiel laatste veroorzaakten, wel in staat bleken om een ontstekingsreactie die opgewekt was door blootstelling aan door hitte gedode bacteriën te remmen. De ontstekingsreactie die normaal zou ontstaan werd verminderd door extra productie van ontstekingsremmende signaalmoleculen, terwijl er tijdens een 'gezonde', klachtenvrije periode geen effecten te zien waren. Stammen met dit profiel leken dus erg geschikt als potentieel medicijn aangezien ze alleen tijdens ontsteking effect zouden hebben.

Verschillende studies hebben aangetoond dat er een negatief verband is tussen de relatieve hoeveelheid *Feacaliumbacterium prausnitzii* bacteriën in de darm van een patiënt en de ernst van darmontsteking. Hoewel het dus logisch lijkt dat een tekort aan deze bacteriesoort de darmontsteking zou veroorzaken is een definitief oorzakelijk verband nog niet bewezen. Maar het is wel aangetoond dat als men muizen bepaalde stammen van deze *F. prausnitzii* bacterie toedient, dat dit de klinische symptomen van darmontsteking (colitis) verminderde. In **hoofdstuk 3** hebben we daarom specifiek gekeken naar 28 stammen van de bacterie soort *F. prausnitzii*. Na uitvoerig onderzoek moeten we echter vaststellen dat de immunomodulerende eigenschappen van deze bacteriesoort opnieuw niet specifiek zijn en dat de verschillende stammen grote verschillen laten zien in de geteste eigenschappen. Zowel de hoeveelheden signaalmoleculen en NO die geproduceerd werden, als de activering van de alarm functie (NF-κB via TLR), kwamen niet overeen met de evolutionaire verwantschap (fylogenetische clustering) van de soorten. Wel konden binnen de 28 stammen alle drie de verschillende immuunprofielen die we eerder vonden hadden opnieuw geobserveerd worden. Bovendien bleek de algemene aanname dat alle *F. prausnitzii* stammen altijd hoge waardes van het ontstekingsremmende IL-10 uitscheiden ook niet correct, aangezien we een aantal 'stille' stammen ontdekten, die amper IL-10 uitscheidden. Interessant was ook, dat een van de stammen die de sterkste activator was van de alarmfunctie (NF-κB signalering), amper zorgde voor productie van signaalmoleculen in witte bloedcellen. Dit is erg vreemd omdat normaal gesproken de activering van de alarmfunctie de productie van de signaalmoleculen in gang zet. De eigenschappen van deze 'stille' stam waren erg interessant en vroegen om vervolg *in vivo* onderzoek.

Tijdens de hierboven beschreven *in vitro* screeningprocedures viel ons op dat van alle geteste stammen het medium waarin de bacteriën groeiden in staat was om de door hitte gedode bacteriën geïnduceerde ontsteking te remmen. Verder onderzoek toonde aan dat het oorspronkelijke groeimedium (zelfs zonder aanwezige bacteriën), en vooral de korte keten vetzuren (SCFA) in dit medium, ook in staat waren ontstekingen te remmen. Van SCFA was al bekend dat het ontstekingsremmende effecten had, maar deze onderzoeken waren niet allemaal consistent. De meeste studies toonden aan dat het vetzuur butyraat, de afgifte van het ontstekingsremmende IL-10 door immuuncellen stimuleerde en daardoor de ontwikkeling van bepaalde regulerende witte bloedcellen (ontstekingsremmende regulerende T cellen, Tregs) veroorzaakte.

In **hoofdstuk 4** hebben we de effecten van de vetzuren acetaat en butyraat op verschillende afweermechanismen van de witte bloedcellen vergeleken. We vonden dat gemiddeld tot hoge concentraties butyraat de levensvatbaarheid van cellen verlaagde, terwijl vergelijkbare of zelfs hogere concentraties van acetaat de levensvatbaarheid van deze cellen niet beïnvloedden. Interessant is dat, zowel acetaat als butyraat in staat waren om de door hitte gedode bacteriën geïnduceerde afgifte van ontstekingsbevorderende signaalmoleculen te verminderen. Alleen acetaat was in staat om afgifte van het ontstekingsremmende IL-10 te verhogen. Wat nog belangrijker is, butyraat verminderde zelfs de afgifte van het ontstekingsremmende IL-10. Deze verminderde IL-10-afgifte zou kunnen leiden tot een sterkere ontstekingsreactie (lagere IL-10/IL-12-verhouding) in vergelijking met de reactie die veroorzaakt werd door acetaat. Om te onderzoeken hoe butyraat en acetaat hun effecten opwekten, probeerden we het mechanisme te bepalen waarmee ze de afgifte van signaal moleculen (cytokinesecretie) beïnvloedden. Met specifieke remmers hebben we bepaalde receptoren (G-eiwit-gekoppelde receptoren (GPCR)) geremd in een bepaald type witte bloed cel (MDDC). Daarna werden de ontstekingsremmende effecten van butyraat nog steeds waargenomen, dus de regulatie van de afgifte van signaalmoleculen is GPCR-onafhankelijk. Van butyraat (en in mindere mate acetaat) is ook bekend dat het histonacetylering beïnvloedt en daardoor het aflezen van erfelijke informatie (gentranscriptie) kan beïnvloeden. We hebben ontdekt dat butyraat inderdaad de acetylering van histonen verhoogde, en daarmee de afgifte van signaalmoleculen zou kunnen beïnvloeden. Interessant is dat ook de activatie van de alarmfunctie (NF-κB) verschilde voor acetaat vergeleken met butyraat, hoewel het onderliggende mechanisme nog niet is opgehelderd.

Omdat we duidelijke effecten van zowel acetaat als butyraat op de afgifte van signaal moleculen (cytokinesecretie) door witte bloedcellen vonden, vroegen we ons af of ook andere biologische routes zouden worden beïnvloed. We stimuleerden daarom een bepaald type witte bloedcellen (CD14+ monocyten) met acetaat en butyraat (met of zonder toevoeging van door hitte gedode bacteriën om een ontsteking na te bootsen) en onderzochten vervolgens het effect op gentranscriptie in **hoofdstuk 5**. Ook in onze monocyten zagen we dezelfde vermindering van de ontstekingsreactie als we hadden waargenomen bij de eerdere experimenten met witte bloedcellen. Verder veroorzaakte acetaat geen grote effecten op het aantal gereguleerde genen, butyraat daarentegen had een significante invloed op de regulatie van veel verschillende (immuun) routes en de genen daarin.

In hoofdstuk 6 beschrijven de vergelijking van de uitwerking die de korte vetzuren (SCFA) zouden kunnen hebben op darmwand (epitheel) cellen met de effecten die we vonden op witte bloedcellen. Deze effecten werden bekeken in een minidarm die we hadden opgekweekt in een petrischaal (*ex-vivo* 3D porcine ileum organoid model) in **hoofdstuk 6**. We hebben deze minidarm (organoid) cellen blootgesteld aan acetaat en butyraat vervolgens bekeken wat het effect was op gentranscriptie. Wederom, vergelijkbaar met de resultaten van de

witte bloedcellen, bleek butyraat grotere veranderingen in genexpressie op te wekken dan acetaat en beïnvloedde gecontroleerde celdood (apoptose) en celcyclus-gerelateerde routes aanzienlijk. Acetaat daarentegen had voornamelijk invloed op het cellulaire metabolisme, wat een minder schadelijk effect op de darmwand functie suggereert in vergelijking met butyraat.

Om onze studies af te ronden, hebben we verschillende bacteriestammen die veelbelovend leken in de *in vitro* proeven getest in een *in vivo* muis model voor darmontsteking (DSS geïnduceerd colitis-model) in **hoofdstuk 7**. We zagen vermindering van de klinische symptomen zoals gewichtsverlies, diarree en bloed in de ontlasting, van de darmontsteking na toevoeging van onze 'stille' stammen. Hiermee konden we onze hypothese dat de bacteriestammen die een 'stil' profiel induceerden de darmontsteking zouden kunnen verminderen, bevestigen.

In het laatste hoofdstuk, **hoofdstuk 8**, vatten we de gecombineerde resultaten van dit proefschrift samen en bespreken we deze in de context van andere studies naar interacties tussen gastheer en bacterie/ probiotica en de effecten van korte vetzuren. We leggen uit hoe onze bevindingen bijdragen aan een beter begrip van de ontstekingsremmende eigenschappen van darmbacteriën en hun afgifte producten (metabolieten) en geven suggesties voor toekomstig onderzoek.

ACKNOWLEDGEMENTS

It was a long and winding road to finally reach the end of my PhD journey, and I would like to acknowledge some people for their support. I received a lot of academic, technical and financial support, as well as moral support while pursuing my PhD. First of all, I would like to thank my scholarship provider **Indonesia Endowment Fund for Education (LPDP)** and **Chr. Hansen A/S** for their financial support to pursue a Doctoral program and complete my PhD project in Host-Microbe Interactomics Group, Wageningen University & Research.

I would like convey my sincere gratitude to my promotor, **Jerry Wells**. Thank you for giving me an opportunity to pursue my PhD in HMI and for guiding me to navigate this project until the end. I learned a lot from uncountable discussions, meetings, and personal conversations with you. Even though there were times when I got a little irritated when you challenged my conclusions or suggested the need for additional experiments, deep down I know that it is the way you helped me to develop critical thinking as an independent scientist. Six experimental chapters! Personally, I think it was a great achievement to wrap up my PhD. Thank you for your countless feedback during the writing process. Dear Jerry, I teased you a lot that as a Chair holder you have an endless meeting schedule throughout the day and the week, but actually I truly admire the way you try really hard to accommodate everybody's needs (and demands) while balancing family time, and even having the time to cook for your family! You care a lot about each member of HMI, guest researcher and students. I notice that you always try to ask how we are doing and make conversation whenever get a chance, even in the small gaps between appointments in your demanding schedule. You are truly a great Chair holder. I am so thankful for your endless support and help during the most difficult time of my life and my PhD journey when I lost my mother. Thank you for believing in me when I insisted on meeting the deadline for submission of the thesis, at this disorientating time in my life. Without you, that would have been impossible. I would also like to thank for you hospitality to welcome the delegation from Universitas Brawijaya. I look forward to future collaboration between HMI and Faculty of Medicine, Universitas Brawijaya.

I would also like to thank my co-promotor and daily supervisor, **Ellen Kranenbarg-Stolte**. At first, I was a bit worry when you were appointed as my daily supervisor and co-promotor, as we had limited opportunity to interact with each other during my master thesis in HMI previously. Also at first glance, you look super strict and kind of a cold person. However, you are a perfect example of the phrase "don't judge a book from its cover". Along the way I got to know you much better, you are wonderfully warm and caring person. Dear Ellen, thank you for your endless support and help during my PhD journey, you were always there during my ups and downs (which happened a lot). You guided me patiently, even when I freaked out about something and had to bother you ten thousand times a day. I am so sorry and so thankful for that. It was a memorable experience to work side by side with you in this project. You always

managed to help me to look at things “on the bright side”, no matter how disappointing our experimental results! You also played a big role on keeping me on tract; for the lab work and during the writing process. Thank you for countless discussion and feedbacks during those periods. I really enjoyed spending time with you, either during conferences, meetings or social/personal occasions. I still remember you saying that you would rather I treat you as a friend than a supervisor. You are great at being both Ellen, supervisor and a friend. Thank you for sharing the duck eggs with me, listening to my worrying thoughts, and thousands other things you did for me. For being someone, I can rely on during the darkest time when I lost my mother and faced the deadline of my thesis submission. Thanks for always taking care and making time for me, I am forever grateful to have you as a friend and supervisor. I also impressed that you manage to arrange a strict schedule, always balance between work and family. I set you as a great example of wonderful planner, always managing to make time for your family and doing what you enjoy (running, playing volley ball, helping in petting zoo, etc.) in between your work. As you enjoy being a lecturer right now, I hope someday you can come together with Jerry to Faculty of Medicine, Universitas Brawijaya to give guest lecture and help to set up collaboration between HMI and Brawijaya. I look forward to welcome you in Indonesia!

Furthermore, I would like to extend my sincere gratitude to the **microbiome consortium** members: **Eleni**, **Hermi** and **Carrien** (UMCG); **Paul**, **Alan** and **Sylvia** (University of Aberdeen); **Gemma**, **Johan** and **Wendy** (Chr. Hansen A/S). Thank you for a great collaboration. It is an honor and great opportunity to work together with all of you. I learned a lot from you during our collaboration. I also enjoyed the nice conversations over lunches and dinners during our intense project meeting. Our caretakers **Bert**, **Wilma** and **Rene**. Thank so much for all your help with the 5 *in vivo* experiments. What wonderful team work during those exhausting DSS-induced colitis studies, and I really enjoyed working with all of you. My students **Marye**, **Bart**, **Mojtaba**, **Dyonne**, **Emilie**, **Rick**, **Joachem** and **Editha**, I want to say thank you so much for your contributions and help throughout this project. As supervisor, I learned a lot from all of you. Each of you left a meaningful impression for me as I am learning to become a better supervisor. I hope you all had a good experience while working on this project. Best wishes for your future studies and career. **Bart**, my student who eventually become a PhD colleague and equal contributor for Chapter 6, I have to admit that I learned a lot more from you than you probably did from me. It is nice to work with you and it is great to have you as a friend and colleague. I always enjoy the scientific discussions and casual conversations with you. Let’s try to publish Chapter 6 as soon as possible!

Sincere thanks to **Monica Missja** (Laboratory of Microbiology) for the help growing some difficult anaerobic bacterial strains. **Bart** (Human and Animal Physiology) for the discussion and help to run western blot for histone protein, and **Vincent** (Human and Animal Physiology) for useful discussion about the histone acetylation experiment.

Special thanks to my paranymphs; **Berdien**, my officemate and friend, I really enjoy our conversation together, we talked about anything, PhD life, religion, family, personal stuff, etc. I also enjoyed the walks around the campus, which helped a lot to refresh our minds. Thank you also for sharing our emergency cookies/chocolates and for hunting bananas in the fruit basket downstairs! Thank you for being such a good listener and a great supporter for me in difficult times. Thanks also for for your help to deal with R and other computer-related stuff, I am really sorry that I bothered you a lot with this. You are someone I can rely on to calm me down when I am panicking about something. I am so grateful that I can always count on you, including the important role as one of my paranymphs. I wish you a great success on finishing your PhD, and I look forward to meeting up during your future travel around Indonesia. **Yuda**, Mas Yuda, thank you for being a great friend and paranymph! Your cooking skills saved me from starvation and some urgent international dinners. I love taking over and enjoy the lazy time in your comfy room (Bornsesteeg 1-10B3) together with Mbak Linda, but more importantly, I really enjoyed all the conversations we shared. You were often my personal sounding board, and sometimes my stylist! I really enjoyed all the trips, cycling, jogging, doing groceries and shopping spree together with you, or helping you to shake all the pots containing sand for your experiment (I didn't imagine that as a scientist you would need such strong arms to shake those pots!). I wish you the best in the final stage of PhD! and I look forward to our travel plan when we are back to Indonesia.

I would like to thank one of the biggest supporters during my PhD journey, my **Host-microbe Interactomics (HMI) family**. I was lucky to have such wonderful colleagues during my PhD in this group. I love the family-like atmosphere in our group. We help, support and care for each other a lot. I hope this will not change in the future, as our group continuously grows. **Michiel**, at the beginning of my PhD, I was nervous by your critical questions during my presentations. However, gradually I learned to deal with your questions. Your critical feedbacks were always greatly appreciated. Michiel, I must tell that I really admire your presentation skill. You are an excellent presenter who never fail to engage your audience and keep them with you. I always enjoy your talks during lab meeting or conferences. I also enjoy our brief chat on Sunday afternoon in the office when we were both came to do some work. Peter thank you for the help and discussion about Ingenuity Pathway Analysis (IPA). I am really sorry for the time I accidentally locked us out of the IPA program! **Peter**, I really enjoy your out-of-the-box presentations in our lab meetings. I am also impressed by your paperless work style which means your desk always looks super tidy!

Anja and **Nico**, our super research technicians, but also parent-like figures to me in the Netherlands. **Anja**, thank you for your help with countless PBMC experiments. We made great teamwork and I really enjoyed to work side-by-side with you during those experiments. Also, thank for your help with histology and technical help during section day of animal experiments. **Nico**, our lab manager, you bruised my heart *lol* when you kicked my fridge

and freezer out of the cell lab. You put them close to the anaerobic chamber, “in the smelly corner” in your own words. You teased me a lot because of the smell in my fridge (which I actually find not that bad). Dear Nico, thank you for helping me to provide organoids culture for my experiment and countless help solving technical problems during my experiments. Anja and Nico, thank you for your great support during my PhD, for taking care of me, for the dinner invitations and organizing all the fun events for us. I always enjoy your warm hospitality. I hope one day in the future you will be able to visit me in Indonesia, so I can return your hospitality. **Loes**, our beloved secretary and fairy godmother, with a single click of your magic button you always manage to solve all administrative problems. Thank you for all your help on organizing many administrative stuff for us. More importantly, thank you for constantly reminding us to have a short coffee break, lunch, or to take holiday in between our busy schedule. Not to forget for hosting Sinterklaas celebration for our group. For all of those efforts, I would really like to say thank you for taking care our mental health. **Marjolein**, I would like to thank you for your help to secure a scholarship and for your advice at the beginning of my PhD. I am glad that we still manage to keep in touch from time to time and I hope it will not change in the future.

To all my PhD colleagues, the comrades who fight together in this PhD journey. **Jonna**, my PhD sister, we started and ended our PhD journey on the same days! It is amazing how we were “clicked” since the first time we met at the HMI lab outing in 2015. Dear Jonna, I really enjoyed undertaking this PhD journey with you from the start until the end. You are a great colleague and friend, and I love how we help and support each other along the journey. Thank you for everything Jonna, especially for your support. I hope we can keep in touch and for sure you have to visit me in Indonesia somewhere in the future. **Blanca**, my officemate, I am happy to share the office together with you (and Berdien). I really enjoy the talks we shared together in between our busy activities. Even though you are travel away a lot due to research demand, you are always missed. Dear **Raka**, thank you for the nice conversations we had together, about PhD life, culture and personal life. You are such a warm and caring person, I really admire the way you confidently conveyed your opinions and wise thoughts, a quality I need to learn from you. **Isabela**, I love your bright spirit and warm personality. It is lovely to have you as colleague and friend. It was also a nice experience to do bacteriocin work together with you. I hope I can to convince you to take over the anaerobic chamber when I am gone. **Jori**, you are the reason I learned how to cook rendang. Even though I cannot beat your cooking skills for other Indonesian food, with this recipie I can pass as an Indonesian! **Simen**, a unique character I would say, I like to tease you a lot because of that. Simen, thank you for helping me to deal with microbiota analysis. I really appreciate your help and I am happy to share the co-authorship with you in Chapter 7. **Simon**, I was always impressed about your bright ideas and knowledge in various fields. Also how convincing you can be when delivering those ideas in front of people. **Alex**, we do not interact so much except during some social occasion or my visit to the super computer. Nevertheless, I enjoy

our conversations during those times. **Avis**, my only Indonesian colleague in HMI. Even though we have limited interaction due to different workplace (NIZO), it was nice to catch up with you whenever you came to HMI. **Matthew**, it was nice to briefly work together with you during bacteriocin and PBMC experiments. I wish all my PhD student colleagues success finishing their PhD!

Furthermore, I would like to thank my other HMI colleagues. **Marcela**, our HMI darling, we really noticed the quietness of your absence lately. You are one of the most cheerful persons I know, it is always nice to talk with you. Thank you for your encouragement and help during my PhD journey! **Linda**, I enjoyed working together with you during the pilot of colitis experiments. Thank you for your advice, help and your moral support during my PhD. I love to share my stash of chocolates with you! **Edo**, you are one of the most fun persons in the group! I always enjoy a good laugh whenever you join our social events. I also admire your knowledge and interest in various science fields. Thank you for always trying your best to help me whenever I came to you with some questions. **Laura**, I always appreciate your warm personality. I especially enjoy our talks about Korean drama and gossip. It was really nice to have a colleague who can share the fun about Korean stuff. **Femke**, you fitted perfectly in our group from the day you first arrived at HMI. Always so kind and caring. Thank you for proof-reading a few chapters of my PhD thesis, which helped a lot to improve the final draft. **Tim**, I always enjoy our brief conversations from time to time. It was nice experience to come to you PhD defence in Groningen, which you defended very well. I hope I can do the same. **Saartje**, we rarely interact with each other, except sometimes during the coffee break or during a social event. I wish I had more opportunity to get to know you better as a colleague. **Joyce**, our newest and youngest research technician, always so quiet, yet so helpful. Thank you for all your help! In return it was also a pleasure to help you with the anaerobic chamber.

My previous officemates **Sam**, **Niru**, **Kim**, **Aga** I really appreciate the time we spent together as officemates and friends. It was also a great pleasure to be a part of your PhD journey and keep in touch, even though we are now apart. I wish you all good luck in your career! My former PhD and Postdoc colleagues: **Nadya**, the strong-willed and solitary lady, the-smart-and-witty-guy, **Rogier** and **Bruno**, the person who helped me a lot with the colitis study and enjoyed the ice-skating with HMI members. Thank you for all your help and useful discussions during the time you spent in HMI, I learned a lot from all of you. It was also nice to interact with all of you!

Other people I would like to thank, **Olaf**, a previous colleague from the neighboring group (Cell Biology and Immunology), I really enjoy our conversation and discussion. I am also glad that we can share PBMCs sometimes. **Ben** (Cell Biology and Immunology), thank you for your help with Flow cytometry and immune staining. I wish you a great success in your current career! **Henk** also from a neighboring group (Experimental Zoology), you are always kind to

me and always interested in the Indoneasian snacks I brought to HMI. I was touched by your warm encouragement during my difficult time.

Mas Indraningrat, my big brother, I cannot thank you enough for all help and support since our MSc study until now. I really enjoy our talks together, and as we both are scorpion, we are tune to each other really well. I was also happy to help during your PhD defence, it was an honor and pleasure to be your paranymph. I wish you a great success in your career together with your wife, **Titi**. I look forward to have a future research collaboration with you! **Mbak Linda**, the tiger lady, thank you for being a big sister for me. I am so grateful for your help and support, especially during the hardest time. I also enjoyed the time we spent together and deep conversations we shared. I especially admire your skill to cook some sophisticated Indonesian food and you passion as well as dedication as a wildlife warrior. **Mbak Titis**, my Kpop partner. I really enjoyed chasing up our idols all the way to Paris with you. But most of all, I really enjoy to spend time having a good discussion with you. Thank you for all the help and support as well. Also, **Mas Emil** (also **Mbak lina**, **Nathans**), **Mas Taufik**, **Kang Dasep**, **Mbak Nila** (also **Mas Anto**, **Ammare**, **Unni-Adek**), **Silvi**, **Mbak Eka** (also **Mas Yusuf**, **Kirana**), we started our MSc study together as one big family, and I was glad to keep this family during PhD journey. **Ceu' Ayu**, my scorpion sister, thank you for always having a time for me whenever I come home. I really enjoy our talks and arguments we shared together. Thank you for helping me to write the short biography for my thesis book. Your name will be forever engraved in the special part of my thesis book. **Teh Dewi**, thanks for the good advice, you are a mother-like figure as well as a big sister for me. **Bang Zulham**, and other member of Indonesian MSc 2011 family (**Gerombolan WUR 2011 CS**), I am happy that our bond is still going strong.

Pak Eko, I am glad to have a colleague from Universitas Brawijaya (UB) in WUR. I am so grateful that we can share our problems and help each other a lot. Also a great teamwork to welcome UB delegations at WUR during our study. I want to thank your wife as well, **Mbak Andra**, for providing delicious Indonesian snacks and food from time to time. **Mbak Atik**, **Mbak Aviv** and **Mbak Nurmi**, thank you for the laughs, conversations and nice food we shared together over special lunches and dinners. **Teh Novi** thank you for the great advice, **Mas Indra**, **Gumi**, **Gendis**, **Hachi**, **Alim**, **CaLo**, **Vina**, **Mbak Windy**, **Belinda** and other members of Indonesian PhD in WUR, I am happy to be a part of or big Indonesian family in WUR.

Genk PhD kebelet (**Mbak Yusnita**, **Mas Nanda**), thank you for the good laughs and nice talks despite the distance (Netherlands – Australia). It was nice to be able to share our burdens and jokes together along this PhD journey, it helped to keep me sane. My soul adores you! I am so thankful that I can ease my worries whenever I talk to you both. I look forward to see you all when we are back home! **Mbak Siwi**, **Nova**, **Denny** you are all special friends for me, thank you for your support during my PhD. **Irja** thank you for the nice chillin' time we

spent together, it is always nice to catch up with you. **Nana**, **Vivi** and other friends in **ABD community** (anak kolong) group, I love how we grew up together and still manage to keep in touch until now.

I would also like to convey my gratitude to some people in my home institute, Universitas Brawijaya (UB). I would like to thank the former Dean of Faculty of Medicine **Dr. dr. Sri Andarini**, **M.Kes** and the current Dean, **Dr. dr. Wisnu Barlianto**, **M.Si.Med**, **SpA(K)**. Thank you for the support and help to pursue my PhD. I sincere thank the former Vice Dean, **Prof. Dr. dr. Loeki Enggar Fitria**, **SpParK**, for her immerse support and helps throughout my study. I was happy to be able to welcome you during official visits in WUR. I would also like to thank **Dr.rer.nat. Dra. Tri Yudani Mardining Raras**, **M.App.Sc**, the head of Biomedical Laboratory for the support during my study. Also for all technical researchers in Biomedical Laboratory and administrative staff of UB, **Mas Yuda**, **Mbak Suci**, **Mbak Asnah**, **Mbak Dian**, **Mbak Tarina**, **Mbak Bunga**, **Mbak Fitri**, **Mbak Dini**, **Isty** who are like family for me. **Mbak Yanti** and **mbak lilik**, administration staff at Faculty of Madicine who helped a lot for administrative requirement during my study. **Ucup (Yusuf)** and **Mbak Annisa**, my colleagues and close friends in the Faculty of Medicine, thank you for your help and support from afar. **Dra. Dwi Listyorini, M.Si, D.Sc.**, my former supervisor and also a mentor during my bachelor studies at State University of Malang (UM). Thank you so much for your never-ending support and great advice.

I would also like to sincerely thank **Penawangan family** and **Banjarnegara family**, thank you for all support and encouragement to finish my PhD. Especially to Dek Andhika, thank you for keeping an eye and taking care of my parents health during my absence. Success on your training as a medical doctor!

Last, but not least, I want to thank the biggest supporter of my PhD journey, **my family**. My dear sisters, **Bak yan** and **Aci**. I could not thank you enough for taking care of our parents during my absent. I am really sorry that you both had to sacrifice a lot to fill my shoes. I relied on both of you a lot to take care of our parents. Thank you for your never-ending support to pursue my dream. My dear niece **Chanza** and nephew **Ganesh**, you both are my little sunshine, I love you! My brothers-in-law **Mas Arik** and **Mas Wawan**, thank you for taking care of our family.

To my beloved **father**, **Bapak**, you are the one who encouraged me to pursue my dream to study abroad. You never doubted that I would be able to achieve my dream and always praised me for being the pride of our family. Thank you for your eternal support and countless prayers for me, also for patiently waiting for me to finish my study. More importantly, thank you for always believing in me. I would not have been able to come this far without you. I hope I can be the rock for you to lean on during this difficult time. Let's walk on a flowery

path from now on, Dad. My dear **mother**, **Mama**, when I lost you a month before the thesis submission deadline, my world collapsed. I almost give up. The only thing that keep me going is the promise I made to finish my PhD. Words fail me, to say how much I regret for not being by your side during your difficult times. Being far away from home, I lost so much time I could have spent with you. I wish I had more time to make you happy, and how I wish you could be here with me to share the joy of my academic achievement. You see, I did it, I keep my promise to you, mom. I know you feel so proud of me even though you cannot be here with me. The words I cannot say enough to you, I am sorry, I love you and thank you.

ABOUT THE AUTHOR

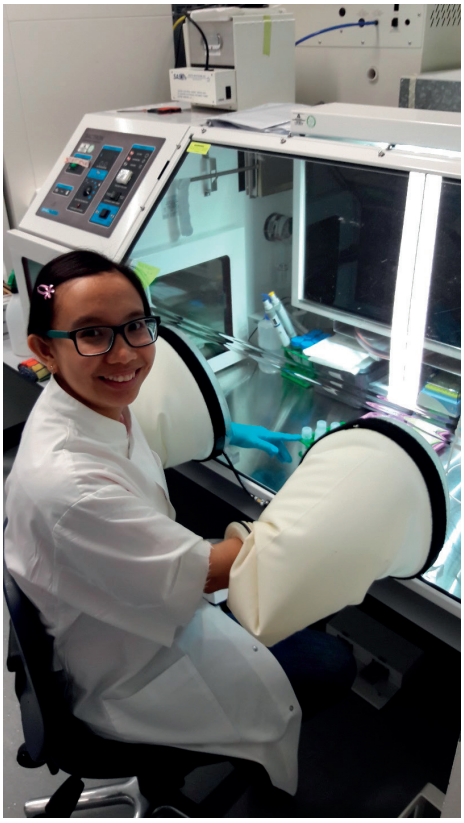

Nuning Winaris was born in Malang, East Java on 6th November 1987. As a middle child of two siblings, Nuning has developed her passion and interest in science since from a young age. Unlike most children Nuning's dream was to go into deep space as a mission specialist of NASA. In 2005 Nuning started her bachelor education in the Biology program in order to fulfil her childhood dream. She successfully obtained her bachelor degree in science in 2009.

In 2010, Nuning was granted Beasiswa Unggulan, a scholarship from Ministry of Research and Technology (DIKTI), Indonesia. This scholarship enabled her to pursue her passion in science by attending Master program of Biotechnology, specialization in Medical Biotechnology at Wageningen University & Research, The Netherlands. During her two-year study program, she learned a lot about medical research and its impact on human health and well-being. She was also involved in a NESTEC II project for her major and minor MSc thesis in Host-Microbe Interactomics (HMI) Group, under supervision of Dr. Marjolein Meijerink and Dr. Annick Mercenier. Her dream of becoming a mission specialist in the medical field seemed within reach.

Unfortunately, life led her to different direction. After completing her master program in 2013, this Javanese lady went back to her hometown, Malang, and in 2014 started her new journey as a lecturer in the Faculty of Medicine, Universitas Brawijaya. Nuning set a new ambition to become an academic scholar, a good lecturer and a researcher that could contribute significantly to medical science.

Shortly after obtaining her new position, she was fortunate to win another scholarship, this time from Indonesia Endowment Fund for Education (LPDP), Ministry of Finance, to take the next level of her education. She went back to Holland and HMI Group in September 2015 to pursue a PhD program in Mucosal Immunology under supervision of Prof. Dr. Jerry M. Wells

and Dr. Ir. Ellen Kranenbarg-Stolte. Her project aimed to find a new therapeutic candidate to treat and prevent chronic inflammation diseases such as IBD.

Nuning put a lot of her time and effort into this project, but did not forget to have some fun. In her leisure time, this purple colour lover likes reading science fiction books and enjoying the performances of her favourite Kpop idols such as EXO, BTS and SuJu. She believes that korean wave ('hallyu') is an influential global phenomenon in the 21st century. Despite giving up her dream to be a mission specialist, Nuning always keeps her keen interest about the space mission, as it was reflected in one of her proposition about NASA's twins study. Upon completing her PhD, Nuning is expected to resume her position as a lecturer in Faculty of Medicine, Universitas Brawijaya. Even though she is not working as a mission specialist, we still hope that her contribution in medical science would be a small step that leads to giant leap for human beings.

by Rahayu Handayani
MSc. MID 2013 WUR

OVERVIEW OF COMPLETED TRAINING ACTIVITIES

Discipline specific activities

17th Gut Day, Gut flora Foundation, Rotterdam, Netherlands, 2015

Laboratory Animal Science, Utrecht University, Utrecht, Netherlands, 2016

The Intestinal Microbiome and Diet in Human and Animal Health, VLAG, Wageningen, Netherlands, 2017 - poster presentation

3rd PhD symposium 'Diversity in Science', Wageningen PhD Council (WPC), Wageningen, Netherlands, 2016

KNVM & NVMM Scientific Spring Meeting, KNVM & NVMM, Papendal, Netherlands, 2016
18th Gut Day, Gut flora Foundation, Venlo, Netherlands, 2016

Wageningen Indonesia Scientic Expose (WISE), WUR-Indonesian PhD in WUR, Wageningen, Netherlands, 2016 - poster presentation

Wageningen Indonesia Scientic Expose (WISE), WUR-Indonesian PhD in WUR, Wageningen, Netherlands, 2017 - oral presentation

KNVM & NVMM Scientific Spring Meeting, KNVM & NVMM, Papendal, Netherlands, 2017

International Scientific Conference Probiotic and Prebiotic (IPC), IPC 2017 Committee, Budapest, Hungary, 2017 – oral presentation

KNVM & NVMM Scientific Spring Meeting, KNVM & NVMM, Papendal, Netherlands, 2018

20th Gut Day, Gut flora foundation, Wageningen, Netherlands, 2018

Host and the Environment in IBD: Scientific Advances Leading to New Therapeutics, Keystone Symposia, Taos, New Mexico, United States, 2019 - poster presentation

Wageningen Indonesia Scientic Expose (WISE), WUR-Indonesian PhD in WUR, Wageningen, Netherlands, 2019 - poster presentation

KNVM & NVMM Scientific Spring Meeting, KNVM & NVMM, Papendal, Netherlands - 2019

Integrating Experimental and Theoretical Approaches in Immunology, WIAS-VLAG, Wageningen, Netherlands, 2019

General courses

VLAG PhD week, VLAG, Baarlo, Netherlands, 2015

Scientific Publishing, WGS, Wageningen, Netherlands, 2018

Introduction to R, VLAG, Wageningen, Netherlands, 2018

PhD workshop Carousel, WGS, Wageningen, Netherlands, 2018

Applied Statistics, VLAG, Wageningen, Netherlands, 2018

Supervising BSc and MSc thesis students, WGS, Wageningen, Netherlands, 2018

The Essentials of Scientific Writing & Presenting, WGS, Wageningen, Netherlands, 2019

The Final Touch: Writing the General Introduction and Discussion, WIAS, Wageningen, Netherlands, 2019

Optionals

VLAG PhD proposal, VLAG, Wageningen, Netherlands, 2015 - 2016

Organizing Wageningen Indonesia Scientic Expose (WISE), WUR-Indonesian PhD in WUR, Wageningen, Netherlands, 2016

Organizing Wageningen Indonesia Scientic Expose (WISE), WUR-Indonesian PhD in WUR, Wageningen, Netherlands, 2017

HMI weekly lab meetings, HMI, Wageningen, Netherlands, 2015 - 2019

Project Meeting, Microbiome consortium, Hørsholm - Denmark (2016), Aberdeen - United Kingdom (2017), Wageningen - Netherlands (2017), Hørsholm - Denmark (2018)

The research described in this thesis was financially supported by Indonesian Endownment for Education (LPDP) under grant agreement number 20150422022974 for Nuning Winaris. Additional financial support was also given by Chr. Hansen A/S.

Colophon

Cover: schematic image of immune regulation by colonic bacteria and SCFA in the gut
Cover design: H. Sigit Pamungkas and Nuning Winaris
Printed by: DigiForce || ProefschriftMaken

Financial support from LPDP and Host-Microbe Interactomics Group, Wageningen University for printing this thesis is gratefully acknowledged.